Heinrich-Heine-Universität Düsseldorf

Inaugural-Dissertation

Entanglement in multipartite quantum systems in the context of graph states

Author:
Junyi WU

Supervisor:
Prof. Dagmar BRUß

zur Erlangung des Doktorgrades
der Mathematisch-Naturwissenschaftlichen Fakultät
Düsseldorf, April 22, 2015

Aus dem Institut für Theoretische Physik, Lehrstuhl III
der Heinrich-Heine-Universitt Düsseldorf

Gedruckt mit der Genehmigung der
Mathematisch-Naturwissenschaftlichen Fakultät der
Heinrich-Heine-Universitt Düsseldorf

Referent: Prof. Dr. Dagmar Bruß
Koreferent: PD. Dr. Hermann Kampermann
Tag der mündlichen Prüfung:

Acknowledgements

I'm thankful for the support and guidance, which I obtained during my stay at the Institute of Theoretical Physics III of Heinrich-Heine-Universität Düsseldorf.

I owe my deepest gratitude to Prof. Dr. Dagmar Bruß, who taught me many basic concepts and gave me lots of suggestions, guidance and supervision.

I am heartily thankful to PD. Dr. Hermann Kampermann for his inspiration regarding my projects and many useful discussions and guidance.

I would like to express my gratitude to Dr. Marcus Huber and Mr. Claude Klöckl for the collaboration on the project *"Determining lower bounds on a measure of multipartite entanglement from few local observables"*.

I would like to express my gratitude to Prof. Dr. Chiara Macchiavello, Prof. Dr. Leong Chuang Kwek, Dr. Matteo Rossi and Dr. Simone Severini for the collaboration on the project *"Randomized graph states and their entanglement properties"*.

I thank Prof. Dr. Otfried Gühne and Prof. Dr. Mio Murao for their useful comments and suggestions in discussions.

I thank Mr. Jochen Szangolies, Mr. Michael Epping and Mr. Felix Bischof for their help on the proofreading of this thesis.

I thank Dr. Markus Mertz, Dr. Alexander Streltsov, Dr. Silvestre Abruzzo, Dr. Sylvia Bratzik, Mr. Michael Epping, Mr. Jochen Szangolies, Mr. Felix Bischof and all the group members for helpful discussions and the wonderful breakfast/lunch time.

I want to express my most deepest appreciation to my parents and friends who have rendered their whole hearted support at all times for the successful completion of this dissertation.

List of publications

Determining lower bounds on a measure of multipartite entanglement from few local observables

J.-Y. Wu, H. Kampermann, D. Bruß, C. Klöckl and M. Huber

Phys. Rev. A, 86, 022319 (2012)

Contribution: first author, scientific work and preparation of the manuscript 70%

Randomized graph states and their entanglement properties

J.-Y. Wu, M. Rossi, H. Kampermann, S. Severini, L.C. Kwek, C. Macchiavello, D. Bruß

Phys. Rev. A, 89, 052335 (2014)

Contribution: first author, scientific work and preparation of the manuscript 75%

X-chains reveal substructures of graph states

J.-Y. Wu, H. Kampermann, D. Bruß,

E-print: arXiv:1504.03302,(2015) (submitted to PRA)

Contribution: first author, scientific work and preparation of the manuscript 90%

Abstract

Entanglement in multipartite quantum systems is studied with respect to its detection, generation and representation.

For multipartite entanglement detection, lower bounds on a type of genuine multipartite entanglement (GME) measure are derived in *Phys. Rev. A, 86, 022319 (2012)*. A positive value of these lower bounds indicates the presence of GME in a multipartite quantum system.

As a special multipartite entangled system, the preparation of graph states with imperfect gates are considered in *Phys. Rev. A, 89, 052335 (2014)*. The bipartite and multipartite entanglement of the end-product states (called randomized graph (RG) states) is analysed using the positive partial transpose (PPT) criterion and GME witnesses, respectively. RG states are characterized by a randomness parameter p, which is the success probability of the imperfect gates. The critical randomness parameter p_c, beyond which GME is present, is estimated via its upper bounds.

As a tool for this analysis, a representation of graph states in the X-basis is derived in *E-print: arXiv:1504.03302,(2015)*. This representation is simpler than the known one in the Z-basis, and more efficient for the calculation of graph state overlaps, which are needed in the GME analysis of RG states. This representation is derived with the help of so-called X-chains, which are special vertex subsets corresponding to the graph state stabilizers containing only σ_X-Pauli operators. Besides graph state overlaps, the X-chain approach can efficiently determine the Schmidt decomposition of graph states in the X-basis, which has a further application to error correction in entanglement localization of certain graph states.

Zusammenfassung

Wir studieren multipartite Quantumsysteme und deren Verschränkung hinsichtlich ihrer Detektion, Erzeugung und Darstellung.

Zur Detektion multipartiter Verschränkung leiten wir untere Schranken für ein Maß für genuine Mehrteilchenverschränkung her in *Phys. Rev. A, 86, 022319 (2012)*. Ein positiver Wert einer solchen Schranke zeigt das Vorhandensein genuiner Mehrteilchenverschränkung an.

Als ein besonderes System mit Mehrteilchenverschränkung studieren wir die Erzeugung von Graphenzuständen mit imperfekt realisierten Quantengattern in *Phys. Rev. A, 89, 052335 (2014)*. Die bipartite und multipartite Verschränkung der finalen Zustände (genannt randomized graph (RG)-Zustände) wird mit Hilfe des PPT-Kriteriums sowie von GME-Verschränkungszeugen untersucht. RG-Zustände sind durch einen stochastischen Parameter p charakterisiert, welcher die Erfolgswahrscheinlichkeit der Quantengatter angibt. Der kritische Wert p_c, jenseits dessen genuine Mehrteilchenverschränkung vorhanden ist, wird durch obere Schranken abgeschätzt.

Als Werkzeug für diese Analyse erarbeiten wir eine Darstellung von Graphenzuständen in der X-Basis in *E-print: arXiv:1504.03302,(2015)*. Diese Darstellung ist von einfacherer Form als die bekannte Z-Basis Darstellung, und kann zur effizienteren Berechnung des Überlapps zweier Graphenzustände, welcher für die Analyse genuiner Mehrteilchenverschränkung von RG-Zuständen vonnöten ist, verwendet werden. Diese Darstellung wird mit Hilfe sogenannter X-chains abgeleitet, bei welchen es sich um spezielle Untermengen von Knoten, die denjenigen stabilisierenden Operatoren, die nur σ_X-Pauli Operatoren beinhalten, zugeordnet sind, handelt. Neben dem Überlapp von Graphenzuständen kann mittels des X-Chain Ansatzes auf effiziente Weise die Schmidt-Zerlegung von Graphenzuständen in der X-Basis bestimmt werden, was weitergehende Anwendungen für die Fehlerkorrektur bezüglich der Verschränkungslokalisierung bestimmter Graphenzustände hat.

Contents

1. Introduction

Soon after the discovery of quantum mechanics, debates regarding its completeness started. In 1935, Einstein, Podolsky, and Rosen [1] disputed the completeness of quantum mechanics with the so-called EPR-paradox, in which a bipartite system was shown to be non-locally correlated, such that measurement on one party simultaneously affects the measurement outcome on the other, causally separated, party. Since they were unwilling to accept non-local influences in a physical theory, they argued that, in order to account for their predictions, quantum mechanics would have to be augmented with additional parameters, and is hence incomplete.

However, since the 1970s the non-locality of quantum mechanics was verified by various Bell test experiments [2–9], which were constructed based on the Bell inequalities [10–12]. The violation of a Bell inequality by a quantum system ρ indicates that ρ possesses correlations that are not describable by any local hidden variable (LHV) model. The resources used in these experiments are the so-called *Bell states* (EPR-pairs). The non-classical bipartite correlation of these Bell states is called *entanglement*, after Schrödinger [13].

In 1990, Werner clarified the distinction between non-locality and entanglement with the *Werner state* and clarified the definition of entanglement for mixed states [14]. Based on this definition, Peres proposed a separability criterion (PPT) [15] for determining the entanglement of general bipartite states [15] in 1996. In the same year, Horodecki established the general basic theory of separability criteria [16]. Since then various separability criteria were discovered [17–20]. Besides separability criteria, entanglement witnesses [21–25] were proposed for detecting entanglement in experiments.

On the practical side, entanglement was found to be the resource for various applications, e.g. quantum key distribution [26], quantum teleportation [27], quantum dense coding [28], quantum computation [29–31], quantum error correction [32–35] and so on. In these applications, e.g. in faithful quantum teleportation, it was found that different entangled states have different strengths and efficiencies. As a result of this, entanglement was pragmatically quantified by entanglement measures, which are defined to be non-increasing under local operations and classical communication (LOCC) [36–39].

Beyond bipartite entanglement, the entanglement in multipartite systems is far richer in structure. It is a resource for many quantum algorithms [40] and allows various applications in quantum information theory, e.g. GHZ states [41] in quantum secret sharing [42], W-states [43] in quantum memory [44] , graph states [45] in measurement based quantum computation (MBQC) [46] and so on. Multipartite entanglement is stratified into different classes by stochastic local operation and classical communication (SLOCC). In 3-qubit systems, there are two classes of entangled states, namely the GHZ-class and W-class [47]. These entangled states are all *genuinely multipartite (GM) entangled*, that means they cannot be decomposed into mixtures of biseparable states. GME can be detected and quantified with GME witnesses [47,48] and measures [49], respectively. We derived

lower bounds on a type of GME measure in Ref. [50]. With these lower bounds one can detect GME in experimentally feasible measurement settings.

For an n-qubit system with $n \geq 4$, there is a new type of entangled states additionally to the GHZ or W states, i.e. the graph states [45,51], which are resources in measurement based quantum computation (MBQC). They are quantum states that can be described in terms of mathematical graphs [52]. In Ref. [53], a preparation approach for graph states via only 1- and 2-qubit gates was proposed. However, the current realizations of 2-qubit entangling gates are far from being perfect. Therefore in Ref. [54], we considered a type of imperfect preparation of graph states, which is implemented by a type of probabilistic gates called repeat-until-success (RUS) gates [55–57]. The end products in such a preparation model are called *randomized graph (RG) states*. They are weighted according to the success probability p of the control-Z (CZ) operation in a RUS gate. We call the success probability p *randomness parameter*. The entanglement of RG states is different from that of pure graph states. The local unitary (LU) equivalence of pure graph states does not hold any more for RG states. The entanglement of RG states is determined by the randomness parameter p. We employed the PPT criterion and a projector GME witness [47,58,59] to determine the critical randomness parameter p_c[1] for bipartite and GM-entanglement, respectively. Upper bounds on p_c for GME are found via an approximation approach.

To calculate the GME witness employed in Ref. [54], we need a simpler representation of graph states in the computational basis. In Ref. [60], we introduced the so-called *X-chains*, which are a special type of vertex subsets corresponding to the graph state stabilizers consisting of only σ_X-Pauli operators. The set of X-chains of a graph state is a group with symmetric difference as its group operation. It hence allows the so-called *X-chain factorization*, from which a simpler representation of graph states in the X-basis can be derived. The larger the X-chain group is, the simpler is the graph state represented in the X-basis.

As a result of this representation, the overlap of two graph states can be efficiently calculated via the X-chain group. For this problem, no efficient algorithms were known before. X-chain factorization can also be employed for finding the Schmidt decomposition of graph states in the X-basis. This can be further applied to error correction in entanglement localization [61] of certain graph states, which could be useful for quantum repeaters [62].

This thesis is organized as follows. Three publications [50, 54, 60] are summarized in section 3.2.3, 4.3 and 4.4, respectively. To introduce the background of these projects, we review briefly the formalism of quantum mechanics in section 1.1 and the development of entanglement theory in section 1.2. Before we dive into multipartite entanglement theory, we first review the mathematical techniques employed in entanglement detection and quantification of bipartite systems in chapter 2. Then in chapter 3, entanglement in multipartite systems is reviewed with respect to its classification in section 3.1 and its detection and quantification in section 2.1 and 2.2. Then we summarize our results on the lower bounds of a type of GME measure [50] in subsection 3.2.3.

Finally, special multipartite entangled systems, namely graph states, are studied in chapter 4. We review their definition and entanglement properties in section 4.1 and 4.2. Then we summarize our results regarding the investigation of the entanglement properties of RG states [54] in section 4.3 and the representation of graph states with the help of X-chain factorization [60] in section 4.4.

[1] The randomness parameter p_c is the critical value, where for $p > p_c$ it is guaranteed that a certain type of entanglement occurs in the RG state.

1.1 Formalism of quantum mechanics

Quantum mechanics describes a quantum system on a Hilbert space $\mathbb{H}$ as a quantum state ρ, whose information content can be accessed by orthogonal projection measurement (von Neumann measurements) $\mathcal{M}_{\pi,\perp} = \{|e_i\rangle\langle e_i|\}_i$ ($\{|e_i\rangle\}$ is a basis of $\mathbb{H}$). Every basis state $|e_i\rangle$ corresponds to an outcome indexed by i. The scalar product $p_i = \langle e_i|\rho|e_i\rangle$ is interpreted as the probability of the outcome i. Since probability is non-negative and sum up to 1, a state ρ is mathematically described as a positive-semidefinite bounded linear operator on $\mathbb{H}$, with trace 1.

Definition 1.1.1 (Quantum states)**.** A quantum state is represented by a density matrix ρ,

$$\rho \in \mathcal{B}(\mathbb{H}) \text{ with } \rho \geq 0 \text{ and } \sum_i \langle e_i|\rho|e_i\rangle = 1, \tag{1.1}$$

where $\mathcal{B}(\mathbb{H})$ denotes the set of bounded linear operators on $\mathbb{H}$.

The similarity between two quantum states can be quantified by the so-called *fidelity*.

Definition 1.1.2. The *fidelity* of two quantum states ρ and σ is

$$F(\rho,\sigma) := \mathrm{tr}(\sqrt{\sqrt{\sigma}\rho\sqrt{\sigma}}). \tag{1.2}$$

If $\sigma = |\psi\rangle\langle\psi|$ is a pure state, then the fidelity is the square root of expectation value

$$F(\rho, |\psi\rangle\langle\psi|) = \sqrt{\langle\psi|\,\rho\,|\psi\rangle}. \tag{1.3}$$

A *quantum operation* is a linear map $\mathfrak{O} : \mathcal{B}(\mathbb{H}_1) \to \mathcal{B}(\mathbb{H}_2)$ mapping a quantum system $\rho \in \mathcal{B}(\mathbb{H}_1)$ to another *valid* quantum system $\mathfrak{O}(\rho) \in \mathcal{B}(\mathbb{H}_2)$. To ensure that $\mathfrak{O}(\rho)$ is a valid quantum state, $\mathfrak{O}$ *has to be a positive map*, i.e. $\mathfrak{O}(\rho) \geq 0$ for all $\rho \geq 0$.

Futhermore, let $\rho \in \mathcal{B}(\mathbb{H}_1 \otimes \mathbb{H}')$ be a quantum state in a larger Hilbert space. A quantum operation $\mathfrak{O}$ acting on the subsystem $\mathbb{H}_1$ of ρ should preserve the whole state as a valid quantum system, i.e.

$$[\mathbb{1}_{\mathbb{H}'} \otimes \mathfrak{O}](\rho) \geq 0, \tag{1.4}$$

for any $\mathbb{H}'$ and any state $\rho \in \mathcal{B}(\mathbb{H}_1 \otimes \mathbb{H}')$ with $\rho \geq 0$. This implies that a $\mathfrak{O}$ is *completely positive (CP)*[2].

Additionally, the sum of probabilities of measurement outcomes of the state $\mathfrak{O}(\rho)$ should not exceed 1, i.e. $\mathrm{tr}(\mathfrak{O}(\rho)) \leq \mathrm{tr}(\rho)$. Therefore $\mathfrak{O}$ must be *trace-non-increasing*. In summary, a quantum operation is defined as follows.

Definition 1.1.3 (Quantum operations)**.** A quantum operation $\mathfrak{O}$ is a linear map $\mathfrak{O} : \mathcal{B}(\mathbb{H}_1) \to \mathcal{B}(\mathbb{H}_2)$, which is *completely positive (CP)* and *trace-non-increasing*.

According to Choi's theorem [63], every quantum operation can be represented as a set of Kraus operators (operator-sum representation) [64–66]. More generally, any Kraus operator (completely positive (CP) map) can be lifted up to a unitary transformation in a higher dimensional Hilbert space according to the Stinespring factorization theorem [67].

[2] A linear map L is *completely positive (CP)*, if $\mathbb{1}_k \otimes L$ is positive for all $k \in \mathbb{N}$.

Theorem 1.1.4 ([66] Kraus operators, operator sum representation)**.** Let $\rho \in \mathcal{B}(\mathbb{H}^n)$ with finite dimension n, and $\mathfrak{O} : \mathcal{B}(\mathbb{H}^n) \to \mathcal{B}(\mathbb{H}^m)$ be a quantum operation, then the operation $\mathfrak{O}(\rho)$ can be expressed as a sum of linear operators,

$$\mathfrak{O}(\rho) = \sum_{i=1}^{k} L_i \rho L_i^\dagger, \tag{1.5}$$

with $\{L_i\}_i$ being a set of linear operators, $k \leq n \times m$ and $\sum_i L_i^\dagger L_i \leq \mathbb{1}$.

Theorem 1.1.5 ([67] Stinespring factorization theorem)**.** Let $\rho \in \mathcal{B}(\mathbb{H}^n)$ with finite dimension n, and $\mathfrak{O} : \mathcal{B}(\mathbb{H}^n) \to \mathcal{B}(\mathbb{H}^m)$ be a quantum operation, then there exists a bounded operator $V : \mathcal{B}(\mathbb{H}^n \otimes \tilde{\mathbb{H}}) \to (\mathbb{H}^m \otimes \tilde{\mathbb{H}})$, such that the operation $\mathfrak{O}(\rho)$ is equivalent to tracing out the subsystem $\tilde{\mathbb{H}}$ of the state under the transformation V on $\rho \otimes |0_{\tilde{H}}\rangle \langle 0_{\tilde{H}}|$, i.e.

$$\mathfrak{O}(\rho) = \sum_{i=1}^{k} L_i \rho L_i^\dagger = \mathrm{tr}_{\tilde{H}} \left[V \left(\rho \otimes |0_{\tilde{H}}\rangle\langle 0_{\tilde{H}}| \right) V^\dagger \right] \tag{1.6}$$

with $k \leq n \times m$.

Note that if the Hilbert space $\tilde{H}$ is the environment, this operation describes the couplings of the quantum system to the environment.

The information of a quantum system is accessible via quantum measurements. A type of quantum measurements is given by the *von Neumann measurements*.

Definition 1.1.6 (von Neumann measurements)**.** A von Neumann measurement $\mathcal{M}_{\pi,\perp}$ is a set of orthogonal projectors $\{|e_i\rangle \langle e_i|\}_i$ with $\sum_i |e_i\rangle \langle e_i| = \mathbb{1}$, where the basis vector $|e_i\rangle$ represents a measurement outcome, and $\langle e_i| \rho |e_i\rangle$ is its probability.

The generalization of von Neumann measurements, where one gives up the restriction of orthogonality, are the so-called positive operator-valued measure (POVM) measurements.

Definition 1.1.7 (POVM measurements)**.** A positive operator-valued measure (POVM) measurement $\mathcal{M}_+$ is a set of positive-semidefinite operators $\{E_i\}_i$ such that $\sum_i E_i = \mathbb{1}$ with $\mathrm{tr}(\rho E_i)$ being the probability of the i-th measurement outcome.

An observable returns the value of a physical quantity from an quantum system via quantum measurements.

Definition 1.1.8 (Observables)**.** An observable $\mathcal{Q}$ is a Hermitian operator, which can be expressed as the sum of the projectors of its orthogonal eigenstates $\{|\mu_i\rangle\}_i$ with real number eigenvalues $\{\mu_i\}_i$,

$$\mathcal{Q} = \sum_i \mu_i |\mu_i\rangle \langle \mu_i| . \tag{1.7}$$

The trace $\mathrm{tr}(\mathcal{Q}\rho)$ is the expectation value of the physical quantity $\mathcal{Q}$ of the quantum system ρ.

A linear operator L_i in a quantum operation (Theorem 1.1.4) can be generally expressed as the product of a projection $P_i : \mathcal{B}(\mathbb{H}^n \otimes \tilde{\mathbb{H}}) \to \mathcal{B}(\mathbb{H}^n)$ and the bounded operator V in Eq. (1.6)[3], i.e.

$$L_i = VP_i. \tag{1.8}$$

If P_i sum up to $\mathbb{1}_{\mathbb{H}^n}$, then one can implement this Kraus operator with the POVM $\mathcal{M}_+ = \{P_i\}_i$. Contrarily, if the range of $\{P_i\}_i$ does not span the whole space $\mathbb{H}^n$, post-selection on the measurement outcomes are then necessary for the implementation of the quantum operation. That means the quantum operation can not be implemented deterministically. Since the desired measurement outcome only occurs with a certain probability, such a quantum operator is *stochastic*.

Definition 1.1.9 (Stochastic quantum operator)**.** A quantum operation is *stochastic*, if post-selection on measurement outcomes is necessary in its implementation.

1.2 Discovery of entanglement

In 1935, Einstein, Podolsky and Rosen published their famous EPR-paradox [1], in which they tried to disprove the *completeness* of quantum mechanics. In this paper, they considered, a priori, nature as

A-EPR1 real (i.e. every measurement outcome (physical quantity) returns the information of an element of pre-existing physical reality.)

A-EPR2 and local (i.e. two physical quantities in causally separate systems should not affect each other).

Further they assumed that

A-EPR3 quantum mechanics is complete.

Under these assumptions (A-EPR1 - A-EPR3), they showed the existence of a causally separable system A and B,

$$|\Psi_{AB}\rangle = \sum_k |u_k\rangle_A |\psi_k\rangle_B = \sum_l |v_l\rangle_A |\phi_l\rangle_B, \tag{1.9}$$

which can be decomposed as the superposition of $|u_k\rangle |\psi_k\rangle$ or $|v_l\rangle |\phi_l\rangle$, where $\{|u_k\rangle\}_k$, $\{|v_l\rangle\}_l$, $\{|\psi_k\rangle\}_k$ and $\{|\phi_l\rangle\}_l$ are the eigenbases (eigen wave functions) of the observables $\mathcal{Q}_U^{(A)}$, $\mathcal{Q}_V^{(A)}$, $\mathcal{Q}_\psi^{(B)}$ and $\mathcal{Q}_\phi^{(B)}$, with eigenvalues u_k, v_l, ψ_k and ϕ_l, respectively. The observables $\mathcal{Q}_\psi^{(B)}$ and $\mathcal{Q}_\phi^{(B)}$ were tailored to be noncommutative,

$$\left[\mathcal{Q}_\psi^{(B)}, \mathcal{Q}_\phi^{(B)}\right] = \frac{h}{2\pi i}. \tag{1.10}$$

This noncommutativity implies the uncertainty relation of the quantities $\mathcal{Q}_\psi^{(B)}$ and $\mathcal{Q}_\phi^{(B)}$. If one predicts $\mathcal{Q}_\psi^{(B)}$ with 100% certainty on the subsystem B, then the value of $\mathcal{Q}_\phi^{(B)}$ is complete unpredictable. Hence it is said that ψ_k and ϕ_l are simultaneous elements of reality.

However, by observing the state $|\Psi_{AB}\rangle$ on the subsystem A with $\mathcal{Q}_U^{(A)}$ and $\mathcal{Q}_V^{(A)}$, respectively, A will obtain the outcomes u_k and v_l, such that he/she can then predict the states $|\psi_k\rangle$ and $|\phi_l\rangle$ on the casually disconnected system B with 100% certainty. This violates the uncertainty relationship between $\mathcal{Q}_\psi^{(B)}$ and $\mathcal{Q}_\phi^{(B)}$.

[3] A unitary U is the special case that $V = U \otimes |0_{\tilde{\mathbb{H}}}\rangle \langle 0_{\tilde{\mathbb{H}}}|$ and $P_i = \mathbb{1}_{\mathbb{H}^n} \otimes |0_{\tilde{\mathbb{H}}}\rangle \langle 0_{\tilde{\mathbb{H}}}|$.

Such a contradiction indicates that at least one of the three presumptions (A-EPR1 - A-EPR3) in is wrong. Therefore they concluded that quantum mechanics is incomplete for describing nature, which is a priori assumed to possess the features of locality and realism. Hence, they suggested additional *LHVs* to complete the quantum mechanics.

However in 1964, Bell proved a measurable upper bound of an inequality (Bell inequality) in the LHV model of quantum mechanics [10]. In the LHV model, one adopts the assumptions of

A-Bell1 realism and

A-Bell2 locality.

With quantum mechanics, one can obtain measurement results on particular states that violate the Bell inequality. Once the Bell inequality is violated in an experiment, then at least one of the assumptions (A-Bell1 - A-Bell2) must be wrong. Therefore one can conclude that *either realism or locality is not a property of nature.*

CHSH inequality: Later in 1969, Clauser, Horne, Shimony and Holt generalized the Bell inequality, and proposed the so-called *CHSH inequality* to experimentally test quantum non-locality [11], as well as the CH74 inequality in [12]. In their proposal of CHSH inequality, two measurement settings $\{A_1, A_2\}$ and $\{B_1, B_2\}$ are available to Alice and Bob, respectively. The possible outcomes of each measurement are ± 1. They showed that for any LHV model the expectation values $E(A_1, B_1)$, $E(A_1, B_2)$, $E(A_2, B_1)$ and $E(A_2, B_2)$ should fulfil the following inequality

$$|E(A_1, B_1) + E(A_1, B_2) + E(A_2, B_1) - E(A_2, B_2)| \leq 2. \tag{1.11}$$

On the other hand, the EPR-pairs, which are called *Bell states*

$$|\phi^+\rangle := \frac{1}{\sqrt{2}} \left(|0_A 0_B\rangle + |1_A 1_B\rangle\right), \tag{1.12}$$

$$|\phi^-\rangle := \frac{1}{\sqrt{2}} \left(|0_A 0_B\rangle - |1_A 1_B\rangle\right), \tag{1.13}$$

$$|\psi^+\rangle := \frac{1}{\sqrt{2}} \left(|0_A 1_B\rangle + |1_A 0_B\rangle\right), \tag{1.14}$$

$$|\psi^-\rangle := \frac{1}{\sqrt{2}} \left(|0_A 1_B\rangle - |1_A 0_B\rangle\right) \tag{1.15}$$

violate the CHSH-inequality with the maximal quantum bound $2\sqrt{2}$ [68] for certain measurements. For example, the state $|\psi^-\rangle$ violates the CHSH inequality in 1.11 with the value $2\sqrt{2}$ given the measurements

$$A_1 = Z_A, A_2 = X_A, B_1 = -\frac{Z_B + X_B}{\sqrt{2}} \text{ and } B_1 = \frac{Z_B - X_B}{\sqrt{2}}. \tag{1.16}$$

In this case,

$$\left|\langle A_1, B_1\rangle_\psi + \langle A_1, B_2\rangle_\psi + \langle A_2, B_1\rangle_\psi - \langle A_2, B_2\rangle_\psi\right| = 2\sqrt{2}. \tag{1.17}$$

Hence, the Bell states are optimal resources in Bell test experiments. The first series of convincing Bell tests was carried out by Aspect *et al.* [4,5]. Although it is now 50 years after Bell's first paper, Bell tests are still facing two main challenges, namely the locality and detection loopholes. The locality loophole was closed by Weihs, Zeilinger et. al [6] and detection loophole was closed with different materials in [7–9]. To close the locality loophole and detection loophole, one needs fast

measurements and detectors with high efficiency, respectively. Nowadays it is still hard to combine these two requirements. Hence, to construct a locality and detection loophole-free Bell test is still a challenging task. Despite the existence of loopholes, most physicists are already convinced that nature violates Bell inequalities. As most physicists believe realism is more basic than locality, commonly people regard our world as *nonlocal* and *real*.

Entanglement: Besides the loopholes, in the 80s and 90s, another obstacle to Bell test experiments is the generation of quantum system that produce non-locality, e.g. the Bell states. The non-local property of the Bell states comes from the superposition of two orthogonal product state basis vectors $|0_A\rangle|0_B\rangle$ and $|1_A\rangle|1_B\rangle$, which are also orthogonal on the both subsystems A and B. Such a basis is called *Schmidt basis*, and the expression of a state in the superposition of Schmidt basis vectors is the *Schmidt decomposition*. The number of the basis vectors in the Schmidt decomposition is called the *Schmidt rank* of a state. The non-classical structure of Bell states with Schmidt rank 2 is called "Verschränkung" according to Schrödinger [13], which means "*entanglement*" in English. For bipartite systems, the *entanglement of pure states* is defined as follows.

Definition 1.2.1 (Bipartite entanglement of pure states)**.** A quantum state $|\psi\rangle \in \mathbb{H}_A \otimes \mathbb{H}_B$ is entangled regarding the bipartition $A|B$, if its Schmidt rank in the $A|B$-bipartite Schmidt decomposition is greater than one, i.e. it cannot be written as a product state.

That means there exist at least two nonzero singular values $s_1, s_2 > 0$ in the $A|B$-bipartite Schmidt decomposition,

$$|\psi^{(A|B)}\rangle = \sum s_i |e_i^{(A)}\rangle |f_i^{(B)}\rangle. \tag{1.18}$$

Here the sets of the states $\{|e_i^{(A)}\rangle\}_i$ and $\{|f_i^{(B)}\rangle\}_i$ are bases of the subsystem A and B, respectively. A state, which can be factorized as a tensor product of two basis states, $|\psi\rangle = |e_i^{(A)}\rangle\,|f_i^{(B)}\rangle$, is called *separable*.

It was shown by Gisin that *every bipartite entangled pure state can violate a certain Bell inequality* in appropriately selected measurement settings [69, 70]. Hence not only the Bell states, but also general entangled states are the resources for Bell tests. The research of nonlocal realism shed light on a new research field, namely quantum information theory, while the techniques of entanglement creation facilitate the realization of many applications of quantum information theory. Various applications were facilitated by entanglement, e.g. quantum key distribution [26], quantum teleportation [27], quantum dense coding [28], quantum computation [29–31], quantum error correction [32–35], and others.

At the beginning, people could not distinguish the difference between non-locality and entanglement until 1989, when Werner extended the definition of entanglement to mixed states [14]. There, Werner defined the *separability of a mixed quantum state* as its decomposability as a mixture of separable pure states.

Definition 1.2.2 ([14] Bipartite entanglement of mixed states)**.** A state ρ_{AB} in the Hilbert space $\mathcal{H}_A \otimes \mathcal{H}_B$ is *separable*, if and only if it can be expressed as

$$\rho_{AB} = \sum p_i \rho_i^{(A)} \otimes \rho_i^{(B)}. \tag{1.19}$$

A state which is not separable is called *entangled*.

In [14], Werner showed that *no separable quantum state (no matter pure or mixed) can violate any Bell inequality*, and concluded that *non-locality (violation of a Bell inequality) in a system implies entanglement* [14]. Together with the result of Gisin [69], this statement links *non-locality and entanglement as equivalent properties for bipartite pure states*. However, in the same paper, Werner proved the existence of *an entangled mixed state, which admits a LHV model*. The counterexample for the equivalence of non-locality and bipartite entanglement is a $d \times d$ dimensional mixed state, which is called the *Werner state* and parameterized as [14, 71]

$$\rho_{\text{Werner}}(p_{\text{sym}}) = p_{\text{sym}} \frac{P_+}{\text{tr}(P_+)} + (1 - p_{\text{sym}}) \frac{P_-}{\text{tr}(P_-)}, \tag{1.20}$$

where $P_\pm = (1 \pm S)/2$ are the projectors on the symmetrization operator $S = \sum_{ij} |i\rangle\langle j| \otimes |j\rangle\langle i|$ with $\text{tr}(P_\pm) = \left(d^2 \pm d\right)/2$. According to the positive partial transpose (PPT) criterion, which will be formulated in Theorem 2.1.5, $\rho_{\text{Werner}}(p_{\text{sym}})$ is entangled if

$$p_{\text{sym}} < 1/2. \tag{1.21}$$

Meanwhile there exists a LHV model describing the correlation of measurements on $\rho_{\text{Werner}}(p_{\text{sym}})$, if

$$p_{\text{sym}} = (d+1)/(2d^2). \tag{1.22}$$

For dimension $d \geq 2$ and $p_{\text{sym}} < 1/2$, the Werner state $\rho_{\text{Werner}}(p_{\text{sym}})$ is entangled and can be described by a LHV model[4]. Therefore entanglement is only a necessary condition for non-locality. It is conceptually different from non-locality. The discrepancy between entanglement and non-locality inspires the detection of entanglement beyond Bell tests. To this end, several separability criteria were derived based on the fact that the convex combination of two separable states is separable. This convexity is a direct result of the definition of entanglement (Def. 1.2.2).

Lemma 1.2.3 ([16] Closed convexity of separable states)**.** The set of separable states is closed convex.

[4]Note that Popescu and Rohrlich also found another counterexample in [72].

2. Entanglement in bipartite quantum systems

2.1 Entanglement detection

After Werner [14], Popescu and Rohrlich [72] found that noisy entanglement (the entanglement in mixed states) in general admits LHV model in the early 90s, people started to find new criteria other than Bell inequalities for detecting noisy entanglement, which does not violate any Bell inequality. The first separability criterion is the *positive partial transpose (PPT) criterion* discovered by Peres [15] and Horodecki [16] in 1996. Although it cannot be implemented physically (nonoperational)[1], it helps understanding entanglement in theoretical analysis. Positivity of the partial transpose is necessary for separability and is shown to be sufficient for 2×2 and 2×3 bipartite systems [16]. The PPT criterion is derived from a decomposable positive and not completely positive (PnCP) map, namely the transpose. Note that from any positive and not completely positive (PnCP) map Λ, one can derive an entanglement criterion[2]. Partial transpose is the optimal decomposable PnCP map for entanglement detection [16]. To study the sufficiency of PPT for the system with dimension higher than 2×3, Horodecki proposed the *range criterion* in 1997 [17], which was derived from an indecomposable PnCP map. It can detect PPT entanglement [17, 18, 20]) in 3×3 and 2×4 bipartite systems, which implies insufficiency of PPT criterion for systems with dimension higher than 2×3. Another PnCP-type criterion, the *reduction criterion*, was discovered by Cerf *et al.* [19] and Breuer [74, 75].

Besides the nonoperational criteria, experimentally implementable Hermitian operators called *entanglement witnesses* can also be exploited to detect entanglement [16, 21]. In 2000, Lewenstein *et al.* proposed a systematic approach to construct the optimal entanglement witnesses, which are indecomposable and able to detect PPT entangled states [22, 23]. Other entanglement witnesses were developed in [24, 25]. All the above mentioned witnesses are linear Hermitian operators. Furthermore, in 2006, a nonlinear entanglement witness was proposed by Gühne and Lütkenhaus [76].

Convexity - the cornerstone: The closed convexity of the set of separable states (Lemma 1.2.3) allows us to enclose all the separable states with a set of hyperplanes (Hahn-Banach theorem). This statement was shown in [16] and results in the following entanglement criterion.

[1] Up to date, it can only be approximately implemented in experiments [73].

[2] One can show that for a k-positive map, the non-positive $\mathbb{1}_{k+1} \otimes \Lambda$ operator always maps a separable state ρ_{sep} to a valid quantum state, i.e. $\mathbb{1}_{k+1} \otimes \Lambda\rho_{sep} \geq 0$.

Theorem 2.1.1 ([16] Hahn-Banach theorem for entanglement)**.** A state $\rho \in \mathcal{B}(\mathbb{H}_A \otimes \mathbb{H}_B)$ is $A|B$-entangled iff there exists a Hermitian operator O_{hp}[3], such that

$$\text{tr}(O_{\text{hp}}(\rho)) < 0 \text{ and } \text{tr}(O_{\text{hp}}(\rho_{\text{sep}})) \geq 0 \tag{2.1}$$

for all separable states ρ_{sep}.

This theorem can be reversely reformulated as:

Theorem 2.1.2 (Hahn-Banach theorem for separable states)**.** A state $\rho \in \mathcal{B}(\mathbb{H}_A \otimes \mathbb{H}_B)$ is $A|B$-separable iff

$$\text{tr}(O_{\text{hp}}(\rho)) \geq 0 \tag{2.2}$$

for all hyperplane operators O_{hp} enclosing the set of separable states.

Due to Choi's theorem, the set of hyperplane operators O_{hp} is equivalent to the set of tensor product extensions of positive maps

$$\{O_{\text{hp}}\} = \{\mathbb{1}_A \otimes \Lambda_+ : \ \Lambda_+ \text{ positive maps } \mathcal{B}(\mathbb{H}_B) \to \mathcal{B}(\mathbb{H}_A)\}. \tag{2.3}$$

As a result, the theorems above are equivalent to the following separability criterion:

Theorem 2.1.3 ([16] Separability criterion (Horodecki))**.** A state $\rho \in \mathcal{B}(\mathbb{H}_A \otimes \mathbb{H}_B)$ is $A|B$-separable iff

$$\text{tr}([\mathbb{1}_A \otimes \Lambda_B^+](\rho)) \geq 0 \tag{2.4}$$

for all positive maps $\Lambda_B^+ : \mathcal{B}(\mathbb{H}_B) \to \mathcal{B}(\mathbb{H}_A)$.

These necessary and sufficient criteria are the cornerstones of several separability criteria and entanglement witnesses.

2.1.1 Nonoperational separability criteria

According to Theorem 2.1.3, given a local positive map Λ_B^+ on the Hilbert space $\mathbb{H}_B$, the positivity $[\mathbb{1}_A \otimes \Lambda_B^+](\rho) \geq 0$ is necessary for the state ρ being $A|B$-separable. If $\Lambda_B^+ = \Lambda_{\text{CP}}$ is a CP map, the condition $[\mathbb{1}_A \otimes \Lambda_{\text{CP}}](\rho) \geq 0$ is fulfilled by any quantum state ρ including all the entangled states. Hence, Λ_{CP} does not lead to any separability criterion. The nontrivial maps, from which one can derive a meaningful necessary separability criterion, are the positive and not completely positive (PnCP) maps Λ_{PnCP}.

Corollary 2.1.4 (Separability criterion (PnCP map))**.** Consider a bipartite system $\mathbb{H}_A \otimes \mathbb{H}_B$, let $\Lambda_{\text{PnCP}} : \mathcal{B}(\mathbb{H}_B) \to \mathcal{B}(\mathbb{H}_A)$ be a positive and not completely positive (PnCP) map. Then for all $A|B$-separable states ρ_{sep} it holds

$$[\mathbb{1}_A \otimes \Lambda_{\text{PnCP}}](\rho_{\text{sep}}) \geq 0. \tag{2.5}$$

Therefore the non-positivity $[\mathbb{1}_A \otimes \Lambda_{\text{PnCP}}](\rho) \ngeq 0$ implies $A|B$-entanglement of ρ. Since the transpose operator T is PnCP, the partial transpose operator $\mathbb{1}_A \otimes T_B$ leads to a necessary criterion for separability, namely the *PPT criterion*.

[3]The subscript "hp" stands for "hyperplane".

Theorem 2.1.5 ([15] positive partial transpose (PPT) criterion (Peres)). If a state ρ is $A|B$-separable, then its partial transpose ρ^{Γ} [4] is positive semi-definite.

The PPT criterion is a special case of PnCP separability criterion. The strength of a PnCP separability criteria depends on the *decomposability* of the PnCP operator Λ_{PnCP}.

Definition 2.1.6 ([67, 77, 78] Decomposable positive maps). A positive map $\Lambda_{\mathrm{decomp}}$ is decomposable if it is a convex combination of a completely positive map Λ_{CP} and the product of a second completely positive map and the transpose operator $\Lambda'_{\mathrm{CP}}T$, i.e.

$$\Lambda_{\mathrm{decomp}} = \Lambda_{\mathrm{CP}} + \Lambda'_{\mathrm{CP}}T. \tag{2.6}$$

In 2×2 and 2×3 dimensional Hilbert spaces, all PnCP operators of the form $\Lambda_{\mathrm{PnCP}} : \mathcal{B}(\mathbb{H}_{d=2,3}) \to \mathcal{B}(\mathbb{H}_{d=2})$ are decomposable [79], therefore all operators of the form $\mathbb{1}_A \otimes \Lambda_{\mathrm{PnCP}}$ can be reduced to the partial transpose $\mathbb{1}_A \otimes T_B$. As a result of the Horodecki criterion (Theorem 2.1.3), the PPT criterion is not only necessary, but also sufficient in the 2×2 and 2×3 dimensional Hilbert spaces.

Theorem 2.1.7 ([16] Sufficiency of PPT criterion (Horodecki)). A state $\rho \in \mathcal{B}(\mathbb{H}_A \otimes \mathbb{H}_B)$ with dimension 2×2 or 2×3 is separable iff its partial transpose is positive semidefinite.

Since all decomposable positive maps can be reduced to the transpose operator (Def. 2.1.6), the PPT criterion is the strongest one among the criteria derived from decomposable PnCP maps. However, the PPT criterion is not sufficient in bipartite systems with dimension larger than $d_A \times d_B = 6$. There are *PPT entangled states* [17,18,20][5], which are not detectable by the PPT criterion. In order to detect PPT entanglement, one needs separability criteria not weaker than the PPT criterion. The sole candidates are the indecomposable PnCP maps.

The entanglement of a PPT entangled state can not be distilled from an infinite number of copies to a single maximally entangled state via local operations and classical communication [80]. Such a type of entanglement is called *bound entanglement* . In [80], Horodecki proved that non-positive partital transpose (NPT) is necessary for distillability. However, the existence of non-positive partital transpose (NPT) bound entangled states is still an open question. As a result, distillability, NPT and entanglement have the following relationship.

$$\begin{array}{ccccc} & \Rightarrow & & \Rightarrow & \\ \text{Distillability} & & \text{NPT} & & \text{Entanglement} \\ & \overset{?}{\Leftarrow} & & \not\Leftarrow & \end{array} \tag{2.7}$$

In summary, the set of separable states is convex and enclosed by the hyperplanes characterized by the tensor extension of PnCP maps $\mathbb{1}_A \otimes \Lambda_{\mathrm{PnCP}}$ (see Fig. 2.1.1). Each hyperplane leads to a necessary separability criterion. These criteria are divided into two classes, which correspond to decomposable and indecomposable PnCP maps, respectively. All the criteria derived from decomposable PnCP maps (e.g. the red solid curve in Fig. 2.1.1) are weaker than the PPT

[4] ρ^{Γ} denotes either the partial transpose ρ^{T_A} on A or ρ^{T_B} on B. Here "Γ" is employed as the half part of the transpose "T".

[5] Entangled states with positive partial transpose.

criterion, which is derived from the partial transpose operator $\mathbb{1}_A \otimes T_B$. The PPT entangled states are therefore not detectable by any of these criteria. On the contrary, the criteria derived from indecomposable PnCP maps (e.g. the blue solid curve in Fig. 2.1.1) are able to detect certain PPT entangled states. A PPT entangled state is not distillable, if such 'bound entanglement' exists for any NPT state is still an open question. As the complete positivity is a prerequisite for quantum operations (Def. 1.1.3), all these PnCP criteria are not physically implementable, unless one performs the full tomography [81] of a state to reveal its density matrix, which is a tough task. To detect entanglement experimentally without full state tomography, one needs another method using entanglement witnesses.

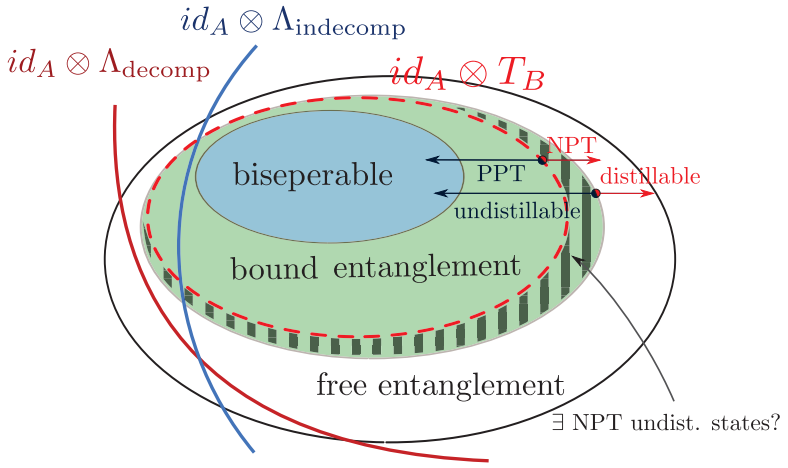

Figure 2.1: Summary of separability criteria: for the explanation please refer to the main text.

2.1.2 Entanglement witnesses

Full knowledge of the testing state is a prerequisite for entanglement detection via separability criteria. This requires a large number of observables (measurements)[6] in experiments, to implement full state tomography. A more efficient approach for entanglement detection is to certify entanglement with a single observable W. Such an operator W is called *entanglement witness* and defined as follows.

Definition 2.1.8 ([21] Entanglement witness)**.** A quantum observable $W \in \mathcal{B}(\mathbb{H}_A \otimes \mathbb{H}_B)$ is an $A|B$-bipartite entanglement witness, if it satisfies

$$\text{tr} W \rho_{\text{sep}} \geq 0, \tag{2.8}$$

for all $A|B$-separable ρ_{sep} and there exists an $A|B$-bipartite entangled state ρ_{ent} such that

$$\text{tr} W \rho_{\text{ent}} < 0. \tag{2.9}$$

From a PnCP map Λ_{PnCP}, one can derive an entanglement witness W_Λ with the help of the Jamiołkowski-isomorphism [22, 82, 83]. The basic idea is as follows. Let $\Lambda_B : \mathcal{B}(\mathbb{H}_B) \to \mathcal{B}(\mathbb{H}_A)$ be

[6] E.g. one need 9 observables for a 2-qubit quantum system

a PnCP operator, where $d_{\mathbb{H}_A} = n$ and $d_{\mathbb{H}_B} = m$, then

$$[\mathbb{1}_A \otimes \Lambda_B](\rho) = \sum_{i=1}^{nm}\sum_{j=1}^{nm} r_{ij}\,[\mathbb{1}_A \otimes \Lambda_B](|i\rangle\langle j|), \tag{2.10}$$

where $\rho = \sum_{ij} r_{ij}|i\rangle\langle j| \in \mathcal{B}(\mathbb{H}_A \otimes \mathbb{H}_B)$. We choose a pure test state $|\psi\rangle \in \mathbb{H}_A \otimes \mathbb{H}_B$ to check the positivity of $\Lambda(\rho)$ via the quantity $\langle\psi|\Lambda(\rho)|\psi\rangle$, which can be reformulated as

$$\begin{aligned}\langle\psi|\Lambda(\rho)|\psi\rangle &= \sum_{i=1}^{n}\sum_{j=1}^{m} r_{ij}\langle\psi|[\mathbb{1}_A \otimes \Lambda_B](|i\rangle\langle j|)|\psi\rangle \\ &= tr(\rho W_{\Lambda_B,\psi})\end{aligned} \tag{2.11}$$

with

$$W^{ji}_{\Lambda_B,\psi} := \mathrm{tr}\left([\mathbb{1}_A \otimes \Lambda_B](|i\rangle\langle j|)\,|\psi\rangle\langle\psi|\right). \tag{2.12}$$

If $\mathrm{tr}(\rho W_{\Lambda_B,\psi}) < 0$, then $\mathbb{1}_A \otimes \Lambda_B(\rho)$ is not positive, which implies that ρ is $A|B$-entangled (Theorem 2.1.3). On the other hand, for all $A|B$-separable states ρ_{sep}, the expectation value $\mathrm{tr}(W_{\Lambda_B,\psi}\rho_{\mathrm{sep}}) \geq 0$, since $[\mathbb{1}_A \otimes \Lambda_B](\rho_{\mathrm{sep}}) \geq 0$.

We take the transposition $\Lambda_B = T$ as an example and consider a bipartite quantum system $\mathcal{B}(\mathbb{H}_A \otimes \mathbb{H}_B)$ with dimension $dim(\mathbb{H}_A) \times dim(\mathbb{H}_B) = 2 \times 2$. We choose the Bell state $|\phi^+\rangle$ (Eq. 1.12) as the test state. The witness derived from $\mathbb{1}_A \otimes T$ and $|\phi^+\rangle$ is

$$W_{T,|\phi^+\rangle} = \frac{1}{2}\begin{pmatrix} 1 & 0 & 0 & 0 \\ 0 & 0 & 1 & 0 \\ 0 & 1 & 0 & 0 \\ 0 & 0 & 0 & 1 \end{pmatrix} = \frac{1}{2}\mathbb{1} - |\psi^-\rangle\langle\psi^-|, \tag{2.13}$$

where $|\psi^-\rangle$ is another Bell state orthogonal to $|\phi^+\rangle$. The state $|\phi^+\rangle$ is the eigenstate of $\mathbb{1} \otimes T(|\psi^-\rangle\langle\psi^-|)$ with the negative eigenvalue $-1/2$. Vice versa, $|\psi^-\rangle$ is the eigenstate of the witness $W_{T,|\phi^+\rangle}$ with the negative eigenvalue $-1/2$. The $W_{T,|\phi^+\rangle}$ can be implemented by a Bell measurement [81], in which the expectation value $\langle\psi^-|\,\rho\,|\psi^-\rangle$ can be determined. This quantity is equal to the fidelity $F(\rho, |\psi^-\rangle)$. The witness $W_{T,|\phi^+\rangle}$ can only detect the entanglement of the states which have high fidelity with $|\psi^-\rangle$. The entanglement of the other three Bell states $|\phi^+\rangle$, $|\phi^-\rangle$ and $|\psi^+\rangle$, which are orthogonal to $|\psi^-\rangle$, is not detectable by $W_{T,|\phi^+\rangle}$.

The relation between a PnCP map (e.g. transposition T) and its entanglement witnesses is shown in Fig. 2.2. An entanglement witness $W_{\Lambda_B,\rho}$ is a hyperplane separating certain entangled states from separable states. It is not stronger than the criterion derived from the map $\mathbb{1}_A \otimes \Lambda_B$ (Corollary 2.1.4). However, geometrically, the set of the entanglement witnesses $\{W_{\Lambda_B,\rho} : \rho \in B(\mathbb{H})\}$ is the set of all the hyperplanes outside the cone of $\mathbb{1}_A \otimes \Lambda_B$. Therefore $\{W_{\Lambda_B,\rho}\}_\rho$ and $\mathbb{1}_A \otimes \Lambda_B$ are equivalent, and have the same entanglement detection strength.

A witness derived from a decomposable positive map is called *decomposable witness*. According to the definition of decomposable positive maps (Def. 2.1.6), a decomposable witness can be decomposed as follows.

Definition 2.1.9 ([22] Decomposable positive witness)**.** A witness W_{dec} is decomposable if it can

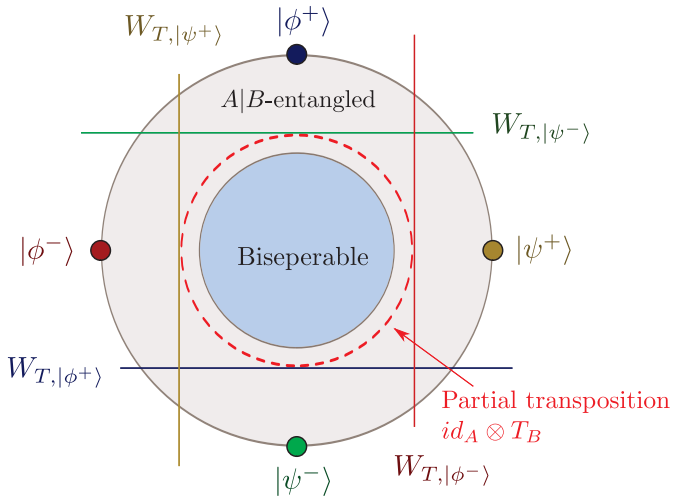

Figure 2.2: The relation between a PnCP map and its entanglement witnesses.

be written as

$$W_{\text{dec}} = P + Q^{\Gamma} \tag{2.14}$$

with P and Q being both positive and Γ being the partial transpose.

The set of all decomposable witnesses characterize the convex set of PPT states.

Continue with the example in Eq. (2.13). If the testing state $|\phi^+\rangle$ is mixed with white noise, i.e.

$$\rho_p := (1-p)\frac{\mathbb{1}}{4} + p\,|\phi^+\rangle\langle\phi^+|\,, \tag{2.15}$$

the strength of the entanglement witness W_{T,ρ_p} depends on the mixing fraction p. As the fraction p of the Bell state decreases, the set of detectable entangled states of W_{T,ρ_p} shrinks (see Fig. 2.3). If $p \leq 1/3$, the partial transpose of the state ρ_p is positive. Hence the operator W_{T,ρ_p} is also positive. Its expectation value on any quantum state is therefore positive and cannot be used as an entanglement witness. In Fig. 2.3, one observes that the hyperplane of W_{T,ρ_p} moves farther from the convex cone of PPT states as the fraction p of the Bell state decreases. This implies that the entanglement of quantum states is not just a question of "to be or not to be" entangled, but also a question of "how much to be" entangled, i.e. "what is the amount of the entanglement in a quantum system". This will be the topic of the next section.

Note that the witness $W_{T,|\phi^+\rangle}$ in Eq. (2.13) can be also derived from the following simple approach.

Proposition 2.1.10. For any entangled state $|\psi\rangle$, one can construct an entanglement witness

$$W_\psi := \lambda\mathbb{1} - |\psi\rangle\langle\psi|\,, \tag{2.16}$$

where λ is the maximum of the square of the overlap between $|\psi\rangle$ and separable states $|\sigma\rangle$,

$$\lambda := \max_{|\sigma\rangle \text{ sep.}} |\langle\psi|\sigma\rangle|^2 \tag{2.17}$$

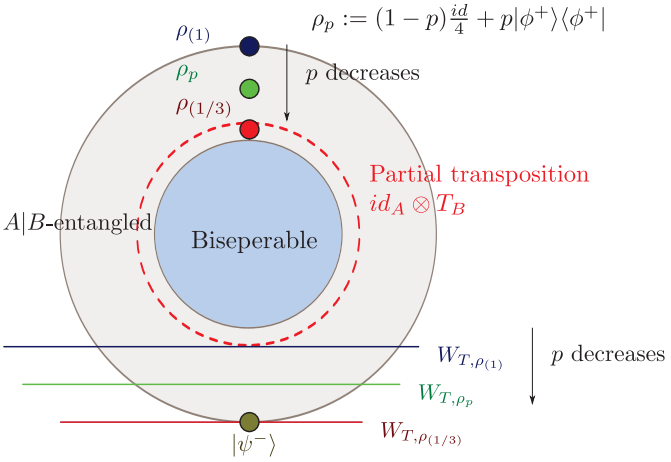

Figure 2.3: The relation between a PnCP map and its entanglement witnesses.

Proof. Let $\rho = \sum_i p_i |\sigma_i\rangle\langle\sigma_i|$ be separable as a mixture of separable $|\sigma_i\rangle$. Then $\mathrm{tr}(W_\psi \rho) = \lambda - \sum_i p_i |\langle\psi|\sigma_i\rangle|^2 \geq 0$. On the other hand, $\mathrm{tr}(W_\psi |\psi\rangle\langle\psi|) = \lambda - 1 < 0$, since $|\psi\rangle$ is entangled, $\lambda < 1$. □

The inequality $\mathrm{tr}(W_\psi \rho) \geq 0$ is maximally violated by $|\psi\rangle$. Therefore this witness is tailored for detecting the entangled states "close"[7] to $|\psi\rangle$.

2.2 Entanglement quantification

Separability criteria and entanglement witnesses can qualitatively determine the presence of entanglement. However, a quantitative measure for comparing entanglement among different states is still missing. Since entanglement can be detected by Bell inequalities, the amount of violation of a Bell inequality was the first candidate for an entanglement measure. However, the CHSH-inequality was found not to yield a measure of entanglement in Ref. [84], since its violation by particular states was shown to increase under local operations. A proper entanglement measure for pure states is the *entropy of entanglement*, which is the von-Neumann entropy of the reduced quantum states of the subsystems. However, for mixed states, their entropy can be non-zero even for separable system. In 1996, Bennett *et. al.* introduced two entanglement measures for mixed states, namely *distillable entanglement* and the *entanglement of formation*, which do not increase under LOCC [36, 85]. They are derived from a pragmatical perspective, namely the *entanglement distillation and dilution*.

Indeed there is no unique definition of entanglement measures up to date. In different contexts, different sets of postulates are adopted for entanglement measures [36–38]. Among these different sets of postulates, one is necessary, which is the non-increasing behaviour under LOCC. Accordingly, Vidal introduced the so-called *entanglement monotones* [36, 39] as follows.

[7] Here, two states are "close" to each other, if they have high fidelity.

Definition 2.2.1 ([39] (LOCC) Entanglement monotone)**.** A scalar valued function of quantum states is an *entanglement monotone*, if it does not increase (on average) under LOCC, i.e.

$$\mathcal{E}(\rho) \geq \mathcal{E}(\Lambda\rho) \tag{2.18}$$

for all LOCC operations Λ.

In [39], the necessary and sufficient conditions for a function being an entanglement monotone are given. Besides the entanglement monotone an entanglement measure is necessarily vanishing for all separable states. Together, there are therefore two necessary postulates for entanglement measures.

Postulate 2.2.2 (Entanglement measure)**.** A scalar valued function of a quantum state $\mathcal{E}(\rho)$ is an entanglement measure, if it is

1. an entanglement monotone, i.e. $\mathcal{E}(\Lambda(\rho)) \leq \mathcal{E}(\rho)$, for all LOCC operation Λ,
2. vanishing for separable states, i.e. $\mathcal{E}(\sigma) = 0$ for all separable states σ.

Note that in [36, 37], LU-invariance was also required for entanglement measures, i.e.

$$\mathcal{E}(U_A \otimes U_B \rho U_A^\dagger \otimes U_B^\dagger) = \mathcal{E}(\rho). \tag{2.19}$$

Since LUs are special local operations which are reversible, i.e.

$$\rho_1 \overset{\text{LU}}{\to} \rho_2 \Leftrightarrow \rho_2 \overset{\text{LU}}{\to} \rho_1, \tag{2.20}$$

two LU equivalent states are therefore equivalent with respect to any entanglement monotone, i.e. $\mathcal{E}(\rho_1) = \mathcal{E}(\rho_2)$. Therefore LU-invariance is satisfied by all entanglement monotones.

Other additional properties, which are also considered as requirements for entanglement measures by different authors [36–38], are the following:

1. additivity [36], i.e. $\mathcal{E}(\rho_1 \otimes \rho_2) = \mathcal{E}(\rho_1) + \mathcal{E}(\rho_2)$;
2. tightness on separable states, i.e. $\mathcal{E}(\sigma) = 0$ only if σ is separable;
3. convexity, i.e. $\mathcal{E}(\sum p_i \rho_i) \leq \sum p_i \mathcal{E}(\rho_i)$.

The key notion in entanglement quantification is LOCC. However, still in the 90s, LOCC were confused with separable Kraus operators, which were proved to be more general than LOCC in [86]. Up to date, the description of LOCC is still very sophisticated. In order to understand the quantification of entanglement, one first needs to understand LOCC. Therefore we start this section with a review of quantum operations on composite systems (section 2.2.1). Then we will review 4 entanglement measures, namely *distillable entanglement*, *entanglement of formation*, *negativity* and *concurrence*, which are all entanglement monotones satisfying different optional axioms. At the end, a summary of these entanglement measures will be given in section 2.2.7.

2.2.1 Quantum operations on composite systems

In this section, we take bipartite systems as an example of composite systems to review different types of local quantum operations [87]. Quantum operations on multipartite systems can be extended from bipartite systems straightforwardly.

As the discussion of Eq. (1.8) shows that quantum operations can be classified as deterministic (D) and stochastic (S). In a composite system, the local implementability of a quantum operation should be additionally taken in to account. Since classical correlations CC of local quantum operations can be implemented via classical communications, it is another pragmatic aspect of quantum operation classification. Hence, three properties of quantum operations come into consideration:

(D/S) Do we need post-selections in measurements to implement this operation?

(LO/GO) Is it implementable with local quantum operations (LOs) on the subsystems, or is a global operation (GO) needed?

CC Are the local operations classically correlated via classical communication (CC)?

The classes of quantum operations within the combinations of $\{\mathrm{D/S}, \mathrm{LO/GO}, \mathrm{CC}\}$ on a composite system are listed in Table 2.1. Usually, the term "LOCC" refer to a deterministic "DLOCC", which also holds for the terms "LO" and "GO".

post-selection (PS) / local implementability	deterministic (without PS)	stochastic (with PS)
local operations without CC	DLO	SLO
local operations with CC	DLOCC	SLOCC
global (joint) operations	DGO	SGO

Table 2.1: Quantum operations in a composite system: CC stands for classical communication, DLO for deterministic local operation, SLO for stochastic local operation, DLOCC for deterministic local operation and classical communication, SLOCC for stochastic local operation and classical communication, DGO for deterministic global operation and SGO for stochastic global operation, respectively.

Local operation (LO) and stochastic local operation (SLO)

Definition 2.2.3 (LO and SLO)**.** A *local operation (LO)* $\mathfrak{O}_{\mathrm{LO}}$ is a set of Kraus operators $\{L_i\}_i$, which can be decomposed into two independent $\{A_\alpha\}_\alpha$ and $\{B_\beta\}_\beta$, with $L_i = A_\alpha \otimes B_\beta$ and $i = (\alpha, \beta)$ being an index comprising α and β.

$$\mathfrak{O}_{\mathrm{LO}}(\rho) = \sum_{\alpha,\beta} A_\alpha \otimes B_\beta \rho A_\alpha^\dagger \otimes B_\beta^\dagger. \tag{2.21}$$

The $\mathfrak{O}_{\mathrm{LO}}$ is a *stochastic local operation (SLO)*, if post-selections of measurements are necessary in its implementation, that means it succeeds only with a certain probability.

The operation $\mathfrak{O}_{\rm LO}$ is deterministic, if and only if it preserves the trace of all ρ, i.e. $\mathrm{tr}(\mathfrak{O}_{\rm LO}\rho) = 1$, which is equivalent to $\sum_{\alpha,\beta} A_\alpha A_\alpha^\dagger \otimes B_\beta B_\beta^\dagger = \mathbb{1}$. Reversely, if $\mathfrak{O}_{\rm LO}$ does not preserve the trace, i.e. $\mathrm{tr}(\mathfrak{O}_{\rm LO}\rho) < 1$, which we denote as $\sum_{\alpha,\beta} A_\alpha A_\alpha^\dagger \otimes B_\beta B_\beta^\dagger < \mathbb{1}$, then it is stochastic. Since $\{A_\alpha\}_\alpha$ and $\{B_\beta\}_\beta$ are totally independent, one can not generate any correlation (neither quantum or classical) from a product state $\rho = \rho_A \otimes \rho_B$ with the local operation (LO), i.e.

$$\mathfrak{O}_{\rm LO}(\rho_A \otimes \rho_B) = \sum_{\alpha,\beta} A_\alpha \rho_A A_\alpha^\dagger \otimes B_\beta \rho_B B_\beta^\dagger. \tag{2.22}$$

Local operations and classical communication (LOCC)

Definition 2.2.4 (LOCC)**.** A *LOCC* operation $\mathfrak{O}_{\rm LOCC}$ is a local operation, in which the operations on two subsystems are correlated classically via classical communication. If it can be implemented deterministically without post-selection, then it is deterministic LOCC, while it is stochastic (SLOCC), if post-selection is necessary.

The conceptual definition of LOCC can be clearly phrased. However, the mathematical characterization of LOCCs is sophisticated. A LOCC operation can be generally formulated as a sequence of local operations with dependence on measurement outcomes on each subsystem. Let Alice and Bob first implement A_{α_1} and B_{β_1} on their systems with the outcomes α_1 and β_1, respectively. They share these results (α_1, β_1) via classical communications. Based on these results, they take a decision to perform the subsequent operations $A_{\alpha_2|(\alpha_1,\beta_1)}$ and $B_{\beta_2|(\alpha_1,\beta_1)}$ in the second round. The outcomes (α_2, β_2) in the second round will determine the subsequent operation in the next round. Up to the n-th round, this operation is formulated as

$$A_{\alpha_n|(\alpha_1,\beta_1,\ldots,\alpha_{n-1},\beta_{n-1})} \cdots A_{\alpha_2|(\alpha_1,\beta_1)} A_{\alpha_1} \otimes B_{\beta_n|(\alpha_1,\beta_1,\ldots,\alpha_{n-1},\beta_{n-1})} \cdots B_{\beta_2|(\alpha_1,\beta_1)} B_{\beta_1}. \tag{2.23}$$

The restriction of this operation is that in each round no outcomes are redundant (no post-selections), that means each outcome either stimulates a subsequent operation or arrives at an ultimate desired state, i.e.

$$\begin{aligned} \mathbb{1} &= \sum_{\alpha_k} A^\dagger_{\alpha_k|(\alpha_1,\beta_1,\ldots,\alpha_{k-1},\beta_{k-1})} A_{\alpha_k|(\alpha_1,\beta_1,\ldots,\alpha_{k-1},\beta_{k-1})} \\ &= \sum_{\beta_k} B^\dagger_{\beta_k|(\alpha_1,\beta_1,\ldots,\alpha_{k-1},\beta_{k-1})} B_{\beta_k|(\alpha_1,\beta_1,\ldots,\alpha_{k-1},\beta_{k-1})} \end{aligned} \tag{2.24}$$

for all $k \leq n$. One can redefine the sequence of operations as a single operation indexed by i, i.e.

$$\begin{aligned} A_i &:= A_{\alpha_n|(\alpha_1,\beta_1,\ldots,\alpha_{n-1},\beta_{n-1})} \cdots A_{\alpha_2|(\alpha_1,\beta_1)} A_{\alpha_1}, \\ B_i &:= B_{\beta_n|(\alpha_1,\beta_1,\ldots,\alpha_{n-1},\beta_{n-1})} \cdots B_{\beta_2|(\alpha_1,\beta_1)} B_{\beta_1} \end{aligned} \tag{2.25}$$

with $i = (\alpha_1, \beta_1, ..., \alpha_{k-1}, \beta_{k-1}, \alpha_k, \beta_k)$. The determinism of LOCC (Eq. 2.24) leads to $\sum A_i^\dagger A_i = \sum B_i^\dagger B_i = \mathbb{1}$. Hence this reformulation results in a so-called *separable (Kraus) operator (SOP)*, which is defined as follows.

Definition 2.2.5 (SOP)**.** A separable (Kraus) operator (SOP) $\mathfrak{O}_{\rm SOP}$ is expressed as

$$\mathfrak{O}_{\rm SOP}(\rho) = \sum_i A_i \otimes B_i \rho A_i^\dagger \otimes B_i^\dagger \tag{2.26}$$

with $\{A_i\}_i$ and $\{B_i\}_i$ being two sets of linear operators and $\sum_i A_i A_i^\dagger \otimes B_i B_i^\dagger = \mathbb{1}$.

In the 90s, separable (Kraus) operators (SOPs) were thought to be equivalent to LOCCs [37]. However, in 1999, Bennett *et al.* showed that a particular separable operator, which is used for state discrimination of an unextendible product basis, can not be implemented locally without post-selection [86]. That means there exists an unextendible product basis which can be perfectly distinguished by a SOP, but not by any LOCC. Therefore the SOP are more general than LOCC,

$$LOCC \subsetneq SOP. \tag{2.27}$$

However, besides in the context of state discrimination, it is not obvious to see the difference between SOP and LOCC in entanglement quantification, since both of them can create classical correlations from product states and create entanglement from separable states. Despite the unclear roles of SOP and LOCC in entanglement, LOCC is conventionally adopted as the ordering operation in entanglement quantification (see the definition of entanglement monotone in Def. 2.2.1). Meanwhile due to its mathematical simplicity, SOP is employed for verifying the monotonicity of entanglement monotones. We call a monotonically non-increasing function with respect to SOP a SOP entanglement monotone.

Definition 2.2.6 (SOP entanglement monotones)**.** A SOP entanglement monotone is a scalar function $\mathcal{E}_{\mathrm{SOP}}$, which does not increase under SOPs, i.e.

$$\mathcal{E}_{\mathrm{SOP}}(\rho) \geq \mathcal{E}_{\mathrm{SOP}}(\mathfrak{O}(\rho)). \tag{2.28}$$

for all $\mathfrak{O}$ being SOP.

Since LOCCs are special SOPs (Eq. (2.27)), SOP entanglement monotones are certainly LOCC entanglement monotones.

$$\text{SOP entanglement monotones } \subseteq \text{LOCC entanglement monotones .} \tag{2.29}$$

However, the reverse was not refuted until 2009, when Chitambar and Duan showed the existence of a LOCC entanglement monotone, which can increase under SOP [88].

Stochastic local operation and classical communication (SLOCC) *Stochastic local operations and classical communication (SLOCC)* are *LOCC* which need post-selection. SOP, that are not LOCC, are SLOCC. If a set of Kraus operators $\{A_i \otimes B_i\}_i$ has $\sum_i A_i A_i^\dagger \otimes B_i B_i^\dagger < \mathbb{1}$ then it is certainly SLOCC. The relation between LOCC, SOP and SLOCC is illustrated in Fig 2.4.

Global operation (GO) and Stochastic global operation (SGO) A *global operation (GO)* is a set of Kraus operators $\{A_i\}_i$, which can not be decomposed as LO or SOP. It can generate classical correlations from product states and entanglement from separable states. A *stochastic global operation (SGO)* is a global operation (GO) with post-selection, i.e. $\sum_i A_i A_i^\dagger < \mathbb{1}$. The relation between stochastic global operation (SGO) and GO is illustrated in Fig 2.4.

2.2.2 The unit of entanglement

In this section, we will compare the entanglement of pure states using a unit defined by the "maximally" entangled states, e.g. the Bell states in a 2×2 dimensional Hilbert space. Such

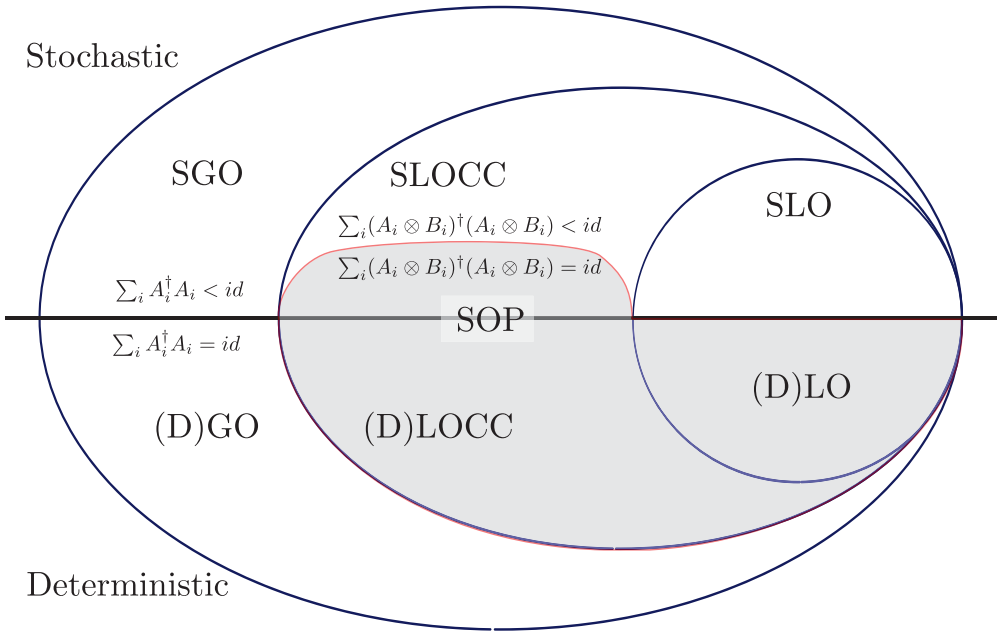

Figure 2.4: The summary of quantum in composite systems: for explanation, please refer to the main text.

comparison is allowed, since in the asymptotic limit $n \to \infty$, n copies of an entangled pure state $|\psi\rangle$ can be created from m_n copies of Bell states $|Bell\rangle$ via LOCC, and conversely one can create m_n copies of Bell states via LOCCs [89]. As a result, the entanglement of $|\psi\rangle^{\otimes n}$ is equivalent to that of $|Bell\rangle^{\otimes m_n}$, i.e.

$$\mathcal{E}_{add}(|Bell\rangle^{\otimes m_n}) \leq \mathcal{E}_{add}(|\psi\rangle^{\otimes n}) \leq \mathcal{E}_{add}(|Bell\rangle^{\otimes m_n}) \tag{2.30}$$

$$\Downarrow$$

$$\mathcal{E}_{add}(|\psi\rangle^{\otimes n}) = \mathcal{E}_{add}(|Bell\rangle^{\otimes m_n}). \tag{2.31}$$

If $\mathcal{E}_{add}$ is an entanglement measure which is additive *for pure states*, i.e. $\mathcal{E}_{add}(|\psi\rangle^{\otimes n}) = n\mathcal{E}_{add}(|\psi\rangle)$, then

$$\mathcal{E}_{add}(|\psi\rangle) = \frac{m_n}{n}\mathcal{E}_{add}(|Bell\rangle). \tag{2.32}$$

For $n \to \infty$, m_n/n is equal to the entropy of subsystems $S_{ent}(|\psi\rangle)$, which is called *entropy of entanglement (for pure states)*.

Definition 2.2.7 ([85] Entropy of entanglement)**.** The entropy of entanglement of a pure state $|\psi\rangle$ is defined as the entropy of the reduced state $\rho_\psi^{(A)} := tr_B(|\psi\rangle\langle\psi|)$ or $\rho_\psi^{(B)} := tr_A(|\psi\rangle\langle\psi|)$, i.e.,

$$S_{ent}(|\psi\rangle) = S(\rho_\psi^{(A)}) = S(\rho_\psi^{(B)}). \tag{2.33}$$

Consequently, the entanglement of $|\psi\rangle$ can be expressed as a fraction of the one of $|Bell\rangle$

$$\mathcal{E}_{add}(|\psi\rangle) = S_{ent}(|\psi\rangle)\mathcal{E}_{add}(|Bell\rangle), \tag{2.34}$$

for an additive entanglement measure $\mathcal{E}_{add}$. Since $S_{ent}(|\psi\rangle) \leq 1$ for pure states, according to Eq. (2.34), the entanglement of Bell states has the maximum value among pure states. Bell states are therefore *maximally entangled*. As a result, one can quantify the entanglement of any pure state $|\psi\rangle$ with the unit of entanglement called *e-bit*, which is defined as the value $\mathcal{E}_{add}(|\psi_{\max}\rangle)$ with $|\psi_{\max}\rangle$ (e.g. $|Bell\rangle$) being the maximally entangled states[8]. The process of transforming n copies of $|\psi\rangle$ to m_n copies of a maximally entangled state is called *entanglement distillation*, while the reverse is called *entanglement dilution.*

For pure states, the entropy of entanglement is an entanglement measure, since it is a LOCC monotone that vanished for all separable pure states. Additionally it is additive, i.e $S_{ent}\left(|\psi\rangle^{\otimes n}\right) = nS_{ent}\left(|\psi\rangle\right)$, due to the additivity of von Neumann entropy for independent systems and the equality

$$tr_B\left(|\psi\rangle\langle\psi|^{\otimes n}\right) = tr_B\left(|\psi\rangle\langle\psi|\right)^{\otimes n}. \tag{2.35}$$

Therefore the quantity $S_{ent}(|\psi_{\max}\rangle)$ can be used as the unit of entanglement *e-bit*.

In summary, the entropy of entanglement is a practical entanglement measure for pure states, which indicates the operational potential of a state in entanglement distillation and the resource demands for its entanglement dilution. However, for separable mixed states which are classically correlated, e.g. $\rho = 1/2\,|00\rangle\langle 00| + 1/2\,|11\rangle\langle 11|$, the entropy of entanglement is non-zero. The reason is that the entropy of entanglement implies mixedness of the subsystems. It does not only quantify entanglement but also the degree of mixedness. Therefore the entropy of entanglement is not a valid entanglement measure for mixed states.

2.2.3 Distillable entanglement and entanglement of formation

As shown in Eq. (2.30), in the asymptotic limit, the number $m_n^{(\text{dist})}$ of Bell states, which one can distill from n copies of a pure state $|\psi\rangle$, is identical to the number $m_n^{(\text{form})}$ of Bell states, which are required for the creation of n copies of $|\psi\rangle$. For pure states, in the asymptotic limit, the number $\lim_{n\to\infty} m_n^{(\text{dist})}$ and $\lim_{n\to\infty} m_n^{(\text{form})}$ refer to *distillable entanglement* and *entanglement of formation*, respectively. Different from pure states, the distillable entanglement and entanglement of formation of a mixed state ρ do not coincide with each other. There are entangled states which are not distillable (bound entanglement) [80], but can be created from maximally entangled states. *Distillable entanglement* and *entanglement of formation* are introduced as entanglement measures for mixed states in [36].

Distillable entanglement The distillable entanglement is an operational entanglement measure stemming from quantum teleportation, in which subsystems of n copies of maximally entangled states $|\psi_{\max}\rangle$ are transmitted through a noisy channel, e.g. depolarizing channel, from Alice to Bob. At the end, Alice and Bob will share n copies of mixed states, i.e.

$$\rho_{\psi_{\max}}^{\otimes n}, \text{with } \rho_{\psi_{\max}} = f\frac{1}{d_A \times d_B}\mathbb{1} + (1-p)|\psi_{\max}\rangle\langle\psi_{\max}|, \tag{2.36}$$

with d_A and d_B being the dimension of $\mathbb{H}_A$ and $\mathbb{H}_B$, respectively. In order to achieve a faithful quantum teleportation, one needs to distill (originally called 'concentrate' or 'purify'[9]) n copies of the mixed states $\rho_{\psi_{\max}}^{\otimes n}$ to m_n copies of the pure maximally entangled state $|\psi_{\max}\rangle$ [85, 90].

[8] One of the maximally entangled states in $d_A \times d_B$ Hilbert space is $|\phi_{\max}\rangle = \sum_{i=1}^{d} |i_A i_B\rangle$ where $d = \min(d_A, d_B)$. The other maximally entangled states can be obtained via local unitaries.

[9] One should not confuse the purification of noisy states in entanglement distillation with the purification of a mixed state to a pure state in higher dimension.

The maximum value of $\lim_{n\to\infty}(m_n/n)$ over all possible LOCCs is defined as the *distillable entanglement*. A mathematical definition of distillable entanglement is formulated using a distance measure [91].

Definition 2.2.8 ([91] Distillable entanglement)**.** The distillable entanglement of a state is an entanglement measure defined as

$$\mathcal{E}_D(\rho) = \sup_r \left[r : \lim_{n\to\infty} \left(\inf_{\Lambda\in \mathrm{LOCC}} \left\| \Lambda(\rho) - |\psi_{\max}\rangle\langle\psi_{\max}|^{\otimes rn} \right\|_1 \right) \right], \tag{2.37}$$

where $\|\cdot\|_1$ is the trace norm.

Entanglement of formation Diluting the entanglement from pure maximally entangled states to a mixed entangled state is more straightforward than entanglement distillation. A mixed state ρ can be always decomposed into a mixture of pure states $|\psi_i\rangle$, i.e. $\rho = \sum_i p_i |\psi_i\rangle\langle\psi_i|$, with $\sum_i p_i = 1$. That means that a mixed state ρ can be generated from an ensemble of pure states $\{p_i, |\psi_i\rangle\}_i$. Since each pure state $|\psi_i\rangle$ can be created with $S_{ent}(|\psi\rangle)$ maximally entangled states in the asymptotic limit, ρ can be created from $\sum_i p_i S_{ent}(|\psi\rangle)$ maximally entangled states. Note that the decomposition $\{p_i, |\psi_i\rangle\}_i$ is not unique, therefore the infimum over all possible decompositions is employed to express the minimum requirement on the maximally entangled resources in entanglement dilution. This minimum requirement is called the *entanglement of formation*.

Definition 2.2.9 ([36] Entanglement of formation)**.** The entanglement of formation for mixed states is

$$\mathcal{E}_F(\rho) := \inf_{\{p_i,|\psi_i\rangle\}} \left\{ \sum_i p_i \mathcal{E}_F(|\psi_i\rangle) : \rho = \sum_i p_i |\psi_i\rangle\langle\psi_i| \right\} \tag{2.38}$$

where $\mathcal{E}_F(|\psi_i\rangle) = S_{ent}(|\psi_i\rangle)$.

Entanglement of formation is an entanglement measure due to its convexity, i.e.

$$\mathcal{E}_F(\Lambda(\rho)) \le \sum_i p_i \mathcal{E}_F(\Lambda(|\psi_i\rangle)) \le \sum_i p_i \mathcal{E}_F(|\psi_i\rangle) = \mathcal{E}_F(\rho). \tag{2.39}$$

This approach is called *convex roof extension*. It can be exploited in the extension of pure state entanglement measures to mixed state.

Proposition 2.2.10 ([36] Convex roof extension)**.** Let $\mathcal{E}_{\mathrm{pure}}$ be an entanglement measure for pure states, then the convex roof extension

$$\mathcal{E}_{\mathrm{mix}} = \inf_{\{p_i|\psi_i\rangle\}} \left\{ \sum_i p_i \mathcal{E}_{\mathrm{pure}}(|\psi_i\rangle) : \rho = \sum_i p_i |\psi\rangle\langle\psi| \right\} \tag{2.40}$$

is a convex entanglement measure.

Every entanglement measure obtained via convex roof extension is convex. The problem of convex roof extension is its compatibility. Since one needs to calculate the infimum over all possible decompositions of the density matrix, which is infinite, it is in general impossible to obtain a global infimum.

According to the definition of distillable entanglement and entanglement of formation, one can find a LOCC protocol, such that from $n\mathcal{E}_F(\rho)$ copies of a maximally entangled state $|\psi_{\max}\rangle$, n copies of ρ are created. Subsequently, from these n copies of ρ one can distill $n\mathcal{E}_D(\rho)$ copies of $|\psi_{\max}\rangle$. Therefore the entanglement of formation $\mathcal{E}_F(\rho)$ of a state ρ is a upper bound on its distillable entanglement $\mathcal{E}_D(\rho)$, i.e. $\mathcal{E}_D \leq \mathcal{E}_F$. Otherwise, given a number of maximally entangled states, one can then create maximally entangled states via LOCC, which is impossible.

2.2.4 Concurrence

In order to quantify the entanglement of formation, Hills and Wootters introduced the so-called *concurrence* as a mathematical tool [92–94]. For a two-qubit pure state $|\psi\rangle$, the concurrence is defined as the overlap of $|\psi\rangle$ and its spin-flipped state $|\tilde{\psi}\rangle$.

Definition 2.2.11 ([92–94] Concurrence (two-qubit pure states))**.** Let $|\psi\rangle$ be a two-qubit pure state, its concurrence is

$$\mathcal{E}_{\text{con}}(|\psi\rangle) = \left\langle \psi \middle| \tilde{\psi} \right\rangle \tag{2.41}$$

with $|\tilde{\psi}\rangle := \sigma_y \otimes \sigma_y |\psi^*\rangle$ and $|\psi^*\rangle$ being the complex conjugation of $|\psi\rangle$.

If $|\psi\rangle$ is separable, the operation $\sigma_y \otimes \sigma_y |\psi^*\rangle$ flips the spin direction of $|\psi\rangle$ on the Bloch-sphere. E.g. let $|\psi\rangle = |\phi_A\rangle \otimes |\phi_B\rangle$ be a product state, then

$$\begin{aligned} |\psi\rangle\langle\psi| &= \frac{1}{2}(\mathbb{1} + \vec{v}_A \cdot \vec{\sigma}) \otimes \frac{1}{2}(\mathbb{1} + \vec{v}_B \cdot \vec{\sigma}) \\ &\Big\downarrow \; |\tilde{\psi}\rangle = \sigma_y \otimes \sigma_y |\psi^*\rangle \\ |\tilde{\psi}\rangle\langle\tilde{\psi}| &= \frac{1}{2}(\mathbb{1} - \vec{v}_A \cdot \vec{\sigma}) \otimes \frac{1}{2}(\mathbb{1} - \vec{v}_B \cdot \vec{\sigma}) \end{aligned} \tag{2.42}$$

with $\vec{v}_A$ and $\vec{v}_B$ being the Bloch-vectors of $|\phi_A\rangle$ and $|\phi_B\rangle$, respectively, and $\vec{\sigma} = (\sigma_x, \sigma_y, \sigma_z)$. Concurrence is a measure of the similarity of a state and its "spin-flipped" counterpart. If a state is orthogonal to its "spin-flipped" state then it is separable. On the other hand, maximally entangled states are invariant under the "spin-flipping" operator.

For mixed states, concurrence is extended by convex roof extension.

Proposition 2.2.12 ([92–94] Concurrence (two-qubit mixed states))**.** Let ρ be a two-qubit state. Its concurrence is

$$\mathcal{E}_{\text{con}}(\rho) = \inf_{\{p_i, |\psi_i\rangle\}} \left\{ \sum_i p_i \mathcal{E}_{\text{con}}(|\psi_i\rangle) : \rho = \sum_i p_i |\psi_i\rangle\langle\psi_i| \right\}. \tag{2.43}$$

It is equivalent to

$$\mathcal{E}_{\text{con}}(\rho) = \max\{0, \sqrt{\lambda_1} - \sqrt{\lambda_2} - \sqrt{\lambda_3} - \sqrt{\lambda_4}\} \tag{2.44}$$

with $\{\lambda_i\}_i$ being the eigenvalues of the matrix $\rho\tilde{\rho}$, where $\tilde{\rho} = \sigma_y \otimes \sigma_y \rho^* \sigma_y \otimes \sigma_y$ is the "spin-flipped" state of ρ.

Since $\mathcal{E}_F(\rho)$ is monotonically increasing with respect to the concurrence $\mathcal{E}_{\text{con}}(\rho)$, concurrence $\mathcal{E}_{\text{con}}$ is an entanglement measure itself. In 2-qubit systems, the exact value of the entanglement of formation is directly related to the concurrence [93].

Proposition 2.2.13 ([92–94] Concurrence and entanglement of formation)**.** The entanglement of formation of a two-qubit state ρ can be given by its concurrence, i.e.

$$\mathcal{E}_F(\rho) = h\left(\frac{1+\sqrt{1-\mathcal{E}_{\text{con}}(\rho)^2}}{2}\right) \tag{2.45}$$

with

$$h(x) = -x\log_2 x - (1-x)\log_2(1-x) \tag{2.46}$$

being the binary Shannon entropy of the probability distribution of $\{p_1 = x, p_2 = 1-x\}$.

In the general case, entanglement of formation is lower bounded by the expression of concurrence on the right hand side of Eq. (2.45).

***I*-concurrence** The concurrence can be extended from 2-qubit systems to more general states with different approaches [95,96]. One of these approaches is called *"universal state inversion"* [96], in which Rungta *et al.* extended the "spin-flipping" operator to the "universal state inversion" superoperator I, i.e.

$$\mathcal{I}(\rho) = \mathbb{1} - \rho. \tag{2.47}$$

Then they defined the *I-concurrence* for pure states as follows.

Definition 2.2.14 ([96] I-concurrence)**.** The *I-concurrence* of a pure state $|\psi\rangle$ is

$$\begin{aligned}\mathcal{E}_{\mathcal{I}}(|\psi\rangle) &= \sqrt{\text{tr}(|\psi\rangle\langle\psi|\ \ [\mathcal{I}\otimes\mathcal{I}](|\psi\rangle\langle\psi|))} \\ &= \sqrt{2\,(1-\text{tr}\rho_A^2)},\end{aligned} \tag{2.48}$$

where $\rho_A = \text{tr}_B(|\psi\rangle\langle\psi|)$ is the reduced state of $|\psi\rangle$ on the subsystem A. For mixed states, *I-concurrence* is defined by convex roof extension, i.e.

$$\mathcal{E}_{\mathcal{I}}(\rho) = \inf_{\{p_i,|\psi_i\rangle\}}\left\{\sum_i p_i\mathcal{E}_{\mathcal{I}}(|\psi_i\rangle) : \rho = \sum_i p_i\,|\psi_i\rangle\langle\psi_i|\right\}. \tag{2.49}$$

Note that in general, I-concurrence is not related to entanglement of formation.

2.2.5 Negativity

The *Negativity* [97] is an entanglement measure related to the PPT criterion 2.1.5. It is the sum of the negative eigenvalues of the partial transpose of states, i.e.

$$\mathcal{N}(\rho) = -\sum_{\lambda_-<0}\lambda_- \tag{2.50}$$

where λ_- are the negative eigenvalues of ρ^Γ. Mathematically it is defined by the trace norm.

Definition 2.2.15 ([97] Negativity)**.** The *negativity* of a state ρ is

$$\mathcal{N}(\rho) = \frac{\left\|\rho^\Gamma\right\|_1 - 1}{2}, \tag{2.51}$$

where $\|\rho\|_1 = \mathrm{tr}(\sqrt{\rho^\dagger \rho})$ is the trace norm and ρ^Γ is the partial transpose of ρ.

The negativity is computable and convex. However, it is not additive, since $\|\rho_1 \otimes \rho_2\|_1 = \|\rho_1\|_1 \|\rho_2\|_1$. It can be rescaled by logarithm, such that it admits additivity.

Definition 2.2.16 ([97] Logarithmic negativity)**.** The *logarithmic negativity* of a state ρ is

$$\mathcal{E}_{\mathcal{N}}(\rho) = \log_2 \left\|\rho^\Gamma\right\|_1 . \tag{2.52}$$

Although the logarithmic negativity is additive, it is not convex due to the concavity of logarithms. Note that it is lower bounded by distillable entanglement, i.e. $\mathcal{E}_D(\rho) \leq \mathcal{E}_{\mathcal{N}}(\rho)$. Neither negativity nor logarithmic negativity is tight on separable states, as they both vanish for bound entangled states.

2.2.6 Witnessed entanglement

It is clear that any quantity lower bounding an entanglement measure detects entanglement, if it is positive. Conversely, one can construct an entanglement measure from a *compact* set of entanglement witnesses $\mathcal{W}$ according to the theory in [98, 99]. Such an entanglement measure is called *witnessed entanglement*, which is defined as follows.

Definition 2.2.17 ([98, 99] Witnessed entanglement)**.** Let $\mathcal{W}$ be a *compact* set of entanglement witnesses. The following quantity is called the *$\mathcal{W}$-witnessed entanglement* of ρ.

$$\mathcal{E}_{\mathcal{W}}(\rho) = \max\{0, -\min_{W \in \mathcal{W}} \mathrm{tr}(W\rho)\} \tag{2.53}$$

It is shown that any *$\mathcal{W}$-witnessed entanglement* $\mathcal{E}_{\mathcal{W}}$ is

- LOCC-monotonic,
- vanishing for separable states, and
- convex.

If $\mathcal{W}_{\mathrm{all}}$ contains all the entanglement witnesses, then $\mathcal{E}_{\mathcal{W}_{\mathrm{all}}}$ is also tight on separable states, i.e. $\mathcal{E}_{\mathcal{W}_{\mathrm{all}}}(\rho) = 0$ if and only if ρ is separable. For example, negativity is witnessed by $\mathcal{W}_{\mathrm{decomp}}$, which is the set of decomposable witnesses, i.e.

$$\mathcal{E}_{\mathcal{W}_{\mathrm{decomp}}} = \mathcal{N}. \tag{2.54}$$

2.2.7 Summary of entanglement measures

Here we summarize and give an overview of all the entanglement measures reviewed in this chapter. Different from other scalar physical measures, e.g. length, temperature, energy, etc., the measures of entanglement are not unique. Most of them are not even comparable with each other, i.e. they have different orderings under LOCC. Moreover, although the LOCC transformation $\rho_2 = \Lambda(\rho_1)$ implies the ordering of the states with respect to an entanglement measure, i.e. $\mathcal{E}(\rho_1) \geq \mathcal{E}(\rho_2)$, conversely, this entanglement measure ordering in general does not imply the existence of a LOCC transformation from ρ_1 to ρ_2. E.g. let $\mathcal{E}_a$ and $\mathcal{E}_b$ be two entanglement measures, and $\rho_1 = \Lambda_1(\rho)$

and $\rho_2 = \Lambda_2(\rho)$ be two resulting states of ρ under the LOCCs Λ_1 and Λ_2, respectively. Assume that $\mathcal{E}_a(\rho_1) \geq \mathcal{E}_a(\rho_2)$, then one has

$$\mathcal{E}_a(\rho) \geq \mathcal{E}_a(\rho_1) \geq \mathcal{E}_a(\rho_2). \tag{2.55}$$

Since it is possible that there exist no LOCC transformations from ρ_1 to ρ_2, ρ_1 and ρ_2 can admit a different ordering with respect to the entanglement measure $\mathcal{E}_b$, i.e.,

$$\mathcal{E}_b(\rho) \geq \mathcal{E}_b(\rho_2) \geq \mathcal{E}_b(\rho_1).$$

Therefore there must be certain profound insights on the quantification of entanglement, that might enhance a unique entanglement ordering, which are still not well understood.

Nevertheless, several relations between these measures have been shown. *First*, the distillable entanglement $\mathcal{E}_D$ and the entanglement of formation $\mathcal{E}_F$ are both identical to the entropy of entanglement S_{ent} for pure states, i.e.

$$\mathcal{E}_D(|\psi\rangle) = S_{ent}(|\psi\rangle) = \mathcal{E}_F(|\psi\rangle). \tag{2.56}$$

For mixed states, the distillable entanglement $\mathcal{E}_D$ is upper bounded by the entanglement of formation $\mathcal{E}_F$ and the logarithmic negativity $\mathcal{E}_{\mathcal{N}}$, i.e.

$$\mathcal{E}_D(\rho) \leq \mathcal{E}_F(\rho) \text{ and } \mathcal{E}_D(\rho) \leq \mathcal{E}_{\mathcal{N}}(\rho). \tag{2.57}$$

Second, the entanglement of formation can be expressed through the (I-)concurrence for two-qubit states, i.e.

$$\mathcal{E}_F(\rho) = \mathcal{E}_{\mathcal{I}}(\rho) \text{ for all } \rho \in B(\mathbb{H}_2 \otimes \mathbb{H}_2). \tag{2.58}$$

The entanglement measures reviewed in this chapter fulfill different axioms. We compare them in Table 2.2.

	Entanglement measure	Tightness	Additivity	Convexity
Entropy of entanglement S_{ent}	× (*)	×	✓	concave
Negativity $\mathcal{N}$	✓	×	×	✓
Logarithmic negativity $\mathcal{E}_{\mathcal{N}}$	✓	×	✓	×
Distillable entanglement $\mathcal{E}_D$	✓	×	(†)	(†)
Concurrence $\mathcal{E}_{\text{con}}$	✓	—	—	✓
Entanglement of formation $\mathcal{E}_F$	✓	✓	(‡)	✓
Witnessed entanglement $\mathcal{E}_{\mathcal{W}}$	✓	(§)	—	✓

Table 2.2: Comparison of different entanglement measures: The "tightness" of an entanglement measure $\mathcal{E}$ indicates whether $\mathcal{E}(\sigma) = 0$ only for separable states σ. (*) Entropy of entanglement is only an entanglement measure for pure states. (†) Distillable entanglement is not additive or convex, if there exist NPT bound entangled states [100], which is still an open question. (‡) Entanglement of formation is additive for pure states, but for mixed states its additivity is still an open question [94]. (§) $\mathcal{E}_{\mathcal{W}}$ is tight, if $\mathcal{W}$ contains all possible entanglement witnesses.

3. Entanglement in multipartite quantum systems

The study of multipartite entanglement started with the GHZ state, which was introduced by Greenberger, Horne and Zeilinger in 1989 [41]. The original GHZ state was given as

$$|\mathrm{GHZ}_4\rangle = \frac{1}{\sqrt{2}}(|0011\rangle - |1100\rangle). \tag{3.1}$$

It was proposed for constructing quantum systems for Bell tests. They showed that no LHV model can reproduce the quantum predictions for this state in certain measurement settings. Later in [101], Greenberger, Horne, Shimony and Zeilinger also proposed a gedankenexperiment for Bell's theorem in 3-qubit systems.

$$|\mathrm{GHZ}_3\rangle = \frac{1}{\sqrt{2}}(|000\rangle + |111\rangle). \tag{3.2}$$

This GHZ state can be generalized to n-partite systems.

Definition 3.0.18 (GHZ states)**.** An n-partite GHZ state $|\mathrm{GHZ}_n\rangle$ is equivalent to the following state up to local unitaries,

$$|\mathrm{GHZ}_n\rangle \overset{LU}{=} \frac{1}{\sqrt{2}}(|0_1 \cdots 0_n\rangle + |1_1 \cdots 1_n\rangle). \tag{3.3}$$

Compared with bipartite entanglement, multipartite entanglement is richer in its structure for various quantum information applications. For instance, GHZ states can be employed for quantum secret sharing [42], W-states [43] for quantum memories [44], graph states [45] for measurement based quantum computation (MBQC) [46], hypergraph states [102, 103] for Deutsch-Josza algorithm [29], and so on. In this chapter, we will present a brief review of the characterization of multipartite entanglement, including its classification, detection and quantification.

3.1 Classification of multipartite entanglement

Multipartite entanglement is richer than bipartite entanglement regarding its classification under SLOCC. The simplest multipartite system is the tripartite system $\rho \in \mathcal{B}(\mathbb{H}_A \times \mathbb{H}_B \times \mathbb{H}_C)$. A state can be $A|BC$-separable, but $B|C$-entangled, e.g. $|\psi\rangle = |0_A\rangle \otimes (|0_B 0_C\rangle + |1_B 1_C\rangle)/\sqrt{2}$. The state $|\psi\rangle$ is *biseparable* with respect to the subsystem split $A|BC$. Meanwhile it is also 2-*particle entangled* in the subsystem BC. A state can be also $A|B|C$-separable $|\psi\rangle$, which is then a product state, e.g. $|\psi\rangle = |0_A\rangle\,|0_B\rangle\,(|0_C\rangle + |1_C\rangle)/\sqrt{2}$. In this case, $|\psi\rangle$ is 3-*separable* containing no entanglement, and hence *fully separable*.

We adopt the notion of "biseparability" in [47][1]. A tripartite state ρ is *biseparable*, if it can be written as a convex combination of biseparable states, i.e.

$$\rho = c_1\rho_{A|BC} + c_2\rho_{B|AC} + c_3\rho_{C|AB}, \tag{3.4}$$

where $\rho_{A|BC}$, $\rho_{B|AC}$ and $\rho_{C|AB}$ are biseparable with respect to the bipartitions $A|BC$, $B|AC$ and $C|AB$, respectively. If a state is not *biseparable* then it is *genuinely multipartite (GM) entangled* (see Fig. 3.1). Contrary to the case of bipartite states, where all entangled states can be either

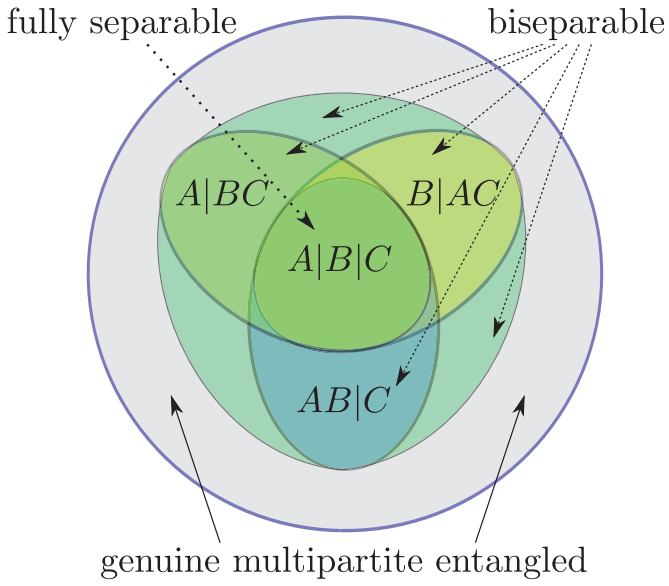

Figure 3.1: Genuine multipartite entanglement in tripartite states

distilled via LOCC or transformed via SLOCC to Bell states, tripartite GM-entangled states fall into two different classes under SLOCC [43]. The first class is the GHZ-class, which is the set of tripartite GM-entangled states that can be transformed via SLOCC to the GHZ state (Def. 3.0.18). The second class is the W-class, which is the set of tripartite GM-entangled states that can be transformed via SLOCC to the W-state, i.e.

$$|W_3\rangle = \frac{1}{\sqrt{3}}(|001\rangle + |010\rangle + |100\rangle). \tag{3.5}$$

In general, an n-partite W-state is defined as

$$|W_n\rangle = \frac{1}{\sqrt{n}}(|0_1\cdots 0_{n-1}1_n\rangle + \cdots + |0\cdots 01_i0\cdots 0\rangle + \cdots + |1_10_2\cdots 0_n\rangle). \tag{3.6}$$

Entanglement of multipartite states can only be ordered within the same class under LOCC. The maximally entangled GHZ-type state is $|GHZ\rangle$, while maximally entangled W-type state is $|W\rangle$. However there is no unified maximally tripartite GM-entangled state for the both GHZ-class and W-class.

Since the theory of multipartite entanglement is still in development, many mathematical defi-

[1]Some authors adopt the notion of "biseparability" only with repect to a fixed split.

nitions related to this notion do not agree among different authors. Here we adopt the definitions of separability, producibility and entanglement in [47, 104] to classify multipartite entanglement.

3.1.1 Multipartite separability and genuine multipartite entanglement

We first extend biseparability to *P-separability*, with P being a multi-partition of the particles in a quantum system.

Definition 3.1.1 (P-separability)**.** Let $\rho \in B(\mathbb{H}_1 \otimes \mathbb{H}_2 \cdots \otimes \mathbb{H}_n)$ be a state in an n-particle system, and $P = (\pi_1|...|\pi_m)$ be a partition of these n-particles, with π_i being disjoint and $\bigcup_{i=1}^{m} \pi_i = \{1, ..., n\}$. The state ρ is *P-separable* if it can be written as

$$\rho = \sum_j p_j \left|\psi_j\right\rangle \left\langle\psi_j\right|, \tag{3.7}$$

where $|\psi_j\rangle$ can be factorized into

$$|\psi_j\rangle = |\phi_j^{(\pi_1)}\rangle \otimes \cdots \otimes |\phi_j^{(\pi_m)}\rangle \tag{3.8}$$

with $|\phi_j^{(\pi_i)}\rangle$ being a state on the Hilbert space $\mathbb{H}^{(\pi_i)}$ of the subsystem π_i. If ρ is not *P-separable*, then it is *P-entangled*.

The partition P can be decomposed into m bipartitions, i.e.

$$P = \Pi_1 \wedge \cdots \wedge \Pi_m, \tag{3.9}$$

with $\Pi_i := (\pi_i|\bigcup_{j\neq i} \pi_j)$ being a bipartition. The wedge operation "$\wedge$" of two partitions is the combination of two splits, e.g. $(A|BC) \wedge (AB|C) = (A|B|C)$. Hence, P-entanglement can be detected and quantified via the analysis of Π_i-entanglement with the criteria, witnesses and measures for bipartite entanglement given in section 2.1 and 2.2.

Let $\mathbb{P}_n^{(l)} = \{P_i^{(l)}\}_i$ be the set of all l-partitions of an n particle system, e.g.

$$\mathbb{P}_4^{(2)} = \{(1|234), (2|134), (3|124), (4|123), (12|34), (13|24)\}. \tag{3.10}$$

The set of all $P_i^{(l)}$-separable states is not convex, since e.g. the convex combination

$$\frac{1}{2}\left|0\right\rangle\left\langle 0\right|_{\{1\}} \otimes \left|\mathrm{GHZ}_3\right\rangle\left\langle \mathrm{GHZ}_3\right|_{\{2,3,4\}} + \frac{1}{2}\left|\mathrm{GHZ}_3\right\rangle\left\langle \mathrm{GHZ}_3\right|_{\{1,2,3\}} \otimes \left|0\right\rangle\left\langle 0\right|_{\{4\}} \tag{3.11}$$

is neither $(1|234)$-separable nor $(123|4)$-separable. $P^{(l)}$-separability is extended to so-called *l-(partite-)separability* via including the convex hull of $P_i^{(l)}$-separable states, instead of considering a fixed partition.

Definition 3.1.2 (L-partite separability and genuine l-partite entanglement)**.** A state $\rho \in B(\mathbb{H}_1 \otimes \mathbb{H}_2 \cdots \otimes \mathbb{H}_n)$ is *l-(partite-)separable* ($l < n$), if there exists a set of partitions,

$$\mathbb{P}^{(\geq l)} = \{P_i : P_i \text{ is } k\text{-partition of } \{1, ..., n\} \text{ with } k \geq l\}_i, \tag{3.12}$$

whose elements contain at least l-parties, such that ρ can be decomposed into a convex combination of the P_i-separable states ρ_{P_i}.

$$\rho = \sum_i p_i \rho_{P_i}. \tag{3.13}$$

If ρ is not l-partite separable, then it is *genuinely l-partite entangled*. A *genuinely bipartite entangled* state is *genuinely multipartite (GM) entangled*.

Fig. 3.2 illustrates the relation between the different degrees of multipartite separability. An n-partite separable state is *fully separable*. The set of l-separable states is definitionally convex (Eq. (3.13)). Since an l-partition can be considered as an $(l-1)$-partition, an l-separable state is then certainly $(l-1)$-separable. The maximum number of particles in a single party of an n-particle l-separable state $\rho_n^{(l)}$ is $n-l+1$. Therefore, the l-separability of $\rho_n^{(l)}$ indicates that its can be created in l number of independent parties (subsystems), which consists of $n-l+1$ particles.

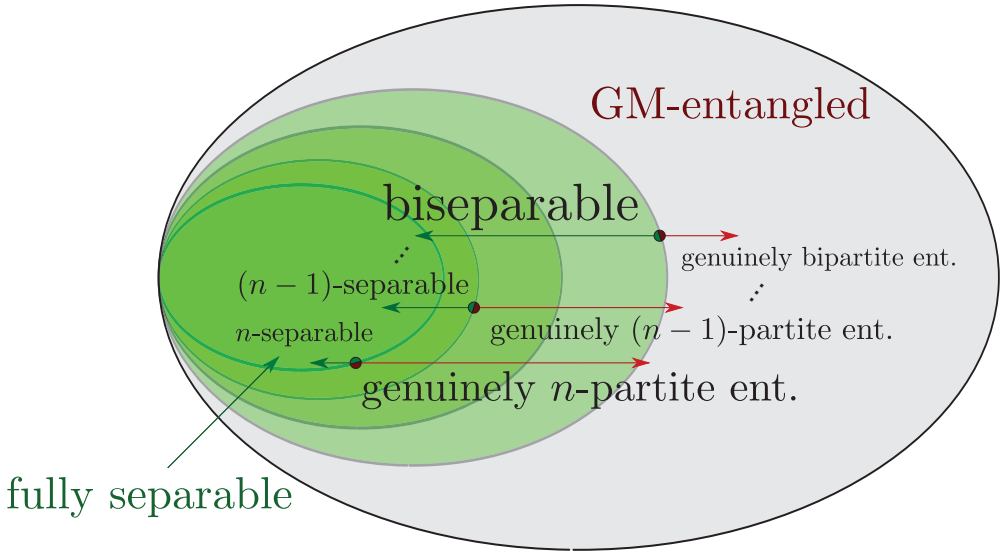

Figure 3.2: L-partite separability and genuine l-partite entanglement: The length of the arrows indicates the domain of l-separability (green arrows) and genuine l-partite entanglement (red arrows), as well as the font-sizes of the texts(the area covered by the texts of a class is the domain of this class).

3.1.2 Multi-particle producibility and multi-particle entanglement

Although l-partite separability determines the requirements on the number and dimension of independent parties for state creation, the degree of entanglement in each party is also an important information, which is not directly involved in l-partite separability. Therefore Gühne *et al.* introduced the *multi-particle producibility* to describe the requirements on the entangling capacity of quantum apparatuses in multipartite entanglement creation [104]. The minimum entangling capacity requirement of quantum apparata is given by the *k-(particle-)entanglement*[2], which is defined as follows.

Definition 3.1.3 ([104] Multi-particle producibility and multi-particle entanglement)**.** A pure state $|\psi\rangle$ is *producible with k-partite GM entangled states*, shortly *k-producible*, if it can be written

[2]In order to distinguish from l-partite separability (Def. 3.1.2, we exploit the nomenclature "k-(particle-)entanglement" instead of "k-(party-)entanglement", which is used in [104])

as the tensor product of states with maximally k particles, i.e.

$$|\psi\rangle = |\phi_1\rangle \otimes \cdots \otimes |\phi_m\rangle\,, \tag{3.14}$$

with $|\phi_i\rangle \in \mathbb{H}^{\otimes k_i}$ and $k_i \leq k$ for all $i \in \{1, ..., m\}$. A mixed state ρ is *k-producible*, if it can be decomposed as a convex combination of *k-producible* pure states. A state is k-(particle-)entangled, if it is not $(k-1)$-producible.

Note that k-particle entanglement is a different concept from l-partite GM entanglement (Def. 3.1.2). If a state is k-producible, then it is $(k+1)$-producible. The k-producibility of a state ρ provides a sufficient requirement on the creation of rho, which indicates that the available quantum entangling apparata should at least be able to generate k-particle GME. Conversely, if a state is k-particle entangled, then it is $(k-1)$-particle entangled. The k-particle entanglement of ρ indicates that the creation of ρ requires necessarily the quantum entangling apparata to generate k-particle GME. A 1-producible state is *fully separable*, while an n-particle entangled state is *GM entangled*. The relation between multi-particle producibility and entanglement are shown in Fig. 3.3.

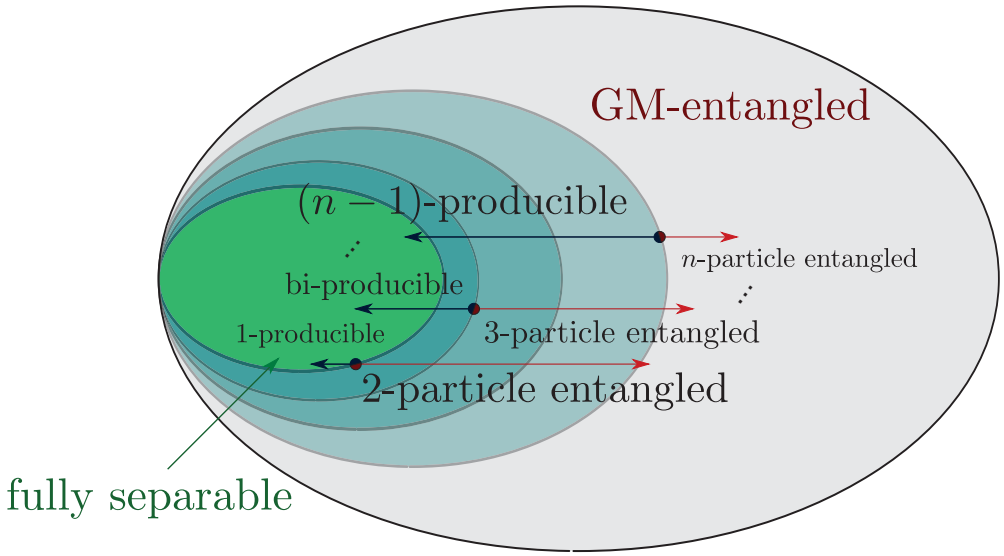

Figure 3.3: Multi-particle producibility and entanglement: The length of the arrows indicates the domain of k-producibility (blue arrows) and k-particle entanglement (red arrows), as well as the font-sizes of the texts (the area covered by the texts of a class is the domain of this class).

For 3-particle states, l-partite separability is identical to $(4-l)$-producibility, while genuine k-partite entanglement is identical to $(5-k)$-particle entanglement. In general, l-partite separability and genuine l-partite entanglement are not directly related to k-producibility and k-particle entanglement. They have different classifications, except two extremum classes, namely full separability and GME:

- n-partite separability is identical to 1-producibility, which is full separability;
- genuine bipartite entanglement is identical to n-particle entanglement, which is GME.

3.2 Detection and quantification of genuine multipartite entanglement

In this section, we will focus on the detection and quantification of genuine multipartite entanglement. Three approaches will be given, which are projector witnesses [47, 48], the PPT-mixer (extension of negativity) [49, 98, 99] and our result [50] on GM I-concurrence [105].

3.2.1 Projector witness

Starting from the range criterion [17], Lewenstein *et al.* proposed an approach to obtain an optimal entanglement witness from the so-called "edge" states [22, 106]. The "edge" states δ_K of an entanglement class K (e.g. PPT-, W- and GHZ-class) lie on the boundary of the set of the states in this class. The witness derived from this approach can be generally expressed in the following *canonical* form,

$$P + Q^{\Gamma} - \epsilon(\delta_K)\mathbb{1}, \tag{3.15}$$

where $\epsilon(\delta_K) \geq 0$ depends on the selected edge state δ_K. From this general approach, Acin, Bruß and Sanpera derived witnesses for detecting GHZ-type and W-type entanglement of tripartite states [47]. The witness for GHZ-entanglement is

$$W_{\mathrm{GHZ}} = \frac{3}{4}\mathbb{1} - |\mathrm{GHZ}\rangle\langle\mathrm{GHZ}|, \tag{3.16}$$

while for W-entanglement, we have

$$W_{W_1} = \frac{2}{3}\mathbb{1} - |\mathrm{W}\rangle\langle\mathrm{W}| \tag{3.17}$$

and

$$W_{W_2} = \frac{1}{2}\mathbb{1} - |\mathrm{GHZ}\rangle\langle\mathrm{GHZ}|. \tag{3.18}$$

Each of these three witnesses is an GME witness for 3-qubit systems. Let $|\psi_{\mathrm{GME}}\rangle$ be a GM-entangled state. In general, one can construct a GME witness for detecting the GM entangled states close to $|\psi_{\mathrm{GME}}\rangle$ via the extension of Proposition 2.1.10. Such witnesses are introduced in [48] as follows

Proposition 3.2.1 ([48] GME-projector witness)**.** From a GM entangled state $|\psi_{\mathrm{GME}}\rangle$, one can construct a GME witness

$$W_{\psi_{\mathrm{GME}}} = c\mathbb{1} - |\psi_{\mathrm{GME}}\rangle\langle\psi_{\mathrm{GME}}| \tag{3.19}$$

where

$$c = \max_{|\phi\rangle \text{ bisep.}} |\langle\phi\,|\,\psi_{\mathrm{GME}}\rangle|^2. \tag{3.20}$$

3.2.2 Fully decomposable witnesses and PPT-mixer measure

As an extension of decomposable witnesses (Def. 2.1.9), Jungnitsch, Moroder and Gühne introduced the so-called *fully decomposable witnesses*, which are defined as follows.

Definition 3.2.2 ([49] Fully decomposable witness)**.** An entanglement witness operator W is *fully decomposable*, if it can be decomposed into two positive operators $P_\gamma \geq 0$ and $Q_\gamma \geq 0$ for all bipartitions $\gamma|\bar{\gamma}$, such that

$$W = P_\gamma + Q_\gamma^{\Gamma_\gamma}, \tag{3.21}$$

with $\mathrm{tr}(W) = 1$ and Γ_γ being the partial transpose regarding the bipartition $\gamma|\bar{\gamma}$.

A biseparable state can be generally expressed as $\rho_{\mathrm{bi}} = \sum_\gamma p_\gamma |\psi_\gamma\rangle \langle\psi_\gamma|$ (Def. 3.1.2), where $|\psi_\gamma\rangle$ is $\gamma|\bar{\gamma}$-separable (Def. 3.1.1). Therefore the action of a fully decomposable witness on a biseparable state is

$$W\rho_{\mathrm{bi}} = \sum_\gamma p_\gamma \left[\left(P_\gamma + Q_\gamma^{\Gamma_\gamma} \right) |\psi_\gamma\rangle \langle\psi_\gamma| \right]. \tag{3.22}$$

Since $\langle\psi_\gamma| P_\gamma + Q_\gamma^{\Gamma_\gamma} |\psi_\gamma\rangle \geq 0$ for all γ, $\mathrm{tr}(W\rho_{\mathrm{bi}}) \geq 0$ for all biseparable states ρ_{bi}. A violation of the inequality $\mathrm{tr}(W\rho) \geq 0$ indicates therefore that ρ is GM-entangled. Hence, a fully decomposable witness is a GME witness.

One can extend the notion of witnessed entanglement (Def. 2.2.17) to construct a GME measure via the set of fully decomposable witnesses. As with the example in Eq. (2.54), negativity is identical to the $\mathcal{W}_{\mathrm{decomp}}$-witnessed entanglement, where $\mathcal{W}_{\mathrm{decomp}}$ is the set of decomposable witnesses. Analogously, since the set of all fully decomposable witnesses $\mathcal{W}_{\mathrm{fully}}$ is compact, one can construct a $\mathcal{W}_{\mathrm{fully}}$-witnessed entanglement measure as follows.

Definition 3.2.3 ([49] PPT-mixer measure)**.** The *PPT-mixer measure* is defined as the $\mathcal{W}_{\mathrm{fully}}$-witnessed entanglement, i.e.

$$\mathcal{E}_{\mathrm{pptmixer}}(\rho) = \max \left\{ 0, - \min_{W \text{ fully decomp.}} \mathrm{tr}(W\rho) \right\}. \tag{3.23}$$

The $\mathcal{E}_{\mathrm{pptmixer}}$ is a GME measure, which is numerically computable with semi-definite programs by virtue of the decomposability of its constructing witnesses. Since decomposable witnesses characterize the set of PPT states and detect the NPT entangled states, the set of fully decomposable witnesses can only characterize the states that are mixtures of PPT states, which are called *PPT-mixture* (see Fig. 3.4). Hence, the measure $\mathcal{E}_{\mathrm{pptmixer}}$ derived from fully decomposable witnesses is only tight on the set of PPT-mixture, i.e. it is zero for PPT-entangled states.

3.2.3 (Result) Lower bounds on genuine multipartite I-concurrence

In this section, we will briefly summarize the result in [50], which is attached in Appendix A. In [50], an incomputable GME measure [105] $\mathcal{E}_{\mathcal{I}}^{\mathrm{GM}}$, which is derived from the I-concurrence (Def. 2.2.14), is lower bounded by a quantity Q, which is determined by the off-diagonal elements of a density matrix. This lower bound is computable and experimentally feasible. Note that a positive value of Q indicates the presence of GME.

The I-concurrence (Def. 2.2.14) was extended for GME in [105]. There, a GME measure for pure states is defined as

$$\mathcal{E}_{\mathcal{I}}^{\mathrm{GM}}(|\psi\rangle\langle\psi|) := \min_{\gamma \subseteq \{1,\ldots,n\}} \sqrt{S_L\left(\rho_\gamma\right)} = \min_{\gamma \subseteq \{1,\ldots,n\}} \sqrt{2\left(1 - \mathrm{tr}(\rho_\gamma^2)\right)}, \tag{3.24}$$

where $S_L\left(\rho_\gamma\right)$ is the linear entropy of the γ-reduced density matrix of ρ, i.e. $\rho_\gamma := \mathrm{tr}_{\bar{\gamma}}(|\psi\rangle\langle\psi|)$. The minimum is taken over all possible subsystems $\gamma \subseteq \{1, ..., n\}$, which corresponds to the bipartition $\gamma|\bar{\gamma}$ with $\bar{\gamma}$ being the complement of γ in $\{1, ..., n\}$. A general GME measure for mixed states is then obtained via convex roof extension (Proposition 2.2.10), i.e.

$$\mathcal{E}_{\mathcal{I}}^{\mathrm{GM}}(\rho) := \inf_{\{p_i, |\psi_i\rangle\}} \sum_i p_i \mathcal{E}_{\mathcal{I}}^{\mathrm{GM}}(|\psi_i\rangle\langle\psi_i|), \tag{3.25}$$

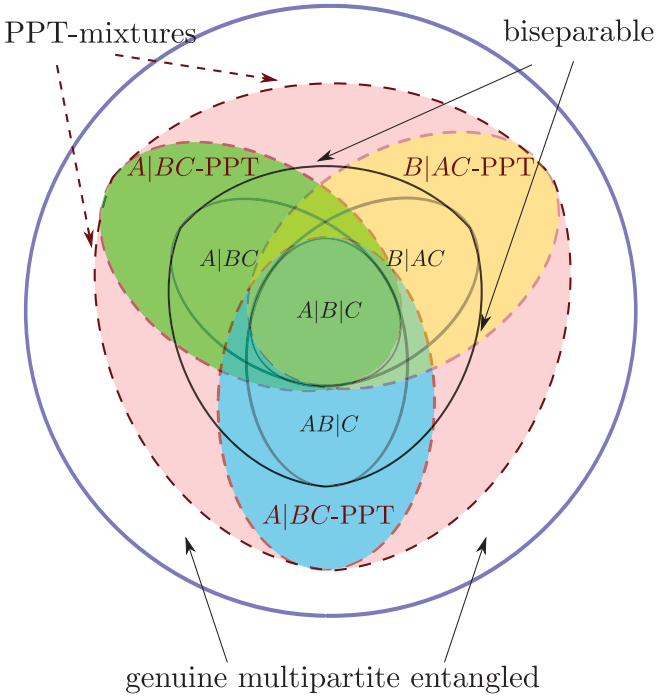

Figure 3.4: Fully decomposable witnesses and PPT-mixtures

where the infimum is taken over all possible decompositions of $\rho = \sum_i p_i |\psi_i\rangle \langle\psi_i|$. This GME measure is, however, not computable due to the infinite number of possible decompositions. To address this, we derived a calculable lower bound, which is also experimentally feasible with small numbers of local measurements, to estimate the GM I-concurrence.

For derivation of the lower bound, a γ-permutation operation on binary numbers is needed,

$$P_\gamma(i,j) = \left(i_\gamma^{[j]}, j_\gamma^{[i]}\right), \tag{3.26}$$

where $i_\gamma^{[j]}$ is the number i with its digits corresponding to the indices in the party γ replaced by the digits of j. E.g. $01213_{\{1,3\}}^{[30121]} = 31113$ and $30121_{\{1,3\}}^{[01213]} = 00221$,

$$P_{\{1,3\}}(01213, 30121) = (31113, 00221). \tag{3.27}$$

The entry $\rho_{(i,j)}$ of a density matrix $\rho \in B(\mathbb{H}_d^n)$ can be indexed by the row-column index pair (i,j) with $i,j \in \{0,1\}^{\otimes n}$. Under the γ-permutation operation, the row-column index pairs of a matrix are divided into different classes,

$$J_c := \{P_\gamma(0_1 \cdots 0_n, c) : \gamma \subseteq \{1,...,n\}\}. \tag{3.28}$$

E.g. in 3-qubit systems, $J_{011} = \{(000,011),(011,000),(001,010),(010,001)\}$ indexes the set of off-diagonal entries, $\{\rho_{000,011}, \rho_{011,000}, \rho_{001,010}, \rho_{010,001}\}$. Now one can select a set of index pairs $\mathcal{R}$ from different classes (maximally one pair for each class) to derive a lower bound on $\mathcal{E}_I^{\mathrm{GM}}$ via the following theorem.

Theorem 3.2.4 (Lower bound on genuine multipartite I-concurrence)**.** Let ρ be an n-qudit state. A set of matrix index pairs $\mathcal{R}$ is selected with $(i,j) \neq P_\gamma(i',j')$ for all $(i,j) \neq (i',j') \in \mathcal{R}$ and all $\gamma \subseteq \{1,...,n\}$. The genuine multipartite entanglement measure $\mathcal{E}_I^{\mathrm{GM}}$ has the following lower bound $Q_{\mathcal{R}}(\rho)$:

$$Q_{\mathcal{R}}(\rho) := 2\sqrt{\frac{1}{|\mathcal{R}| - S_{\min}(\mathcal{R})}}\left[\sum_{(i,j)\in\mathcal{R}}\left(|\rho_{ij}| - \sum_{\gamma|\bar{\gamma}\in\Gamma(i,j)}\sqrt{\rho_{i^\gamma i^\gamma}\rho_{j^\gamma j^\gamma}}\right) - \left(\frac{1}{2}\sum_{i\in I_{\mathcal{R}}} S^i_{\max}(I_{\mathcal{R}})\,|\rho_{ii}|\right)\right], \tag{3.29}$$

where $\rho_{ij} := \langle i|\rho|j\rangle$, $(i^\gamma, j^\gamma) := P_\gamma(i,j)$, $\Gamma(i,j) := \{\gamma|\bar{\gamma} : (i^\gamma, j^\gamma)$ and $(i^{\bar{\gamma}}, j^{\bar{\gamma}}) \notin \mathcal{R}\}$ and $I_{\mathcal{R}} := \{i : \exists j$ that (j,i) or $(i,j) \in \mathcal{R}\}$ is the set of indices i, which appear in $\mathcal{R}$. $S_{\min}(\mathcal{R})$ is the minimal value of $|\mathcal{S}_\gamma(\mathcal{R})|$ over all possible bipartitions $\gamma|\bar{\gamma}$, where $\mathcal{S}_\gamma(\mathcal{R}) \subseteq \mathcal{R}$ is the P_γ-invariant subset of $\mathcal{R}$,

$$S_{\min}(\mathcal{R}) := \min_{\gamma\subset\{1,\ldots,n\}}\Big|\underbrace{\{(i,j)\in\mathcal{R} : (i,j) = P_\gamma(i,j) \text{ or } P_{\bar{\gamma}}(i,j)\}}_{=:\mathcal{S}_\gamma(\mathcal{R})}\Big|. \tag{3.30}$$

$S^i_{\max}(I_{\mathcal{R}})$ is the maximal value of $\left|\mathcal{S}^i_\gamma(I_{\mathcal{R}})\right|$ over all possible bipartitions $\gamma|\bar{\gamma}$, where $\mathcal{S}^i_\gamma(I_{\mathcal{R}})$ is the subset of $\mathcal{S}_\gamma(I_{\mathcal{R}})$ whose element contains the index i, .

$$S^i_{\max}(I_{\mathcal{R}}) := \max_{\gamma\subset\{1,\ldots,n\}}\Big|\underbrace{\{(j,j')\in\mathcal{S}_\gamma(\mathcal{R}) : i = j \text{ or } j'\}}_{=:\mathcal{S}^i_\gamma(I_{\mathcal{R}})}\Big|. \tag{3.31}$$

For instance, choose $\mathcal{R}_W = \{(001,010),(001,100),(010,100)\}$, one can lower bound the $\mathcal{E}_I^{\mathrm{GM}}$ by

$$\begin{aligned} Q_{\mathcal{R}_W}(\rho) = \sqrt{2}(&\rho_{001,010} - \sqrt{\rho_{000,000}\rho_{011,011}} + \rho_{001,100} - \sqrt{\rho_{000,000}\rho_{101,101}} \\ &+ \rho_{100,010} - \sqrt{\rho_{000,000}\rho_{110,110}}) - \frac{\sqrt{2}}{2}\left(\rho_{001,001} + \rho_{010,010} + \rho_{100,100}\right) \end{aligned} \tag{3.32}$$

This quantity can detect the GME of the 3-qubit W-state $|W\rangle = (|001\rangle + |010\rangle + |100\rangle)/\sqrt{3}$,

$$\mathcal{E}_I^{\mathrm{GM}}(|W\rangle\langle W|) \geq Q_{\mathcal{R}_W}(|W\rangle\langle W|) = \frac{\sqrt{2}}{2}. \tag{3.33}$$

In order to obtain an optimal lower bound, the choice of the index pairs should be tailored for different states. In most of the cases, the anti-diagonal entries contribute more strongly to the positive value of $Q_{\mathcal{R}}$ than the other entries. Principally, one chooses those off-diagonal entries $\rho_{(i,j)}$, such that the Hamming weight of $i \oplus j$ is large. In Fig. 3.5 , we highlight the good choices for $\mathcal{R}$ in green (the darker the green is, the better the choice is), while the bad ones, which have the Hamming weight $i \oplus j \leq 1$ and should never be chosen, are highlighted in khaki and red.

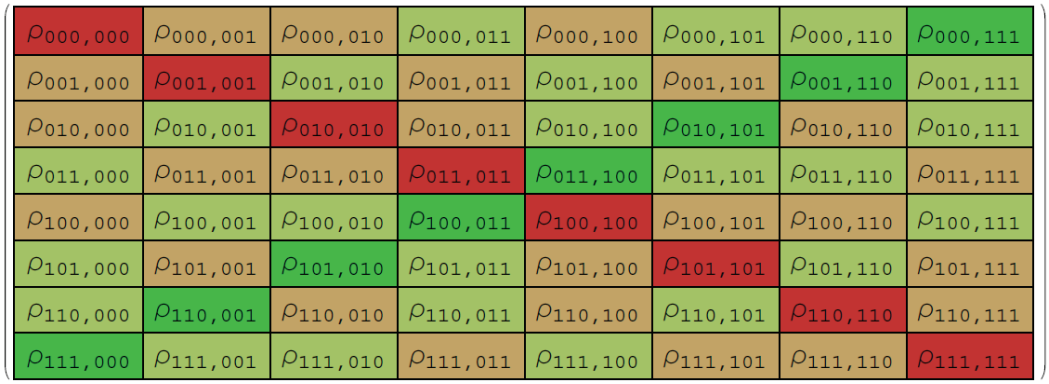

Figure 3.5: The selection of matrix index pairs: the row and column indices in index pairs of dark green entries have the Hamming distance $|i \oplus j| = 3$, while the light green entries have $|i \oplus j| = 2$, khaki entries have $|i \oplus j| = 1$, and red entries have $|i \oplus j| = 0$. The khaki and red entries are never good choices for $\mathcal{R}$ in Theorem 3.2.4.

4. Graph states: A type of entangled multipartite systems

A type of multipartite (n-qubit) entangled states called *linear cluster states*, which are derived from spin interactions in a 1D lattice, were introduced by Briegel and Raussendorf [45] in 2001. Linear cluster states is a type of graph states, which can be general represented by a mathematical 1D grid graph in graph theory (the definition of graph states will be given later). They are distinguished from the GHZ-states and W-states for multipartite systems with $n \geq 4$ with respect to two properties, which are called *persistency* and *maximal connectedness*. Explicitly, 4-qubit linear cluster states up to local unitaries can be expressed as

$$|L_4\rangle = \frac{1}{2}(|0000\rangle + |0011\rangle + |1100\rangle + |1111\rangle), \tag{4.1}$$

with $|0\rangle$ and $|1\rangle$ being computational Z-basis states[1]. Compared with GHZ-state $|\mathrm{GHZ}_4\rangle$ and the W-state $|W_4\rangle$, i.e.

$$|\mathrm{GHZ}_4\rangle = \frac{1}{\sqrt{2}}|0000\rangle + |1111\rangle, \tag{4.2}$$

$$|W_4\rangle = \frac{1}{2}(|0001\rangle + |0010\rangle + |0100\rangle + |1000\rangle), \tag{4.3}$$

one observes that the entanglement of $|L_4\rangle$ and $|W_4\rangle$ are "stronger" than the one of $|\mathrm{GHZ}_4\rangle$ against local Z-measurements. The "strength" refers to the fact that the entanglement of $|\mathrm{GHZ}_4\rangle$ can be totally destroyed with certainty via a Z-measurement on any single qubit, while under the same measurement $|L_4\rangle$ and $|W_4\rangle$ can be still entangled with non-zero probability. This robustness is quantified by the so-called *persistency*.

Definition 4.0.5 ([45] Persistency)**.** The *persistency* of a state is the minimum number of local measurements, such that the state is totally disentangled with certainty after the measurements.

The persistencies of the examples $|\mathrm{GHZ}_4\rangle$, $|L_4\rangle$ and $|W_4\rangle$ are 1, 2 and 3, respectively.

On the other hand, the entanglement of $|\mathrm{GHZ}_4\rangle$ and $|L_4\rangle$ can be localized to maximally entangled Bell states by local measurements onto any bipartite subsystem (v_1, v_2) with 100% certainty, while for $|W_4\rangle$ it is not possible. This concept is referred to as the *"entanglement localization"* [61]. The localizability of the entanglement of a state for any pair of qubits is referred to as *maximal connectedness*.

[1] A computational Z-basis state $|i_Z\rangle$ is the eigenstate of σ_Z such that $\sigma_Z |i_Z\rangle = (-1)^i |i\rangle$.

Multipartite system	Persistency	Maximal connectedness
GHZ states $\|\mathrm{GHZ}_n\rangle$	1	✓
W states $\|W_n\rangle$	$n-1$	×
Cluster states (linear) $\|L_n\rangle$	$n/2$	✓

Table 4.1: The persistency and maximal connectedness of different multipartite systems.

Definition 4.0.6 ([45] Maximal connectedness)**.** A state is called *maximally connected*, if one can project the state via local measurements into a Bell state on any pair of its qubits with certainty.

The differences between GHZ-states, W-states and cluster states regarding their persistency and maximal connectedness are shown in Table 4.1. Since cluster states possess high persistency and are maximally connected at the same time, they are the resources for measurement based quantum computation (MBQC) [46], in which one employs local measurements to consume the entanglement of the quantum system to implement universal quantum computations.

Actually, cluster states are a special type of *graph state*, which can be represented using mathematical *graphs* [52]. In this chapter, we will follow [51] to review the definition of graph states, as well as their entanglement properties in section 4.1 and 4.2, respectively. Following this, we will summarize our results, i.e. the entanglement in an error model of imperfect graph staph preparation [54] and a useful representation of graph states in X-basis [60], in section 4.3 and 4.4, respectively.

4.1 Definition

Graph theory A graph state is a quantum state, which can be represented by a mathematical graph. A mathematical *graph* $G = (V, E)$ consists of a set of n vertices V and a set of l edges E [52]. The *vertices*, $V_G = \{v_1, ..., v_n\}$, are depicted as nodes and represent individual objects like locations, particles etc. The *edges*, $E_G = \{e_1, ..., e_l\}$, are depicted as lines and describe relations between two vertices. A symmetric relation between two vertices v_1 and v_2, e.g. a two-way road between two cities, can be represented by the vertex pair $e = \{v_1, v_2\}$; such an edge is *undirected*. Let $\xi_a, \xi_b \subseteq V_G$ be two subsets of V_G. The edges between ξ_a and ξ_b are the edges $e = \{v_a, v_b\}$, which connect one vertex $v_a \in \xi_a$ and one vertex $v_b \in \xi_b$. We denote the set of these edges by $E_G(\xi_a : \xi_b)$. A vertex v_1 is a *neighbor* of v_2, if they are connected by an edge. The neighborhood of v is the set of all neighbors of v and denoted as N_v. A graph is *connected*, if for any pair of vertices $\{v, v'\}$, there exists a set of edges (called *path*) P, such that from v one can reach v' through a sequence of edges in $P = \{\{v, v_{i_1}\}, \{v_{i_1}, v_{i_2}\}, ..., \{v_{i_{m-1}}, v_{i_m}\}, \{v_{i_m}, v'\}\}$. In Table 4.2, we list the relevant types of graphs that will be considered in this chapter.

A graph F is a *subgraph* of G, if its vertices and edges are subsets of the vertex set and the edge set of G, respectively, i.e., $V_F \subseteq V_G$ and $E_F \subseteq E_G$. If $V_F = V_G$, then F is a spanning subgraph of G. Let $\xi \subseteq V_G$ be a vertex subset, then the ξ-induced subgraph of G is defined as

$$G[\xi] := (\xi, E_G(\xi : \xi)), \tag{4.4}$$

which consists of the vertex subset ξ and edges between vertices inside the set ξ.

Type of graph	Example	Definition
Empty graph $E_n^{\emptyset}$		Graphs which contain no edges.
Complete graph K_n	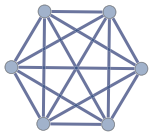	Graphs which contain all possible edges.
Star graph S_n	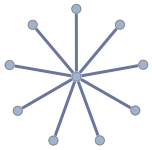	Graphs for which the center vertex has $n-1$ neighbors and all the others have the center vertex as their only neighbor.
Cycle graph C_n	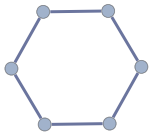	Connected graphs for which every vertex has degree 2. They are closed paths.
Grid graph $L_{m\times n}$	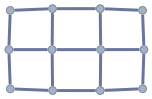	Graphs whose vertices lie on the points of a discrete two-dimensional $m\times n$ lattice and only the nearest vertices are connected by edges. They are the underlying graphs of cluster states.

Table 4.2: The graphs considered in this chapter.

A useful graph operation is the *graph symmetric difference*. Let F and G be two graphs with the same vertices V. Their *symmetric difference* is the graph $F\Delta G = (V_{F\Delta G}, E_{F\Delta G})$ with $V_{F\Delta G} = V_F = V_G$ and $E_{F\Delta G} = (E_F \cup E_G) \setminus (E_F \cap E_G)$. The *symmetric difference* between the graph G with n vertices and the complete graph K_n (the definition see Table 4.2) is called the *inversion* of G, which is denoted by $G^{-1} := K_n \Delta G$.

Definition according to entangling gates As a representation of quantum graph states, the vertices of a graph correspond to the qubits comprising a state. Initially, an empty graph[2] state with n vertices is a product state $|+\rangle^{\otimes n}$, where $|+\rangle$ is the eigenstate of σ_X with eigenvalue $+1$. The edges represent the operations of the entangling gates, which are originally derived from spin Ising-interactions with strength ϕ [45], i.e.

$$e^{-i\phi H^{\{v_1,v_2\}}} = e^{-i\phi\sigma_Z^{(v_1)}\sigma_Z^{(v_2)}}. \tag{4.5}$$

By the choice of the strength $\phi = \pi$, this operator turns into the two-qubit unitary CZ gate,

$$U_Z^{\{v_1,v_2\}} = |0_{v_1}\rangle\langle 0_{v_1}| \mathbb{1}_{v_2} + |1_{v_1}\rangle\langle 1_{v_1}| \sigma_Z^{(v_2)}. \tag{4.6}$$

[2]Definition of empty graph see Table 4.2

With these entangling gates edges can be added to or removed from a graph state. On an empty graph state, by applying $U_Z^{\{v_1,v_2\}}$ one generates an edge between v_1 and v_2. Due to the Hermitian unitarity $(U_Z^{\{v_1,v_2\}})^2 = \mathbb{1}$, applying $U_Z^{\{v_1,v_2\}}$ on a graph state, which contains already the edge $e = \{v_1, v_2\}$, will remove the edge e. Since the operators U_Z^e and $U_Z^{e'}$ commute for all e, e', no matter in which order the edges are created, the product of these two operators generates two edges e and e'. A graph state $|G\rangle$ is then defined as a state generated by a sequence of CZ-operations, which correspond to the edges of G.

Definition 4.1.1 ([45] Graph states (entangling gates))**.** The quantum state $|G\rangle$ represented by a graph G is

$$|G\rangle := (\sum_{e \in E_G} U_Z^e)\,|+\rangle^{\otimes n}\,. \tag{4.7}$$

Stabilizer formalism Besides the definition according to its preparation with entangling gates, a graph state can also be formulated as a state left invariant by a certain set of operators, the so-called stabilizers.

Definition 4.1.2 ([45] Graph state (stabilizer formalism))**.** A graph state with the vertices $\{1, ..., n\}$ is the state stabilized by a set of local pauli operators $\{g_i\}$, i.e.

$$g_i\,|G\rangle = |G\rangle\,, \tag{4.8}$$

with $g_i = \sigma_X^{(i)} \sigma_Z^{(N_i)}$, i.e. σ_X applied to the i-th vertex, and σ_Z to the vertices in N_i (the neighborhood of the i-th vertex).

These stabilizers g_i generate the whole stabilizer group $(\mathcal{S}_G, \cdot)$ of the state $|G\rangle$ with multiplication as the group operation, i.e.

$$\mathcal{S}_G = \{s_G^{(\xi)} | \xi \subseteq V_G\} \text{ with } s_G^{(\xi)} := \prod_{i \in \xi} g_i. \tag{4.9}$$

That means $s_G^{(\xi)}\,|G\rangle = |G\rangle$ for all $\xi \subseteq V_G$ and $s_G^{(\xi_1)} \cdot s_G^{(\xi_2)} \in \mathcal{S}_G$ for all $\xi_1, \xi_2 \subseteq V_G$. The stabilizer $s_G^{(\xi)}$ is called the *ξ-induced stabilizer*. Note that the sum of all stabilizers is the graph state itself,

$$|G\rangle\langle G| = \sum_{\xi \subseteq V_G} s_G^{(\xi)}. \tag{4.10}$$

This is also equal to the product of the projectors, which correspond to +1-eigenstates of the stabilizer generators

$$|G\rangle\langle G| = \prod_{i=1}^{n} \frac{\mathbb{1} + g_i}{2}. \tag{4.11}$$

4.2 Multipartite entanglement in graph states

4.2.1 Local unitary equivalence

The number of graph states with n vertices is equal to $2^{\binom{n}{2}}$. Among these graph states, there are some states which can be transformed into each other via the following local Clifford (LC) unitaries [107].

Proposition 4.2.1 ([107] LC-rule)**.** For a graph state $|G\rangle$, the local Clifford (LC) unitary

$$T_i(G) := e^{-i\frac{\pi}{4}\sigma_X^{(i)}} \bigotimes_{j\in N_i} e^{i\frac{\pi}{4}\sigma_Z^{(j)}} \propto \sqrt{g_i} \tag{4.12}$$

can locally map $|G\rangle$ to another graph state

$$T_i(G)|G\rangle = |\tau_i(G)\rangle, \tag{4.13}$$

where τ_i is a *local inversion* of G,

$$\tau_i(G) = K_{N_i}\Delta G \tag{4.14}$$

with $K_{N_i}\Delta G$ being the graph symmetric difference between G and the complete graph K_{N_i} on N_i[3]. A graph state $|G'\rangle$ is *LU-equivalent* or (*LC-equivalent*) to $|G\rangle$, if G' can be transformed from G with a sequence of local inversions, i.e.

$$G' = \left(\cdots \circ \tau_{i_k} \circ \cdots \circ \tau_{i_2} \circ \tau_{i_1}\right)(G) \tag{4.15}$$

with $i_k \in V_G$.

The set of graph states, which are LU-equivalent to each other, form a LC-class. The formation of LC-classes of connected graph states up to 4 qubits is shown in Fig. 4.1.

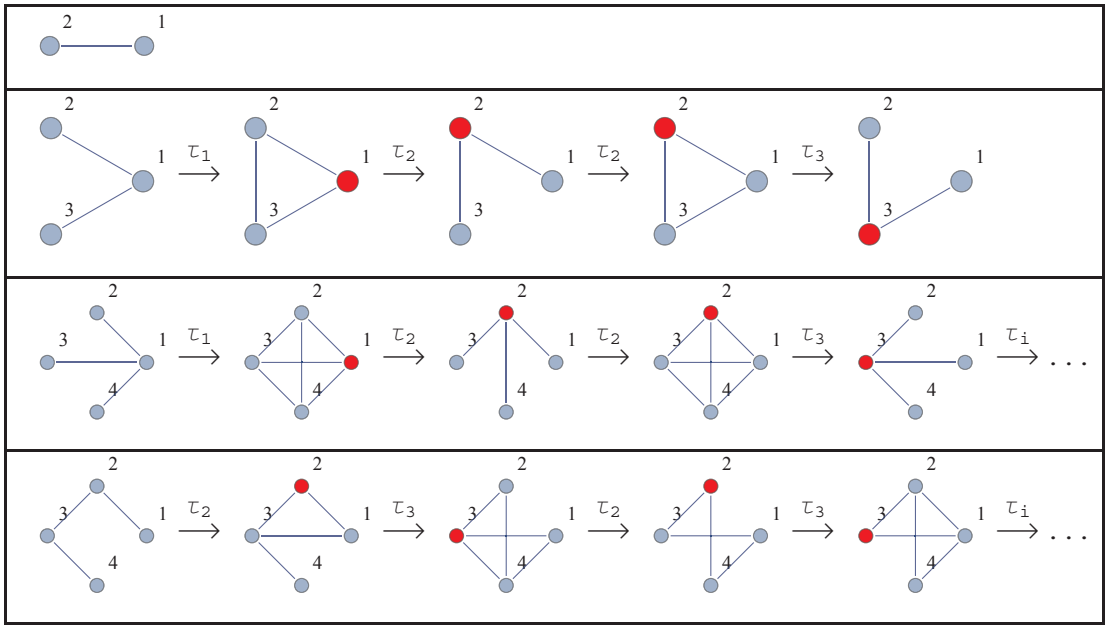

Figure 4.1: Formation of LC-classes of connected graph states: the red vertex in each graph corresponds to the index of the LC-transformation T_i applied to the preceding graph state. For the LC-classes of graph states with more than 4 vertices, please refer to [51, 107].

According to the definition of entanglement measures in Postulate 2.2.2, the entanglement

[3] $K_{N_i}\Delta G$ inverts the N_i-induced subgraph $G[N_i]$ to its complement $(G[N_i])^{-1}$.

properties of two LU-equivalent graph states are identical. Therefore, the LC-classes are also the entanglement classes of graph states. From Fig. 4.1, one observes that despite the large number of connected graph states, they have only 4 entanglement classes for systems of up to 4-qubits.

4.2.2 Multipartite entanglement detection of graph states

In [58,59], Toth and Gühne proposed a GME witness for the stabilizer states $|\psi_S\rangle$, whose stabilizers S_k are products of Pauli operators. The general form of this type of witnesses is

$$\mathcal{W}_s = c_0 \mathbb{1} - \sum_k c_k S_k. \tag{4.16}$$

These witnesses are called *stabilizer witnesses*. Since graph states are a special type of stabilizer state, a witness for graph states is derived based on stabilizer witnesses with the coefficient $c_0 = 1/2$ and $c_k = 1$ [108]. Since the sum of stabilizers of a graph state $|G\rangle$ is the state itself (see Eq. (4.10)), the simplest witness for detecting GME of the states close to the graph state $|G\rangle$ is given by

$$\mathcal{W}_G = \frac{1}{2}\mathbb{1} - |G\rangle\langle G|. \tag{4.17}$$

Note that the underlying graph of the graph state $|G\rangle$ employed in this witness must be connected.

4.3 (Result) Randomized graph states: the imperfect preparation of graph states

Although graph states are rich in their entanglement structures and allow many applications, there is an obstacle to their generation. A graph state is generated with the initialization of the product state $|+\rangle^{\otimes n}$, which is then subsequently entangled via a series of CZ operations U_Z to create the edges (Def. 4.1.1). Since the current experimental realizations of U_Z are not perfect, it is difficult to generate a noiseless graph state [53]. In Ref. [54], we modeled the noisy preparation of graph states using the so-called *RUS* gates [55–57]. A RUS gate creates the desired edge between two qubits with probability p, while with probability $1-p$ it fails and recovers the original state, and thus, is equivalent to the identity operator. The operation of RUS on a 2-qubit empty graph state is mathematically expressed as follows.

Definition 4.3.1 (RUS operations)**.** A RUS (CZ) operation with success probability p is defined as

$$\Lambda_p(|++\rangle\langle++|) = p|\bullet\!\!-\!\!\bullet\rangle\langle\bullet\!\!-\!\!\bullet| + (1-p)|++\rangle\langle++| \tag{4.18}$$

with $|++\rangle$ representing the two-qubit empty graph state, and $|\bullet\!\!-\!\!\bullet\rangle$ denoting the two-qubit connected graph state.

Note that RUS operations Λ_p commute with each other and therefore the order of their application does not change the resulting states.

Instead of perfect CZ gates, we employ these probabilistic RUS gates to create the edges in a graph state, which leads to a *randomized graph (RG) state*.

Definition 4.3.2 (Randomized graph (RG) states)**.** Let $|G\rangle$ be a graph state. A *randomization operator* R_p is defined via

$$R_p(|G\rangle) := \sum_{F \text{ spans } G} p^{|E_F|}\,(1-p)^{|E_G \setminus E_F|}\,|F\rangle\langle F|, \tag{4.19}$$

where F is spanning subgraphs of G, and E_F, E_G are the edge sets of F and G, respectively. The probability p is the *randomness parameter* corresponding to the success probability of the RUS gates in Eq. (4.18). The resulting state $\rho_G^p := R_p(|G\rangle)$ is called the *p-randomization* of $|G\rangle$.

As an example, the randomization of the 3-vertex complete graph state $|$  $\rangle$ is expressed as follows.

$R_p(|$  $\rangle)$

$= p^3\,|$  $\rangle\langle$  $|$

$+ p^2(1-p)\,|$  $\rangle\langle$  $| + p^2(1-p)\,|$  $\rangle\langle$  $| + +p^2(1-p)\,|$  $\rangle\langle$  $|$

$+ p(1-p)^2\,|$  $\rangle\langle$  $| + p(1-p)^2\,|$  $\rangle\langle$  $| + p(1-p)^2\,|$  $\rangle\langle$  $|$

$+ (1-p)^3\,|$  $\rangle\langle$  $|\,.$ (4.20)

Note that such randomized complete graph states are quantum states corresponding to the classical Erdős-Rényi random graphs introduced in Ref. [109].

A RG state ρ_G^p is a mixture of all the subgraph states $|F\rangle$ with $F \subseteq G$. Due to this mixedness, its entanglement properties are different from that of pure graph state $|G\rangle$ with respect to LU equivalence and GME detection.

4.3.1 Unitary equivalence

Pure graph states can be classified via a particular set of local unitaries, $\{T_i(G) \propto \sqrt{g_i}\}_i$ (Proposition 4.2.1). Two graph states in the same LU class possess the same entanglement properties. However, randomized graph states do not fit into the same classification as pure graph states. We showed this statement via the existence of two LU-equivalent graph states, whose randomization cannot be transformed to each other via global unitaries.

These two graph states are the complete graph state $|K_n\rangle$ and the star graph state $|S_n\rangle$. According to the LC-rule (Proposition 4.2.1), $|K_n\rangle$ and $|S_n\rangle$ are LU-equivalent. However, the rank of the density matrix of the randomized complete graph state is

$$\operatorname{rank}(\rho_{K_n}^p) = 2^n - n, \tag{4.21}$$

while the rank of the randomized star graph state is upper bounded by

$$\operatorname{rank}(\rho_{S_n}^p) \leq 2^n - n - \binom{n-1}{2}. \tag{4.22}$$

Since there exist no global unitaries which can change the rank of a state, the RG states $\rho_{K_n}^p$ and $\rho_{S_n}^p$ are not even global unitary equivalent.

4.3.2 Entanglement of RG states

According to Def. 4.3.2, the fraction of entangled subgraph states $|F\rangle$ in a RG state ρ_G^p increases with respect to the randomness parameter p. For a connected graph G, if $p = 0$, the state $\rho_G^{p=0}$ is fully separable, while for $p = 1$, $\rho_G^{p=1} = |G\rangle$ is GM-entangled. The amount of entanglement depends solely on the randomness parameter p. We plot the negativity (Def. 2.2.15) and the PPT-mixer GME measure (Def. 3.2.3) with respect to the randomness parameter p in Fig. 4.2. One observes monotonically increasing behaviour of bipartite and GM entanglement with respect to p. If this monotonicity holds for all states and entanglement measures, one can conclude the

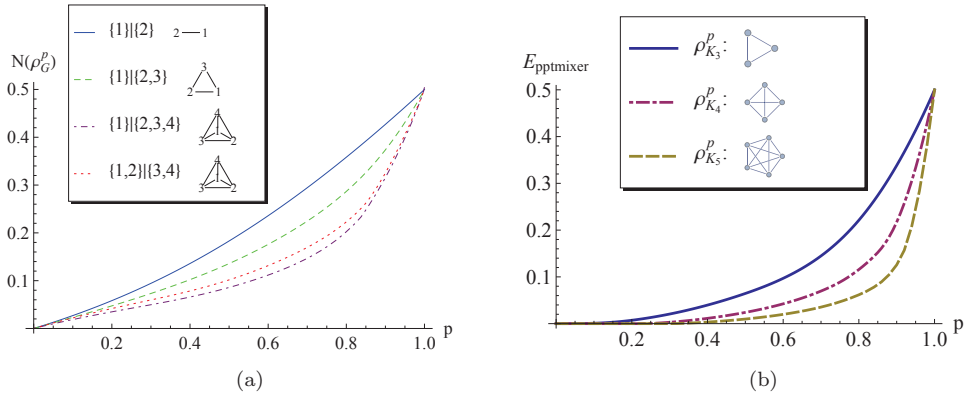

Figure 4.2: Bipartite and GM entanglement in RG states with respect to p: (a) The negativity of all randomized complete graph states ρ_{K_n} with up to $n = 4$ qubits with respect to the randomness parameter p. (b) The PPT-mixer GME measure of randomized complete graph states with up to 5 qubits with respect to the randomness parameter p.

existence of a critical randomness parameter p_c above which entanglement occurs. Although it is an open question if this monotonicity holds for all states and all entanglement measures, we can still verify the critical randomness p_c for bipartite entanglement with the PPT criterion and determine an upper bound on the p_c for GME with the projector GME witness in Eq. 4.17.

From Fig. 4.2a, one observes that the critical randomness parameter p_c for bipartite entanglement is equal to zero. This result can be shown via the PPT criterion (Theorem 2.1.5).

Proposition 4.3.3 (Bipartite entanglement of RG states)**.** Given a graph G, let A and B be a bipartition of the RG state ρ_G^p. ρ_G^p is entangled regarding $A|B$, if there exists at least one edge in G between A and B , and the randomness parameter $p > 0$.

For GME, one observes non-zero critical randomness parameters p_c in Fig. 4.2b. Due to the complexity of computing GME measures for mixed states[4], we estimated the value of p_c via its upper bound found by the projector witness in Eq. (4.17), i.e.

$$\mathcal{W}_G = \frac{1}{2}\mathbb{1} - |G\rangle\langle G|\,. \tag{4.23}$$

[4]E.g. the GM I-concurrence in Eq. (3.25) is incomputable, while the PPT-mixer measure in Def. 3.2.3 is only numerically computable.

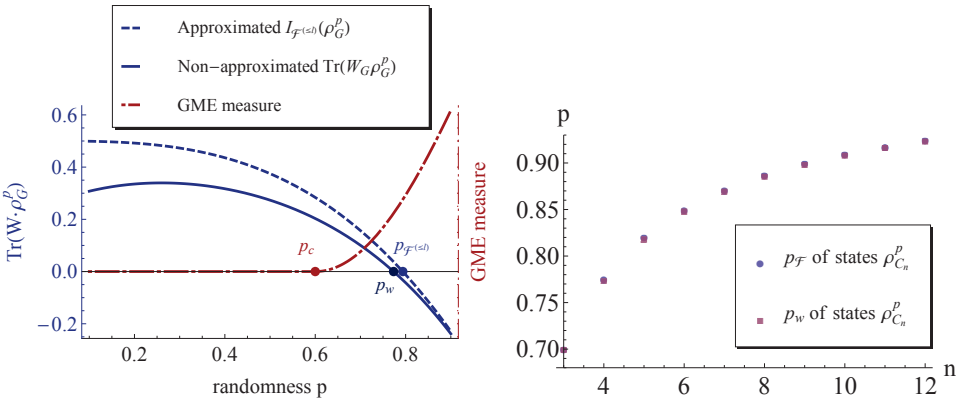

Figure 4.3: (a)The relation between a measure of GME and the expectation value of the projector witness W (Eq. (4.24)). The dashed line depicts the expectation value of the l-level approximated GME witness (Eq. (4.25)). In contrast with the non-approximated one, it is monotonically decreasing for level $l \leq |E_G|/2$ and randomness parameter $1/2 \leq p \leq 1$. The expectation value of the non-approximated GME witness $\mathrm{tr}(W_G\rho_G^p)$ is always smaller than or equal to the l-approximated one $I_{\mathcal{F}^{(\leq l)}}(\rho_G^p)$. (b)The upper bounds $p_{\mathcal{F}^{(\leq 2)}}$ and p_w on the critical randomness parameter p_c of the randomized cycle graph states with up to 12 qubits are plotted.

The relation between the critical randomness parameter p_c and the expectation value of the projector witness $\mathrm{tr}(\mathcal{W}_G\rho)$ is illustrated in Fig. 4.3a. The critical randomness parameter p_c is upper bounded by p_w. Notice that only with monotonically decreasing $\mathrm{tr}(\mathcal{W}_G\rho_G^p)$, one can obtain a definite upper bound p_w, beyond which the expectation value is certainly negative. However, the monotonic behaviour of the expectation value $\mathrm{tr}(\mathcal{W}_G\rho_G^p)$ is not guaranteed.

Moreover this expectation value is difficult to compute, since it depends on the sum of the overlaps of all subgraph states $|F\rangle$ with $|G\rangle$, i.e.

$$\mathrm{tr}(\mathcal{W}_G\rho_G^p) = \frac{1}{2} - \sum_{F \text{ spans } G} p^{|E_F|}(1-p)^{|E_G \setminus E_F|}\,|\langle F|G\rangle|^2\,. \tag{4.24}$$

The first difficulty of this calculation is the graph state overlap $\langle F|G\rangle$, which will be studied in section 4.4. The second difficulty is the large number of summands, which is equal to the number of subgraphs of G, i.e. $2^{|E_G|}$. Therefore, we introduce the *l-level-approximation* of $\mathrm{tr}(\mathcal{W}_G\rho_G^p)$ by dropping the subgraphs $F^{(>l)}$, which differ from G by more than l edges, i.e.

$$I_{\mathcal{F}^{(\leq l)}}(\rho_G^p) = \frac{1}{2} - \sum_{F\subseteq G \text{ and } |E_{F\Delta G}|\leq l} p^{|E_F|}(1-p)^{|E_G \setminus E_F|}\,|\langle F|G\rangle|^2\,. \tag{4.25}$$

This approximated witness is monotonically decreasing with respect to the randomness parameter $p \geq 1/2$ for all $l \leq |E_G|/2$. For the approximation level $l = 2$, one obtains the following GME witness.

Theorem 4.3.4 (Approximated GME witness)**.** Let G be a graph and d_v be the degree of a vertex

v. The expectation value $\mathrm{tr}(\mathcal{W}_G\rho_G^p)$ is upper bounded by $I_{\mathcal{F}^{(\leq 2)}}(\rho_G^p)$, which is equal to

$$\mathrm{tr}(\mathcal{W}_G\rho_G^p) \leq I_{\mathcal{F}^{(\leq 2)}}(\rho_G^p) = \frac{1}{2} - p^{|E_G|} - \frac{1}{4}(1-p)\,p^{|E_G|-1}\,|E_G| - \frac{1}{2^4}(1-p)^2\,p^{|E_G|-2}\left[\binom{|E_G|}{2} + 3\sum_{v\in V_G}\binom{d_v}{2}\right]. \tag{4.26}$$

This quantity can be regarded as a GME witness for ρ_G^p. If $I_{\mathcal{F}^{(\leq 2)}}(\rho_G^p) < 0$, it is then guaranteed that the RG state ρ_G^p is genuinely multipartite entangled.

Since $I_{\mathcal{F}^{(\leq 2)}}(\rho_G^p)$ is greater or equal to $\mathrm{tr}(W_G\rho_G^p)$ and monotonic with respect to p, the point where it equals zero yields an upper bound $p_{\mathcal{F}^{(\leq 2)}}$ on p_c. A randomness parameter $p > p_{\mathcal{F}^{(\leq 2)}}$ guarantees that ρ_G^p is GM-entangled. In Fig 4.3b, we plot the explicit values of $p_{\mathcal{F}^{(\leq 2)}}$ of the randomized cycle graph states with up to 12 qubits.

4.4 (Result) The representation of graph states revealed by X-chains

Graph states can be defined both via entangling gates and the stabilizer formalism (Def. 4.1.1 and 4.1.2), respectively. The explicit form of a graph state $|G\rangle$ in the Z-basis is the superposition of all Z-basis states with non-zero amplitudes $\pi_G(\xi)$ [60, 110], which are called *stabilizer parity* and defined later in Eq. (4.30), i.e.

$$|G\rangle = \frac{1}{2^{n/2}}\sum_{\xi\subseteq V_G}\pi_G(\xi)\,|i_Z^{(\xi)}\rangle. \tag{4.27}$$

with $i_Z^{(\xi)}$ being the binary number corresponding to the vertex subset ξ[5]. In the entangling gates representation (Def. 4.1.1), a graph state $|G\rangle$ needs $|E_G|$ CZ gates, while in the stabilizer formalism, it needs $|V_G|$ stabilizer generators. Yet, the number of Z-basis states in the superposition in Eq. (4.27) grows exponentially ($2^{|V_G|}$) with respect to the number of vertices $|V_G|$. This complicates the calculation of the graph state overlaps in the GME witness in Eq. (4.24). Therefore we need a simpler representation of graph states in the computational basis.

In order to represent graph states explicitly and efficiently, we introduced the so-called *X-chains* in Ref. [60], from which an efficient representation approach was derived. As a result the overlap of two graph states, which could not be determined efficiently up to now, can be calculated efficiently by X-chain groups. Besides, our approach can also determine the Schmidt decomposition of a graph state with respect to a bipartition. It is also useful in entanglement localization [61] for finding repetition codes robust against local measurement errors. The difficulty of the above mentioned tasks decreases as the number of X-chains increases.

4.4.1 X-chains

A graph state with n vertices is associated with n stabilizer generators (see Def. 4.1.2), which generate the whole stabilizer group of the graph state. Each vertex subset $\xi \subseteq V_G$ is associated with the so-called ξ-induced stabilizer (Eq. (4.9)). The explicit form of a ξ-induced stabilizer is given as follows.

[5]For instance, in the system of a 4-vertex graph state, $i^{\{1,3\}} = 1010$.

Proposition 4.4.1 (Form of induced stabilizer)**.** Let $\xi = \{v_1, ..., v_k\}$ be a vertex subset of G. The ξ-induced stabilizer of a graph state $|G\rangle$ is given by

$$s_G^{(\xi)} = \pi_G(\xi)\, \sigma_x^{(\xi)} \sigma_z^{(c_\xi)}, \tag{4.28}$$

where c_ξ is the *correlation index* of ξ and $\pi_G(\xi)$ is the *stabilizer parity* of ξ. The *correlation index* of ξ is defined as the symmetric difference[6] of the neighbourhoods within ξ,

$$c_\xi := N_{v_1} \Delta N_{v_2} \cdots \Delta N_{v_k}, \tag{4.29}$$

where N_{v_i} is the neighbourhood of v_i. The *stabilizer parity* of ξ is the parity of the edge number $\left|E_{G[\xi]}\right|$ of the ξ-induced subgraph $G[\xi]$,

$$\pi_G(\xi) := (-1)^{\left|E_{G[\xi]}\right|}. \tag{4.30}$$

Proof. See [60]. □

There is a class of special vertex subsets, for which the induced stabilizers contain only σ_X operators, which means that the correlation index $c_\xi = \emptyset$. We call such vertex subsets *X-chains*.

Definition 4.4.2 (X-chains)**.** Let $|G\rangle$ be a graph state. A vertex subset $\xi \subseteq V_G$ with empty correlation index, i.e. $c_\xi = \emptyset$, is called an *X-chain* of $|G\rangle$. Its induced stabilizer is called *X-chain stabilizer*.

Consider the 4-vertex star graph state $|S_4\rangle$ in Table 4.3. The $\{1,2\}$-induced stabilizer is given by $-\sigma_X^{\{1,2\}}\sigma_Z^{\{1,2,3,4\}}$, while the $\{2,3\}$-induced stabilizer is $\sigma_X^{\{2,3\}}$, meaning that $\{2,3\}$ is an X-chain. Table 4.3 shows the 4 X-chains of $|S_4\rangle$. The set of X-chains of a given graph state forms a group with the symmetric difference Δ as its group operation. The X-chain group of a graph state $|G\rangle$ is denoted by $\langle \Gamma_G \rangle$, where Γ_G is the set of group generators.

In Ref. [60], we employed X-chain groups $\langle \Gamma_G \rangle$ to derive the representation of graph states in the X-basis, which is simpler[7] than the Z-basis representation [110] (Eq. (4.27)). The algorithm is called *X-chain factorization*, in which the group of vertex subsets $(\mathcal{P}(V_G), \Delta)$ is factorized to the direct product of the X-chain group $\langle \Gamma_G \rangle$ and the so-called *correlation group* $\langle \mathcal{K}_G \rangle$.

$$(\mathcal{P}(V_G), \Delta) \sim (\langle \Gamma_G \rangle, \Delta) \times (\langle \mathcal{K}_G \rangle, \Delta). \tag{4.31}$$

Here $\mathcal{P}(V_G) := \{\xi : \xi \subseteq V_G\}$ is the powerset of V_G, and $\langle \mathcal{K}_G \rangle$ is the quotient subgroup of $\mathcal{P}(V_G)$ factorized by the X-chain group $\langle \Gamma_G \rangle$, i.e.

$$\langle \mathcal{K}_G \rangle = \mathcal{P}(V_G) / \langle \Gamma_G \rangle. \tag{4.32}$$

4.4.2 X-chain factorization

Via the ξ-induction map in Eq.(4.28), the X-chain group Γ_G of a graph state $|G\rangle$ induces the X-chain stabilizer subgroup $\mathcal{S}_{\Gamma_G}$, which projects the Hilbert space of $|G\rangle$ into a subspace spanned

[6] The symmetric difference of two vertex subsets ξ_1 and ξ_2 is $\xi_1 \Delta \xi_2 = (\xi_1 \cup \xi_2) \setminus (\xi_1 \cap \xi_2)$.

[7] A simpler representation means the number of terms in the superposition is smaller.

Graph G	X-chains $\langle \Gamma_G \rangle$	X-chain generators Γ_G
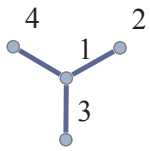 S_4	$\xi_1 = \emptyset$ $\xi_2 = \{2,3\}$ 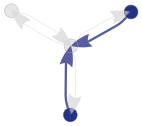 $\xi_3 = \{2,4\}$ 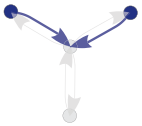 $\xi_4 = \{3,4\}$ 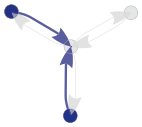	$\{\{2,3\},\{2,4\}\}$

Table 4.3: The X-chain group of the 4-vertex star graph state: The directed graphs shown under the X-chains illustrate the criterion of X-chains. Once a vertex is selected for the vertex subset ξ then one draws arrows from it to its neighbors. A vertex subset ξ is an X-chain if and only if an even number of arrows arrives at each vertex of the graph. The X-chain groups $\langle \Gamma_G \rangle$ are generated by their generating sets Γ_G via the symmetric difference.

by the set of X-basis states $\Psi^{\emptyset}_{\mathcal{K}_G}$, i.e.

$$\Gamma_G : \text{ X-chain group} \tag{4.33}$$

$$\Big\downarrow \xi\text{-induced stabilizers}$$

$$\mathcal{S}_{\Gamma_G} = \left\{ s^{\xi}_G : \xi \in \langle \Gamma_G \rangle \right\} \subseteq \mathcal{S}_G \tag{4.34}$$

$$\Big\downarrow \text{the kernel of } \mathcal{S}_{\Gamma_G}$$

$$\text{span}(\Psi^{\emptyset}_{\mathcal{K}_G}) \text{ with } \Psi^{\emptyset}_{\mathcal{K}_G} := \{ |\psi_{\emptyset}(\xi)\rangle : \xi \in \langle \mathcal{K}_G \rangle \} . \tag{4.35}$$

Here, the states $|\psi_{\emptyset}(\xi)\rangle$ are stabilized by all X-chain stabilizers and called *X-chain states*, which are defined as follows.

Definition 4.4.3 (X-chain states and correlation states)**.** Let $|G\rangle$ be a graph state with the X-chain group $\langle \Gamma_G \rangle$ and the correlation group $\langle \mathcal{K}_G \rangle$, and $\langle \mathcal{K} \rangle \subseteq \langle \mathcal{K}_G \rangle$ be a correlation subgroup. The *$\mathcal{K}$-correlation state* of the graph state $|G\rangle$, $|\psi_{\mathcal{K}}(\xi)\rangle$, is defined as

$$|\psi_{\mathcal{K}}(\xi)\rangle = \frac{1}{2^{|\mathcal{K}|/2}} \sum_{\xi' \in \langle \mathcal{K} \rangle} |\psi_{\emptyset}(\xi' \Delta \xi)\rangle \tag{4.36}$$

with the *X-chain states*

$$|\psi_{\emptyset}(\xi)\rangle = \pi_G(\xi) \, |i_\Gamma \oplus i^{(c_\xi)}\rangle, \tag{4.37}$$

where $|i_\Gamma\rangle$ is the X-basis state stabilized by $\{s^{(\gamma)}_G\}_{\gamma \in \langle \Gamma_G \rangle}$ and $\{\sigma^{(\kappa)}_X\}_{\kappa \in \langle \mathcal{K}_G \rangle}$, and $|i^{(c_\xi)}\rangle$ is the X-basis

state corresponding to the binary notation[8] of the correlation index $c_\xi = \Delta_{j\in\xi} N_j$.

The *X-chain states* and *correlation states* defined in this way satisfy the following proposition.

Proposition 4.4.4 ($\mathcal{K}_G$-correlation states as stabilized states)**.** $\mathcal{K}$-correlation states are stabilized by the graph state stabilizers $\{s_G^{(\kappa)} : \kappa \in \langle\Gamma_G\rangle \times \langle\mathcal{K}\rangle\}$, i.e.

$$s_G^{(\kappa)} |\psi_{\mathcal{K}}(\xi)\rangle = |\psi_{\mathcal{K}}(\xi)\rangle. \tag{4.38}$$

for all $\kappa \in \langle\Gamma_G\rangle \times \langle\mathcal{K}\rangle$

Proof. See Ref. [111]. □

With this proposition one arrives at the representation theorem of graph states in the X-basis.

Theorem 4.4.5 (Representation of graph states in the X-basis)**.** A graph state $|G\rangle$ is the $\mathcal{K}_G$-correlation state, which is the superposition of the X-chain states $|\psi_\emptyset(\xi)\rangle$, i.e.

$$|G\rangle = |\psi_{\mathcal{K}_G}\rangle = \frac{1}{2^{|\mathcal{K}_G|/2}} \sum_{\xi\in\langle\mathcal{K}_G\rangle} |\psi_\emptyset(\xi)\rangle. \tag{4.39}$$

Proof. See Ref. [111]. □

This theorem can be summarized in the so-called *X-chain factorization diagram* in Fig. 4.4. This diagram is obtained from Eq. (4.33)-(4.35) by adding the correlation group $\langle\mathcal{K}_G\rangle$ via the direct product operation into Eq. (4.33), and subsequently projecting the subspace span($\Psi^\emptyset_{\mathcal{K}_G}$) via $\langle\mathcal{K}_G\rangle$ into the $\mathcal{K}_G$-correlation state. Since the $\mathcal{K}_G$-correlation state is stabilized by all the graph state stabilizer of $|G\rangle$ (Proposition 4.4.4), it is identical to the graph state $|G\rangle$.

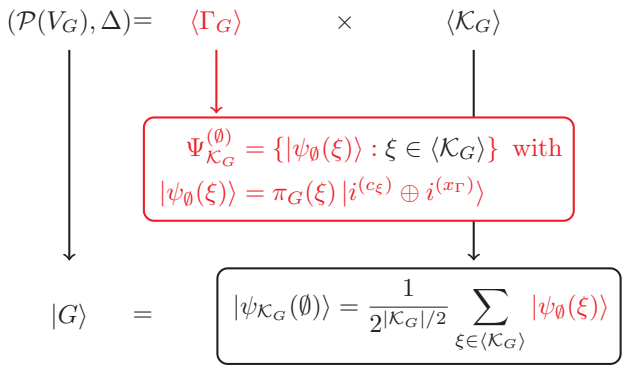

Figure 4.4: X-chain factorization diagram of graph states: A graphical summary of Def. 4.4.3, Proposition 4.4.4 and Theorem 4.4.5. This diagram illustrates the algorithm for representing a graph state in the X-basis.

[8]The binary notation of a vertex subset ξ is defined as $i^{(\xi)} := i_1 i_2 \cdots i_n$ with $i_j = 1$ if $j \in \xi$, otherwise $i_j = 0$. E.g. for $n = 3$, $i^{(\{1,3\})} = 1010$.

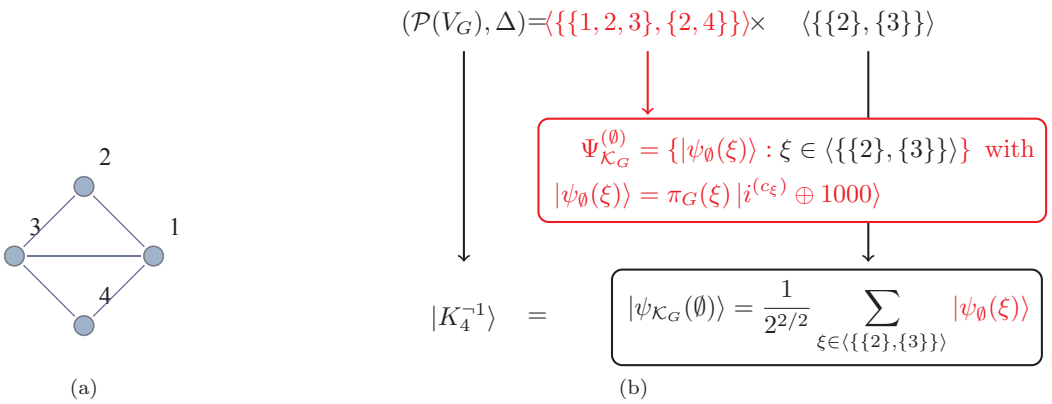

Figure 4.5: X-chain factorization of $|K_4^{\neg 1}\rangle$): (a) The graph state $|K_4^{\neg 1}\rangle$. (b) The factorization diagram of $|K_4^{\neg 1}\rangle$: this state has the X-chain generators $\{\{1,2,3\},\{2,4\}\}$, which leads to the X-chain states $\Psi^{\emptyset}_{\mathcal{K}_G} = \{|1000\rangle, |0010\rangle, |0101\rangle, -|1111\rangle\}$.

In Eq. (4.39), one observes that the number of terms in the superposition of a graph state $|G\rangle$ depends on the number of the correlation group generators $|\mathcal{K}_G|$, which is equal to $n - |\Gamma_G|$. This indicates that the more X-chains a graph state possesses, the simpler is its representation in the X-basis.

As an example, the X-chain factorization for the graph state $|K_4^{\neg 1}\rangle$, whose underlying graph $K_4^{\neg 1}$ is the 4-vertex complete graph with one edge missing, is shown in Fig. 4.5. It has the X-chain generators $\{\{1,2,3\},\{2,4\}\}$ and generators of the correlation group $\{\{2\},\{3\}\}$. As a result of X-chain factorization, the 4 X-chain states are:

$$\begin{aligned} &|\psi_{\mathcal{K}_G}(\emptyset)\rangle = |1000\rangle, && |\psi_{\mathcal{K}_G}(\{2\})\rangle = |0010\rangle, \\ &|\psi_{\mathcal{K}_G}(\{3\})\rangle = |0101\rangle, && |\psi_{\mathcal{K}_G}(\{2,3\})\rangle = -|1111\rangle. \end{aligned} \tag{4.40}$$

Hence the graph states $|K_4^{\neg 1}\rangle$ is represented in the X-basis as follows.

$$|K_4^{\neg 1}\rangle = \frac{1}{2}(|1000\rangle + |0010\rangle + |0101\rangle - |1111\rangle). \tag{4.41}$$

Note that this result can be extended for determining the Schmidt decomposition of a graph state $|G\rangle$ via adding a proper intermediate correlation group $\mathcal{K}_G^{A\rfloor B}$ in the factorization procedure, such that the correlation states $|\psi_{\mathcal{K}_G^{A\rfloor B}}(\xi)\rangle$ form the $A|B$-separable Schmidt basis of $|G\rangle$. As a result, the Schmidt decomposition of $|G\rangle$ is given by

$$|G\rangle = \frac{1}{2^{|\mathcal{K}_G| - \left|\mathcal{K}_G^{A\rfloor B}\right|}} \sum_{\xi \in \langle \mathcal{K}_G \rangle / \langle \mathcal{K}_G^{A\rfloor B} \rangle} |\psi_{\mathcal{K}_G^{A\rfloor B}}(\xi)\rangle. \tag{4.42}$$

For more details please refer to Ref. [111]. A Mathematica package is provided in Ref. [112].

4.4.3 Graph state overlaps

Knowing the X-chain group of a graph state $|G\rangle$, one can directly determine the amplitude of the X-basis state[9] $|0_X\rangle^{\otimes n}$ in the superposition of $|G\rangle$ via Theorem 4.4.5. We call the amplitude $\langle 0_X^{\otimes n}|G\rangle$ the *Z-bias degree* of $|G\rangle$, since it is equal to the difference of positive and negative amplitudes in the Z-basis, and denote it by $\beta(|G\rangle)$. Z-bias degree is related to the overlap of two graph states $|G\rangle$ and $|H\rangle$, since according to the entangling gate definition of graph states (Def. 4.1.1), $\langle G|H\rangle$ can be reformulated to

$$\langle G|H\rangle = \langle 0_X^{\otimes n}|G\Delta H\rangle = \beta(|G\Delta H\rangle). \tag{4.43}$$

Here, $G\Delta H$ is the graph symmetric difference of G and H. As a result of Theorem 4.4.5, graph state overlaps can be determined via the following corollary.

Corollary 4.4.6 (Graph state overlaps and Z-bias degrees)**.** The overlap of two graph states $|G\rangle$ and $|H\rangle$ is equal to the Z-bias degree of the graph state $|G\Delta H\rangle$, i.e.

$$\langle G|H\rangle = \beta(|G\Delta H\rangle). \tag{4.44}$$

The Z-bias degree of a graph state $|G\rangle$ is equal to

$$|\beta(|G\rangle)| = \frac{1}{2^{(n-|\Gamma_G|)/2}} \prod_{\gamma\in\Gamma_G} \delta^1_{\pi_G(\gamma)}, \tag{4.45}$$

where Γ_G is a generating set of the X-chain group of $|G\rangle$, δ is the Kronecker-delta and $\pi_G(\gamma)$ is the stabilizer-parity of the X-chain generator γ.

Proof. See Ref. [60]. □

Since the X-chain group of a graph state can be determined efficiently, graph state overlaps can be then calculated efficiently with this corollary. Eq. (4.45) implies that two graph states are orthogonal, i.e $\langle G|H\rangle = 0$, if there exists an X-chain γ^- of the graph state $|G\Delta H\rangle$ with negative stabilizer parity, i.e. $\pi_{G\Delta H}(\gamma^-) = -1$. For instance, the graph state $|K_4^{\neg 1}\rangle$ (Fig. 4.5) has an X-chain $\{1,2,3\}$ with stabilizer parity -1. Then the graph states $|G\rangle$ and $|H\rangle$ are orthogonal, if $G\Delta H = K_4^{\neg 1}$. In Fig. 4.6, we list three example pairs of orthogonal graph states, whose graph symmetric difference is equal to the graph $K_4^{\neg 1}$.

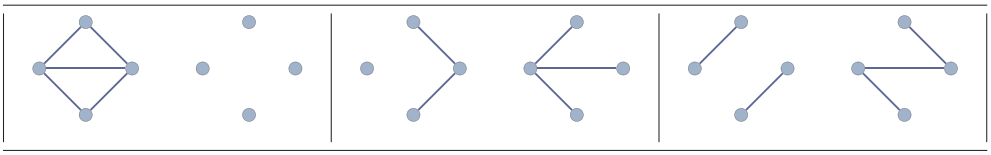

Figure 4.6: Orthogonal graph states derived from the graph state $|K_4^{\neg 1}\rangle$: The graph states in each cell are orthogonal. The graph symmetric difference of each pair $G\Delta H$ is identical to the cycle graph $K_4^{\neg 1}$. The $|K_4^{\neg 1}\rangle$ has an X-chain $\{1,2,3\}$, whose stabilizer parity is -1.

[9] The X-basis state $|0_X\rangle^{\otimes n}$ is the eigenstate of the Pauli operator $\sigma_X^{\otimes n}$ with the eigenvalue $(1_1,...,1_n)$.

5. Conclusion and outlook

Multipartite quantum systems were studied with respect to multipartite entanglement detection. A special class of multipartite entanglement systems called graph states were investigated. The theories of their generation with noisy models, and their representation using X-chains are derived.

We first derived a lower bound Q_R on the GM I-concurrence $\mathcal{E}_{\mathcal{I}}^{\mathrm{GM}}$ in Theorem 3.2.4 (originally in Ref. [50]). For n-partite systems, via selecting a proper set of off-diagonal indices of an $n \times n$ matrix, one can obtain a quantity $Q_R(\rho)$ expressed as a function of particular entries of the density matrix ρ. The quantity $-Q_R(\rho)$ can be employed as a GME witness, which detects GME for $-Q_R(\rho) < 0$. The required local measurement settings for these witnesses are experimentally feasible. In bipartite cases, this lower bound is related to the PPT criterion.

We then investigated the generation of graph states, which are a class of multipartite entangled systems and can be represented in terms of mathematical graphs, in Ref. [54]. For an $n \geq 4$ partite system, graph states are not GHZ-type or W-type entangled states. A graph state $|G\rangle$ can be created from a product state via applying the (control-Z (CZ)) gates on pairs of qubits $e = \{v_1, v_2\}$ corresponding to the edges e of the graph G [45]. In Ref. [54], instead of perfect CZ gates, we considered a type of noisy entangling gates called repeat-until-success (RUS) gates, which can be modeled by a type of probabilistic operation with success probability p. The RUS gates lead to a mixed state ρ_G^p, which is the mixture of all subgraph states $|F\rangle$ ($F \subseteq G$). We called these end products *randomized graph (RG) states* and the success probability p of gates the *randomness parameter*.

The properties of RG states were studied with respect to both bipartite and multipartite entanglement. We found that LU-equivalence of pure graph states does not imply LU-equivalence of their randomized version. The amount of bipartite and GM entanglement of a RG state is shown to increase monotonically with respect to the randomness p in the systems up to 4 qubits. For general cases, we can only detect the presence of entanglement. A randomized edge between the two parties $A|B$ guarantees the $A|B$ bipartite entanglement, if the randomness parameter is non-zero. Meanwhile, the GME can be guaranteed for the randomness parameter p greater than a critical value p_c. This critical value is upper bounded by the value $p_{\mathcal{F}}$ detected by an approximated GME witness $I_{\mathcal{F}}(\rho)$ (Theorem 4.3.4). For $p > p_{\mathcal{F}}$, the state ρ_G^p is GM entangled with certainty. The explicit values of $p_{\mathcal{F}}$ for certain states are given in Ref. [54], where the critical randomness parameter p_{LHV}, beyond which a LHV description is not possible for ρ_G^p, is also determined.

To derive the non-approximated GME witness for RG state in Eq. (4.24), the calculation of graph state overlaps is necessary. To this end, we derived an alternative representation of graph states in the X-basis in Ref. [60] , which is simpler than the known expression of graph states in the Z-basis [110]. We found that a special type of graph state stabilizers, which contains only σ_X-Pauli operators, determine the terms in the superposition of graph states in the X-basis. We called

the vertex subsets associated with these stabilizers *X-chains* (Def. 4.4.2). The set of X-chains of a graph state forms a group and reveals structures of graph states. The group structure of X-chains allows the so-called *X-chain factorization* (Eq. (4.31)) for deriving the representation of graph states in the X-basis, which is the superposition of all X-chain states (Theorem 4.4.5). This algorithm was illustrated in the so-called *X-chain factorization diagram* (Fig. 4.4). We showed that the larger the X-chain group is, the simpler is the representation of the graph state in the X-basis.

Via this representation, we showed that the overlap of two graph states can be efficiently determined via the X-chain group of the state corresponding to their graph symmetric difference (Corollary 4.4.6), for which no efficient algorithm was known before.

Another application of X-chain factorization is to determine the Schmidt decomposition of graph states, which is the superposition of appropriately selected correlation states (Eq. 4.42). A further application of the Schmidt decomposition in the X-basis is the error correction in entanglement localization of graph states in bipartite systems, which could be useful for quantum repeaters [62].

X-chain factorization can be extended to more general graph states, e.g. weighted graph states [113, 114] and hypergraph states [102, 103, 115]. Another prospective use for these results is to represent graph states in a hybrid basis, i.e. a mix of the X-basis and Z-basis. The graph states in such a hybrid basis can even have a smaller number of terms in their superposition than that obtained in Theorem 4.4.5. A simplification of graph state generation can also be derived with the help of X-chains. Besides, we expect that the approach of X-chain factorization may also be useful in the quantification of multipartite entanglement of graph states, which were studied in Ref. [51, 107, 116, 117]. Further, all the above applications can be extended to the states stabilized by a set of particular operators, which are products of certain noncommutative operators.

A. List of publications

Determining lower bounds on a measure of multipartite entanglement from few local observables

J.-Y. Wu, H. Kampermann, D. Bruß, C. Klöckl and M. Huber

Phys. Rev. A, 86, 022319 (2012)

Contribution: first author, scientific work and preparation of the manuscript 70%

Randomized graph states and their entanglement properties

J.-Y. Wu, M. Rossi, H. Kampermann, S. Severini, L.C. Kwek, C. Macchiavello, D. Bruß

Phys. Rev. A, 89, 052335 (2014)

Contribution: first author, scientific work and preparation of the manuscript 75%

X-chains reveal substructures of graph states

J.-Y. Wu, H. Kampermann, D. Bruß,

E-print: arXiv:1504.03302,(2015) (submitted to PRA)

Contribution: first author, scientific work and preparation of the manuscript 90%

PHYSICAL REVIEW A **86**, 022319 (2012)

Determining lower bounds on a measure of multipartite entanglement from few local observables

Jun-Yi Wu, Hermann Kampermann, and Dagmar Bruß
Institut für Theoretische Physik III, Heinrich-Heine-Universität Düsseldorf, D-40225 Düsseldorf, Germany

Claude Klöckl
University of Vienna, Faculty of Mathematics, Nordbergstraße 15, 1090 Wien, Austria

Marcus Huber
University of Bristol, Department of Mathematics, Bristol, BS8 1TW, United Kingdom
(Received 14 May 2012; published 17 August 2012)

We introduce a method to lower bound an entropy-based measure of genuine multipartite entanglement via nonlinear entanglement witnesses. We show that some of these bounds are tight and explicitly work out their connection to a framework of nonlinear witnesses that were published recently. Furthermore, we provide a detailed analysis of these lower bounds in the context of other possible bounds and measures. In exemplary cases, we show that only a few local measurements are necessary to determine these lower bounds.

DOI: 10.1103/PhysRevA.86.022319 PACS number(s): 03.67.Mn, 03.65.Ud, 03.65.Fd, 03.65.Aa

I. INTRODUCTION

Quantum entanglement is central to the field of quantum-information theory. Due to its numerous applications in upcoming quantum technology much research has been devoted to its understanding (for a recent overview consider Ref. [1]). Especially in systems comprised of many particles, entanglement provides numerous challenges and of course potential applications, such as building quantum computers (see Ref. [2]), performing quantum algorithms (the connection to multipartite entanglement is demonstrated in Ref. [3]), and multiparty cryptography (see, e.g., Ref. [4]). Furthermore, the understanding of the behavior of complex systems seems to be closely linked to the understanding of multipartite entanglement manifestations, demonstrated by the connection to phase transitions and ionization in condensed-matter systems (e.g., [5]), the properties of ground states in relation to entanglement (as shown, e.g., in Refs. [6,7]), or potentially even biological systems (such as, e.g., bird navigation [8]). In order to judge the relevance of entanglement in such systems it is crucial to not only detect its presence but also quantify the amount. The structure of entangled states, especially in multipartite systems [9], is very complex and the question whether a given state is entangled is even NP-hard [10]. Thus, in general, it will not be possible to derive a computable measure of entanglement that reveals all entangled states to be entangled and discriminates between different entanglement classes. Furthermore, full information about the state of the system requires a number of measurements that grows exponentially in the size of the system. For the detection of entanglement in multipartite systems most researchers have therefore made it a primary goal to develop entanglement witnesses, which via a limited amount of local measurements can detect the presence of entanglement, even in complex systems (for an overview of multipartite entanglement witnesses, consider Ref. [11]). The expectation value of witness operators are usually expressed in terms of inequalities, which if violated show the presence of entanglement. Nonlinear witnesses (first introduced in Ref. [12]; see also early discussions in, e.g., Ref. [13]) provide a generalization that is no longer a linear function of density matrix elements, but a nonlinear one. Thus one cannot reformulate the criteria in terms of an expectation value of a Hermitian operator (unless one considers coherent measurements on multiple copies of the state, which out of experimental infeasibility we do not discuss in our manuscript). We will henceforth refer to inequalities that involve nonlinear functions of density matrix elements as nonlinear entanglement witnesses.

Recently some authors pointed out a connection between the possible amount of violation of these nonlinear inequalities and quantification of entanglement in multipartite systems (in Refs. [14,15]). The aims of this paper are twofold. First to systematically show the connection of numerous witnesses to a meaningful measure of genuine multipartite entanglement and second to use this established relation for the development of novel witnesses, which by construction give lower bounds on that measure. To that end we follow and generalize the approach from Ref. [15]. It turns out that only a small number of density matrix elements enters into our lower bounds, making the construction experimentally feasible even in larger systems of high dimensionality.

II. A MEASURE OF MULTIPARTITE ENTANGLEMENT AND ITS LOWER BOUNDS

A. A measure of genuine multipartite entanglement (GME)

The entropy of subsystems has often been used in order to quantify entanglement contained in multipartite pure states (e.g., see [1,16–19]). In this paper we will follow the definition first presented in Ref. [16] and define a measure of GME for multipartite pure states as

$$E_m(|\psi\rangle\langle\psi|) := \min_{\gamma} \sqrt{S_L(\rho_\gamma)} = \min_{\gamma} \sqrt{2\left[1 - \mathrm{Tr}\left(\rho_\gamma^2\right)\right]}, \tag{1}$$

where $S_L(\rho_\gamma)$ is the linear entropy of the reduced density matrix of subsystem γ, i.e., $\rho_\gamma := \mathrm{Tr}_{\bar{\gamma}}(|\psi\rangle\langle\psi|)$. The minimum is taken over all possible reductions γ (where the complement is denoted as $\bar{\gamma}$), which corresponds to a bipartite split into

$\gamma|\bar{\gamma}$. As any proper measure of multipartite entanglement for pure states can be generalized to mixed states via a convex roof, i.e.,

$$E_m(\rho) := \inf_{\{p_i,|\psi_i\rangle\}} \sum_i p_i E_m(|\psi_i\rangle\langle\psi_i|)\,.$$

Due to its construction this measure fulfills almost all desirable properties one would expect from measures of GME (see Ref. [15] for details). Because computing all possible pure state decompositions of a density matrix is computationally impossible even if one is given the complete density matrix, we require lower bounds to be calculable for this expression.

Also note that a lower bound on the linear entropy directly leads to a lower bound on the Rényi 2-entropy $S_R^{(2)}(\rho_\gamma)$ via the relation $S_R^{(2)}(\rho_\gamma) = -\log_2(\frac{2-S_L(\rho_\gamma)}{2})$, which also provides one of the physical interpretations of this measure. The Rényi 2-entropy in itself is a lower bound to the von Neumann entropy $S(\rho_\gamma)$ and the mutual information can be expressed as $I_{\gamma\bar{\gamma}} := S(\rho_\gamma) + S(\rho_{\bar{\gamma}}) - S(\rho) = 2S(\rho_\gamma)$. Thus by our lower bound we gain a lower bound on the average minimal mutual information across all bipartitions of the pure states in the decomposition, minimized over all decompositions.

B. Linear entropy and its convex roof

The state vector of an n-partite qudit state can be expanded in terms of the computational basis

$$|\psi\rangle = \sum_{i_1,i_2,\cdots,i_n=0}^{d-1} c_{i_1,i_2,\ldots,i_n}|i_1,i_2,\ldots,i_n\rangle =: \sum_{\eta\in\mathbb{N}_d^{\otimes n}} c_\eta|\eta\rangle\,,$$

where a basis vector is denoted by $\eta = (i_1,i_2,\ldots,i_n) \in \mathbb{N}_d^{\otimes n}$. This vector notation will facilitate the upcoming derivations. A crucial element of the notation in this paper will be the permutation operator acting upon two vectors, exchanging vector components corresponding to the set of indices. For example, the permutation operator $P_{\{1,3\}}(\eta_1,\eta_2)$ will exchange the first and third component of the vector η_1 with the corresponding component of the vector η_2, i.e.,

$$P_{\{1,3\}}(\mathbf{01}2\mathbf{13},\mathbf{30}1\mathbf{21}) = (\mathbf{31}1\mathbf{13},\mathbf{00}2\mathbf{21}).$$

Using this notation one can write down a very simple expression for the linear entropy of a reduced state ρ_γ (see Appendix A for the derivation)

$$S_L(\rho_\gamma) = \sum_{\eta_1\neq\eta_2} \left|c_{\eta_1}c_{\eta_2} - c_{\eta_1^\gamma}c_{\eta_2^\gamma}\right|^2, \tag{2}$$

where $(\eta_1^\gamma,\eta_2^\gamma) = P_\gamma(\eta_1,\eta_2)$. For pure states we can of course find lower bounds on $E_m(|\psi\rangle\langle\psi|)$ by lower bounding the linear entropy for all possible bipartitions. For mixed states we can then provide a lower bound for the convex roof $E_m(\rho)$. We now illustrate our method in one exemplary case and then continue to articulate the main theorem.

Note that the linear entropy of subsystems has been widely used for lower bounding measures of entanglement due to the well-known and simple structure of Eq. (2). None of the previous methods, however, work for lower bounding the inherently multipartite measure $E_m(\rho)$, due to the additional minimization over all bipartitions in each decomposition element of the convex roof.

C. *W* states

In order to demonstrate how our framework works let us start by deriving the explicit lower bound detecting the three-qubit W state $|W\rangle = \frac{1}{\sqrt{3}}(|001\rangle + |010\rangle + |100\rangle)$. For three-qubit states there are three bipartitions (1|23,2|13,3|12) and thus we have three linear entropies to look at in order to calculate $E_m(|\psi\rangle\langle\psi|)$,

$$\sqrt{S_L(\rho_1)} = 2\sqrt{|c_{001}c_{100} - c_{101}c_{000}|^2 + |c_{010}c_{100} - c_{110}c_{000}|^2 + (\cdots)}\,, \tag{3}$$

$$\sqrt{S_L(\rho_2)} = 2\sqrt{|c_{010}c_{100} - c_{110}c_{000}|^2 + |c_{010}c_{001} - c_{011}c_{000}|^2 + (\cdots)}\,, \tag{4}$$

$$\sqrt{S_L(\rho_3)} = 2\sqrt{|c_{001}c_{100} - c_{101}c_{000}|^2 + |c_{010}c_{001} - c_{011}c_{000}|^2 + (\cdots)}\,. \tag{5}$$

Now using $\sqrt{a^2+b^2} \geqslant \frac{1}{\sqrt{2}}(a+b)$ [which is a specific case of the inequality (A5) in Appendix A] and $|a-b| \geqslant |a| - |b|$, it is obvious that

$$\sqrt{S_L(\rho_1)} \geqslant \frac{2(|c_{001}c_{100}| - |c_{101}c_{000}| + |c_{010}c_{100}| - |c_{110}c_{000}|)}{\sqrt{2}}\,, \tag{6}$$

$$\sqrt{S_L(\rho_2)} \geqslant \frac{2(|c_{010}c_{100}| - |c_{110}c_{000}| + |c_{010}c_{001}| - |c_{011}c_{000}|)}{\sqrt{2}}\,, \tag{7}$$

$$\sqrt{S_l(\rho_3)} \geqslant \frac{2(|c_{001}c_{100}| - |c_{101}c_{000}| + |c_{010}c_{001}| - |c_{011}c_{000}|)}{\sqrt{2}}\,. \tag{8}$$

Then using $|ab| - \frac{1}{2}(a^2+b^2) \leqslant 0$ we can add one negative term for each entropy and it will still be a lower bound, i.e., we add $|c_{010}c_{001}| - \frac{1}{2}(|c_{010}|^2 + |c_{001}|^2)$ in the first lower bound, $|c_{100}c_{001}| - \frac{1}{2}(|c_{100}|^2 + |c_{001}|^2)$ in the second, and $|c_{010}c_{100}| - \frac{1}{2}(|c_{010}|^2 + |c_{100})|^2$ in the third. Then we can use that $\min[P - N_1, P - N_2, P - N_3] \geqslant P - N_1 - N_2 - N_3$ and end up with

$$\begin{aligned} E_m(|\psi\rangle\langle\psi|) \geqslant\ & \sqrt{2}(|c_{001}c_{100}| + |c_{001}c_{010}| + |c_{100}c_{010}|) \\ & - \frac{\sqrt{2}}{2}(|c_{010}|^2 + |c_{100}|^2 + |c_{001}|^2) \\ & - \sqrt{2}(|c_{101}c_{000}| + |c_{110}c_{000}| + |c_{011}c_{000}|)\,. \end{aligned} \tag{9}$$

Finally we can bound the convex roof using the following two relations:

$$\inf_{\{p_i,|\psi_i\rangle\}} \sum_i p_i \left| c^i_{\eta_1} c^i_{\eta_2} \right| \geqslant |\langle \eta_1|\rho|\eta_2\rangle| \,, \tag{10}$$

$$\inf_{\{p_i,|\psi_i\rangle\}} \sum_i p_i \left| c^i_{\eta_1} c^i_{\eta_2} \right| \leqslant \sqrt{\langle \eta_1|\rho|\eta_1\rangle\langle \eta_2|\rho|\eta_2\rangle} \,, \tag{11}$$

and end up with a lower bound for mixed states as

$$\begin{aligned} E_m(\rho) \geqslant \sqrt{2}(&|\langle 001|\rho|100\rangle| + |\langle 001|\rho|010\rangle| + |\langle 100|\rho|010\rangle|) \\ &- \frac{\sqrt{2}}{2}(\langle 010|\rho|010\rangle + \langle 100|\rho|100\rangle + \langle 001|\rho|001\rangle) \\ &- \sqrt{2}\sqrt{\langle 101|\rho|101\rangle\langle 000|\rho|000\rangle} \\ &- \sqrt{2}\sqrt{\langle 110|\rho|110\rangle\langle 000|\rho|000\rangle} \\ &- \sqrt{2}\sqrt{\langle 011|\rho|011\rangle\langle 000|\rho|000\rangle} \,. \end{aligned} \tag{12}$$

Surprisingly this leads directly to the nonlinear entanglement witness inequality presented in Refs. [20,21] up to a factor of $\sqrt{2}$. Using only simple algebraic relations, we have thus shown how to lower bound the convex roof construction. The first apparent strength of this lower bound is the limited number of density matrix elements needed to compute it. For example, in our exemplary three-qubit case only 10 out of possibly 64 elements need to be measured. Obviously we can extend the analysis using the same techniques to systems beyond three qubits.

III. A GENERAL CONSTRUCTION OF LOWER BOUNDS ON THE GME MEASURE E_m

Now we can generalize the connection of the three-qubit W-state witness and the measure E_m. Just as for three qubits we can always get lower bounds by summing the coefficient pairs $c_{\eta_1} c_{\eta_2}$ that belong to a certain target pure state and appear in some or all reduced linear entropies. The construction of such general lower bounds also starts by selecting a subset of coefficient pairs that will be translated into off-diagonal elements ρ_{η_1,η_2}, where (η_1,η_2) is the vector basis pair denoting the row and column of the element in density matrix ρ. We denote the selected vector basis pairs as $R := \{(\eta_1,\eta_2)\}$. Then we can repeat the steps analogously to Eqs. (6)–(11) and arrive at a general lower bound on the measure as the following theorem:

Theorem 1. A general lower bound on the GME measure. For a set of row-column pairs $R = \{(\eta_1,\eta_2)\}$, the genuine multipartite entanglement measure E_m has the following lower bound:

$$E_m \geqslant 2\sqrt{\frac{1}{|R| - N_R}} \left[\sum_{(\eta_1,\eta_2)\in R} \left(\left|\rho_{\eta_1\eta_2}\right| - \sum_{\gamma\in\Gamma(\eta_1,\eta_2)} \sqrt{\rho_{\eta_1^\gamma \eta_1^\gamma} \rho_{\eta_2^\gamma \eta_2^\gamma}} \right) - \left(\frac{1}{2} \sum_{\eta\in I(R)} N_\eta |\rho_{\eta\eta}| \right) \right] . \tag{13}$$

The right-hand side of Eq. (13) defines a GME witness $W_R(\rho)$, where $\rho_{\eta_1,\eta_2} := \langle \eta_1|\rho|\eta_2\rangle$, $(\eta_1^\gamma,\eta_2^\gamma) := P_\gamma(\eta_1,\eta_2)$, $\Gamma(\eta_1,\eta_2) := \{\gamma : (\eta_1^\gamma,\eta_2^\gamma) \notin R\}$, and $I(R) := \{\eta : \exists\eta'$ that (η',η) or $(\eta,\eta') \in R\}$ is the set of basis vectors η, which appear in the set R.

N_R is the maximal (or minimal) value of $|R^\gamma|$ over all possible bipartitions $\gamma|\bar{\gamma}$, where R^γ is the set of coefficient pairs $(c_{\eta_1},c_{\eta_2}) \in R$, which do not contribute to the γ-subsystem entropy.

N_η are normalization constants given by the maximal value of n_η^γ over all possible bipartitions $\gamma|\bar{\gamma}$, where n_η^γ is the number of coefficients c_η from some pairs in R, which are not counted in the γ-subsystem entropy (and how many are counted depends on whether one chooses N_R to be maximal or minimal). See Appendix B for the proof.

It is evident that not every choice of coefficient pairs will yield a useful lower bound, because one really needs to select those that are actually contributing to multipartite entanglement. There is, however, always an obvious choice. The set of coefficient pairs R must be chosen such that in every subsystem at least one of the elements of R contribute to the linear entropy of the reduced state. For example, in the case of GHZ states given in a specific basis $|\{\mathrm{GHZ}\rangle = \frac{1}{\sqrt{2}}(|0\rangle^{\otimes n} + |1\rangle^{\otimes n})$, one would choose the pair $(00\ldots0,11\ldots1)$, which contributes to all reduced entropies. In the general case, however, there is still some freedom of choice left to get a valid lower bound. For some sets R it can happen that the coefficients do not contribute to every subsystem entropy equally (which we show in an exemplary case in Sec. IV A). Then one can choose N_R in different ways, but in all considered cases we found that choosing it maximal or minimal will produce the best bounds (where choosing it maximal usually yields the tightest bounds close to pure states, whereas choosing it minimal improves the noise resistance). Since these coefficients are in general basis dependent, so is also our witness construction. The prefactor $\sqrt{\frac{1}{|R|-N_R}}$ suggests that the optimal basis for constructing such a lower bound is given by the minimal tensor rank representation of the pure state.

IV. APPLICATIONS AND EXAMPLES

A. Four-qubit singlet state

Let us illustrate how to apply Theorem 1 with an explicit example. In an experimental setting where one expects to produce a four-qubit singlet state (which was, e.g., discussed in the context of solving the liar detection problem in Ref. [22]), i.e.,

$$\begin{aligned} |S_4\rangle = \frac{1}{2\sqrt{3}}(&2|0011\rangle + 2|1100\rangle - |0110\rangle \\ &- |1001\rangle - |1010\rangle - |0101\rangle) \,, \end{aligned} \tag{14}$$

one is confronted with the following expected coefficients: $c_{0011}, c_{1100}, c_{0101}, c_{1010}, c_{0110}, c_{1001}$. Following the recipe of Theorem 1 we now select some coefficient pairs. We could choose, e.g., $R_1 = (0011,0101)$, $R_2 = (0011,1010)$, $R_3 = (0011,0110)$, and $R_4 = (0011,1001)$, such that

$R = \{R_1, R_2, R_3, R_4\}$. For this selection we use Theorem 1 to bound the GME measure. We see that in every subsystem at least two of these pairs appear naturally. Although there are more coefficient pairs, we now choose to only take into account two per subsystem entropy and thus choose N_R to be the minimal number of coefficient pairs in every subsystem, which gives $N_R = 2$. Thus we need to add negative terms that compensate for the missing terms just as we did in the three-qubit case, but now we need to do it two times in every subsystem. This results in the following individual prefactors N_η for the diagonal elements: $N_{0011} = 2$ (because this coefficient appears in two missing pairs in every subsystem), $N_{0101} = 1$, $N_{1001} = 1$, $N_{1010} = 1$, and $N_{0110} = 1$ (since those appear maximally once per subsystem entropy). Inserting this in Theorem 1 we end up with the lower bound as

$$\begin{aligned} E_m(\rho) \geqslant \frac{2}{\sqrt{2}}[&|\rho_{R_1}| + |\rho_{R_2}| + |\rho_{R_3}| + |\rho_{R_4}| \\ &- \sqrt{\rho_{0111,0111}\rho_{0001,0001}} - \sqrt{\rho_{0111,0111}\rho_{0010,0010}} \\ &- \sqrt{\rho_{1011,1011}\rho_{0001,0001}} - \sqrt{\rho_{1011,1011}\rho_{0010,0010}} \\ &- \frac{1}{2}(\rho_{0101,0101} + \rho_{1001,1001} + \rho_{1010,1010} + \rho_{0110,0110}) \\ &- \rho_{0011,0011}]\,. \end{aligned} \tag{15}$$

We have thus created a nonlinear witness function that lower bounds our measure. From an experimental point of view this is very favorable, because few local measurement settings suffice to ascertain the needed 13 density matrix elements (especially since the nine diagonal elements can be constructed from a single measurement setting). Of course we could also exploit the connection of our lower bound to the Dicke state witness $Q_2^{(2)}$ (which is discussed in Sec. IV C), which also detects GME in this state (although at the cost of more required measurements). In this case even the resistance to white noise is more favorable with our construction method, since for a state $\rho = p|S_4\rangle\langle S_4| + \frac{1-p}{16}\mathbb{1}$ this exemplary lower bound detects GME until $p = \frac{21}{29} \approx 0.72$, whereas the old witness construction yields a worse resistance up to $p = \frac{27}{35} \approx 0.77$. This shows the versatility of our general approach. By choosing certain coefficients one can tailor these lower bounds to specific experimental situations. If one is confronted with a low noise system it is always beneficial to choose as few coefficients as possible, such that very few local measurements suffice (even a number that is linear in the size of the system is often sufficient). Every additional measurement can then be included in the lower bound and improves the bound and its noise resistance if necessary.

B. Bipartite witnesses and lower bounds on the measure

Although we have presented our theorem and measures in the general case of n qudits, we can always apply the lower bounds also for $n = 2$, because our theorem holds for any n and d. Suppose we are given a bipartite qutrit system and want to lower bound the concurrence with only a few local measurements. If the expected state is, e.g., $|\psi\rangle = \frac{1}{\sqrt{3}}(|00\rangle + |11\rangle + |22\rangle)$ we can use the lower bounding procedure outlined above, yielding

$$\begin{aligned} E_m(\rho) \geqslant \frac{2}{\sqrt{3}}(&\mathrm{Re}[\,\langle 00|\rho|11\rangle\,] - \sqrt{\langle 01|\rho|01\rangle\,\langle |10\rho|10\rangle} \\ &+ \mathrm{Re}[\,\langle 00|\rho|22\rangle\,] - \sqrt{\langle 02|\rho|02\rangle\,\langle 20|\rho|20\rangle} \\ &+ \mathrm{Re}[\,\langle 11|\rho|22\rangle\,] - \sqrt{\langle 12|\rho|12\rangle\,\langle 21|\rho|21\rangle}\,). \end{aligned} \tag{16}$$

To determine the lower bound we have to measure nine different density matrix elements. Of course any density matrix element can always be obtained via local measurements. How these measurements can be performed in a basis consisting of a tensor product of the generalized Gell-Mann matrices we show explicitly in Appendix C.

It turns out that these nine different density matrix elements can be obtained via ten local measurement settings. Let us study the lower bound in the presence of noise. Suppose we have white noise in the system, i.e., $\rho = p|\psi\rangle\langle\psi| + \frac{1-p}{d}\mathbb{1}$. Calculating the lower bound results in $E_m(\rho) \geqslant \frac{2(4p-1)}{\sqrt{27}}$, which is equivalent to the analytical expression of Wootter's concurrence for these systems (as proven in Refs. [23,24]). In this case we have a necessary and sufficient entanglement criterion and a tight lower bound on the concurrence from ten local measurements for a special class of states. Indeed if one generalizes this example to arbitrary dimension d, we find that the bound is always tight for bipartite isotropic states.

C. Dicke states

We will now continue to show how this construction relates to an entanglement witness for the Dicke states, which involves multidimensional generalizations of the W states (which were first introduced in the context of laser emission in Ref. [25]).

In the original article [15], where this approach was first introduced, the authors connected the violation of a witness suitable for GHZ states (first introduced in Ref. [20] and later presented in a more general framework in Ref. [21]) with a lower bound on the measure E_m. We want to follow this approach and establish a general connection between a set of witnesses suitable for all generalized Dicke states introduced in Ref. [26] and generalized in Ref. [27]. To that end let us first introduce a concise notation for those states. Let α be a set containing specific subsystems of a multipartite state. We then define the state $|\alpha^l\rangle$ as a tensor product of states $|l\rangle$ for all subsystems not contained in α and excited states $|l+1\rangle$ in the subsystems contained in α. For example, for the four-partite state $|\{1,3\}^2\rangle$ we have $|3232\rangle$. Using this abbreviated notation we can define a generalized set of Dicke states, consisting of n d-dimensional subsystems, as

$$\left|D_m^d\right\rangle = \frac{1}{\sqrt{\binom{n}{m}(d-1)}} \sum_{l=0}^{d-2} \sum_{\alpha:|\alpha|=m} |\alpha^l\rangle\,, \tag{17}$$

where the parameter m denotes the number of excitations, with $0 < m < n$.

Since the explicit form of the nonlinear witness from Ref. [27] will be used in the following considerations we will repeat it in Appendix D. For all biseparable states this witness

$Q_m^{(d)}$ is strictly smaller than or equal to zero, i.e.,

$$Q(\rho) \leqslant 0 \Leftarrow \rho \text{ is biseparable}$$
$$Q(\rho) > 0 \Rightarrow \rho \text{ is multipartite entangled}.$$

Furthermore, the witness can also detect the "dimensionality" of GME, by which we mean the maximal number of degrees of freedom $f_\rho (f_\rho \leqslant d)$ that occurs in the pure states of an ensemble constituting ρ, minimized over all ensembles (this is the natural generalization of the concept of Schmidt number [28] to multipartite systems, further explored, e.g., in Ref. [27]). That is, the dimensionality is defined as

$$f_\rho := \inf_{\{p_i,|\psi_i\rangle\}} \max_i \{\min_\gamma [\text{rank}(\rho_\gamma)]\}. \tag{18}$$

Since

$$Q_m^{(d)}(\rho) \leqslant f_\rho - 1, \quad \forall\, \rho\,,$$

we can directly infer that

$$Q_m^{(d)}(\rho) > f - 2 \Rightarrow f_\rho \geqslant f.$$

In Fig. 1 we show how $Q_m^{(d)}$ detects the GME dimensionality. The maximal violation of these inequalities is always achieved for m-excitation Dicke states, i.e., $Q_m^{(d)}(|D_m^d\rangle\langle D_m^d|) = d - 1$.

If we can find a proper R, as a result of Theorem 1 that uses the Dicke state coefficients, we can connect a lower bound of the measure E_m with the GME witness $Q_m^{(d)}(\rho)$. Indeed choosing the ordered subset R_σ of the set of coefficients σ used in Eq. (D1), i.e.,

$$R_\sigma = \{(\alpha^a, \beta^b) \in \sigma : a \leqslant b\}\,,$$

we immediately arrive at a lower bound on E_m as

$$E_m(\rho) \geqslant m\sqrt{\frac{1}{|R_\sigma| - N_{R_\sigma}}}\, Q_m^{(d)}(\rho) \geqslant m\sqrt{\frac{1}{|R_\sigma|}}\, Q_m^{(d)}(\rho), \tag{19}$$

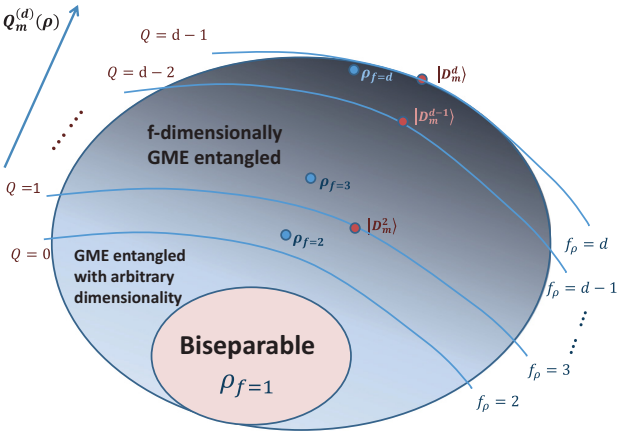

FIG. 1. (Color online) The witness $Q_m^{(d)}$ can quantify the genuine multipartite entanglement with the GME dimensionality f_ρ, where $f_\rho \leqslant d$. A state is biseparable if and only if $f_\rho = 1$, and GM entangled if and only if $f_\rho \geqslant 2$. For Dicke states it holds that $Q_m^{(d)}(|D_m^f\rangle\langle D_m^f|) = f_\rho - 1$.

where $|R_\sigma| = \frac{1}{2}(d-1)^2 \binom{n}{m} m(n-m)$. In this case $N_\eta \leqslant m(n-m-1) + \Theta(d-3)(n-m)$, where Θ is a Heaviside step function.

D. PPT witness and our witness

Using the result on entanglement across bipartitions from the previous section we can explore the relation of our lower bounds to other bipartite entanglement witnesses. In our witness construction, the permutation operator P_γ acting on a pure state is a $\gamma|\bar{\gamma}$-partial transpose operator, i.e., $P_\gamma|\psi\rangle\langle\psi| = (|\psi\rangle\langle\psi|)^{T_{\gamma|\bar{\gamma}}}$ (in the sense that our permutation operator now acts upon the index pairs of the coefficients of the pure state). It is thus intuitive to believe that there is certain connection between our witness and a PPT witness [29]. Indeed our witnesses are related to a standard PPT-witness construction [where the witnesses separate the convex set of states that are positive under partial transpose (PPT) from its complement]. For example, for diagonal GHZ states we can use the standard PPT-witness construction which goes as follows. For $|\text{GHZ}_{\eta_1,\eta_2}\rangle := \frac{1}{\sqrt{2}}(|\eta_1\rangle + |\eta_2\rangle)$ with $\eta_1 + \eta_2 = (d-1, \ldots, d-1)$, we can use the eigenvector belonging to the negative eigenvalue of the $\gamma|\bar{\gamma}$-partial transposed $|\text{GHZ}_{\eta_1,\eta_2}\rangle\langle\text{GHZ}_{\eta_1,\eta_2}|^{T_\gamma}$ which we denote as $|\lambda^-_{\eta_1,\eta_2}\rangle = \frac{1}{\sqrt{2}}(|\eta_1^\gamma\rangle - |\eta_2^\gamma\rangle)$. One can then construct the PPT witness and write its expectation value as

$$\Omega_{\text{PPT}}^{\gamma|\bar{\gamma}}\left(\rho, |\lambda^-_{\eta_1,\eta_2}\rangle\right) = \text{Tr}\left(|\lambda^-_{\eta_1,\eta_2}\rangle\langle\lambda^-_{\eta_1,\eta_2}|^{T_{\gamma|\bar{\gamma}}}\rho\right), \tag{20}$$

For instance in the three-qubit case,

$$|\lambda^-_{001,110}\rangle\langle\lambda^-_{001,110}|^{T_{1|23}} = \frac{1}{2}\begin{pmatrix} 0 & 0 & \cdots & \cdots & 0 & 0 \\ & 0 & & & -1 & \\ & & 1 & 0 & & \\ \vdots & & & & & \vdots \\ \vdots & & 0 & 0 & & \vdots \\ & & 0 & 0 & & \\ & -1 & & & 0 & \\ 0 & & \cdots & \cdots & & 0 \end{pmatrix}. \tag{21}$$

With the PPT-witness construction in Eq. (20) we end up with the following PPT-witness expectation value:

$$\Omega_{\text{PPT}}^{\gamma|\bar{\gamma}}(\rho, |\lambda^-_{\text{GHZ}}\rangle) = \tfrac{1}{2}\left(\rho_{\eta_1^\gamma\eta_1^\gamma} + \rho_{\eta_2^\gamma\eta_2^\gamma}\right) - \text{Re}\left(\rho_{\eta_1\eta_2}\right). \tag{22}$$

Under the fixed bipartition $\gamma|\bar{\gamma}$, we construct our witness by choosing $R = (\eta_1, \eta_2)$ as

$$-W^\gamma_{(\eta_1,\eta_2)}(\rho) = \sqrt{\rho_{\eta_1^\gamma\eta_1^\gamma}\rho_{\eta_2^\gamma\eta_2^\gamma}} - \left|\rho_{\eta_1\eta_2}\right|. \tag{23}$$

It is obvious that $-W^\gamma_{(\eta_1,\eta_2)}(\rho) \leqslant \Omega_{\text{PPT}}^{\gamma|\bar{\gamma}}(\rho, |\lambda_{\text{GHZ}}\rangle)$. Hence we say that the witness $W_R(\rho)$ is stronger than the PPT witness $\Omega_{\text{PPT}}^{\gamma|\bar{\gamma}}(\rho, |\lambda^-_{\eta_1,\eta_2}\rangle)$.

The relation between our witness, the PPT witness, and the PPT-convex set is illustrated in Fig. 2. For clearness we just draw two PPT witnesses in the figure. For the n-qudit case there are $\frac{1}{2}d^n$ such eigenvectors $|\lambda^-_{\eta_1,\eta_2}\rangle$, corresponding to negative

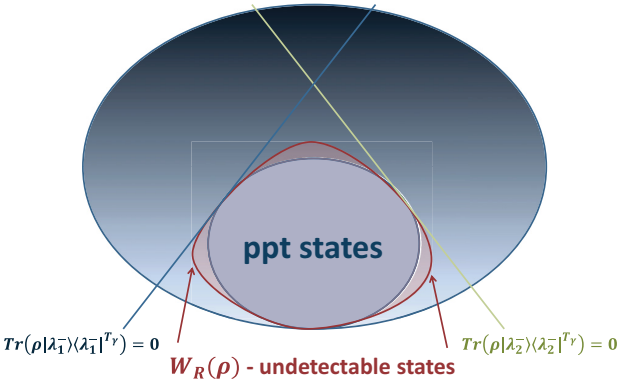

FIG. 2. (Color online) PPT witness compared to our lower bounds [given in terms of the nonlinear witness $W_R(\rho)$]. The set of $W_R(\rho)$ undetectable states denotes the set that is not detected by one specific $W_R(\rho)$ and is strictly larger than the set of PPT states. However, the set of states detected by $W_R(\rho)$ is strictly larger than the set detected by any standard PPT witness.

eigenvalues. Every witness $\Omega^{\gamma|\bar{\gamma}}_{\mathrm{PPT}}(\rho, |\lambda^-_{\eta_1,\eta_2}\rangle)$ is tangent to the set of PPT states (i.e., there exists one PPT state for which the witness yields zero). However, also our witness $W_R(\rho)$ is zero for all these PPT states; i.e., our new witness detects more states than the traditional PPT witness.

V. CONCLUSIONS

In conclusion we have presented a method to derive lower bounds on a measure of genuine multipartite entanglement. We show that in experimentally plausible scenarios (i.e., one knows which state one aims to produce) we can derive such lower bounds simply based on coefficients of the corresponding pure states. We also connected the lower bound construction to a framework of nonlinear entanglement witnesses developed in Refs. [20,21,25–27]. These witnesses are experimentally feasible in terms of required local measurement settings. We provide further evidence in the bipartite case, where we also show that for certain families of mixed states our lower bounds are tight.

Some open questions remain, such as whether this general construction method will work for all kinds of states and how it can be generalized beyond just multi- and bipartite entanglement, but anything in between. We want to point out that recently also other authors have used a similar approach to bound this measure in the bipartite case [23] and for multipartite W states [30].

ACKNOWLEDGMENTS

We thank the QCI group in Bristol and Matteo Rossi for discussions. J.Y.W., H.K., and D.B. acknowledge the financial support of DFG (Deutsche Forschungsgemeinschaft). M.H. gratefully acknowledges support from the EC-project IP "Q-Essence" and the ERC Advanced Grant "IRQUAT."

APPENDIX A: PROOFS OF THE FORMULAS USED IN THE PAPER

1. Reduced linear entropy of pure states

Let $|\psi\rangle = \sum_{\eta\in\mathbb{N}_d^{\otimes n}} c_\eta|\eta\rangle$ be an n-qudit pure state. The linear entropy of $|\psi\rangle$ can be written as

$$S_L(\rho_\gamma) = \sum_{\eta_1\neq\eta_2,\in\mathbb{N}_{d^n}} \left|c_{\eta_1}c_{\eta_2} - c_{\eta_1^\gamma}c_{\eta_2^\gamma}\right|^2, \tag{A1}$$

where $(\eta_1^\gamma,\eta_2^\gamma) = P_\gamma(\eta_1,\eta_2)$.

Proof. The linear entropy regarding a specific partition $\gamma|\bar{\gamma}$ is defined as $S_L(\rho_\gamma) = 2[1-\mathrm{tr}(\rho_\gamma^2)]$, where ρ_γ is the γ-reduced matrix of ρ. The trace of ρ_γ is $\mathrm{tr}(\rho_\gamma^2) = \sum_{\alpha_1,\alpha_2\in H_\gamma}(\rho_\gamma)_{\alpha_1\alpha_2}(\rho_\gamma)_{\alpha_2\alpha_1}$, where H_γ is the subspace of the reduction γ. We separate the summation into diagonal and off-diagonal parts. For the diagonal part we use the normalization condition to evaluate its value:

$$\begin{aligned}
\mathrm{tr}\left(\rho_\gamma^2\right) &= \sum_{\alpha_1=\alpha_2}(\rho_\gamma)^2_{\alpha_1\alpha_1} + \sum_{\alpha_1\neq\alpha_2}(\rho_\gamma)_{\alpha_1\alpha_2}(\rho_\gamma)_{\alpha_2\alpha_1}\\
&= \left(\sum_\alpha(\rho_\gamma)_{\alpha\alpha}\right)^2 - \sum_{\alpha_1\neq\alpha_2}(\rho_\gamma)_{\alpha_1\alpha_1}(\rho_\gamma)_{\alpha_2\alpha_2}\\
&\quad + \sum_{\alpha_1\neq\alpha_2}(\rho_\gamma)_{\alpha_1\alpha_2}(\rho_\gamma)_{\alpha_2\alpha_1}\\
&= 1 - \sum_{\substack{\alpha_1\neq\alpha_2\in H_\gamma\\ \beta_1,\beta_2\in H_{\bar{\gamma}}}}\left|c_{\alpha_1\otimes\beta_1}\right|^2\left|c_{\alpha_2\otimes\beta_2}\right|^2\\
&\quad + \sum_{\substack{\alpha_1\neq\alpha_2\in H_\gamma\\ \beta_1,\beta_2\in H_{\bar{\gamma}}}} c_{\alpha_1\otimes\beta_1}c^*_{\alpha_2\otimes\beta_1}c_{\alpha_2\otimes\beta_2}c^*_{\alpha_1\otimes\beta_2}.
\end{aligned} \tag{A2}$$

By exchanging the indices α_1 and α_2 one has

$$\begin{aligned}
\mathrm{tr}\left(\rho_\gamma^2\right) &= 1 - \frac{1}{2}\sum_{\substack{\alpha_1\neq\alpha_2\in H_\gamma\\ \beta_1,\beta_2\in H_{\bar{\gamma}}}}\left|c_{\alpha_1\otimes\beta_1}c_{\alpha_2\otimes\beta_2} - c_{\alpha_1\otimes\beta_2}c_{\alpha_2\otimes\beta_1}\right|^2\\
&= 1 - \frac{1}{2}\sum_{\eta_1,\eta_2\in\mathbb{N}_{d^n}}\left|c_{\eta_1}c_{\eta_2} - c_{\eta_1^\gamma}c_{\eta_2^\gamma}\right|^2,
\end{aligned} \tag{A3}$$

where $\eta = \alpha\otimes\beta$ and $(\eta_1^\gamma,\eta_2^\gamma) = P_\gamma(\eta_1,\eta_2)$. The linear entropy is then calculated to

$$S_L(\rho_\gamma) = \sum_{\eta_1\neq\eta_2,\in\mathbb{N}_{d^n}}\left|c_{\eta_1}c_{\eta_2} - c_{\eta_1^\gamma}c_{\eta_2^\gamma}\right|^2. \tag{A4}$$

■

2. An important inequality

The following is an inequality, which is crucial for the derivation of the prefactor $\sqrt{\frac{1}{|R|-N_R}}$ in Theorem 1:

$$|I|\sum_{i\in I}|a_i|^2 \geqslant \left|\sum_{i\in I}a_i\right|^2. \tag{A5}$$

Proof. We prove this inequality by constructing two vectors as follows (using $|I| = n$):

$$\vec{x} = \begin{pmatrix} \left.\begin{matrix} a_1 \\ \vdots \\ a_1 \end{matrix}\right\} n \text{ times} \\ \vdots \\ \left.\begin{matrix} a_n \\ \vdots \\ a_n \end{matrix}\right\} n \text{ times} \end{pmatrix}, \quad \vec{y} = \begin{pmatrix} a_1^* \\ \vdots \\ a_n^* \\ \vdots \\ a_1^* \\ \vdots \\ a_n^* \end{pmatrix}. \tag{A6}$$

The right-hand side of Eq. (A5) can be written as the scalar product of $\vec{x}$ and $\vec{y}$:

$$\left|\sum_{i\in I} a_i\right|^2 = \sum_{i,j\in I} a_i a_j^* = |\vec{x}\cdot\vec{y}|. \tag{A7}$$

According to the Cauchy-Schwarz inequality, one can derive

$$|I|\sum a_i^2 = |\vec{x}|\cdot|\vec{y}| \geqslant |\vec{x}\cdot\vec{y}| = \left|\sum_{i\in I} a_i\right|^2. \tag{A8}$$

■

APPENDIX B: PROOF OF THEOREM 1 AND APPROACH OF CONSTRUCTION OF A GME WITNESS

First, one can estimate the lower bound on $S_L(\rho_\gamma)$ by summing its elements over a selected region R, and dropping the other non-negative summands (i.e., lower bounding them with 0),

$$\begin{aligned} S_L\left(\rho_\gamma^i\right) &\geqslant 4 \sum_{(\eta_1,\eta_2)\in R} \left|c_{\eta_1}^i c_{\eta_2}^i - c_{\eta_1^\gamma}^i c_{\eta_2^\gamma}^i\right|^2 \\ &= 4 \sum_{(\eta_1,\eta_2)\in R\setminus R^\gamma} \left|c_{\eta_1}^i c_{\eta_2}^i - c_{\eta_1^\gamma}^i c_{\eta_2^\gamma}^i\right|^2. \end{aligned} \tag{B1}$$

Here we add a prefactor 4 in Eq. (B1), since the symmetric factor of all (η_1,η_2) equals 4. That means for every (η_1,η_2) there are three other $(\tilde{\eta}_1,\tilde{\eta}_2)$ having the same value of $|c_{\tilde{\eta}_1} c_{\tilde{\eta}_2} - c_{\tilde{\eta}_1^\gamma} c_{\tilde{\eta}_2^\gamma}|$ as (η_1,η_2). Here we choose a nondegenerate vector basis set R, and therefore need a prefactor 4 in the lower bound. The set R^γ is the subset of R, whose elements do not contribute to the linear entropy, i.e., $R^\gamma := \{(\eta_1,\eta_2)\in R : (\eta_1^\gamma,\eta_2^\gamma) = (\eta_1,\eta_2) \text{ or } (\eta_2,\eta_1)\}$. Now we use the inequality (A5) to bound the square root of $S_L(\rho_\gamma^i)$:

$$S_L\left(\rho_\gamma^i\right) \geqslant \frac{4}{|R\setminus R^\gamma|}\left(\sum_{\eta_1,\eta_2\in R} \left|c_{\eta_1}^i c_{\eta_2}^i - P_\gamma c_{\eta_1}^i c_{\eta}^i\right|\right)^2, \tag{B2}$$

$$\Downarrow$$

$$\sqrt{S_L\left(\rho_\gamma^i\right)} \geqslant 2\sqrt{\frac{1}{|R|-|R^\gamma|}} \sum_{(\eta_1,\eta_2)\in R} \left|c_{\eta_1}^i c_{\eta_2}^i - c_{\eta_1^\gamma}^i c_{\eta_2^\gamma}^i\right|. \tag{B3}$$

According to Eq. (IIA) together with Eq. (B3), the lower bound reads

$$\begin{aligned} E_m \geqslant 2 \inf_{\{p_i,|\psi_i\rangle\}} &\sum_i p_i \\ &\times \left[\sqrt{\frac{1}{|R|-|R^{\gamma_i}|}} \sum_{\eta_1,\eta_2\in R} \left(\left|c_{\eta_1}^i c_{\eta_2}^i\right| - \left|c_{\eta_1^{\gamma_i}}^i c_{\eta_2^{\gamma_i}}^i\right|\right)\right], \end{aligned} \tag{B4}$$

where γ_i is the partition in which the linear entropy $S_L(|\psi_i\rangle\langle\psi_i|_\gamma)$ of $|\psi_i\rangle\langle\psi_i|$ has its minimum. By defining the normalization factor $N_R := \min_\gamma |R^\gamma|$, which is the minimal value of $|R^\gamma|$ over all possible bipartitions $\{\gamma|\bar{\gamma}\}$, we can extract the prefactor from the convex roof summation.

$$\begin{aligned} E_m \geqslant 2\sqrt{\frac{1}{|R|-N_R}} \inf_{\{p_i,|\psi_i\rangle\}} &\sum_i p_i \\ &\times \left[\sum_{\eta_1,\eta_2\in R} \left(\left|c_{\eta_1}^i c_{\eta_2}^i\right| - \left|c_{\eta_1^{\gamma_i}}^i c_{\eta_2^{\gamma_i}}^i\right|\right)\right]. \end{aligned} \tag{B5}$$

The most difficult part of detecting entanglement of mixed states is a result of the mixing of the decomposition coefficients $c_{\eta_1}^i c_{\eta_2}^i$. In the laboratory we have only the information about the mixed density matrix element $\rho_{\eta_1\eta_2}$ but not $c_{\eta_1}^i c_{\eta_2}^i$, therefore we must exchange the two summations in Eq. (B5), and mix the coefficients $c_{\eta_1}^i c_{\eta_2}^i$ into density matrix elements. Therefore we estimate the summands with a bound, which is independent of the specific partition $\gamma_i|\bar{\gamma}_i$, by adding a summation of nonpositive terms $\sum_{R^{\gamma_i}}[|c_{\eta_1}^i c_{\eta_2}^i| - \frac{1}{2}(|c_{\eta_1}^i|^2 + |c_{\eta_2}^i|^2)]$ into the summands:

$$\begin{aligned} &\sum_{(\eta_1,\eta_2)\in R\setminus R^{\gamma_i}} \left(\left|c_{\eta_1}^i c_{\eta_2}^i\right| - \left|c_{\eta_1^{\gamma_i}}^i c_{\eta_2^{\gamma_i}}^i\right|\right) \\ &\quad\geqslant \sum_{(\eta_1,\eta_2)\in R}\left(\left|c_{\eta_1}^i c_{\eta_2}^i\right| - \sum_{\gamma\in\Gamma(\eta_1,\eta_2)} \left|c_{\eta_1^\gamma}^i c_{\eta_2^\gamma}^i\right|\right) \\ &\quad\quad - \frac{1}{2}\sum_{R^{\gamma_i}} \left(\left|c_{\eta_1}^i\right|^2 + \left|c_{\eta_2}^i\right|^2\right) \\ &\quad\geqslant \sum_{(\eta_1,\eta_2)\in R}\left(\left|c_{\eta_1}^i c_{\eta_2}^i\right| - \sum_{\gamma\in\Gamma(\eta_1,\eta_2)} \left|c_{\eta_1^\gamma}^i c_{\eta_2^\gamma}^i\right|\right) \\ &\quad\quad - \frac{1}{2}\sum_{\eta\in I(R)} n_\eta^{\gamma_i}\left|c_\eta^i\right|^2, \end{aligned} \tag{B6}$$

where $I(R) := \{\eta\in\mathbb{N}_d^{\otimes n} : \exists(\eta,\eta') \text{ or } (\eta',\eta)\in R\}$ is the set of indices contained in the set R, $\Gamma(\eta_1,\eta_2) = \{\gamma|P(\eta_1,\eta_2)\notin R\}$, and $n_\eta^{\gamma_i}$ is the number of vector pairs in R^{γ_i} containing index η. To eliminate the dependence of the partition γ^i, we define the maximal value of n_η^γ over all possible partitions $\{\gamma|\bar{\gamma}\}$ as $N_\eta := \max_\gamma n_\eta^\gamma$. Then one can estimate the GME measure with Eqs. (B5) and (B6) as

$$\begin{aligned} E_m(\rho) \geqslant 2\sqrt{\frac{1}{|R|-N_R}} \sum_{\eta_1,\eta_2\in R} \Bigg[&\inf_{\{p_i,\psi_i\}} \sum_i p_i \\ &\times \left(\left|c_{\eta_1}^i c_{\eta_2}^i\right| - \sum_{\gamma\in\Gamma(\eta_1,\eta_2)} \left|c_{\eta_1^\gamma}^i c_{\eta_2^\gamma}^i\right|\right) - \frac{1}{2}\sum_{\eta\in I(R)} N_\eta \left|c_\eta^i\right|^2\Bigg]. \end{aligned} \tag{B7}$$

Now one can safely exchange the summation in Eq. (B7) and lower bound it with the triangle inequality (i.e., $\sum_{p_i} p_i|c_{\eta_1}^i c_{\eta_2}^i| \geqslant |\rho_{\eta_1\eta_2}|$) and the Cauchy-Schwarz inequality (i.e., $\sum_{p_i} p_i|c_{\eta_1^\gamma}^i c_{\eta_2^\gamma}^i| \leqslant \sqrt{\rho_{\eta_1^\gamma\eta_1^\gamma}\rho_{\eta_2^\gamma\eta_2^\gamma}}$). Finally we arrive at the

result

$$E_m(\rho) \geqslant 2\sqrt{\frac{1}{|R| - N_R}}\left[\sum_{\eta_1,\eta_2\in R\text{-}}\left(\left|\rho_{\eta_1\eta_2}\right| - \sum_{\gamma\in\Gamma(\eta_1,\eta_2)}\sqrt{\rho_{\eta_1^\gamma\eta_1^\gamma}\rho_{\eta_2^\gamma\eta_2^\gamma}}\right) - \frac{1}{2}\sum_{\eta\in I(R)} N_\eta\rho_{\eta\eta}\right], \tag{B8}$$

where $\rho_{\eta_1\eta_2} := \langle\eta_1|\rho|\eta_2\rangle$.

Above is the proof of Theorem 1 in the case of $N_R := \min_\gamma |R^\gamma|$. For the choice of $N_R := \max_\gamma |R^\gamma|$, one just needs to calculate $\max_\gamma |R^\gamma|$ at the first step, i.e., Eq. (B1), then pick up $|R| - \max_\gamma |R^\gamma|$ elements from $R\backslash R^\gamma$ as the summation region in the second line and then repeat the whole proof above. At the end we will attain the same expression for the lower bound on E_m as Eq. (B8), but with different N_η from the ones before $N_R = \min_\gamma |R^\gamma|$. N_η in this maximum choice is greater or equal to the one derived in the minimal case. In the four-qubit singlet example in Sec. IV A, the value of N_η is exactly the same for both choices. Therefore we choose the maximum, i.e., $N_R = 2$, to get a tighter lower bound on E_m.

APPENDIX C: EXPLICIT DECOMPOSITION OF THE BIPARTITE WITNESS INTO LOCAL OBSERVABLES

The measurements needed to ascertain the relevant density matrix elements in the bipartite scenario can be performed in a basis consisting of a tensor product of the generalized Gell-Mann matrices. We continue to provide for each of the density matrix elements above their respective coefficients. The density matrix elements are either off-diagonal elements or diagonal elements. The off-diagonal elements can be obtained by expectation values of the symmetric and antisymmetric generalized Gell-Mann matrices:

$$\Lambda_s^{12} = \begin{pmatrix}0&1&0\\1&0&0\\0&0&0\end{pmatrix}, \quad \Lambda_s^{13} = \begin{pmatrix}0&0&1\\0&0&0\\1&0&0\end{pmatrix}, \quad \Lambda_s^{23} = \begin{pmatrix}0&0&0\\0&0&1\\0&1&0\end{pmatrix}, \tag{C1}$$

$$\Lambda_a^{12} = \begin{pmatrix}0&-i&0\\i&0&0\\0&0&0\end{pmatrix}, \quad \Lambda_a^{13} = \begin{pmatrix}0&0&-i\\0&0&0\\i&0&0\end{pmatrix}, \quad \Lambda_a^{23} = \begin{pmatrix}0&0&0\\0&0&-i\\0&-i&0\end{pmatrix}. \tag{C2}$$

They can be written as follows:

$$\mathrm{Re}\left[\langle 00|\rho|11\rangle\right] = \tfrac{1}{2}\left\langle\Lambda_s^{12}\otimes\Lambda_s^{12} - \Lambda_a^{12}\otimes\Lambda_a^{12}\right\rangle, \tag{C3}$$

$$\mathrm{Re}\left[\langle 00|\rho|22\rangle\right] = \tfrac{1}{2}\left\langle\Lambda_s^{13}\otimes\Lambda_s^{13} - \Lambda_a^{13}\otimes\Lambda_a^{13}\right\rangle, \tag{C4}$$

$$\mathrm{Re}\left[\langle 11|\rho|22\rangle\right] = \tfrac{1}{2}\left\langle\Lambda_s^{23}\otimes\Lambda_s^{23} - \Lambda_a^{23}\otimes\Lambda_a^{23}\right\rangle. \tag{C5}$$

We now consider the terms obtained via the diagonal generalized Gell-Mann matrices. $\Lambda_d^0 = \left(\begin{smallmatrix}1&0&0\\0&1&0\\0&0&1\end{smallmatrix}\right)$, $\Lambda_d^1 = \left(\begin{smallmatrix}1&0&0\\0&-1&0\\0&0&0\end{smallmatrix}\right)$, $\Lambda_d^2 = \frac{1}{\sqrt{3}}\left(\begin{smallmatrix}1&0&0\\0&1&0\\0&0&-2\end{smallmatrix}\right)$. We will expand the sought-after terms into coefficients, utilizing the following basis:

$$b = \begin{pmatrix}\Lambda_d^0&\otimes&\Lambda_d^0\\ \Lambda_d^0&\otimes&\Lambda_d^1\\ \Lambda_d^0&\otimes&\Lambda_d^2\\ \Lambda_d^1&\otimes&\Lambda_d^0\\ \Lambda_d^1&\otimes&\Lambda_d^1\\ \Lambda_d^1&\otimes&\Lambda_d^2\\ \Lambda_d^2&\otimes&\Lambda_d^0\\ \Lambda_d^2&\otimes&\Lambda_d^1\\ \Lambda_d^2&\otimes&\Lambda_d^2\end{pmatrix}. \tag{C6}$$

For further reference the coefficients are given as

$$\langle 01|\rho|01\rangle = \left\langle b * \left(\frac{1}{9},\frac{1}{6},\frac{1}{6\sqrt{3}},-\frac{1}{6},-\frac{1}{4},-\frac{1}{8\sqrt{3}},\frac{1}{6\sqrt{3}},\frac{1}{4\sqrt{3}},\frac{1}{12}\right)\right\rangle,$$

$$\langle 10|\rho|10\rangle = \left\langle b * \left(\frac{1}{9},-\frac{1}{6},\frac{1}{6\sqrt{3}},\frac{1}{6},-\frac{1}{4},\frac{1}{8\sqrt{3}},\frac{1}{6\sqrt{3}},-\frac{1}{4\sqrt{3}},\frac{1}{12}\right)\right\rangle,$$

$$\langle 02|\rho|02\rangle = \left\langle b * \left(\frac{1}{9},\frac{1}{6},\frac{1}{6\sqrt{3}},0,0,0,-\frac{1}{3\sqrt{3}},-\frac{1}{2\sqrt{3}},-\frac{1}{6}\right)\right\rangle,$$
$$\langle 20|\rho|20\rangle = \left\langle b * \left(\frac{1}{9},0,-\frac{1}{3\sqrt{3}},\frac{1}{6},0,-\frac{1}{4\sqrt{3}},\frac{1}{6\sqrt{3}},0,-\frac{1}{6}\right)\right\rangle,$$
$$\langle 12|\rho|12\rangle = \left\langle b * \left(\frac{1}{9},-\frac{1}{6},\frac{1}{6\sqrt{3}},0,0,0,-\frac{1}{3\sqrt{3}},\frac{1}{2\sqrt{3}},-\frac{1}{6}\right)\right\rangle,$$
$$\langle 21|\rho|21\rangle = \left\langle b * \left(\frac{1}{9},0,-\frac{3}{3\sqrt{3}},-\frac{1}{6},0,\frac{1}{4\sqrt{3}},\frac{1}{6\sqrt{3}},0,-\frac{1}{6}\right)\right\rangle.$$

APPENDIX D: EXPLICIT FORM OF THE GME WITNESS $Q_m^{(d)}$

Here we recall the explicit form of the nonlinear witness from Ref. [27]. Using the notation for Dicke states introduced in Sec. IV C we arrive at the following lower bound:

$$Q_m^{(d)} = \frac{1}{m}\left[\sum_{l,l'=0}^{d-2}\sum_{\sigma}\left(|\langle\alpha^l|\rho|\beta^{l'}\rangle| - \sum_{\delta\in\Delta}\sqrt{\langle\alpha^l|\otimes\langle\beta^{l'}|P_\delta^\dagger\rho^{\otimes 2}P_\delta|\alpha^l\rangle\otimes|\beta^{l'}\rangle}\right) - N_D\sum_{l=0}^{d-2}\sum_{\alpha}\langle\alpha^l|\rho|\alpha^l\rangle\right], \tag{D1}$$

with

$$m\in\{1,\ldots,\lfloor n/2\rfloor\},\quad N_D=(d-1)\,m\,(n-m-1),\quad \sigma:=\{(\alpha,\beta):|\alpha\cap\beta|=m-1\},\quad \Delta:=\begin{cases}\alpha, & l'=l\\ \{\delta|\delta\subset\overline{\alpha\backslash\beta}\}, & l'<l\\ \{\delta|\delta\subset\overline{\beta\backslash\alpha}\}, & l'>l\end{cases}. \tag{D2}$$

The properties of this witness are discussed in the main text.

[1] R. Horodecki, P. Horodecki, M. Horodecki, and K. Horodecki, Rev. Mod. Phys. **81**, 865 (2009).
[2] R. Raussendorf and H.-J. Briegel, Phys. Rev. Lett. **86**, 5188 (2001).
[3] D. Bruß and C. Macchiavello, Phys. Rev. A **83**, 052313 (2011).
[4] S. Schauer, M. Huber, and B. C. Hiesmayr, Phys. Rev. A **82**, 062311 (2010).
[5] D. Akoury *et al.*, Science **318**, 949 (2007).
[6] D. Bruß, N. Datta, A. Ekert, L. C. Kwek, and C. Macchiavello, Phys. Rev. A **72**, 014301 (2005).
[7] S. M. Giampaolo, G. Gualdi, A. Monras, and F. Illuminati, Phys. Rev. Lett. **107**, 260602 (2011).
[8] E. M. Gauger, E. Rieper, J. J. L. Morton, S. C. Benjamin, and V. Vedral, Phys. Rev. Lett. **106**, 040503 (2011).
[9] A. Acin, D. Bruß, M. Lewenstein, and A. Sanpera, Phys. Rev. Lett. **87**, 040401 (2001).
[10] L. Gurvits, in *Proceedings of the 35th ACM Symposium on Theory of Computing* (ACM, New York, 2003), p. 10.
[11] O. Gühne and G. Toth, Phys. Rep. **474**, 1 (2009).
[12] P. Horodecki, Phys. Rev. A **68**, 052101 (2003).
[13] O. Gühne and Norbert Lütkenhaus, Phys. Rev. Lett. **96**, 170502 (2006).
[14] B. Jungnitsch, T. Moroder, and O. Gühne, Phys. Rev. Lett. **106**, 190502 (2011).
[15] Z.-H. Ma, Z.-H. Chen, J.-L. Chen, Ch. Spengler, A. Gabriel, and M. Huber, Phys. Rev. A **83**, 062325 (2011).
[16] D. T. Pope and G. J. Milburn, Phys. Rev. A **67**, 052107 (2003).
[17] P. Love *et al.*, Quant. Inf. Proc. **6**, 187 (2007).
[18] B. C. Hiesmayr and M. Huber, Phys. Rev. A **78**, 012342 (2008).
[19] B. C. Hiesmayr, M. Huber, and Ph. Krammer, Phys. Rev. A **79**, 062308 (2009).
[20] O. Gühne and M. Seevinck, New J. Phys. **12**, 053002 (2010).
[21] M. Huber, F. Mintert, A. Gabriel, and B. C. Hiesmayr, Phys. Rev. Lett. **104**, 210501 (2010).
[22] A. Cabello, Phys. Rev. A **68**, 012304 (2003).
[23] S. M. Hashemi Rafsanjani and S. Agarwal, arXiv:1204.3912 [quant-ph].
[24] P. Rungta and C. M. Caves, Phys. Rev. A **67**, 012307 (2003).
[25] R. H. Dicke, Phys. Rev. **93**, 99 (1954).
[26] M. Huber, P. Erker, H. Schimpf, A. Gabriel, and B. C. Hiesmayr, Phys. Rev. A **83**, 040301(R) (2011).
[27] Ch. Spengler, M. Huber, A. Gabriel and B. C. Hiesmayr, Quant. Inf. Proc. (2012), doi: 10.1007/s11128-012-0369-8.
[28] B. M. Terhal and P. Horodecki, Phys. Rev. A **61**, 040301 (2000).
[29] M. Lewenstein, B. Kraus, J. I. Cirac, and P. Horodecki, Phys. Rev. A **62**, 052310 (2000).
[30] Z.-H. Ma, Z.-H. Chen, J.-L. Chen, and S. Severini, Phys. Rev. A **85**, 062320 (2012).

PHYSICAL REVIEW A **89**, 052335 (2014)

Randomized graph states and their entanglement properties

Jun-Yi Wu,[1] Matteo Rossi,[2] Hermann Kampermann,[1] Simone Severini,[3]
Leong Chuan Kwek,[4] Chiara Macchiavello,[2] and Dagmar Bruß[1]
[1]*Institut für Theoretische Physik III, Heinrich-Heine-Universität Düsseldorf, D-40225 Düsseldorf, Germany*
[2]*Dipartimento di Fisica and INFN-Sezione di Pavia, via Bassi 6, 27100 Pavia, Italy*
[3]*Department of Computer Science, University College London, Gower Street, London WC1E 6BT, United Kingdom*
[4]*Centre for Quantum Technologies, National University of Singapore, 3 Science Drive 2, Singapore 117543, Singapore*
(Received 15 March 2014; published 30 May 2014)

We introduce a class of mixed multiqubit states, that corresponds to a randomized version of graph states. Such states arise when a graph state is prepared with noisy or imperfect controlled-Z gates. We study the entanglement features of these states by investigating both bipartite and genuine multipartite entanglement. Bipartite entanglement is studied via the concepts of connectedness and persistency, which are related to measurement based quantum computation. The presence of multipartite entanglement is instead revealed by the use of witness operators which are subsequently adapted to study nonlocal properties through the violation of suitable Bell inequalities. We also present results on the entanglement detection of particular randomized graph states, by deriving explicit thresholds for entanglement and nonlocality in terms of the noise parameter that characterizes the controlled-Z gates exploited for their generation. Finally, we propose a method to further improve the detection of genuine multipartite entanglement in this class of states.

DOI: 10.1103/PhysRevA.89.052335 PACS number(s): 03.67.Bg, 03.67.Mn, 03.65.Ud

I. INTRODUCTION

Graph states and especially cluster states are at the heart of measurement based quantum computation (MBQC) [1]. Given a cluster state, this prominent model of quantum computation provides a way to perform universal computing with only local gates and measurements, by avoiding the use of two-qubit entangling gates. Under this light, the entanglement content of cluster states can then be regarded as a quantum resource that is consumed throughout the process. However, despite the fact that all the operations involved in MBQC can nowadays be easily implemented in various hardware, the hardest task from an experimental point of view is represented by the preparation of the initial cluster state.

The preparation of general graph states always starts from a product state of qubits corresponding to the vertices of a graph with no edges, which is then subsequently processed via an Ising-like interaction [2]. This interaction is tuned in such a way that its action can be regarded as a series of controlled-Z (CZ) gates, connecting the vertices according to the target graph. In Ref. [3] a preparation method involving only one- and two-qubit gates for graph states up to 12 qubits is proposed. As a matter of fact, the current experimental realization of a CZ gate is far from being perfect, and in practice it is very difficult to create a noiseless graph state [3].

A possible way to model a noisy CZ gate is to assume that, with probability p it creates the desired edge between its qubits, while with probability $1-p$ it fails. For heralded entanglement [4], if the gate fails, one could recover the original state, i.e., $|{+}{+}\rangle$. This has the same effect as an identity operator. A physical realization of this probabilistic CZ gate was suggested in [4–6].

In this paper, we aim at studying the *randomized graph state* (for short, RG state), that is, states that arise whenever a probabilistic CZ gate is applied for every edge in a graph. Given a graph state, its randomized version is thus a mixture of all the states corresponding to its subgraphs. These are weighted according to a single parameter p, which we call *randomness parameter*, physically related to the success probability of the CZ gate.

Besides addressing the issue of the unitary equivalence of general RG states, we will mainly focus on the amount of entanglement in RG states, both in the bipartite and the multipartite case [7]. Regarding the former, we will especially discuss the concepts of persistency and connectedness, which have a clear application in terms of the usefulness of RG states for MBQC [2]. For the quantification of the latter, we will use a genuine multipartite entanglement witness [8–10]. We will be able in this way to define a critical value p_c for the randomness parameter, above which the state shows genuine multipartite entanglement properties. Finally, nonlocal realistic features of RG states will be discussed with the help of suitable Bell inequalities developed for graph states.

Notice that not only are RG states interesting and highly nontrivial *per se*, but they are a useful tool to investigate and understand the presence of noise in MBQC. Furthermore, complete RG states are a plausible quantum counterpart to the classical Erdős-Rényi random graphs introduced in [11] (Ref. [12] is a detailed survey on the topic), and recently studied in the context of complex systems [13,14].

The present paper is organized as follows. In Sec. II we review some basic definitions about mathematical graphs, random graphs, and quantum graph states. We define randomized graph states in Sec. III. We then study the rank of RG states to answer the question of unitary equivalence and bipartite and multipartite entanglement in Secs. IV–VI, respectively. In Sec. VI, an approximation to a witness for multipartite entanglement is introduced, which allows us to determine a threshold probability. A further analysis on nonlocal realism is carried out in Sec. VII. We conclude in Sec. VIII with a summary of the achieved results and future perspectives.

II. PRELIMINARIES

In this section, we briefly review the definition of graphs as used in the paper and the mathematical concept of Erdős-Rényi random graphs. We then remind the reader of the well-known class of quantum graph states and introduce the notation that will be used throughout the paper.

A. Graphs

A *graph* $G = (V,E)$ is defined as a pair consisting of a set $V_G = \{v_1,\ldots,v_n\}$, whose elements are called *vertices*, and a set $E_G = \{e_1,\ldots,e_l\}$, whose elements are called *edges* and consist of unordered pairs of different vertices [15]. A graph F with $V_F \subseteq V_G$ and $E_F \subseteq E_G$ is called a *subgraph* of G. If $V_F = V_G$ then F is said to be a *spanning subgraph* of G; in such a case, we say that F *spans* G. Two vertices are *neighbors* if they are connected by an edge. The *degree* of a vertex v_i, d_{v_i}, is the number of its neighbors. A graph is *empty* if it has no edges. The empty graph on n vertices is denoted by $G_n^{\emptyset}$. On the other hand, the *complete* (or fully connected) graph on n vertices, K_n, contains all possible $\binom{n}{2}$ edges. Other relevant types of graphs that will be considered along the paper are the following ones:

(1) (i) *Star graphs*, S_n: graphs where one vertex has degree $n-1$ and all others have degree 1.

(2) (ii) *Cluster graphs*, $L_{m\times n}$: graphs whose vertices correspond to the points of a discrete two-dimensional lattice with m times n. When $m = 1$, we simply write L_n. This is a *linear cluster*, or, equivalently, a path on n vertices. Notice that in the graph-theoretic literature $L_{m\times n}$ is usually called a grid graph or a lattice graph. We use a different terminology given the link with MBQC.

(3) (iii) *Cycle graphs*, C_n: graphs where all vertices have degree 2. These are closed linear clusters.

A very useful concept in the remainder of the paper is the symmetric difference. Letting F and G be two graphs on the same set of vertices V, their *symmetric difference* is the graph $F\Delta G$, such that $V_{F\Delta G} = V_F = V_G$ and $E_{F\Delta G} = E_F \cup E_G \setminus E_F \cap E_G$.

B. Erdős-Rényi random graphs

Random graphs are a well-developed mathematical subject touching both graph theory and probability theory [12]. In the Erdős-Rényi (ER) random graph on n vertices, each edge is included with probability p independently of any other edge. Notice that, as p is uniform for all edges, then the probability of a subgraph $G \subseteq K_n$ with a number of edges $|E_G|$ is given by $P(G) = p^{|E_G|}(1-p)^{\binom{n}{2}-|E_G|}$. As an illustration, Fig. 1 shows all possible subgraphs of the complete graph K_3.

C. Graph states

We will briefly review here the well-known concept of a graph state of n qubits and its connection to graphs [16,17]. Given a graph $G = (V,E)$ on n vertices, the corresponding graph state is denoted by $|G\rangle$ and defined as follows. First, assign to each vertex a qubit and initialize it as the state $|+\rangle = \frac{1}{\sqrt{2}}(|0\rangle + |1\rangle)$, so that the initial n-qubit state is given by $|+\rangle^{\otimes n}$. Then, perform a CZ operation between any two qubits associated to vertices that are connected by an edge. This operation is defined as $\mathrm{CZ} = \mathrm{diag}(1,1,1,-1)$, in the computational basis $\{|0\rangle,|1\rangle\}$ for each qubit. By performing the CZ operation on any two connected qubits i_1 and i_2, we get the corresponding graph state

$$|G\rangle := \prod_{\{i_1,i_2\}\in E} (\mathrm{CZ})_{i_1 i_2} |+\rangle^{\otimes n}. \tag{1}$$

Notice that the number of distinct graph states of n qubits is equal to $2^{\binom{n}{2}}$, which is the number of labeled graphs with n vertices.

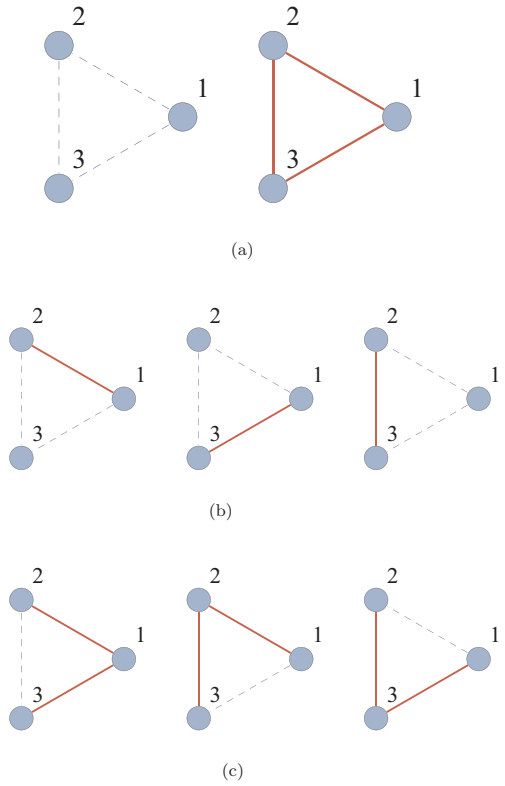

FIG. 1. (Color online) All possible subgraphs on three vertices, and the related probabilities, as instances of the ER random graph. (a) The empty $G_3^{\emptyset}$ and the complete K_3 subgraphs with probability $(1-p)^3$ and p^3, respectively. (b) The subgraphs composed of a single edge with probability $p(1-p)^2$. (c) The subgraphs composed of two edges with probability $p^2(1-p)$.

III. RANDOMIZED GRAPH STATES

In this section, we will introduce the class of randomized graph (RG) states. The main idea is to start from a graph G and to apply probabilistic gates Λ_p to the state $|+\rangle^{\otimes n}$ instead of the perfect CZ gates. Λ_p is defined as

$$\Lambda_p(|++\rangle\langle++|) = p|\!\multimap\!\circ\rangle\langle\circ\!\multimap\!\circ| + (1-p)|++\rangle\langle++|, \tag{2}$$

with $|++\rangle$ representing the two-qubit empty graph state, and $|\!\multimap\!\circ\rangle$ denoting the two-qubit connected graph state. In other words, we consider a noisy implementation of the gate CZ, where one realizes the desired CZ gate with probability p, but one fails and does nothing with probability $1-p$ [4–6].

Notice that all gates Λ_p acting on any pair of qubits commute and therefore we do not have to specify the order of application.

As an illustration, suppose we want to generate the GHZ state $|$  $\rangle$ by employing the aforementioned procedure, namely by applying the probabilistic gates Λ_p to create edges. It is easy to see that the resulting state is a mixture of subgraph states of $|$  $\rangle$, namely

$$R_p(|\text{  }\rangle) = \Lambda_p^{\{1,2\}} \circ \Lambda_p^{\{2,3\}}(|+++\rangle\langle+++|)$$
$$= p^2|\text{  }\rangle\langle\text{}| + p(1-p)|\text{}\rangle\langle\text{}|$$
$$+p(1-p)|\text{  }\rangle\langle\text{}| + (1-p)^2|\text{  }\rangle\langle\text{}|. \quad (3)$$

The above state is then said to be the RG state associated to the graph  . The above example shows that the RG state ρ_G^p associated to a graph G, or equivalently to a pure graph state $|G\rangle$, can be derived by applying the randomization operation R_p in agreement with the following definition.

Definition III.1 (Randomized graph state). Let $|G\rangle$ be a graph state. A *randomization operator* R_p is defined via

$$R_p(|G\rangle) := \sum_{F \text{ spans } G} p^{|E_F|}(1-p)^{|E_G \setminus E_F|}|F\rangle\langle F|, \quad (4)$$

where F are spanning subgraphs of G, E_F and E_G are the sets of edges of F and G, and p is the randomness parameter corresponding to the success probability of the CZ gate in Eq. (2). The resulting state $\rho_G^p := R_p(|G\rangle)$ is the randomized version of $|G\rangle$ with randomness parameter p, or, shortly, a p *randomization* of $|G\rangle$.

This randomization operator corresponds to the preparation of graph states showed in the probabilistic gate model of Eq. (2). It maps a pure graph state $|G\rangle$ into a mixture of all its spanning subgraph states. Since the two extreme cases $p = 0,1$ correspond to the empty graph and the pure graph state, respectively, the parameter p plays a fundamental role to determine the entanglement features of RG states.

In addition, it is useful to remark a difference between mathematical ER random graphs and RG states: in ER random graphs all possible edges among the vertices are considered; in RG states the randomization is restricted to the edges of a given graph. In other words, ER random graphs are always related to the fully connected graph, while RG states can be generated by the randomization process on any graph. From this viewpoint, we can say that RG states are more general than random graphs, since only in the case of $G = K_n$ does the corresponding RG state $\rho_{K_n}^p$ have the same combinatorial properties as the ER random graph of n vertices. It is then evident that our model is in close analogy with bond percolation. Of course, the questions that we ask are not directly related to the main question in percolation theory, which is traditionally concerned with the global behavior of infinite graphs as a function of the randomness parameter (see [18]).

In this paper we will denote the p randomization of the important graph states $|K_n\rangle$, $|S_n\rangle$, $|L_n\rangle$, and $|C_n\rangle$ by $\rho_{K_n}^p$, $\rho_{S_n}^p$, $\rho_{L_n}^p$, and $\rho_{C_n}^p$, respectively.

Notice that a different definition of random graph states is also given in [19]. In that model, a vertex with degree d is represented by a d-qubit system and two vertices a and b are said to be connected by an edge if one qubit in a is maximally entangled with one qubit in b. A random unitary matrix describes the coupling between subsystems of a vertex. The random graph states considered in [19] are then an ensemble of pure states. In contrast, in our definition each vertex is a single-qubit system, and a randomized graph state is always a mixed state for any value of the randomness parameter $0 < p < 1$. Notice that other ways to define mixed quantum states from graphs have been studied in the literature (see, e.g., Ref. [20]).

IV. RANK OF RANDOMIZED GRAPH STATES AND UNITARY EQUIVALENCE

In this section, we investigate the question of *local unitary* (LU) equivalence of RG states. Two n-qubit quantum states ρ and σ are *LU equivalent* if and only if there exist local unitaries $U^{(1)}, \ldots, U^{(n)}$ such that $\rho = U^{(1)} \otimes \cdots \otimes U^{(n)} \sigma U^{(1)\dagger} \otimes \cdots \otimes U^{(n)\dagger}$. LU equivalent states have identical entanglement properties.

The LU equivalence classes of graph states have been intensively studied in Ref. [16]. Pure graph states up to six qubits can be classified in 19 different LU classes. Graph states in the same class can be transformed into each other via local unitaries, and hence share the same entanglement properties. However, in most cases the RG states derived from two LU equivalent graph states, say $|G_1\rangle$ and $|G_2\rangle$, are not LU equivalent and, in general, not even equivalent under *global unitaries* (GUs).

In order to see this, consider for instance the graph states $|G_1\rangle = |$  $\rangle$ and $|G_2\rangle = |$$\rangle$, that are known to be LU equivalent. The corresponding RG states are given by $\rho_{G_1}^p = R_p(|$$\rangle)$, see Eq. (3), and

$$\rho_{G_2}^p = p^3|\text{}\rangle\langle\text{}| + p^2(1-p)|\text{  }\rangle\langle\text{}| + \cdots$$
$$+p(1-p)^2|\text{  }\rangle\langle\text{}| + \cdots$$
$$+(1-p)^3|\text{  }\rangle\langle\text{}|. \quad (5)$$

For any value of $p \neq 0,1$ the above two states can be shown by direct calculation to have different ranks, namely $\text{rank}(\rho_{G_1}^p) = 4$, and $\text{rank}(\rho_{G_2}^p) = 5$. Therefore, the RG states $\rho_{G_1}^p$ and $\rho_{G_2}^p$, defined starting from LU equivalent graph states, cannot even be transformed into each other by a GU operation. In other words, these are not unitary equivalent and, in particular, not LU equivalent. This reasoning can be generalized to an arbitrary number of qubits by introducing the following concepts:

Definition IV.1 (G-subgraphs state space). Let G be a graph and F a spanning subgraph of G. The space spanned by the states $|F\rangle$ is called *G-subgraphs state space* and is denoted as

$$\Sigma_G := \text{span}(\{|F\rangle\}_{F \subseteq G, V_F = V_G}). \quad (6)$$

This definition prompts to two observations concerned with the complete graph. The respective proofs are in Appendix A.

Theorem IV.2 (Dimension of Σ_{K_n}). The K_n-subgraphs state space Σ_{K_n} has dimension $2^n - n$.

Theorem IV.3 (Rank of randomized graph states). The rank of the randomized graph state $\rho_{K_n}^p$ is $2^n - n$, for all $0 < p < 1$.

A direct consequence of Theorem IV.3 is that the rank of $\rho^p_{K_n}$ is maximum over all RG states of n qubits, as long as $p \neq 0,1$. An interesting question is whether there exists any other randomized graph state ρ_{G_n} with maximum rank. The answer is in the negative. This can be explained by the following argument. Suppose we have a graph G_n given by the complete graph K_n where, without loss of generality, we delete a single edge between vertices 1 and 2. It can be easily seen that the state $|1100\ldots00\rangle$ appears with a plus sign in the graph state $|G_n\rangle$ and all the corresponding subgraph states. Therefore, the state $|0000\ldots00\rangle - |1100\ldots00\rangle$ cannot be obtained as a superposition of the subgraphs of G_n (see the proof of Theorem IV.2 in Appendix A for an explanation). Thus, the rank of ρ_{G_n} is always strictly smaller than $2^n - n$.

The above argument also holds for the case of states that correspond to graphs $G_n^{\neg m}$ with m edges missing with respect to the complete graph, i.e., with $\binom{n}{2} - m$ edges. The rank of the corresponding RG states is then bounded as

$$\operatorname{rank}\left(\rho_{G_n^{\neg m}}\right) \leqslant 2^n - n - m. \tag{7}$$

To prove this, the above argument about the state $|1100\ldots00\rangle$ corresponding to 1's for the qubits that are not connected by an edge can be repeated for all the other m pairs of qubits where the edges are missing, and the above upper bound then follows. From the above reasoning we can thus infer that the randomized graph state $\rho_{G_n^{\neg m}}$ can never be GU equivalent to ρ_{K_n}.

An interesting example in this sense is provided by the two graph states $|K_n\rangle$ and $|S_n\rangle$, which are known to be LU equivalent. As we have observed, $\operatorname{rank}(K_n) = 2^n - n$, while, since the star graph S_n can be obtained from the complete graph K_n by deleting $\binom{n-1}{2}$ edges, the rank of ρ_{S_n} can be bounded as

$$\operatorname{rank}\left(\rho_{S_n}\right) \leqslant 2^n - n - \binom{n-1}{2}. \tag{8}$$

This proves that, although the star graph state $|S_n\rangle$ and the complete graph state $|K_n\rangle$ are LU equivalent, their corresponding RG states ρ_{S_n} and ρ_{K_n} are not even GU equivalent.

V. BIPARTITE ENTANGLEMENT

In this section, we analyze the bipartite entanglement properties of RG states. We show that RG states exhibit some properties which are analogous to bipartite entanglement of pure graph states, while others are different. A pure graph state is entangled regarding a bipartition if there exists at least one edge across the partition. The following proposition shows that the same result holds for RG states.

Proposition V.1. Given a graph G, let A and B be disjoint subsets such that $A \cup B = V_G$. A RG state ρ^p_G is entangled regarding the bipartition $A|B$, if there exists at least one randomized edge between A and B with randomness $p > 0$.

Proof. Let us first consider the graph state composed of two qubits, namely the Bell state $|\text{Bell}\rangle = |\!\multimap\!\circ\rangle$. The RG state ρ^p_{Bell} associated to it is thus given by

$$\rho^p_{\text{Bell}} = \frac{1}{4}\begin{pmatrix} 1 & 1 & 1 & 1-2p \\ 1 & 1 & 1 & 1-2p \\ 1 & 1 & 1 & 1-2p \\ 1-2p & 1-2p & 1-2p & 1 \end{pmatrix}. \tag{9}$$

Since the partial transpose of ρ^p_{Bell} has one negative eigenvalue for $p > 0$, ρ^p_{Bell} is entangled whenever $p > 0$ [21]. Let us now move to the general case and show that there is always a nonzero probability to project a given RG state ρ^p_G onto a randomized Bell state of vertices $a \in A$ and $b \in B$, by using local σ_z measurements. Notice that this is never possible if ρ^p_G is separable across the bipartition $A|B$. Recall that a σ_z measurement on the vertex v_i of $|G\rangle$ results in the graph state $|G - v_i\rangle \otimes |+\rangle_{v_i}$, where all the edges touching the vertex v_i have been deleted, whenever the outcome $+1$ occurs [16]. Therefore, if we now measure all the vertices except a and b, i.e., $V\backslash\{a,b\}$, there is a nonvanishing probability that all the outcomes are $+1$, and thus a nonzero probability to delete all the randomized edges of ρ^p_G except the one between $a \in A$ and $b \in B$. As a result, there is a nonzero probability to obtain a randomized Bell state ρ^p_{Bell} between the vertices a and b, which finally shows that the state ρ^p_G is entangled with respect to $A|B$ for any $p > 0$. ■

This shows that, for $p > 0$, RG states show entanglement across any bipartition connected by at least one randomized edge, thus even the action of an imperfect probabilistic CZ gate creates entanglement between the two connected parties.

We now consider two different bipartite entanglement properties, namely maximal connectedness and persistency, specifically introduced in [2] for cluster states, and of particular interest with regard to MBQC. A state is said to be *maximally connected* if we can project any pair of vertices onto a Bell state with certainty, by using only local measurements. The following proposition shows that RG states never enjoy this property.

Proposition V.2. A randomized graph state is never maximally connected for $p < 1$.

Proof. Since for any pair of vertices $\{i,j\}$ there is a nonzero probability that either vertex i or j is isolated, the state cannot be projected onto a Bell state $|\text{Bell}\rangle_{i,j}$ with certainty. ■

The *persistency* $\mathcal{P}$ of a state is instead the minimal number of local measurements needed to completely disentangle the state. In Ref. [2], it was shown that, while every cluster state is maximally connected, the persistency depends on its specific structure. Results are known for one-dimensional (1D) cluster states $|L_n\rangle$, where the persistency $\mathcal{P}$ equals the Schmidt rank $n/2$, and for two- or three-dimensional cluster states where $\mathcal{P}$ approaches $n/2$ only asymptotically. The following proposition shows that the RG state ρ^p_G is less robust than the graph state $|G\rangle$.

Proposition V.3. The persistency of a randomized graph state $\mathcal{P}(\rho^p_G)$ is always smaller or equal than $\mathcal{P}(|G\rangle)$:

$$\mathcal{P}\left(\rho^p_G\right) \leqslant \mathcal{P}(|G\rangle). \tag{10}$$

Proof. Let $\mathcal{P}(|G\rangle) = m$, and $\{M_1,\ldots,M_m\}$ be the measurements that totally disentangle $|G\rangle$. Then the same set of measurements $\{M_1,\ldots,M_m\}$ totally disentangles ρ^p_G too, as it

disentangles each spanning subgraph state of $|G\rangle$. Therefore the inequality $\mathcal{P}(\rho_G^p) \leqslant m$ follows. ■

The two propositions above show that the bipartite entanglement of a given RG state is never as robust as the one of the corresponding pure graph state. This observation is expected, due to the method of construction, and is of particular interest with regard to MBQC.

We finally quantify the amount of bipartite entanglement by considering the negativity, evaluated with respect to all possible bipartitions of the qubits. The *negativity* of a bipartite state ρ_{AB} is defined [22] as

$$N(\rho_{AB}) = \frac{\left\|\rho_{AB}^{\Gamma_A}\right\| - 1}{2}, \tag{11}$$

where Γ_A represents the partial transposition with respect to the subsystem A, and $\|X\| = \mathrm{Tr}[\sqrt{X^\dagger X}]$ is the trace norm. Notice that this is one of the few computable measures of entanglement when mixed states are concerned.

We have evaluated the negativity numerically for some RG states composed of a small number of qubits. The results for the negativity of states corresponding to the complete graph K_n and the star graph S_n up to $n = 4$ vertices are reported in Fig. 2. As can be seen, in the studied cases the negativity exhibits a monotonic behavior in terms of the randomness parameter p. This suggests that the entanglement content might increase monotonically in p with respect to any bipartition. Actually, since for the extreme cases $p = 0$ and $p = 1$ we have a fully separable state and an entangled state, respectively, one might expect that, as the weight of entangled subgraph states in ρ_G^p increases with increasing p, a corresponding growth of the entanglement content of the RG state ρ_G^p. However, even though this conjecture is supported by numerical evidence, it is an open question whether the monotonic behavior of the negativity in terms of the randomness p is a common feature to all RG states.

VI. GENUINE MULTIPARTITE ENTANGLEMENT

In this section, we consider genuine multipartite entanglement (GME) properties of RG states. We remind the reader that a state which cannot be written as a convex combination of biseparable states is called *genuinely multipartite entangled* (GME) [7]. For example, in the case of three qubits, a state ρ is genuinely multipartite entangled, if it cannot be expanded in the following decomposition:

$$\rho = c_1\rho_{1|23} + c_2\rho_{2|13} + c_3\rho_{3|12}, \tag{12}$$

where $\rho_{i|jk}$ is a biseparable state regarding the bipartition $\{i\}|\{jk\}$, and $\sum_{i=1}^{3} c_i = 1$, with $c_i \geqslant 0$. The condition of being genuine multipartite entangled is thus stronger than showing bipartite entanglement. As a direct consequence, the recognition and evaluation of GME becomes much harder, especially for mixed states. Nonetheless some investigations can be still made for RG states.

As was the case for bipartite entanglement in Fig. 2, we expect the randomness parameter p to tune the amount of GME of a connected RG state from zero to its maximum value. Since the two extreme cases $p = 0, 1$ correspond to a fully separable and a genuine multipartite entangled state, respectively, we wonder whether the GME content of a general RG state ρ_G^p might still follow a monotonically increasing behavior in terms of p.

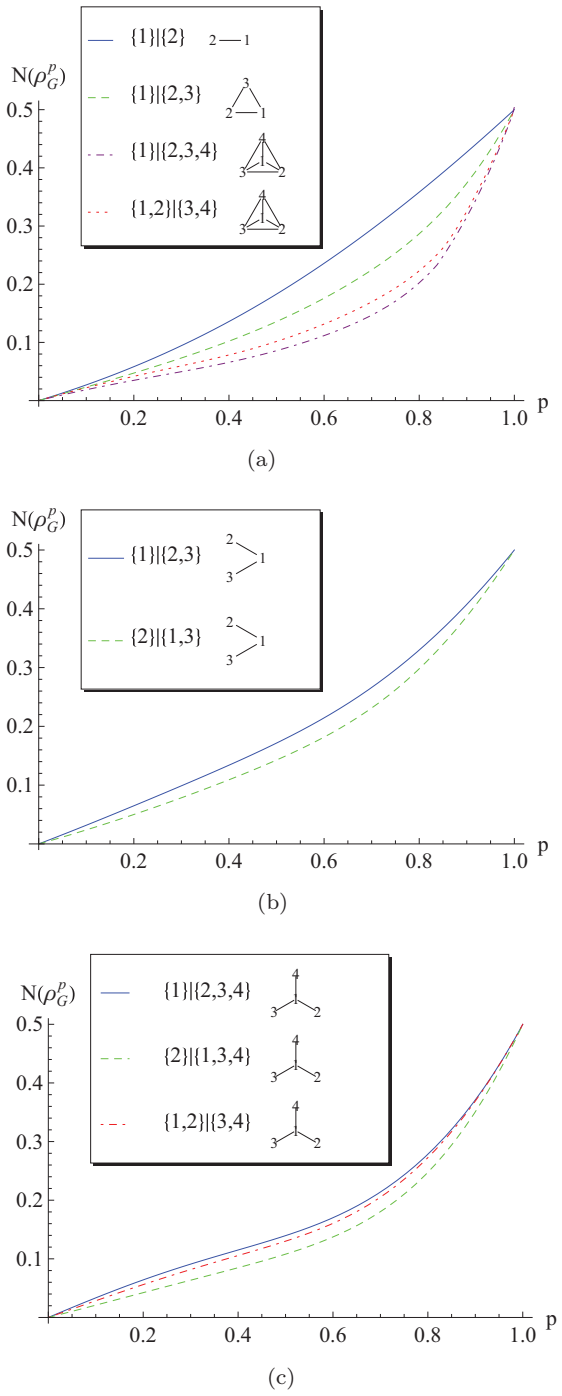

FIG. 2. (Color online) Negativity of some special RG states composed of few qubits. "$\{a_1, \ldots\}|\{b_1, \ldots\}$" indicates the bipartition with respect to which the negativity has been calculated. (a) Negativity of all RG states ρ_{K_n} states up to $n = 4$ qubits. (b) Negativity of RG states ρ_{S_n} composed of $n = 3$ qubits. (c) Negativity of RG states ρ_{S_n} composed of $n = 4$ qubits.

In order to support this intuition, we have followed the PPT mixer approach developed in Ref. [23]. In this approach

one uses a semidefinite program to make an optimization over all fully decomposable witnesses. An entanglement witness is a Hermitian operator W such that there exists a ρ with $\mathrm{Tr}[W\rho] < 0$ and $\mathrm{Tr}[W\rho_{\mathrm{sep}}] \geqslant 0$ for all separable states ρ_{sep}. A fully decomposable witness W is a witness operator that can be decomposed into two positive semidefinite operators P_γ and Q_γ for all bipartitions γ, such that

$$W = P_\gamma + Q_\gamma^{\Gamma_\gamma}, \tag{13}$$

with $\mathrm{Tr}(W) = 1$, $P_\gamma \geqslant 0$, $Q_\gamma \geqslant 0$ and Γ_γ being the partial transpose regarding bipartition γ. Such a witness is a GME witness, if there exists a GME state ρ with $\mathrm{Tr}[W\rho] < 0$, and $\mathrm{Tr}[W\rho'] \geqslant 0$ for all non-GME states ρ'. With a semidefinite program one can minimize the expectation value $\mathrm{Tr}(W\rho)$ over all fully decomposable witnesses, such that one can numerically calculate the quantity

$$E_{\mathrm{pptmixer}}(\rho) = \left|\min\left(0, \min_{W \text{ fully decomp.}} \mathrm{Tr}(W\rho)\right)\right|. \tag{14}$$

Since E_{pptmixer} is an entanglement monotone, it cannot solely detect the presence of GME but also bound the amount of GME [23]. Moreover it turns out to be necessary and sufficient for entanglement detection in permutationally invariant states up to three qubits [24], thus leading to a well defined measure of GME. Notice that, for graph states and their randomization, only the ones which are generated by complete graphs are permutationally invariant. Hence we can solely use this PPT mixer approach as GME measure for the three-qubit RG state $\rho_{K_3}^p$, while as a GME monotone for the other RG states. With the help of the online program [25], we obtain the numerical results for RG states with three, four, and five qubits. These are shown in Fig. 3. The behavior of the monotone of GME derived from the PPT mixer is monotonic in p, supporting our intuition. Whether the multipartite entanglement of RG states is generally increasing with p remains an open question.

If the quantity $\mathrm{Tr}[W\rho_G^p]$ is monotonically decreasing with respect to p, then it allows us to find a critical value of the randomness parameter, p_w, such that whenever $p > p_w$ the state is guaranteed to show GME. A depiction of what could happen is illustrated in Fig. 4. There, the expectation value of a GME witness on the RG state ρ_G^p is plotted as a function of p, and compared with the expected behavior of a general measure of GME. By assuming the existence of a threshold p_c above which the state shows GME (according to the GME measure), it is clear that p_w is an upper bound for p_c, i.e., $p_c \leqslant p_w$. Note that the presence of a threshold p_c is supported by results shown in Fig. 3, and that any negative expectation value for a witness leads to a lower bound for a corresponding entanglement measure [26].

A suitable witness to detect GME in a RG state ρ_G^p turns out to be the projector-based witness [7–10],

$$W_G = \tfrac{1}{2}\mathbb{1} - |G\rangle\langle G|. \tag{15}$$

Notice that the operator above involves only the projector onto the pure graph state $|G\rangle$ that generates ρ_G^p, disregarding all its subgraphs. In order to see whether W_G of Eq. (15) provides a negative expectation value for the state ρ_G^p, one has to compute the overlap $\mathrm{Tr}[|G\rangle\langle G|\rho_G^p]$. Therefore we introduce the next definition:

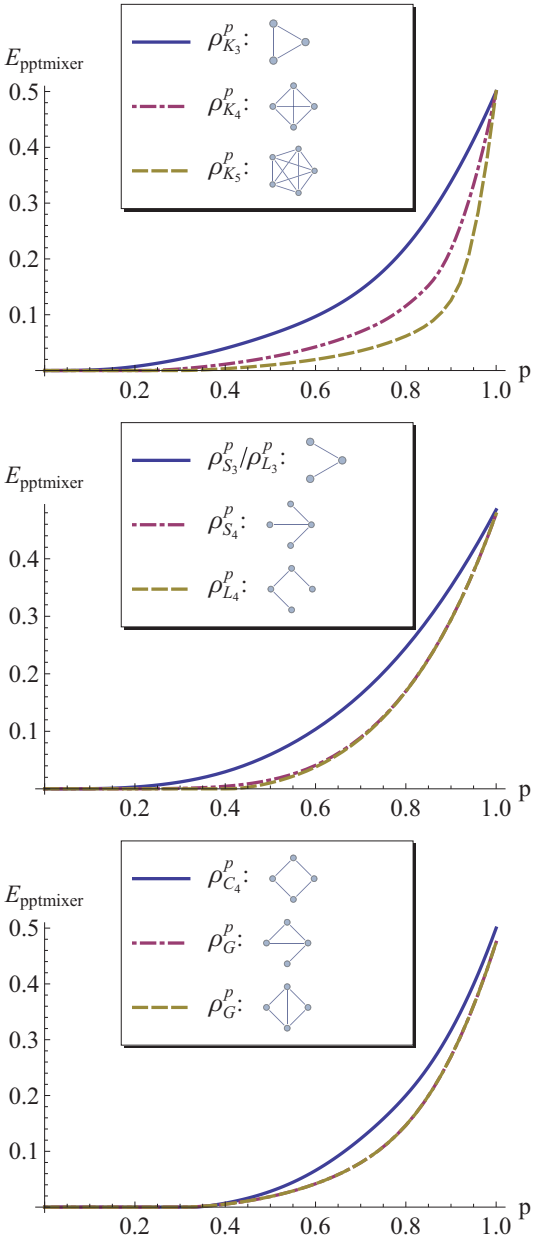

FIG. 3. (Color online) Multipartite entanglement monotone derived from the PPT mixer as a function of the randomness p for RG states up to five qubits; see Eq. (14).

Definition VI.1 (Randomization overlap). The overlap of a graph state $|G\rangle$ and its randomization ρ_G^p is the randomization overlap of ρ_G^p, i.e.,

$$L(\rho_G^p) := \mathrm{Tr}\left[|G\rangle\langle G|\rho_G^p\right] = \sum_{F \text{ spans } G} p^{|E_F|}(1-p)^{|E_G \setminus E_F|}\mathrm{Tr}[|G\rangle\langle G|F\rangle\langle F|]. \tag{16}$$

Due to the linearity of the trace, the calculation of the randomization overlap $L(\rho_G^p)$ of Eq. (16) thus reduces to the calculation of the scalar product of the graph state $|G\rangle$ with all its possible subgraph states $|F\rangle$. Furthermore, exploiting the

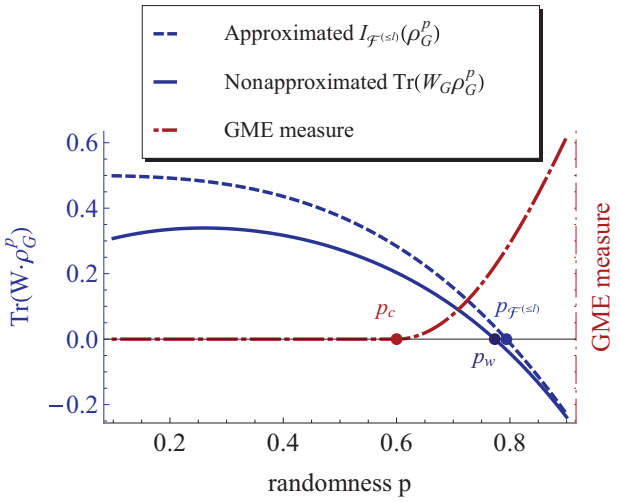

FIG. 4. (Color online) Relation between a measure of GME and the expectation value of the witness W. The critical probability p_c is upper bounded by p_w, i.e., the value of p where the expectation value becomes negative. Notice that the existence of p_c and the monotonically increasing behavior of the GME measure are not guaranteed. The same considerations apply to the monotonic decreasing behavior of the expectation value. The dashed line depicts an l-level approximated GME witness introduced in Sec. VI B. In contrast with the nonapproximated witness, it is monotonically decreasing for level $l \leqslant |E_G|/2$ and randomness $1/2 \leqslant p \leqslant 1$. The value of the nonapproximated GME witness $\mathrm{Tr}(W_G\rho_G^p)$ is always smaller than or equal to the l-approximated GME witness $I_{\mathcal{F}^{(\leq l)}}(\rho_G^p)$.

symmetric difference defined in Sec. II A and the definition of a graph state in Eq. (1), each contribution $\mathrm{Tr}[|G\rangle\langle G|F\rangle\langle F|]$ can be rewritten as

$$\mathrm{Tr}[|G\rangle\langle G|F\rangle\langle F|] = \mathrm{Tr}[|G^{\emptyset}\rangle\langle G^{\emptyset}|G\Delta F\rangle\langle G\Delta F|], \qquad (17)$$

where $|G^{\emptyset}\rangle$ is associated with the empty graph. Therefore, the overlap of any two graph states can be recast as the overlap of the graph defined by the symmetric difference and the empty one. However, even in this form the scalar product remains highly nontrivial to compute. By the help of a specifically developed algorithm [27], some special cases can be computed efficiently and even an analytical formula can be given (see Table I), especially when a small number of edges is concerned. However, in the general case the overlap can be given only via some iterative formula [28], which unfortunately scales exponentially in the number of vertices.

TABLE I. Scalar product of some special graph states with $|G^{\emptyset}\rangle$. The cluster graphs L_n in the table are one-dimensional. The results are attained by using the formulas derived in Ref. [27].

Graph $\lvert G\rangle$	Overlap $\lvert\langle G^{\emptyset}\rvert G\rangle\rvert^2$
L_{2n}	$1/2^{2n}$
L_{2n+1}	$1/2^{2n}$
C_{2n}	$1/2^{2n-2}$
C_{2n+1}	0
S_n	1/4

Besides the difficulty to compute each single overlap, another problem that inevitably affects the computation of the randomization overlap $L(\rho_G^p)$ consists of the large number of contributions we have to account for. As a matter of fact, since a RG state contains $2^{\binom{|E_G|}{2}}$ possible subgraphs, that is exponentially increasing in the number of edges, the number of overlaps contributing to $L(\rho_G^p)$ increases exponentially fast as well. Nonetheless there exist some special cases that can be treated explicitly and where an analytical solution can be found. These cases will be treated in the following, before moving to a possible efficient approximation of the randomization overlap $L(\rho_G^p)$.

A. Calculation of the witness for special RG states

In Appendix B, we derive the randomization overlap of both the RG state $\rho_{S_n}^p$, corresponding to the star graph S_n, and the randomized 1D cluster $\rho_{L_n}^p$. The expectation value of the witness W_{S_n} on the state $\rho_{S_n}^p$ takes the form

$$\mathrm{Tr}\left[W_{S_n}\rho_{S_n}^p\right] = \tfrac{1}{4} - \tfrac{3}{4}p^{n-1}, \qquad (18)$$

which is monotonically decreasing with respect to p. Therefore the threshold probability turns out to be $p_w = 3^{-1/(n-1)}$, and upper bounds the critical randomness p_c.

For the randomized 1D cluster state $\rho_{L_n}^p$ the witness gives instead the following expectation value:

$$\mathrm{Tr}\left[W_{L_n}\rho_{L_n}^p\right] = \frac{1}{2} - \frac{1}{\sqrt{\lambda_p}}\left(1 - \frac{p}{2} + \frac{\sqrt{\lambda_p}}{2}\right)\left(\frac{p}{2} + \frac{\sqrt{\lambda_p}}{2}\right)^n + \frac{1}{\sqrt{\lambda_p}}\left(1 + \frac{p}{2} + \frac{\sqrt{\lambda_p}}{2}\right)\left(\frac{p}{2} - \frac{\sqrt{\lambda_p}}{2}\right)^n, \qquad (19)$$

where $\lambda_p = 1 - p + p^2$ (see Appendix B for details). Notice that this function is also monotonically decreasing with respect to p. Solving the above polynomial in p thus provides an upper bound p_w on p_c for the RG state $\rho_{L_n}^p$. Both the expectation values above are plotted in Fig. 5.

The nonapproximated values p_w of the RG cycle state $\rho_{C_n}^p$ can also be computed numerically by the use of the algorithm developed in Ref. [27], which will be compared with approximated values in Fig. 6 in the next section.

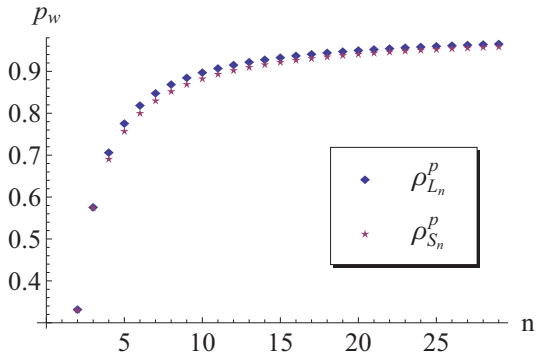

FIG. 5. (Color online) Probability p_w for the randomized star graph state $\rho_{S_n}^p$ and the randomized 1D cluster state $\rho_{L_n}^p$.

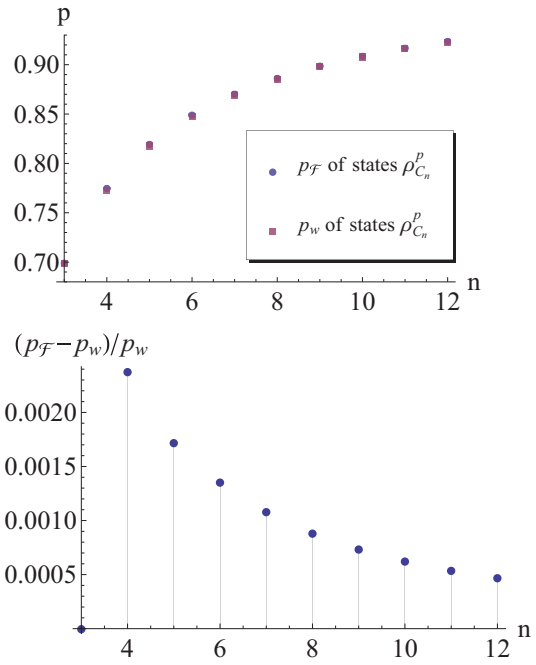

FIG. 6. (Color online) Accuracy of the approximated GME witness $L_{\mathcal{F}^{(\leqslant 2)}}(\rho^p_{C_n})$ for the cycle RG graph $\rho^p_{C_n}$. The parameter for comparison is the threshold probability p_w, calculated according to the algorithm explained in Ref. [27].

It is worth mentioning that, as expected, p_w increases rapidly as the number of vertices increases. From an experimental point of view, this means that the more edges one creates, the higher gate quality is required to guarantee the presence of GME in the final state.

In the following we will follow a different approach, namely we will approximate the witness neglecting all contributions of subgraphs too "different" from the generating one. This approximation holds whenever the randomness parameter p is high enough.

B. Approximated witness

Due to the structure of a general RG state, the computation of the scalar product of the pure graph state with all spanning subgraph states turns out to be too complex. Therefore, we introduce an approximation of the randomization overlap $L(\rho^p_G)$, that defines the expectation value W_G. Here we define the *l-level approximation* of a randomization overlap by dropping its subgraph components $F^{(>l)}$ which differ from G by more than l edges, i.e.,

$$L_{\mathcal{F}^{(\leqslant l)}}\left(\rho^p_G\right) := \mathrm{Tr}(|G\rangle\langle G|\rho_{\mathcal{F}^{(\leqslant l)}}), \tag{20}$$

where $\rho_{\mathcal{F}^{(\leqslant l)}}$ is defined as

$$\rho_{\mathcal{F}^{(\leqslant l)}} = \sum_{F \text{ s.t. } |E_{F\Delta G}|\leqslant l} p^{|E_F|}(1-p)^{|E_G\setminus E_F|}|F\rangle\langle F|. \tag{21}$$

The l-level approximated witness then reads

$$I_{\mathcal{F}^{(\leqslant l)}}\left(\rho^p_G\right) := \tfrac{1}{2} - L_{\mathcal{F}^{(\leqslant l)}}\left(\rho^p_G\right). \tag{22}$$

The proof of the next statement is in Appendix C.

Proposition VI.2. The l-level approximated randomization overlap $L_{\mathcal{F}^{(\leqslant l)}}(\rho^p_G)$ is monotonically increasing with respect to the randomness $p \geqslant 1/2$ for all $l \leqslant |E_G|/2$.

A good approximation, when p is close enough to 1, consists in neglecting the subgraphs $\mathcal{F}^{(>2)}$ that differ from G by more than two edges. This corresponds to a reduced RG state of $|G\rangle$ where only the most relevant subgraphs appear. The following theorem states that instead of using the full randomization overlap $L(\rho^p_G)$ in the GME witness, we can focus just on $L_{\mathcal{F}^{(\leqslant 2)}}(\rho^p_G)$ with the advantage to make the calculation easier.

Theorem VI.3 (Approximated GME witness). Let G be a graph and d_v be the degree of a vertex v. The quantity $L_{\mathcal{F}^{(\leqslant 2)}}(\rho^p_G)$ is a lower bound for the randomization overlap $L(\rho^p_G)$, namely

$$L\left(\rho^p_G\right) \geqslant L_{\mathcal{F}^{(\leqslant 2)}}\left(\rho^p_G\right) = p^{|E_G|} + \frac{1}{4}(1-p)p^{|E_G|-1}|E_G| + \frac{1}{2^4}(1-p)^2 p^{|E_G|-2}\left[\binom{|E_G|}{2} + 3\sum_{v\in V_G}\binom{d_v}{2}\right]. \tag{23}$$

For $p \gg 1/2$, $L(\rho^p_G) \simeq L_{\mathcal{F}^{(\leqslant 2)}}(\rho^p_G)$. The following quantity can be regarded as a GME witness for ρ^p_G:

$$I_{\mathcal{F}^{(\leqslant 2)}}\left(\rho^p_G\right) := \tfrac{1}{2} - L_{\mathcal{F}^{(\leqslant 2)}}\left(\rho^p_G\right). \tag{24}$$

If $I_{\mathcal{F}^{(\leqslant 2)}}(\rho^p_G) < 0$, it is then guaranteed that the RG state ρ^p_G is genuinely multipartite entangled.

See Appendix C for a proof. Notice that the value of the randomness parameter $p_{\mathcal{F}}$ that makes $I_{\mathcal{F}^{(\leqslant 2)}}(\rho^p_G)$ vanishing is still an upper bound of the critical randomness p_c for the RG state ρ^p_G. Notice that by construction the following chain of inequalities holds: $p_c \leqslant p_w \leqslant p_{\mathcal{F}}$. Furthermore, according to Proposition VI.2, the witness $I_{\mathcal{F}^{(\leqslant 2)}}(\rho^p_G)$ is monotonically decreasing as a function of p. Hence whenever $p > p_{\mathcal{F}}$ the RG state ρ^p_G shows GME.

By employing this theorem one can detect GME even for a graph with relatively many edges, however a study about how well the approximated witness performs is now needed. In order to check the accuracy of our approximation, we consider as an example the cycle RG graph $\rho^p_{C_n}$ and plot the relative difference between $p_{\mathcal{F}}$ and p_w. As we can see in Fig. 6, for $n = 3$ the value of $p_{\mathcal{F}}$ equals p_w, while for higher n the approximation becomes more and more accurate as the number of vertices increases. Note that the equality for $n = 3$ results from the fact that the single neglected contribution $\mathrm{Tr}[|G^{\emptyset}\rangle\langle G^{\emptyset}|C_3\rangle\langle C_3|]$ in $L_{\mathcal{F}^{(\leqslant 2)}}(\rho^p_{C_3})$ is equal to zero.

In order to show the quality of our approximation we consider here other relevant RG states, that is randomized 2D and 3D cluster states. For these states we plot the approximated $p_{\mathcal{F}}$ in Figs. 7 and 8, as a function of the number of vertices along each direction of the cluster. As we can see in Fig. 7, $p_{\mathcal{F}}$ for the two-dimensional RG state $\rho^p_{L_{m\times n}}$ increases as the sum $m+n$ grows, where m and n are the number of vertices along the x and y axes, respectively. It also turns out that the values of $p_{\mathcal{F}}$ for two RG cluster states $\rho^p_{L_{m_1\times n_1}}$ and $\rho^p_{L_{m_2\times n_2}}$ are very close to each other whenever $m_1+n_1 = m_2+n_2$. The same

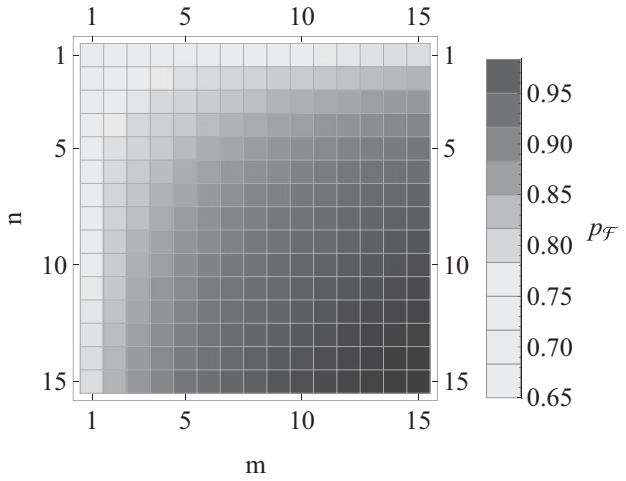

FIG. 7. Threshold probability $p_{\mathcal{F}}$ for randomized 2D cluster states $\rho_{L^p_{n\times m}} = R_p(|L_{n\times m}\rangle)$. Here, m and n represent the number of vertices along the x and y axes of the 2D cluster, respectively. The quantity $p_{\mathcal{F}}$ is depicted as a map in a (m,n) grid.

arguments hold also for the three-dimensional randomized cluster state (see Fig. 8).

Notice that the approximated witness given in Eq. (24) can be exploited to obtain a value of the randomness parameter p above which the RG state shows GME. Vice versa, if we have at disposal only CZ gates with a fixed parameter p, we can then use the estimates given by the witness to find out possible multipartite entangled RG states one could create (see Figs. 5 and 6).

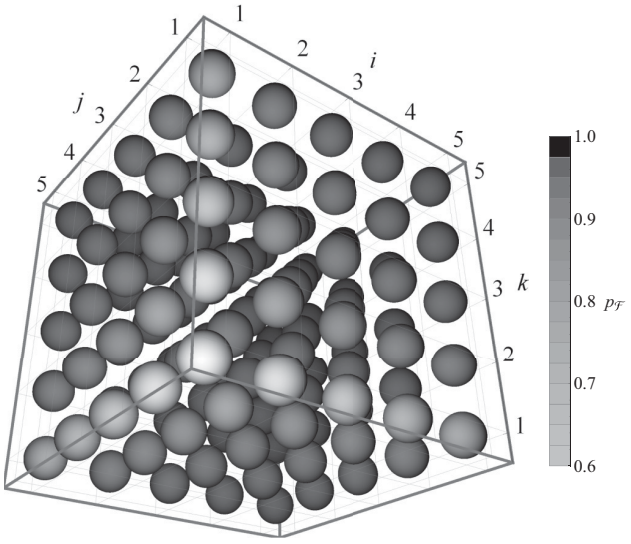

FIG. 8. Threshold probability $p_{\mathcal{F}}$ for randomized 3D cluster states $\rho^p_{L_{i\times j\times k}} = R_p(|L_{i\times j\times k}\rangle)$. The indices i, j, and k represent the number of vertices along the x, y, and z axes of the 3D cluster, respectively. The quantity $p_{\mathcal{F}}$ is depicted in grayscale in a (i,j,k) grid.

VII. BELL INEQUALITIES

In this section, we investigate when RG states cannot be described in terms of *local hidden variable* (LHV) models [29–31]. Any LHV model has to fulfill the constraints of realism and locality. These two facts result in bounds on the strength of correlations, which can be formally captured in terms of Bell inequalities [29]. A violation of such an inequality excludes the description of the correlations in terms of an LHV model [30,31]. We will show that RG states violate Bell inequalities developed for pure graph states, whenever the randomization parameter p is high enough. In order to do so we review the stabilizer description of graph states [17].

Given a graph G, we can associate to each vertex i a *stabilizing operator* g_i as follows:

$$g_i = X^{(i)} \bigotimes_{j\in N(i)} Z^{(j)}, \tag{25}$$

where $N(i)$ is the neighborhood of the vertex i, i.e., the set of vertices connected to i. Here, $X^{(i)},Y^{(i)},Z^{(i)}$ denote the Pauli matrices $\sigma_x,\sigma_y,\sigma_z$, acting on the ith qubit. The graph state $|G\rangle$ associated with the graph G is the unique n-qubit state fulfilling

$$g_i|G\rangle = |G\rangle, \quad \text{for} \quad i = 1,\ldots,n. \tag{26}$$

The n operators g_i turn out to be the generators of a group, called stabilizer and denoted by $S(G)$. The group $S(G)$ can be shown to be Abelian and is composed of 2^n elements s_j. By this definition it straightforwardly follows that $\langle G|s_j|G\rangle = 1$ for any $j = 1,\ldots,2^n$. As any s_j can be expressed as a product of n dichotomic local observables, we can thus define the following Bell operator [32]:

$$\mathcal{B}(G) = \frac{1}{2^n}\sum_{j=1}^{2^n} s_j. \tag{27}$$

Furthermore since a graph state is a product of projectors of its stabilizer generators, i.e., $|G\rangle\langle G| = \prod_i(\mathbb{1}+g_i)/2 = \mathcal{B}(G)$, the expectation value of $\langle\mathcal{B}(G)\rangle$ reaches its maximum value 1 only for the state $|G\rangle$. By defining the quantity

$$\mathcal{D}(G) = \max_{\text{LHV}} |\langle\mathcal{B}(G)\rangle|, \tag{28}$$

where the maximum is taken over all LHV models, equivalently taken over all possible expectation values of local observables $\langle X^{(i)}\rangle$, $\langle Y^{(i)}\rangle$, $\langle Z^{(i)}\rangle$ within $\{-1,+1\}$, we then have the following Bell inequality [32]:

$$\langle\mathcal{B}(G)\rangle \leqslant \mathcal{D}(G). \tag{29}$$

As a straightforward consequence, given the graph state $|G\rangle$, we are guaranteed that it cannot be described by a LHV model whenever $\mathcal{D}(G) < 1$.

For our purpose it is more convenient to rephrase the Bell inequality (29) in terms of a detection operator. Keeping in mind that the Bell operator $\mathcal{B}(G)$ is exactly the projector $|G\rangle\langle G|$, the following witness operator can be found [32,33]:

$$W_{\text{LHV}} = \mathcal{D}(G)\mathbb{1} - |G\rangle\langle G|. \tag{30}$$

Hence, whenever $\text{Tr}[W_{\text{LHV}}\rho] < 0$, i.e., the expectation value of W_{LHV} on the quantum state ρ is negative, the state ρ violates local realism, and thus cannot be described by LHV models.

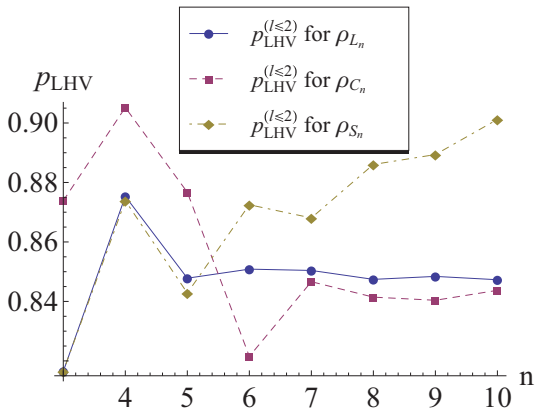

FIG. 9. (Color online) The probability thresholds $p_{\mathrm{LHV}}^{(l\leqslant 2)}$ for some important RG states. These thresholds are the zero crossings of Eq. (31). Due to the complexity of the calculation of the classical bounds $\mathcal{D}(G)$, only the thresholds for the states up to ten qubits are analyzed. The behavior of $p_{\mathrm{LHV}}^{(l\leqslant 2)}$ is explained at the end of Sec. VII.

Note that the witness W_{LHV} is similar to the witness for GME of Eq. (15). They indeed differ only in the value of the coefficient of the identity operator. Notice furthermore that the approximation techniques developed so far apply here too, allowing us to proceed as in Eq. (22) in the previous section, i.e.,

$$I_{\mathrm{LHV}}^{(\leqslant l)}\left(\rho_G^p\right) := \mathcal{D}(G) - L_{\mathcal{F}^{(\leqslant l)}}\left(\rho_G^p\right). \tag{31}$$

In [32], the quantity $\mathcal{D}(G)$ has been calculated for different graphs with number of qubits n up to 10. Our analysis consists of calculating the approximated threshold $p_{\mathrm{LHV}}^{l\leqslant 2}$ for a given graph state $|G\rangle$, such that $I_{\mathrm{LHV}}^{(\leqslant 2)}(\rho_G^{p_{\mathrm{LHV}}}) = 0$. Since $I_{\mathrm{LHV}}^{(\leqslant 2)}(\rho_G^p)$ is monotonically decreasing with respect to p for $p > 1/2$ (see Proposition VI.2), any randomness parameter $p > p_{\mathrm{LHV}}^{(l\leqslant 2)}$ will then lead to a RG state that cannot be described in terms of a LHV model.

In Fig. 9, we show the achieved result for several important RG states. In this figure one can see that the classical bounds $\mathcal{D}(G)$ are crucial for the behavior of p_{LHV}. For a given type of graph, since the classical bound $\mathcal{D}(G)$ is decreasing with respect to the number of vertices n, the threshold p_{LHV} is not monotonically increasing with respect to n. The ordering of p_{LHV} among different types of graphs can be explained via the ordering of $\mathcal{D}(G)$. For $n \leqslant 5$, $\mathcal{D}(C_n) = \mathcal{D}(L_n) = \mathcal{D}(S_n)$ holds. Therefore $p_{\mathrm{LHV}}(C_n) > p_{\mathrm{LHV}}(L_n) > p_{\mathrm{LHV}}(S_n)$ has the same ordering as the threshold p_{GME} for GME; see Figs. 5 and 6. For $n > 5$, the ordering of the threshold values $p_{\mathrm{LHV}}(S_n) > p_{\mathrm{LHV}}(L_n) > p_{\mathrm{LHV}}(C_n)$ reflects the ordering of the classical bounds for the different types of graphs, i.e., $\mathcal{D}(S_n) > \mathcal{D}(L_n) > \mathcal{D}(C_n)$. For larger n, we observe that the nonlocality of the randomized star graph states is fragile with respect to our noise model. This is analogous to the noise resistance of GME for star graph states. The fragility of GME states for other noise models has been investigated in [34].

Similar to the previous section, we can use the results provided by I_{LHV} of Eq. (31) in order to generate nonlocal multiqubit states by using only CZ gates with a given success probability p. For instance, if we have CZ gates with success probability $p = 0.84$, we can then create a nonlocal six-qubit system via generating a six-qubit randomized cycle graph state by subsequently connecting the six qubits using solely the CZ gates at disposal.

VIII. CONCLUSIONS

In this paper, we introduced a class of n-qubit mixed states that we called randomized graph (RG) states because they can be derived from pure graph states by applying a randomization procedure. They represent a quantum analog of random graphs. These states can also be regarded as the resulting states in an imperfect graph state generation procedure [4–6]. We studied in particular the entanglement properties of such states and it turned out that their entanglement classification is quite different from the one for graph states. We investigated whether local unitary (LU) equivalence of pure graph states implies LU equivalence of their randomized version, and answered this question in a negative way. Although the presence of a randomized edge guarantees bipartite entanglement between the two parties that are linked by the edge, the bipartite entanglement of RG states is more fragile under the action of local measurements with respect to the one of their corresponding graph states. We investigated this aspect by evaluating the connectedness and persistency of RG states. We then studied the multipartite entanglement properties of RG states. Due to the fact that these multiqubit states are mixed, we could evaluate the multipartite entanglement content only in some particular cases, namely for states up to four qubits. In such cases we could show that multipartite entanglement exhibits a monotonic behavior as a function of the randomness parameter p, while it is still an open problem whether the entanglement of a general RG state grows monotonically with p. In the general case we could define a critical value p_c for the randomness parameter above which the RG states are guaranteed to be multipartite entangled by employing suitable multipartite entanglement witnesses. The threshold p_c also provides an estimate of how much noise the CZ gates can be in order to guarantee GME in the generated state. Furthermore, the same approach was exploited to study the possibility to describe such RG states in terms of local hidden variable (LHV) models. Again, we could find a critical probability p_{LHV} above which the quantum state surely violates a Bell inequality. The threshold p_{LHV} also gives a hint regarding which kind of nonlocal multiqubit states can be created by using solely controlled-Z gates with a given success probability.

We point out that RG states have possible applications in measurement based quantum computation, quantum key distribution, quantum networks, etc. Since RG states are derived by the use of imperfect controlled-Z gates, which is unavoidable in a laboratory, it is more natural to consider these states instead of pure graph states in the quantum information processing task one wants to pursue.

As an outlook, the emergence of giant components of RG states and the properties of RG states in the asymptotic limit $n \to \infty$ are interesting theoretical topics that deserve further investigation. Other interesting questions that still need to be addressed are for example the possibility of identifying a Hamiltonian which has a RG state as eigenstate, or the possibility of designing a protocol to herald the components

of a RG state, such that one can perform a preselection of the RG state to extract certain subgraph states from it.

ACKNOWLEDGMENTS

We thank O. Gühne for useful discussions. J.W., D.B., and H.K. were financially supported by DFG and SFF of Heinrich-Heine-University Düsseldorf. K.L.C. was supported by the National Research Foundation & Ministry of Education, Singapore. S.S. was supported by the Royal Society.

APPENDIX A: PROOFS OF THEOREMS IV.2 AND IV.3

The proofs of Theorems IV.2 and IV.3 are given below. Notice that for Theorem IV.2 two proofs are provided, the former being more intuitive, the latter being more formal.

Proof of Theorem IV.2. Let us denote the n-qubit state with a single qubit in state 1 at position i as $|1_i\rangle$. Then, from the definition of graph states in terms of CZ operations [Eq. (1)] it follows that the n linearly independent (but not mutually orthogonal) states given by

$$|00\ldots0\rangle - |1_i\rangle \quad \text{for every} \quad i = 1,\ldots,n \tag{A1}$$

are orthogonal to any subgraph state $|G_i\rangle$ of K_n. Thus it follows that $\dim(\Sigma_{K_n}) \leqslant 2^n - n$, where Σ_{K_n} is the subspace spanned by all possible subgraph states of K_n, i.e., all possible graph states with n vertices. To prove that the equality holds, we have to show that the state $|D_n\rangle = |00\ldots0\rangle + \sum_{i=1}^{n} |1_i\rangle$ and any state with a number of qubits in state 1 (excitations) larger than 2, denoted by $|\mathrm{exc}_n \geqslant 2\rangle$, can be expressed as a linear combination of graph states. This is clearly true in the simplest case of two qubits, as $|D_2\rangle \propto |{+}{+}\rangle + |{\circ}\!\!-\!\!{\circ}\rangle$ and $|11\rangle \propto |{+}{+}\rangle - |{\circ}\!\!-\!\!{\circ}\rangle$. In order to show that it holds for generic n we proceed by induction. Suppose that for n qubits it is always possible to express both $|D_n\rangle$ and the states $|\mathrm{exc}_n \geqslant 2\rangle$ as $\sum_i \alpha_i |G_i\rangle$. Then, it can be easily proved that one can achieve both $|D_{n+1}\rangle$ and $|\mathrm{exc}_{n+1} \geqslant 2\rangle$ as follows.

Start from the state $|\mathrm{exc}_n \geqslant 2\rangle|{+}\rangle$, that by hypothesis can be written as $\sum_i \alpha_i |G_i\rangle|{+}\rangle$. Apply then a CZ on the qubit $n+1$ and on one of the qubits that correspond to state 1 in $|\mathrm{exc}_n \geqslant 2\rangle$ so that the resulting state is $\mathrm{CZ}|\mathrm{exc}_n \geqslant 2\rangle|{+}\rangle$. Then, take the following linear combination of the two states: $|\mathrm{exc}_n \geqslant 2\rangle|{+}\rangle$ and $\mathrm{CZ}|\mathrm{exc}_n \geqslant 2\rangle|{+}\rangle$ such that $|\mathrm{exc}_{n+1} \geqslant 2\rangle \propto |\mathrm{exc}_n \geqslant 2\rangle|{+}\rangle \pm \mathrm{CZ}|\mathrm{exc}_n \geqslant 2\rangle|{+}\rangle$. It can be easily seen that in this way almost all states of $n+1$ qubits with more than two excitations $|\mathrm{exc}_{n+1} \geqslant 2\rangle$ can be created (apart from some with two excitations that will be discussed in the following). Actually $2(2^n - n - 1)$ states of the computational basis can be derived from the procedure above. In order to generate the $n+1$ missing states [to achieve all the $2^{n+1} - (n+1)$ desired states] it is sufficient to start from the state $|D_n\rangle|{+}\rangle = \sum_i \alpha_i |G_i\rangle|{+}\rangle$ (instead of $|\mathrm{exc}_n \geqslant 2\rangle|{+}\rangle$) and apply again the same reasoning. If we now apply all possible CZ gates between the qubit $n+1$ and the rest we can derive the state $|D_{n+1}\rangle$. If we apply a single CZ we can achieve the n missing states with two excitations (one in the qubit $n+1$ and the other in each of the n qubits).

Therefore we have proved in this way that $\dim(\Sigma_{K_n}) \geqslant 2^n - n$ and thus the equality $\dim(\Sigma_{K_n}) = 2^n - n$ follows. ■

We now introduce the following lemma that is needed for proving Theorem IV.3.

Lemma A.1 (Rank of a general ρ). Suppose that $\rho = \sum_{i=1}^{D} p_i |v_i\rangle\langle v_i|$ with $p_i > 0$ and $\sum_{i=1}^{D} p_i = 1$, where the states $\{|v_i\rangle\}_{i=1,\ldots,D}$ span the space V of dimension $d \leqslant D$ (thus the set $\{|v_i\rangle\}_{i=1,\ldots,D}$ generally includes linearly dependent vectors). Then the rank of ρ is

$$\mathrm{rank}(\rho) = d. \tag{A2}$$

Proof. It is straightforward to see that $\mathrm{rank}(\rho) \leqslant d$. In order to prove that the rank is exactly d, let us reason by contradiction. Suppose that there exists $|l\rangle$ belonging to a basis $\{|j\rangle\}_{j=1,\ldots,d}$ of V such that $\rho|l\rangle = 0$. By rewriting $|v_i\rangle = \sum_{j=1}^{d} c_j^i |j\rangle$, it follows that

$$\rho|l\rangle = \sum_{i=1}^{D} p_i \sum_{j=1}^{d} c_j^i c_l^{i*} |j\rangle = \sum_{j=1}^{d} \alpha_{jl} |j\rangle = 0, \tag{A3}$$

with $\alpha_{jl} = \sum_{i=1}^{D} p_i c_j^i c_l^{i*}$. This implies that for every j, $\alpha_{jl} = 0$. In particular, for $j = l$ we have

$$\alpha_{ll} = \sum_{i=1}^{D} p_i \left|c_l^i\right|^2 = 0. \tag{A4}$$

The equation above, as $p_i > 0$, implies that $c_l^i = 0$ for every i, contradicting the hypothesis that the space V has dimension d. ■

Proof of Theorem IV.3. It is sufficient to apply the above lemma and Theorem IV.2 to ρ_{K_n}. ■

In the following we provide an alternative proof of Theorem IV.2, via the following lemma concerning a useful way to expand a pure state in Σ_G in terms of single qubit states.

Lemma A.2 (Expansion of states in Σ_G). Let $|\psi\rangle = \sum_{F \text{ spans } G} c_F |F\rangle$ be a state in the G-subgraphs state space Σ_G. Then $|\psi\rangle$ can be decomposed with respect to the bipartition involving the single vertex v as

$$|\psi\rangle = \frac{1}{\sqrt{2}} (|0\rangle_v |\phi^0\rangle + |1\rangle_v |\phi^1\rangle), \tag{A5}$$

with

$$\begin{aligned} |\phi^0\rangle &= \sum_{F \text{ spans } G} c_F |f_F\rangle, \\ |\phi^1\rangle &= \sum_{F \text{ spans } G} \sigma_z^{\otimes N_v(F)} c_F |f_F\rangle. \end{aligned} \tag{A6}$$

Here $f_F = F - v$ is the graph achieved by removing the vertex v from F (and deleting all edges connected with v), and $N_v(F)$ is the neighborhood of the vertex v.

The state $|\phi^0\rangle$ is state in the $(G-v)$-subgraphs state space $\Sigma_{(G-v)}$.

Proof. Obviously, any spanning subgraph state $|F\rangle$ can be generated by adding edges incident to the vertex v to a suitable subgraph state $|{+}\rangle_v |F - v\rangle$. In formulas, this fact can be expressed as

$$|F\rangle = \prod_{v_i \in N_v(F)} (\mathrm{CZ})_{v,v_i} |{+}\rangle_v |F - v\rangle. \tag{A7}$$

Therefore, any spanning subgraph $|F\rangle$ can be rewritten as

$$|F\rangle = \frac{1}{\sqrt{2}} \left(|0\rangle_v \otimes |f_F\rangle + |1\rangle_v \otimes \sigma_z^{\otimes N_v(F)} |f_F\rangle\right), \tag{A8}$$

with $|f_F\rangle = |F - v\rangle$. Now applying what was just found in the general decomposition of $|\psi\rangle = \sum_{F \text{ spans } G} c_F |F\rangle$, Eq. (A5) follows. Since f_F are subgraphs of $(G - v)$, the state $|\phi^0\rangle$ belongs to the space $\Sigma_{(G-v)}$. ■

Alternative proof of Theorem IV.2. Let us first prove that $\dim(\Sigma_{K_n}) \leqslant 2^n - n$ by showing that the n mutually orthogonal states $\sigma_z^{v_i}|G_n^{\emptyset}\rangle$ $(i = 1, \ldots, n)$ are not in the space Σ_{K_n}. In order to prove this we reason by induction. For $n = 2$, it is trivial that there never exist coefficients $c_{\emptyset}$ and c_{S_2} such that

$$\sigma_z^{v_i}\big|G_2^{\emptyset}\big\rangle = c_{\emptyset}\big|G_2^{\emptyset}\big\rangle + c_{S_2}|S_2\rangle. \tag{A9}$$

There $\sigma_z^{v_i}|G_2^{\emptyset}\rangle \notin \Sigma_{K_2}$.

We then assume that $\sigma_z^{v_i}|G_n^{\emptyset}\rangle$ is not in Σ_{K_n}, and want to prove that this is the case for $n + 1$ vertices too. Suppose now by contradiction that $\sigma_z^{v_i}|G_{n+1}^{\emptyset}\rangle \in \Sigma_{K_{n+1}}$, by employing Lemma A.2 and without loss of generality, we can then find for the first vertex v_1 that

$$\sigma_z^{v_1}\big|G_{n+1}^{\emptyset}\big\rangle = \frac{1}{\sqrt{2}}\left(|\phi^0\rangle|0\rangle_{v_{n+1}} + |\phi^1\rangle|1\rangle_{v_{n+1}}\right), \tag{A10}$$

with $|\phi^0\rangle \in \Sigma_{K_n}$. On the other hand, the left-hand side of the above equation is

$$\sigma_z^{v_1}\big|G_{n+1}^{\emptyset}\big\rangle = \frac{1}{\sqrt{2}}\left(\sigma_z^{v_1}\big|G_n^{\emptyset}\big\rangle|0\rangle_{v_{n+1}} + \sigma_z^{v_1}\big|G_n^{\emptyset}\big\rangle|1\rangle_{v_{n+1}}\right), \tag{A11}$$

which leads to

$$\sigma_z^{v_1}\big|G_n^{\emptyset}\big\rangle = |\phi^0\rangle \in \Sigma_{K_n}. \tag{A12}$$

This contradicts the assumption that no solution exists for n vertices.

In order to prove that $\dim(\Sigma_{K_n}) \geqslant 2^n - n$ we show that the space spanned by Σ_{K_n} and $\{\sigma_z^{v_i}|G_n^{\emptyset}\rangle\}_{i=1,\ldots n}$ is the full Hilbert space composed of n qubits. To this end we prove that

$$\sigma_z^{V_G}\big|G_n^{\emptyset}\big\rangle = \sum_{i=1}^{n}\left[(-1)^i 2\big|S_{V_G\setminus V_i}^{v_{i+1}}\big\rangle\big|G_{V_i}^{\emptyset}\big\rangle - (-1)^i\left(\sigma_z^{v_{i+1}} + 1\right)\big|G_n^{\emptyset}\big\rangle\right], \tag{A13}$$

where $V_i = \{v_1, \ldots, v_i\}$ is a set of i vertices and $|S_{V_G\setminus V_i}^{v_{i+1}}\rangle$ is a star graph state on vertices $V_G\setminus V_i$ and v_{i+1} as the central vertex. According to Lemma A.2 we can write

$$\big|S_n^{v_1}\big\rangle = \frac{1}{\sqrt{2}}\left(|0\rangle_{v_1} \otimes \big|G_{n-1}^{\emptyset}\big\rangle + |1\rangle_{v_1} \otimes \sigma_z^{V_G\setminus v_1}\big|G_{n-1}^{\emptyset}\big\rangle\right), \tag{A14}$$

and, since $|0\rangle_{v_1}|G_{n-1}^{\emptyset}\rangle = \frac{1}{\sqrt{2}}(\sigma_z^{v_1}|G_n^{\emptyset}\rangle + |G_n^{\emptyset}\rangle)$, we can write

$$|1\rangle_{v_1} \otimes \sigma_z^{V_G\setminus v_1}\big|G_{n-1}^{\emptyset}\big\rangle = \sqrt{2}\big|S_n^{v_1}\big\rangle - \frac{1}{\sqrt{2}}\left(\sigma_z^{v_1}\big|G_n^{\emptyset}\big\rangle + \big|G_n^{\emptyset}\big\rangle\right). \tag{A15}$$

It is also easy to see that

$$\sigma_z^{V_G}\big|G_n^{\emptyset}\big\rangle = |+\rangle_{v_1} \otimes \sigma_z^{V_G\setminus v_1}\big|G_{n-1}^{\emptyset}\big\rangle - \sqrt{2}|1\rangle_{v_1} \otimes \sigma_z^{V_G\setminus v_1}\big|G_{n-1}^{\emptyset}\big\rangle, \tag{A16}$$

and, by employing Eq. (A15), we finally arrive at the following expression:

$$\sigma_z^{V_G}\big|G_n^{\emptyset}\big\rangle = -2\big|S_n^{v_1}\big\rangle + \left(\sigma_z^{v_1} + 1\right)\big|G_n^{\emptyset}\big\rangle - \sigma_z^{V_G\setminus v_1}\big|G_n^{\emptyset}\big\rangle. \tag{A17}$$

Hence, by using Eq. (A17) recursively we can achieve Eq. (A13). Therefore, for any subset of vertices $V \subseteq V_G$, we have that the state $\sigma_z^V|G_n^{\emptyset}\rangle$ can be expressed as a superposition of vectors in the subspaces Σ_{K_n} and $\{\sigma_z^{v_i}|G_n^{\emptyset}\rangle\}_{i=1,\ldots n}$. As the set of all vectors $\sigma_z^V|G_n^{\emptyset}\rangle$ forms the Hadamard basis, this finally proves that

$$\dim\left(\Sigma_{K_n}\right) \geqslant 2^n - n. \tag{A18}$$

■

APPENDIX B: RANDOMIZATION OVERLAP OF SOME SPECIAL RG STATES

In this appendix we derive an explicit analytical result for the randomization overlap of random star states $\rho_{S_n}^p$ and random 1D cluster states $\rho_{L_n}^p$.

Solution B.1. Let S_n be an n-vertex star graph; its randomization overlap is then

$$L\left(\rho_{S_n}^p\right) = \tfrac{1}{4} + \tfrac{3}{4}p^{n-1}. \tag{B1}$$

Proof. The scalar product of $|S_n\rangle$ and any of its spanning subgraph states $|F\rangle$ always equals $\frac{1}{4}$ (apart from the case when $|F\rangle = |S_n\rangle$). therefore

$$\begin{aligned} L\left(\rho_{S_n}^p\right) &= \frac{1}{4}\sum_{k=1}^{n-1}\binom{n-1}{k}p^{n-1-k}(1-p)^k + p^{n-1} \\ &= \frac{1}{4} + \frac{3}{4}p^{n-1}. \end{aligned} \tag{B2}$$

■

Solution B.2. Let L_n be a linear cluster graph on n vertices, its randomization overlap then reads

$$\begin{aligned} L\left(\rho_{L_n}^p\right) = {} & \frac{1}{\sqrt{\lambda_p}}\left(1 - \frac{p}{2} + \frac{\sqrt{\lambda_p}}{2}\right)\left(\frac{p}{2} + \frac{\sqrt{\lambda_p}}{2}\right)^n \\ & - \frac{1}{\sqrt{\lambda_p}}\left(1 + \frac{p}{2} + \frac{\sqrt{\lambda_p}}{2}\right)\left(\frac{p}{2} - \frac{\sqrt{\lambda_p}}{2}\right)^n, \end{aligned} \tag{B3}$$

with $\lambda_p = 1 - p + p^2$.

Proof. Let us define $\mathcal{F}_{\text{even}}^{(n)}$ $(\mathcal{F}_{\text{odd}}^{(n)})$ as the set of spanning subgraphs of the cluster L_n that have paths with even (odd) number of edges connected to the last vertex v_n (see Fig. 10 for a pictorial explanation). The randomization overlap can thus be rewritten as

$$L\left(\rho_{L_n}^p\right) = f_{\text{even}}^{(n)}(p) + f_{\text{odd}}^{(n)}(p), \tag{B4}$$

where $f_{\text{even}}^{(n)}(p) := \text{Tr}[|L_n\rangle\langle L_n| \sum_{F\in\mathcal{F}_{\text{even}}^{(n)}} p_F|F\rangle\langle F|]$, and $f_{\text{odd}}^{(n)}(p) := \text{Tr}[L_n\rangle\langle L_n| \sum_{F\in\mathcal{F}_{\text{odd}}^{(n)}} p_F|F\rangle\langle F|]$. From the results in Table I, it is then not difficult to notice that the following recursive relations hold:

$$f_{\text{odd}}^{(n+1)}(p) = \frac{1-p}{4}f_{\text{even}}^{(n)}(p), \tag{B5}$$

$$f_{\text{even}}^{(n+1)}(p) = f_{\text{odd}}^{(n)}(p) + pf_{\text{even}}^{(n)}(p). \tag{B6}$$

Imposing the initial conditions $f_{\text{even}}^{(2)} = p$ and $f_{\text{odd}}^{(2)} = (1-p)/4$, the above relations can be solved, leading to the randomization overlap (B3). ■

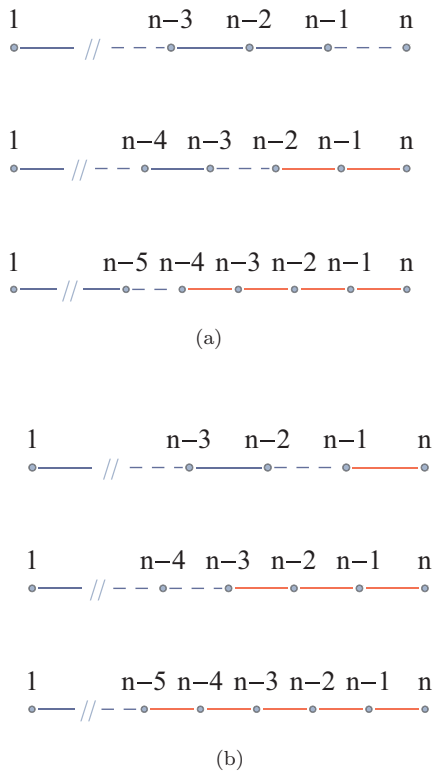

FIG. 10. (Color online) Examples of $\mathcal{F}_{\text{even}}(n)$ and $\mathcal{F}_{\text{odd}}(n)$. (a) Examples of linear clusters in $\mathcal{F}_{\text{even}}(n)$. (b) Examples of linear clusters in $\mathcal{F}_{\text{odd}}(n)$.

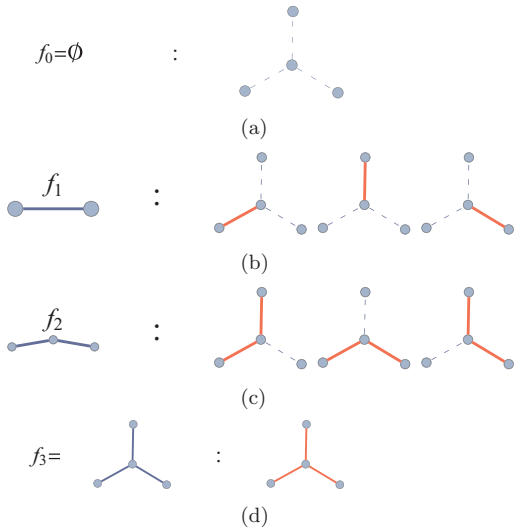

FIG. 11. (Color online) Four different isomorphic classes of star graphs on four vertices. (a) The single graph isomorphic to the empty graph. (b) Graphs isomorphic to the two-vertex graph S_2. (c) Graphs isomorphic to the star graph S_3 with three vertices. (d) The graph isomorphic to the four-vertex star graph S_4.

APPENDIX C: APPROXIMATION OF GME WITNESS

Before proving Theorem VI.3, it is convenient to first make the following observation. The randomization overlap can be easily rewritten in terms of the symmetric difference $\tilde{F} := F\Delta G$ as

$$\frac{1}{p^{|E_G|}} L(\rho_G^p) \tag{C1}$$

$$= \sum_{F \text{ spans } G} \left(\frac{1-p}{p}\right)^{|E_{F\Delta G}|} \text{Tr}[|G^{\emptyset}\rangle\langle G^{\emptyset}|F\Delta G\rangle\langle F\Delta G|],$$

$$= \sum_{\tilde{F} \text{ spans } G} \underbrace{\left(\frac{1-p}{p}\right)^{|E_{\tilde{F}}|} \text{Tr}[|G^{\emptyset}\rangle\langle G^{\emptyset}|\tilde{F}\rangle\langle\tilde{F}|]}_{=:c_G^p(\tilde{F})}. \tag{C2}$$

Equation (C2) makes it clear that the randomization overlap can be recast as a sum of terms where any contribution $c_G^p(\tilde{F})$ depends on both the number of edges $|E_{\tilde{F}}|$ and the scalar product of $|\langle G^{\emptyset}|\tilde{F}\rangle|$. It is clear that two isomorphic graphs $\tilde{F}_1, \tilde{F}_2$, i.e., graphs that can be mapped into each other by just relabeling the vertices, have the same contribution. Therefore, it is convenient to divide the whole set of subgraphs $\tilde{F}$ into different graph-isomorphic classes (as an example, Fig. 11 reports the isomorphic classes of subgraphs of the four-vertex star graph). For values of the randomness parameter $p \geqslant 1/2$, the isomorphic classes with fewer edges contribute the most to the randomization overlap. Therefore, whenever $p \geqslant 1/2$ holds, it makes sense to approximate the randomization overlap as

$$L(\rho_G^p) \geqslant p^{|E_G|} \sum_{\tilde{f} \in \mathcal{F}^{(\leqslant 2)}} |\tilde{f}| c_G^p(\tilde{f}), \tag{C3}$$

where we have defined $\mathcal{F}^{(\leqslant 2)} := \{\tilde{f} : |E_{\tilde{f}}| \leqslant 2\}$, i.e., any $\tilde{f}$ represents an isomorphic class of graphs with a number of edges smaller than 2. Notice that, since any $\tilde{F} \in \tilde{f}$ contributes equally, $c_G^p(\tilde{f})$ can be regarded as $c_G^p(\tilde{F})$ in Eq. (C2), where $\tilde{F}$ represents any element of the class $\tilde{f}$.

We are now ready to prove Proposition VI.2, which states that the l-level approximated randomization overlap $L_{\mathcal{F}^{(\leqslant l)}}(\rho_G^p)$ is monotonically increasing for any $l \leqslant |E_G/2|$, whenever $p \geqslant 1/2$.

Proof of Proposition VI.2. Let

$$\lambda_k := \frac{1}{\binom{|E_G|}{k}} \sum_{F \text{ s.t. } |E_F|=k} \text{Tr}(|F\rangle\langle F|G\rangle\langle G|) \tag{C4}$$

be the average overlap $\text{Tr}(|F\rangle\langle F|G\rangle\langle G|)$ of all subgraphs F with a fixed number of edges k. Since the overlap $\text{Tr}(|F\rangle\langle F|G\rangle\langle G|) \leqslant 1$, we have $\lambda_k \leqslant 1$, and thus the l-level approximated randomization overlap becomes

$$L_{\mathcal{F}^{(\leqslant l)}}(\rho_G^p) = \sum_{k=1}^{l} \lambda_k \binom{|E_G|}{k} p^k (1-p)^{|E_G|-k}. \tag{C5}$$

Now we order the indices k's as follows. First we group together the indices k's that lead to the same value of the coefficients λ_k, then we order all these sets for increasing values of the coefficients λ_k. In the end we get the following partition: $\{k_1^{(1)}, \ldots, k_{i_1}^{(1)}\}, \{k_1^{(2)}, \ldots, k_{i_2}^{(2)}\}, \ldots, \{k_1^{(j)}, \ldots, k_{i_j}^{(j)}\}$, where $\lambda_{k_1^{(1)}} = \cdots = \lambda_{k_{i_1}^{(1)}} > \lambda_{k_1^{(2)}} = \cdots = \lambda_{k_{i_2}^{(2)}} > \lambda_{k_1^{(j)}} = \cdots =$

FIG. 12. (Color online) All the isomorphic classes $\mathcal{F}^{(\leqslant 2)}$ with a number of edges smaller than or equal to 2.

$\lambda_{k_j^{(j)}}$. For the sake of simplicity we define $\lambda^{(j)} := \lambda_{k_1^{(j)}}$ and $\kappa^{(j)} := \{k_1^{(j)}, \ldots, k_{i_j}^{(j)}\}$.

Furthermore, we need the help of the following function:

$$f(\kappa) = \sum_{F \text{ s.t. } |E_{F\Delta G}| \notin \kappa \, |E_{F\Delta G}| \leqslant l} p_F, \tag{C6}$$

which represents the probability of finding a subgraph F having k edges different from G, where $k \leqslant l$ and it is not contained in κ. The above formula can be conveniently rewritten as

$$\begin{aligned} f(\kappa) &= \sum_{k=1}^{l} \binom{|E_G|}{k} p^k (1-p)^{|E_G|-k} \\ &\quad - \sum_{k \in \kappa} \binom{|E_G|}{k} p^j (1-p)^{|E_G|-k} \qquad \text{(C7)} \\ &= 1 - \sum_{k \notin \kappa} \binom{|E_G|}{k} p^k (1-p)^{|E_G|-k} \\ &\quad - \sum_{k=l+1}^{|E_G|} \binom{|E_G|}{k} p^k (1-p)^{|E_G|-k}. \qquad \text{(C8)} \end{aligned}$$

This function turns out to be monotonically increasing for randomness $p \geqslant 1/2$ and $l \leqslant |E_G|/2$. The l-level approximated randomization overlap can be expressed in terms of functions $f(\kappa)$ as

$$\begin{aligned} L_{\mathcal{F}^{(\leqslant l)}}(\rho_G^p) &= \lambda^{(1)} f(\emptyset) + (\lambda^{(2)} - \lambda^{(1)}) f(\kappa^{(1)}) \\ &\quad + (\lambda^{(3)} - \lambda^{(2)}) f(\kappa^{(1)} \cup \kappa^{(2)}) \\ &\quad + \cdots + (\lambda^{(j)} - \lambda^{(j-1)}) f(\kappa^{(1)} \cup \cdots \cup \kappa^{(j-1)}) \\ &\quad + (1 - \lambda^{(j)}) f(\kappa^{(1)} \cup \cdots \cup \kappa^{(j)}). \end{aligned} \tag{C9}$$

Since $(\lambda^{(i+1)} - \lambda^{(i)}) > 0$ and every $f(\kappa^{(1)} \cup \cdots \cup \kappa^{(i)})$ is monotonically increasing for randomness $p \geqslant 1/2$ and $l \leqslant |E_G|/2$, the l-level approximated overlap $L_{\mathcal{F}^{(\leqslant l)}}(\rho_G^p)$ is monotonically increasing whenever $p \geqslant 1/2$ and $l \leqslant |E_G|/2$. ■

Finally we prove Theorem VI.3 concerning a possible approximation of the GME witness.

Proof of Theorem VI.3. The main idea of the approximation is to neglect the subgraphs of G that contain more than two edges and thus to calculate only the contribution of the isomorphic classes of subgraphs with at most two edges (see Fig. 12). The approximated randomization overlap can thus be expressed as in Eq. (C3) and, with the help of the results listed in Table II, can be explicitly rewritten as

TABLE II. The cardinalities of isomorphic classes and their single element contributions: d_v is the vertex degree of vertex v in G, and E_G is the set of edges of G.

$\tilde{f}$	$\emptyset$	 Bell$_2$, S_2	S_2	 $S_2 \otimes S_2$
$c_G^p(\tilde{f})$	1	$\frac{1}{4}\left(\frac{1-p}{p}\right)$	$\frac{1}{4}\left(\frac{1-p}{p}\right)^2$	$\frac{1}{16}\left(\frac{1-p}{p}\right)^2$
$\lvert\tilde{f}\rvert$	1	$\lvert E_G\rvert = \frac{1}{2}\sum_{v\in V} d_v$	$\sum_{v\in V}\binom{d_v}{2}$	$\binom{E_G}{2} - \sum_{v\in V}\binom{d_v}{2}$

$$\begin{aligned} L_{\mathcal{F}^{(\leqslant 2)}}(\rho_G^p) &= p^{|E_G|} + \frac{1}{4}(1-p)p^{|E_G|-1}|E_G| \\ &\quad + \frac{1}{2^4}(1-p)^2 p^{|E_G|-2}\left[\binom{|E_G|}{2} + 3\sum_{v\in V_G}\binom{d_v}{2}\right], \end{aligned} \tag{C10}$$

where d_v is the degree of any vertex v. Since the contribution of subgraphs with number of edges greater than 2 is always non-negative, it follows that $L(\rho_G^p) \geqslant L_{\mathcal{F}^{(\leqslant 2)}}(\rho_G^p)$. Therefore, we have that

$$I_{\mathcal{F}^{(\leqslant 2)}}(\rho_G^p) := 1/2 - L_{\mathcal{F}^{(\leqslant 2)}}(\rho_G^p) \tag{C11}$$

is also a GME witness, in the sense that a negative value indicates the presence of GME. Notice furthermore that $I_{\mathcal{F}^{(\leqslant 2)}}(\rho_G^p) \leqslant I_w(\rho_G^p)$, i.e., the approximated witness is obviously weaker than the complete one defined as $I_w(\rho_G^p) = \mathrm{Tr}[W_G \rho_G^p]$ where W_G is defined in Eq. (15).

The last point of the theorem says that $p_{\mathcal{F}} \geqslant p_w$, where $p_{\mathcal{F}}$ (p_w) represents the threshold probability for $I_{\mathcal{F}^{(\leqslant 2)}}(\rho_G^p)$ [$I_w(\rho_G^p)$], and thus it is an upper bound for the critical probability p_c also. In order to see this, let us consider the following inequality:

$$\begin{aligned} I_{\mathcal{F}^{(\leqslant 2)}}(\rho_G^{p_w}) &= I_w(\rho_G^{p_w}) + L_{\mathcal{F}^{(>2)}}(\rho_G^{p_w}) \\ &= L_{\mathcal{F}^{(>2)}}(\rho_G^{p_w}) \\ &\geqslant 0 = I_{\mathcal{F}^{(\leqslant 2)}}(\rho_G^{p_{\mathcal{F}}}), \end{aligned} \tag{C12}$$

where $L_{\mathcal{F}^{(>2)}}(\rho_G^{p_w})$ represents the scalar product of $|G\rangle$ with all its subgraphs with a number of edges greater than 2.

Together with the fact that $I_{\mathcal{F}^{(\leqslant 2)}}(\rho_G^p)$ is a monotonically decreasing function of p for $p \geqslant 1/2$ (Proposition VI.2), it follows that $p_{\mathcal{F}}$ is always an upper bound for p_w, whenever $p \geqslant 1/2$. As a last note, notice that the following chain of inequalities thus holds: $p_{\mathcal{F}} \geqslant p_w \geqslant p_c$. ■

[1] R. Raussendorf and H. J. Briegel, Phys. Rev. Lett. **86**, 5188 (2001).

[2] H. J. Briegel and R. Raussendorf, Phys. Rev. Lett. **86**, 910 (2001).

[3] A. Cabello, L. E. Danielsen, A. J. López-Tarrida, and J. R. Portillo, Phys. Rev. A **83**, 042314 (2011).

[4] Y. L. Lim, A. Beige, and L. C. Kwek, Phys. Rev. Lett. **95**, 030505 (2005).

[5] Y. L. Lim, S. D. Barrett, A. Beige, P. Kok, and L. C. Kwek, Phys. Rev. A **73**, 012304 (2006).
[6] A. Beige, Y. L. Lim, and L. C. Kwek, New J. Phys. **9**, 197 (2007).
[7] A. Acín, D. Bruß, M. Lewenstein, and A. Sanpera, Phys. Rev. Lett. **87**, 040401 (2001).
[8] M. Bourennane, M. Eibl, C. Kurtsiefer, S. Gaertner, H. Weinfurter, O. Gühne, P. Hyllus, D. Bruß, M. Lewenstein, and A. Sanpera, Phys. Rev. Lett. **92**, 087902 (2004).
[9] O. Gühne, P. Hyllus, D. Bruß, A. Ekert, M. Lewenstein, C. Macchiavello, and A. Sanpera, Phys. Rev. A **66**, 062305 (2002).
[10] G. Tóth and O. Gühne, Phys. Rev. Lett. **94**, 060501 (2005).
[11] P. Erdős and A. Rényi, Publ. Math. Debrecen **6**, 290 (1959).
[12] S. Janson, T. Łuczak, and A. Rucinski, *Random Graphs* (John Wiley & Sons, New York, 2000).
[13] M. E. J. Newman, SIAM Rev. **45**, 167 (2003).
[14] S. Boccaletti, V. Latora, Y. Moreno, M. Chavez, and D.-U. Hwanga, Phys. Rep. **424**, 175 (2006).
[15] R. Diestel, *Graph Theory*, Graduate Texts in Mathematics Vol. 173 (Springer-Verlag, Heidelberg, 2005).
[16] M. Hein, J. Eisert, and H. J. Briegel, Phys. Rev. A **69**, 062311 (2004).
[17] M. Hein, W. Dür, J. Eisert, R. Raussendorf, M. Nest, and H.-J. Briegel, arXiv:quant-ph/0602096.
[18] G. Grimmett, *Percolation*, 2nd ed. (Springer, New York, 1999).
[19] B. Collins, I. Nechita, and K. Życzkowski, J. Phys. A **43**, 275303 (2010).
[20] S. L. Braunstein, S. Ghosh, and S. Severini, Ann. Combinatorics **10**, 291 (2006).
[21] M. Horodecki, P. Horodecki, and R. Horodecki, Phys. Lett. A **223**, 1 (1996).
[22] G. Vidal and R. F. Werner, Phys. Rev. A **65**, 032314 (2002).
[23] B. Jungnitsch, T. Moroder, and O. Gühne, Phys. Rev. Lett. **106**, 190502 (2011).
[24] L. Novo, T. Moroder, and O. Gühne, Phys. Rev. A **88**, 012305 (2013).
[25] http://www.mathworks.com/matlabcentral/fileexchange/30968.
[26] F. G. S. L. Brandao, Phys. Rev. A **72**, 022310 (2005).
[27] J.-Y. Wu, H. Kampermann, and D. Bruß (unpublished).
[28] S. Niekamp, M. Kleinmann, and O. Gühne, J. Math. Phys. **53**, 012202 (2012).
[29] J. S. Bell, Physics **1**, 195 (1964); Rev. Mod. Phys. **38**, 447 (1966).
[30] N. D. Mermin, Phys. Rev. Lett. **65**, 1838 (1990).
[31] D. M. Greenberger, M. A. Horne, A. Shimony, and A. Zeilinger, Am. J. Phys. **58**, 1131 (1990).
[32] O. Gühne, G. Tóth, P. Hyllus, and H. J. Briegel, Phys. Rev. Lett. **95**, 120405 (2005).
[33] P. Hyllus, O. Gühne, D. Bruß, and M. Lewenstein, Phys. Rev. A **72**, 012321 (2005).
[34] M. Ali and O. Gühne, J. Phys. B **47**, 055503 (2014).

X-chains reveal substructures of graph states

Jun-Yi Wu, Hermann Kampermann, and Dagmar Bruß
Institut für Theoretische Physik III, Heinrich-Heine-Universität Düsseldorf, D-40225 Düsseldorf, Germany

Abstract

A special configuration of graph state stabilizers, which contains only Pauli σ_X operators, is studied. The vertex sets ξ associated with such configurations are defined as the X-chains of graph states. The X-chains of a general graph state can be determined efficiently. With the help of X-chains, one obtains the explicit representation of graph states in the X-basis via the so-called X-chain factorization diagram. We show that graph states with different X-chains can have different probability distributions of X-measurement outcomes, which allows to distinguish certain graph states with X-measurements. We provide an approach to find the Schmidt decomposition of graph states in the X-basis. The existence of X-chains in a subsystem facilitates error correction in the entanglement localization of graph states. In all these applications, the difficulty of the task decreases with increasing number of X-chains. Furthermore, we show that the overlap of two graph states can be efficiently determined via X-chains, while its computational complexity with other known methods increases exponentially.

I. INTRODUCTION

Graph states [1–7] represent specific multipartite entangled quantum systems. They are an important resource for measurement-based quantum computation: there, the multipartite entanglement of cluster states (a special class of graph states) is consumed by local measurements on subsystems. Depending on the measurement outcomes, local unitary transformations of the remaining systems are performed. In this way, certain quantum operations can be implemented.

Graph states can be represented in the stabilizer formalism as eigenstates of certain tensor products of Pauli σ_X- and σ_Z-operators (the graph state stabilizers). The explicit structure of the stabilizer operators depends on the structure of the underlying graph. The stabilizers form a group (under multiplication), which is generated from n generators, where n is the number of vertices of the graph.

In this paper we will introduce the concept of X-chains. X-chains are subsets of vertices of a given graph which correspond to graph state stabilizers that consist *only* of Pauli σ_X-operators. We will show that these X-chains form a group. Not every graph contains an X-chain. However, it will be shown that if a graph does contain X-chains, this fact can be used as an efficient tool to determine essential properties of the corresponding graph state, such as its overlap with other graph states, its entanglement characteristics, and the existence of error correcting code words in subsystems of graph states. Note that the overlap of two graph states cannot be determined efficiently up to date. The X-chains provide an efficient method to solve this problem.

While usually graph states are given in the Z-basis, the concepts and methods developed in this paper show that it is often favorable to represent graph states in the X-basis, in particular when one wants to study overlaps of graph states or determine their entanglement properties. The reason for this fact is that for all graph states originating from the same number of vertices, the probability distribution of outcomes of local Z-measurements are uniform, while they are non-uniform for outcomes of local X-measurements. Different X-measurement outcomes of two graph states reflect their difference in the X-chain groups, as the existence of an X-chain in a graph state implies vanishing probability of certain X-measurement outcomes. Reversely, X-chain groups of graph states determine their representation in the X-basis.

In the present paper we will focus on introducing the concept of X-chains, illustrating it with examples, and presenting some applications. The X-chain group of a given graph state can be efficiently determined, the search of X-chains in a given graph state will be studied in detail elsewhere [8] and a Mathematica package is available in [9].

This paper is organized as follows. In section I A, we review the essential concepts of graph theory and graph states. In section II, we review the representation of graph states in the Z-basis and point out its disadvantage in distinguishing graph states. Then we introduce X-chains and study their properties in section III. The representation of graph states in the X-basis is derived via the so-called X-chain factorization in section IV, where we show how X-chain groups feature the X-measurement outcomes on graph states. In section V, we discuss several applications of X-chains, namely the calculation of the overlap of two graphs states (section V A), the Schmidt decomposition of graph states in the X-basis (section V B) and the entanglement localization [10] of graph states against errors (section V B 1). The proofs are presented in Appendix A, and a list of notations and symbols is given in Appendix B.

A. Basic concepts

Here we review the concepts of graphs [11] and graph states [6, 7], and introduce the notation used in the main text.

a. Graph theory [11]: A *graph* $G = (V, E)$ consists of n vertices V and l edges E. The *vertices*, denoted by $V_G = \{v_1, ..., v_n\}$, are depicted as dots and represent locations, particles etc. The *edges*, denoted by $E_G = \{e_1, ..., e_l\}$, describe a relation network between

Name of graph	Graph	Definition
Star graph S_n		Graphs, for which the center vertex has $n-1$ neighbors and all the others have the center vertex as their only neighbor.
Cycle graph C_n		Graphs, for which every vertex has degree 2. They are closed paths.

TABLE I: The graphs considered in this paper.

vertices. A symmetric relation between two vertices v_1 and v_2, e.g. a two-way bridge between two islands, can be represented by the vertex set $e = \{v_1, v_2\}$, which is called *undirected edge*. Let $\xi_a, \xi_b \subseteq V_G$ be two subsets of V_G, then the edges between ξ_a and ξ_b are the edges $e = \{v_a, v_b\}$, which have one vertex $v_a \in \xi_a$ and the other vertex $v_b \in \xi_b$. The set of these edges is denoted by $E_G(\xi_a : \xi_b)$. A vertex v_1 is a *neighbor* of v_2, if they are connected by an edge. The set of all neighbors of v, called the neighborhood of v, is denoted as N_v. In Table I we list two of the relevant types of graphs, which will be considered in the main text.

A graph F is a *subgraph* of G, if its vertices and edges are subsets of the vertex set and the edge set of G, respectively, i.e., $V_F \subseteq V_G$ and $E_F \subseteq E_G$. A subgraph induced by a vertex set $\xi \subseteq V_G$ is defined as the graph

$$G[\xi] := (\xi, E_G(\xi : \xi)), \tag{1}$$

which has the edge set $E_G(\xi : \xi)$ consisting of edges between vertices inside the set ξ.

b. Binary notation: In this paper, we use binary numbers to denote a subset of vertices of graphs. Let G be a graph with vertices $V_G = \{1, ..., n\}$ and $\xi \subseteq V_G$ be a vertex subset. We denote the binary number of ξ as

$$i^{(\xi)} := i_1 \cdots i_n, \tag{2}$$

with

$$i_j = \begin{cases} 0 & , j \notin \xi \\ 1 & , j \in \xi \end{cases}.$$

E.g. in a 4-vertex graph, $0110 = i^{\{2,3\}}$. The tensor product of Pauli-operators σ_α with $\alpha \in \{x, y, z\}$ is denoted as

$$\sigma_\alpha^{(\xi)} := \sigma_\alpha^{i_1(\xi)} \otimes \cdots \otimes \sigma_\alpha^{i_n(\xi)}, \tag{3}$$

with $\sigma_\alpha^0 = \mathbb{1}, \sigma_\alpha^1 = \sigma_\alpha$. E.g. for $n = 4$, $\sigma_\alpha^{\{2,3\}} := \mathbb{1} \otimes \sigma_\alpha \otimes \sigma_\alpha \otimes \mathbb{1}$.

II. REPRESENTATION OF GRAPH STATES

We review the representation of graph states [6, 7]. A given graph with n vertices has a corresponding quantum state by associating each vertex v_i with a graph state *stabilizer generator* g_i,

$$g_i = \sigma_X^{(i)} \sigma_Z^{(N_i)}. \tag{4}$$

Here, N_i is the neighborhood of the vertex v_i. A graph state $|G\rangle$ is the n-qubit state stabilized by all g_i, i.e.,

$$g_i |G\rangle = |G\rangle, \text{for all } i = 1, ..., n. \tag{5}$$

The n graph state stabilizer generators, g_i, generate the whole stabilizer group $(\mathcal{S}_G, \cdot)$ of $|G\rangle$ with multiplication as its group operation. The group $\mathcal{S}_G$ is Abelian and contains 2^n elements. These 2^n stabilizers uniquely represent a graph state on n vertices. Let us define the"induced stabilizer", which is uniquely associated to a given vertex subset.

Definition 1 (Induced stabilizer)**.**
Let G be a graph on vertices $V_G = \{v_1, v_2, \cdots, v_n\}$. Let $\xi = \{\xi_1, \cdots, \xi_m\}$ be a subset of V_G. We call the product of all g_i with $i \in \xi$, i.e.

$$s_G^{(\xi)} := \prod_{i \in \xi} g_i, \tag{6}$$

the ξ-induced stabilizer *of the graph state $|G\rangle$. Here, g_i is the graph state stabilizer generator of $|G\rangle$ associated with i-th vertex.*

Since this ξ-induction map is bijective, it maps the group $(\mathcal{P}(V_G), \Delta)$ into another stabilizer group $(\mathcal{S}_G, \cdot)$, where $\mathcal{P}(V_G) := \{\xi \subseteq V_G\}$ is the power set (the set of all subsets) of V_G and Δ is the symmetric difference operation acting on two sets as $\xi_1 \Delta \xi_2 = (\xi_1 \setminus \xi_2) \cup (\xi_2 \setminus \xi_1)$.

Proposition 2 (Isomorphism of ξ-induction)**.**
Let $(\mathcal{S}_G, \cdot)$ be the stabilizer group of a graph state $|G\rangle$, $\mathcal{P}(V_G)$ be the power set of the vertex set of G. The vertex-induction operation $s_G^{(\xi)}$ is a group isomorphism between $(\mathcal{P}(V_G), \Delta)$ and $(\mathcal{S}_G, \cdot)$, i.e.

$$(\mathcal{P}(V_G), \Delta) \overset{s_G^{(\xi)}}{\sim} (\mathcal{S}_G, \cdot), \tag{7}$$

where Δ is the symmetric difference operation.

Proof. See Appendix A. □

The summation operation maps the stabilizer group $\mathcal{S}_G$ to its stabilized space, i.e. the density matrix of the graph state $|G\rangle$ [7],

$$\mathcal{S}_G \xrightarrow{\Sigma} |G\rangle\langle G| = \frac{1}{2^n} \sum_{s \in S_G} s. \tag{8}$$

Hence there exists also an operation mapping the group $\mathcal{P}(V_G)$ to graph states

$$\mathcal{P}(V_G) \overset{\Sigma \circ s_G^{(\xi)}}{\longrightarrow} |G\rangle\langle G| = \frac{1}{2^n} \sum_{\xi \subseteq V_G} s_G^{(\xi)} = \prod_{i=1}^{n} \frac{1+g_i}{2}. \quad (9)$$

This is a well-known representation of graph states [7]. The representation of a graph state in the computational Z-basis $|i_Z\rangle$ [12] is given by

$$\mathcal{P}(V_G) \overset{\Sigma \circ s_G^{(\xi)} \text{ in } |i_Z\rangle}{\longrightarrow} |G\rangle = \frac{1}{2^{n/2}} \sum_{i \in \{0,1\}^{\otimes n}} (-1)^{\langle i,i \rangle_{A_G}} |i_Z\rangle. \quad (10)$$

Here $\sigma_z^{\otimes n}|i_Z\rangle = (-1)^{|i|}|i_Z\rangle$, where $|i|$ is the Hamming weight of i. A_G is the adjacency matrix of the graph G, and $\langle i,i\rangle_{A_G} = (i_1,...,i_n)A_G(i_1,...,i_n)^{\mathrm{T}}$. For all graph states with n vertices, the probability amplitudes of Z-basis states $\langle i_Z|G\rangle$ are homogenously distributed for all $|i_Z\rangle$ up to a phase -1, i.e. $|\langle i_Z|G\rangle| = 1/2^{n/2}$. Therefore graph states with the same vertex set all have equivalent probability distribution of local σ_Z-measurement outcomes. This means that the Z-basis representation conceals the inner structure of graph states.

Different from the Z-basis, the representation of graph states in the computational X-basis $|i_X\rangle$ (i.e. $\sigma_X^{\otimes n}|i_X\rangle = (-1)^{|i|}|i_X\rangle$) reveals the structure of graph states to a certain degree. One aim in this paper is to find an efficient algorithm, i.e. a mapping from $\mathcal{P}(V_G)$ to $|G\rangle$, to represent graph states in the computational X-basis:

$$\mathcal{P}(V_G) \overset{?}{\longrightarrow} |G\rangle \text{ in } |i_X\rangle. \quad (11)$$

In the rest of the paper, we denote the X-basis $|i_X\rangle$ as $|i\rangle$. I.e. $|0\rangle = |+_Z\rangle = (|0_Z\rangle + |1_Z\rangle)/\sqrt{2}$ and $|1\rangle = |-_Z\rangle = (|0_Z\rangle - |1_Z\rangle)/\sqrt{2}$.

III. X-CHAINS AND THEIR PROPERTIES

The commutativity of the measurement setting with graph state stabilizers determines whether one can obtain information about a graph state in the laboratory. Graph state stabilizers that commute with σ_X-measurements are the stabilizers consisting of solely σ_X operators. They are the key ingredient in the representation of graph states in the X-basis. We will call the vertex sets ξ inducing such configurations *X-chains* of graph states. In this section, the concept of X-chains will be introduced and their properties will be investigated.

The number of σ_Z-operators in the graph state stabilizer $s_G^{(\xi)}$ depends on the neighborhoods within the vertex set ξ. If a vertex v has an even number of neighbors within ξ, then the Pauli operator $\sigma_Z^{(v)}$ appears an even number of times in $s_G^{(\xi)}$, such that the product becomes the identity. Therefore to find the X-chain configurations of graph states, one needs to study the symmetric difference of neighborhoods within the vertex set ξ, which we define as the *correlation index* of ξ as follows.

Definition 3 (Correlation index)**.**
Let ξ be a vertex subset of a graph G. Its correlation index is defined as the symmetric difference of neighbourhoods within ξ,

$$c_\xi := N_{v_1} \Delta N_{v_2} \cdots \Delta N_{v_k}, \quad (12)$$

where N_{v_i} is the neighbourhood of v_i and $\xi = \{v_1,...,v_k\}$.

The name "correlation index" will become clearer in Theorem 13 and refers to the fact that for vanishing correlation index the corresponding stabilized state is factorized. (These states are called X-chain states in Def.9.) Note that the set c_ξ occurs as an "index" for the σ_Z operator of the induced stabilizer $s_G^{(\xi)}$ (see Proposition 5).

Besides the correlation index, due to the anticommutativity of σ_X and σ_Z, the graph state stabilizers depend also on the so-called *stabilizer parity* of ξ.

Definition 4 (Stabilizer parity)**.**
Let ξ be a vertex subset of a graph G. Its stabilizer parity in $|G\rangle$ is defined as the parity of the edge number $|E_{G[\xi]}|$ of the ξ-induced subgraph $G[\xi]$

$$\pi_G(\xi) := (-1)^{|E_{G[\xi]}|}. \quad (13)$$

The stabilizer parity of ξ, $\pi_G(\xi)$ is positive if the edge number $E(G[\xi])$ is even, otherwise negative. The explicit form of the induced stabilizers is given in the following proposition.

Proposition 5 (Form of the induced stabilizer)**.**
Let ξ be a vertex subset of a graph G. The ξ-induced stabilizer (see Def. 1) of a graph state $|G\rangle$ is given by

$$s_G^{(\xi)} = \pi_G(\xi)\, \sigma_X^{(\xi)} \sigma_Z^{(c_\xi)}, \quad (14)$$

where c_ξ is the correlation index *of ξ and $\pi_G(\xi)$ is the stabilizer parity of ξ.*

Proof. See Appendix A. □

Let us illustrate these concepts with an example: the star graph state $|S_3\rangle$ is shown in Fig. 1a. Its stabilizers

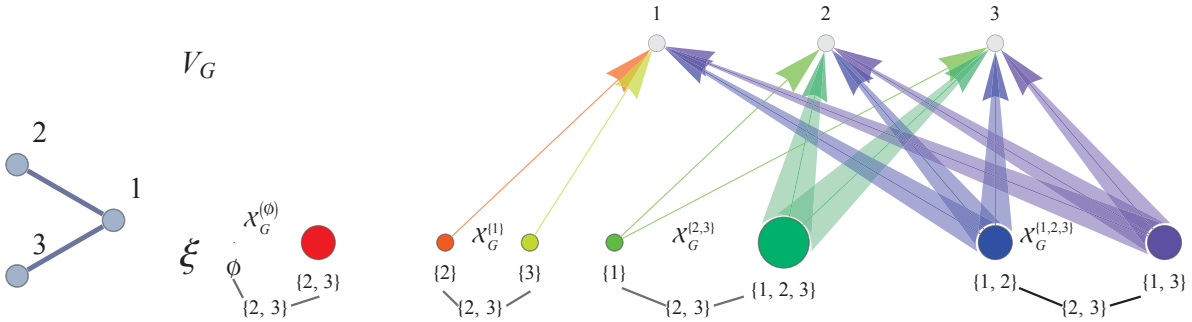

(a) (b)

ξ	$\emptyset$ and $\{2,3\}$	$\{2\}$ and $\{3\}$	$\{1\}$ and $\{1,2,3\}$	$\{1,2\}$ and $\{1,3\}$
$c_\xi \in \mathcal{C}_G$	$\emptyset$	$\{1\}$	$\{2,3\}$	$\{1,2,3\}$
$\lvert E_{G[\xi]}\rvert$	0	0	0 and 2	1
$\pi_G(\xi)$	1	1	1	-1
$s_G^{(\xi)}$	$\mathbb{1}$, $\sigma_X^{\{2,3\}}$	$\sigma_X^{\{2\}}\sigma_Z^{\{1\}}$, $\sigma_X^{\{3\}}\sigma_Z^{\{1\}}$	$\sigma_X^{(1)}\sigma_Z^{\{2,3\}}$, $\sigma_X^{\{1,2,3\}}\sigma_Z^{\{2,3\}}$	$-\sigma_x^{\{1,2\}}\sigma_Z^{\{1,2,3\}}$, $-\sigma_X^{\{1,3\}}\sigma_Z^{\{1,2,3\}}$
$\xi \in \langle\mathcal{K}_G\rangle$	$\emptyset$	$\{2\}$	$\{1\}$	$\{1,2\}$
	$\Gamma_G = \{\{2,3\}\}$, $\mathcal{K}_G = \{\{1\},\{2\}\}$			

(c)

FIG. 1: (Color online) Correlation indices and X-resources: (a) 3-vertex star graph. (b) The mapping from X-resources to correlation indices is illustrated in the incidence structure [13] of the graph S_3. The upper line is the correlation index, while the lower line are the vertex subsets (including the empty set). The arrows go from lower vertex subsets ξ to the upper vertices corresponding to the nonzero entries of their correlation index c_ξ. E.g. the vertex set $\{1,2,3\}$ points to the vertices $\{2,3\}$, indicating that the correlation index of $\{1,2,3\}$ is $c_{\{1,2,3\}} = \{2,3\}$. Especially, the vertex set $\emptyset$ and $\{2,3\}$ are X-chains (see Def. 7), since their correlation index is 0. The resources in the sets $\mathcal{X}_G^{(\emptyset)} = \{\emptyset, \{2,3\}\}$, $\mathcal{X}_G^{\{1\}} = \{\{2\},\{3\}\}$, $\mathcal{X}_G^{\{2,3\}} = \{\{1\},\{1,2,3\}\}$ and $\mathcal{X}_G^{\{1,2,3\}} = \{\{1,2\},\{1,3\}\}$ are all "connected" by $\{2,3\}$ via the symmetric difference operation Δ. (c) Grouping of vertex subsets according to the correlation index. Γ_G and $\mathcal{K}_G$ are the X-chain group generators and correlation group generators, respectively.

can be represented in the following binary matrix

$$\left(\begin{array}{ccc|ccc} 0&0&0&0&0&0\\ 1&0&0&0&1&1\\ 0&1&0&1&0&0\\ 0&0&1&1&0&0\\ 1&1&0&1&1&1\\ 1&0&1&1&1&1\\ 0&1&1&0&0&0\\ 1&1&1&0&1&1 \end{array}\right),$$

in which each row represents a stabilizer: the bit strings on the left hand side of the divider are the possible vertex sets ξ occuring as a superscript for the Pauli σ_X operators in Eq. A2, while the right hand side are their correlation indices c_ξ occurring as superscript for the Pauli σ_Z operators. This is the so-called binary representation of graph states [14–16]. We interpret this binary representation as an incidence structure [13] in Fig. 1b, in which the vertex sets ξ are depicted as the nodes in the lower row, while the upper row interprets the correlation indices c_ξ . In the example of $|S_3\rangle$, one observes that the correlation indices c_ξ do not cover all possible 3-bit binary numbers. The vertex subsets are regrouped according to their correlation indices in Fig. 1c. The concept of regrouping is introduced via the definition of the so-called *X-resources* as follows.

Definition 6 (X-resources of correlation indices)**.** *We denote the set of* correlation indices *of a graph G as*

$$\mathcal{C}_G := \{c_G(\xi) : \xi \subseteq V_G\}.$$

If a vertex set ξ has correlation index c, i.e. $c_G(\xi) = c$, then we call ξ an (X-)resource of c-correlation *in G. The* (X-)resource set of c-correlation *is written as*

$$\mathcal{X}_G^{(c)} := \{\xi \subseteq V_G : c_G(\xi) = c\}. \tag{15}$$

Since in the example of $|S_3\rangle$ the correlation index of $\{2,3\}$ is $\emptyset$, each correlation index $c \in \mathcal{C}_{S_3}$ has two X-resources $\xi^{(c_1)}$ and $\xi^{(c_2)}$ with $\xi^{(c_1)} = \xi^{(c_2)}\Delta\{2,3\}$. The number of X-resources of $|S_3\rangle$ is 2^3. Therefore the graph state $|S_3\rangle$ generates 4 correlation indices corresponding to 4 binary numbers. The other 4 correlation indices are excluded due to the existence of the non-trivial $\emptyset$-correlation resource $\{2,3\}$. This non-trivial $\emptyset$-correlation resource decreases the correlations of the graph state in the X-basis. Explicitly a non-trivial $\emptyset$-correlation resource induces a stabilizer consisting of solely σ_X operators as follows.

$$s_G^{(\xi)} = \pi_G(\xi)\,\sigma_X^{(\xi)}, \text{ for all } \xi \in \mathcal{X}_G^{(\emptyset)}.$$

We will call such vertex sets *X-chains*.

Definition 7 (X-chains)**.** *Let $|G\rangle$ be a graph state. An* X-resource of $\emptyset$-correlation *in G is called an* X-chain *of G. The set of all X-chains is denoted as $\mathcal{X}_G^{(\emptyset)}$.*

The X-chains of the graph states $|S_3\rangle$, $|S_4\rangle$ and $|C_3\rangle$ are given as examples in Table II. The X-chains for certain types of graph states (i.e. linear graph states $|L_n\rangle$, cycle graph states $|C_n\rangle$, complete graph states $|K_n\rangle$ and star graph states $|S_n\rangle$) are studied in [8]. A Mathematica package is provided for finding X-chains in general graph states [9].

We point out that the X-chains form a group with the symmetric difference operation.

Lemma 8 (X-chain groups and correlation groups)**.** *Let $|G\rangle$ be a graph state. The set of X-chains together with the symmetric difference $(\mathcal{X}_G^{(\emptyset)}, \Delta)$, is a normal subgroup of $(\mathcal{P}(V_G), \Delta)$. The quotient group $(\mathcal{P}(V_G)/\mathcal{X}_G^{(\emptyset)}, \Delta)$ is identical to the set of all resource sets*

$$\mathcal{P}(V_G)/\mathcal{X}_G^{(\emptyset)} = \left\{\mathcal{X}_G^{(c)} : c \in \mathcal{C}_G\right\}, \tag{16}$$

which we call call the correlation group *of $|G\rangle$. Let Γ_G and $\mathcal{K}_G$ denote the generating sets of $(\mathcal{X}_G^{(\emptyset)}, \Delta)$ and $(\mathcal{P}(V_G)/\mathcal{X}_G^{(\emptyset)}, \Delta)$, respectively. The stabilizer group $(\mathcal{S}_G, \cdot)$ is isomorphic to the direct product of the X-chain group and the correlation group,*

$$(\mathcal{S}_G, \cdot) \sim (\langle\Gamma_G\rangle, \Delta) \times (\langle\mathcal{K}_G\rangle, \Delta), \tag{17}$$

Graph G	X-chains $\langle\Gamma_G\rangle$	X-chain generators Γ_G
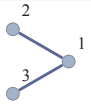 S_3	$\xi_1 = \emptyset$ $\xi_2 = \{2,3\}$ 	{{2,3}}
 C_3	$\xi_1 = \emptyset$ $\xi_2 = \{1,2,3\}$ 	{{1, 2, 3}}
 S_4	$\xi_1 = \emptyset$ $\xi_2 = \{2,3\}$  $\xi_3 = \{2,4\}$  $\xi_4 = \{3,4\}$ 	{{2, 3}, {2, 4}}

TABLE II: X-chain groups of simple graphs: The directed graphs shown under the X-chains illustrate the criterion of X-chains. Once a vertex is selected in a vertex subset ξ then one draws arrows from it to its neighbors. A vertex subset ξ is an X-chain if and only if all vertices of the graph are incident by even number of arrows. The X-chain groups $\langle\Gamma_G\rangle$ are generated by their generating sets Γ_G.

As a result, the graph state $|G\rangle$ is the product of the X-chain group and correlation group inducing stabilizers, i.e.

$$|G\rangle\langle G| = \prod_{\kappa\in\mathcal{K}_G} \frac{1 + s_G^{(\kappa)}}{2} \prod_{\gamma\in\Gamma_G} \frac{1 + s_G^{(\gamma)}}{2}. \tag{18}$$

Proof. See Appendix A. □

Note that the brackets $\langle\Gamma_G\rangle$ and $\langle\mathcal{K}_G\rangle$ denote the group generated by Γ_G and $\mathcal{K}_G$, respectively The correlation group represents the partition of the powerset of vertex set $\mathcal{P}(V_G)$ regarding the correlation index of the vertex subsets $\xi \in \mathcal{P}(V_G)$. The members in the correlation group $\xi \in \langle\mathcal{K}_G\rangle$ possess distinct correlation indices. All the members in the c-correlation resource set $\xi \in \mathcal{X}^{(c)}$ are connected by X-chains. Let $\xi_1^{(c)} \in \mathcal{X}^{(c)}$ and $\xi_2^{(c)} \in \mathcal{X}^{(c)}$ be two X-resources for the same correlation index c, then there must exist an X-chain $\gamma \in \Gamma_G$, such that

$$\xi_2^{(c)} = \xi_1^{(c)}\Delta\gamma. \tag{19}$$

For instance, in the example of $|S_3\rangle$ (Fig. 1b), the resources of correlation $i^{(c)} = 111$ (i.e. $c = \{1,2,3\}$)

are connected by the X-chain $\{2,3\}$, i.e. $\{1,3\} = \{1,2\}\Delta\{2,3\}$. Therefore one can choose one member in $\mathcal{X}^{(c)}$ to represent the whole resource set $\mathcal{X}^{(c)}$. Hence after the X-chain factorization the group $(\mathcal{P}(V_G), \Delta)$ for S_3 becomes $\langle \mathcal{K}_G \rangle = \{\emptyset, \{1\}, \{2\}, \{1,2\}\}$ with $\mathcal{K}_G = \{\{1\}, \{2\}\}$

In Eq. (A8) the Hilbert space $\mathbb{H}_G$ of the graph state $|G\rangle$ is first projected onto the subspace stabilized by the stabilizers $s_G^{(\gamma)}$ with $\gamma \in \Gamma_G$. It is the subspace, $\mathrm{span}(\Psi_\emptyset)$, spanned by the stabilized states $|\psi_\emptyset\rangle$ with

$$\Psi_\emptyset := \left\{ |\psi_\emptyset\rangle : s_G^{(\gamma)} |\psi_\emptyset\rangle = |\psi_\emptyset\rangle, \text{ for all } \gamma \in \Gamma_G \right\}. \quad (20)$$

In this projection, $|\psi_\emptyset\rangle$ are all product states, since every X-chain stabilizer $s_G^{(\gamma)}$ commutes with the $\sigma_X^{\times n}$ operator. After the first projection, the graph state is then obtained via projecting the subspace $\mathrm{span}(\Psi_\emptyset)$ into the state that is stabilized by the stabilizers $s_G^{(\kappa)}$ induced by the correlation group. I.e.

$$\mathbb{H}_G \xrightarrow{\Gamma_G} \Psi_\emptyset \xrightarrow{\mathcal{K}_G} |G\rangle. \quad (21)$$

This approach will be employed in the next section to derive the representation of graph states in the X-basis.

IV. X-CHAIN FACTORIZATION OF GRAPH STATES

We express $|G\rangle$ in the X-basis as $|G\rangle = \sum_{i=1}^{2^n} \alpha_i |i_X\rangle$, with $\sum_i |\alpha_i|^2 = 1$. Since the X-chain stabilizers $s_G^{(\gamma)}$ stabilize $|G\rangle$, it holds

$$\sum \alpha_i |i_X\rangle = \sum \alpha_i s_G^{(\gamma)} |i_X\rangle. \quad (22)$$

Since $s_G^{(\gamma)}$ solely contains σ_X-operators, $s_G^{(\gamma)}|i_X\rangle = \pm|i_X\rangle$. In order to fulfill Eq. (22), however, it follows that only the plus sign is possible, i.e.

$$s_G^{(\gamma)} |i_X\rangle = |i_X\rangle \text{ for all } \alpha_i \neq 0. \quad (23)$$

That means that the possible X-measurement outcomes are solely those X-basis states $|i_G\rangle$, which are stabilized by all X-chain stabilizers $s_G^{(\gamma)}$. A graph state $|G\rangle$ is hence a superposition of such particular X-basis states.

E.g. the star graph state $|S_3\rangle$ in Fig. 1 is stabilized by the X-chain stabilizer $s_{S_3}^{\{2,3\}} = \sigma_X^{\{2,3\}}$. Therefore $|S_3\rangle$ belongs to the space spanned by the states stabilized by $s_{S_3}^{\{2,3\}}$. From the table in Fig. 1, one observes that the X-basis $|i^{(c)}\rangle$, with $c \in \mathcal{C}_{S_3}$ (see Def. 6) corresponding to the correlation indices of $|S_3\rangle$, are stabilized by $s_{S_3}^{\{2,3\}}$, i.e. $\sigma_X^{(\{2,3\})} |i^{(c)}\rangle = |i^{(c)}\rangle$ for all $c \in \mathcal{C}_{S_3}$. That means $|S_3\rangle$ belongs to the subspace, $\mathrm{span}(\Psi)$, spanned by $\Psi = \left\{ |i^{(c)}\rangle, c \in \mathcal{C}_{S_3} \right\} = \{|000\rangle, |100\rangle, |011\rangle, |111\rangle\}$. Thus $|S_3\rangle$ can be represented in solely 4 X-basis states instead of 8 Z-basis states.

In this section, we will derive a general mapping from the X-chain group and correlation group to graph states in the X-basis. This is the question we raised in section II. We first introduce X-chain states and $\mathcal{K}$-correlation states (Definition 9), which span the subspace stabilized by X-chain stabilizers and $\mathcal{K}$-correlation stabilizers, respectively. Given the explicit form of the X-chain states and correlation states in the X-basis (Proposition 10 and 11), one arrives at the X-chain factorization representation of graph states in Theorem 13.

Definition 9 (X-chain states and correlation states)**.** *Let $|G\rangle$ be a graph state with the X-chain group $\langle \Gamma_G \rangle$ and the correlation group $\langle \mathcal{K}_G \rangle$. We define the X-basis state $|i^{(x_{\Gamma_G})}\rangle$ (shortly $|i^{(x_\Gamma)}\rangle$) as the state stabilized by the Pauli σ_X operators such that*

1. *$\pi_G(\gamma)\, \sigma_X^{(\gamma)} |i^{(x_\Gamma)}\rangle = |i^{(x_\Gamma)}\rangle$, for all $\gamma \in \Gamma_G$,*

2. *$\sigma_X^{(\kappa)} |i^{(x_\Gamma)}\rangle = |i^{(x_\Gamma)}\rangle$, for all $\kappa \in \mathcal{K}_G$.*

The local unitary transformed states

$$|\psi_\emptyset(\xi)\rangle = s_G^{(\xi)} \left| i^{(x_\Gamma)} \right\rangle, \xi \in \langle \mathcal{K}_G \rangle \quad (24)$$

are called X-chain states*. Let $\langle \mathcal{K} \rangle \subseteq \langle \mathcal{K}_G \rangle$ be a correlation subgroup, then a* $\mathcal{K}$-correlation state *of graph state $|G\rangle$, $|\psi_\mathcal{K}(\xi)\rangle$, is defined as*

$$|\psi_\mathcal{K}(\xi)\rangle = s_G^{(\xi)} \prod_{\kappa \in \mathcal{K}} \frac{1 + s_G^{(\kappa)}}{\sqrt{2}} |i^{(x_\Gamma)}\rangle \quad (25)$$

with $\xi \in \langle \mathcal{K}_G \rangle / \langle \mathcal{K} \rangle$. Let $\langle \mathcal{K} \rangle \subseteq \langle \mathcal{K}' \rangle \subseteq \langle \mathcal{K}_G \rangle$, a set of $\mathcal{K}$-correlation states are denoted as

$$\Psi_{\mathcal{K}'}^{(\mathcal{K})} = \{ |\psi_\mathcal{K}(\xi)\rangle : \xi \in \langle \mathcal{K}' \rangle / \langle \mathcal{K} \rangle \} \quad (26)$$

In this notation, the set of X-chain states is then written as $\Psi_{\mathcal{K}_G}^{(\emptyset)}$, shortly as $\Psi^{(\emptyset)}$, while the set of all $\mathcal{K}$-correlation states is denoted by $\Psi_{\mathcal{K}_G}^{(\mathcal{K})}$, shortly by $\Psi^{(\mathcal{K})}$. Note that $|\psi_\emptyset(\emptyset)\rangle = |i^{(x_\Gamma)}\rangle$, and X-chain states $|\psi_\emptyset(\xi)\rangle$ are $\emptyset$-correlation states. The X-basis $|i^{(x_\Gamma)}\rangle$ is the fundamental state from which the non-vanishing X-basis components in graph states can be derived. According to its definition, $|i^{(x_\Gamma)}\rangle$ depends on the generating set of the X-chain group and the correlation group of a given graph state. One can employ the following approach to obtain the fundamental X-chain state $|i^{(x_\Gamma)}\rangle$.

Proposition 10 (X-chain states in X-basis)**.**
Let $|G\rangle$ be a graph state with the X-chain group $\langle\Gamma_G\rangle$ and the correlation group $\langle\mathcal{K}_G\rangle$. Let $\Gamma_G = \{\gamma_1, \gamma_2, ...\}$, and $\gamma_i = \{v_{i_1}, v_{i_2}, \cdots\}$. The generating set Γ_G and $\mathcal{K}_G$ can be chosen as

1. *$\Gamma_G = \{\gamma_1, ..., \gamma_k\}$ such that $\gamma_i \not\subseteq \gamma_j$ for all $\gamma_i, \gamma_j \in \Gamma_G$,*
2. *$\mathcal{K}_G = \left\{\{v\} : v \in V_G \backslash \bigcup_{i=1}^{k} \{v_{i_1}\}\right\}$.*

Here, the first element of $\gamma_i = \{v_{i_1}, v_{i_2}, ...\}$ is selected in the way such that $v_{i_1} \neq v_{j_1}$ for all $i \neq j$. Then the X-chain state $|\psi_\emptyset(\emptyset)\rangle$ of $|G\rangle$ is an X-basis state, $|i^{(x_\Gamma)}\rangle$, with

$$x_\Gamma = \{v_{i_1} : \pi_G(\gamma_i) = -1\}. \tag{27}$$

Proof. See Appendix A. □

The vertices v_{i_1} are the key for the determination of $|x_\Gamma\rangle$. First of all, we choose the X-chain generators Γ_G, such that $\gamma_i \not\subseteq \gamma_j$, for all $\gamma_i, \gamma_j \in \Gamma_G$. That means each X-chain generator possesses at least a vertex v_{i_1} as its own vertex exclusively, i.e. $v_{i_1} \in \gamma_i \backslash (\cup_{j\neq i}\gamma_j)$. In other words, the vertex v_{i_1} represents the X-chain generator γ_i uniquely. The correlation group generators are then chosen as the single vertex $V_G \backslash \bigcup_i \{v_{i_1}\}$. At the end, the corresponding vertex set x_Γ of the fundamental X-chain state $|i^{(x_\Gamma)}\rangle$ is the set of v_{i_1}, whose X-chain generator γ_i possesses a negative stabilizer-parity. Note that in general the choice of the X-chain generators Γ_G is not unique, therefore the fundamental X-chain states $|i^{(x_\Gamma)}\rangle$ are neither. However, the above mentioned approach still arrives to the same set $\Psi^{(\emptyset)}$ of X-chain states, since the X-chain group is unique.

Let us illustrate these concepts by an example, the graph state $|K_4^{-1}\rangle$ (Fig. 2a), which corresponds to the graph with one edge missing from the complete graph K_4. Its X-chain generators can be chosen as $\Gamma_G = \{\gamma_1, \gamma_2\} = \{\{1, 2, 3\}, \{2, 4\}\}$ (see Fig. 2c). The exclusive vertex v_1 for γ_1 can be chosen as 1, while v_2 for γ_2 is 4. Since only γ_1 has negative parity, therefore $x_\Gamma = \{1\}$ and the fundamental X-chain state is $|i^{(x_\Gamma)}\rangle = |1000\rangle$.

From the fundamental X-chain state $|i^{(x_\Gamma)}\rangle$ one can derive all the X-chain states and correlation states with the following proposition.

Proposition 11 (Form of X-chain states, $\mathcal{K}$-correlation states)**.**
Let $\xi \in \langle\mathcal{K}_G\rangle$ be an X-resource and $\langle\mathcal{K}\rangle \subseteq \langle\mathcal{K}_G\rangle$. An X-chain state is given as

$$|\psi_\emptyset(\xi)\rangle = \pi_G(\xi) \left| i^{(x_\Gamma)} \oplus i^{(c_\xi)} \right\rangle, \tag{28}$$

where $\pi_G(\xi)$ is the stabilizer parity of ξ (see Eq. (13)), and c_ξ is the correlation index of ξ.

A $\mathcal{K}$-correlation state is the superposition of X-chain states*,*

$$|\psi_\mathcal{K}(\xi)\rangle = \frac{1}{2^{|\mathcal{K}|/2}} \sum_{\xi' \in \langle\mathcal{K}\rangle} |\psi_\emptyset(\xi\Delta\xi')\rangle. \tag{29}$$

Proof. See Appendix A. □

According to this proposition, the X-chain states of $|K_4^{-1}\rangle$ derived from $|i^{(x_\gamma)}\rangle = |1000\rangle$ are given in the table in Fig. 2c. Alternatively, one can also choose the X-chain generators $\Gamma_G = \{\gamma_1, \gamma_2\} = \{\{2, 1, 3\}, \{4, 1, 3\}\}$ (see Fig. 2d). In this case $v_1 = 2$ and $v_2 = 4$. The parities of γ_1 and γ_2 are both negative, hence $|i^{(x_\Gamma)}\rangle = |0101\rangle$. However, the sets of obtained X-chain states $\Psi^{(\emptyset)}$ are identical in both cases.

The correlation states $|\psi_\mathcal{K}(\xi)\rangle$ are then the superposition of their corresponding X-chain states. E.g. in Fig. 2c the correlation state $|\psi_{\{\{2,3\}\}}(\emptyset)\rangle = (|1000\rangle - |1111\rangle)/\sqrt{2}$. The correlation states have the following properties.

Corollary 12 (Properties of $\mathcal{K}$-correlation states)**.**
Let $\langle\mathcal{K}\rangle \subseteq \langle\mathcal{K}_G\rangle$ be a correlation index subgroup, then

1. *$|\psi_\mathcal{K}(\xi)\rangle$ is stabilized by all stabilizers $s_G^{(\kappa)}$ with $\kappa \in \langle\Gamma_G\rangle \times \langle\mathcal{K}\rangle$*

   $$s_G^{(\kappa)} |\psi_\mathcal{K}(\xi)\rangle = |\psi_\mathcal{K}(\xi)\rangle. \tag{30}$$

   Therefore also the space $\mathrm{span}(\Psi^{(\mathcal{K})})$*, see Eq. (26), is stabilized by $s_G^{(\kappa)}$ with $\kappa \in \langle\Gamma_G\rangle \times \langle\mathcal{K}\rangle$.*
2. *For $\xi_1 \in \langle\mathcal{K}_G\rangle$ and $\xi_1 \notin \langle\mathcal{K}\rangle$, it holds*

   $$s_G^{(\xi_1)} |\psi_\mathcal{K}(\xi_2)\rangle = |\psi_\mathcal{K}(\xi_1\Delta\xi_2)\rangle. \tag{31}$$

3. *For $\kappa \in \mathcal{K}_G$ and $\kappa \notin \mathcal{K}$, the $\mathcal{K} \cup \{\kappa\}$-correlation state can be obtained by*

   $$|\psi_{\mathcal{K}\cup\{\kappa\}}(\xi)\rangle = \frac{1 + s_G^{(\kappa)}}{\sqrt{2}} |\psi_\mathcal{K}(\xi)\rangle. \tag{32}$$

Proof. See Appendix A. □

With these properties one can derive the representation of graph states in the X-basis.

Theorem 13 (X-chain state representation of graph states)**.**
Let $|G\rangle$ be a graph state. Then $|G\rangle$ is a $\mathcal{K}_G$-correlation state, which is a superposition of X-chain states $|\psi_\emptyset(\xi)\rangle$, i.e.

$$|G\rangle = |\psi_{\mathcal{K}_G}\rangle = \frac{1}{2^{|\mathcal{K}_G|/2}} \sum_{\xi \in \langle\mathcal{K}_G\rangle} |\psi_\emptyset(\xi)\rangle. \tag{33}$$

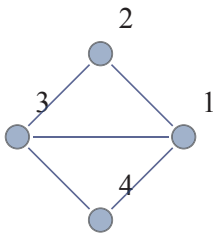

(a)

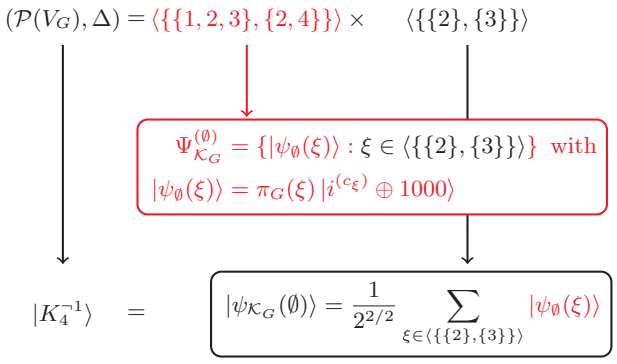

(b)

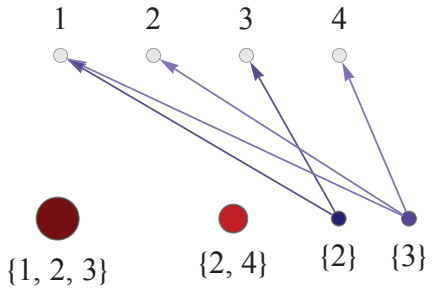

$\gamma \in \Gamma_G$	$\{1,2,3\}$	$\{2,4\}$	$\mathcal{K}_G$	$\{\{2\},\{3\}\}$			
v_{i_1}	1	2	$\xi \in \langle\mathcal{K}_G\rangle$	$\emptyset$	$\{2\}$	$\{3\}$	$\{2,3\}$
$\pi_G(\gamma)$	-1	1	$\pi_G(\xi)$	1	1	1	-1
x_Γ	$\{1\}$		$i^{(c_\xi)}$	0	1010	1101	0111
$\lvert i^{(x_\Gamma)}\rangle$	$\lvert 1000\rangle$		$\lvert\psi_\emptyset(\xi)\rangle$	$\lvert 1000\rangle$	$\lvert 0010\rangle$	$\lvert 0101\rangle$	$-\lvert 1111\rangle$

(c)

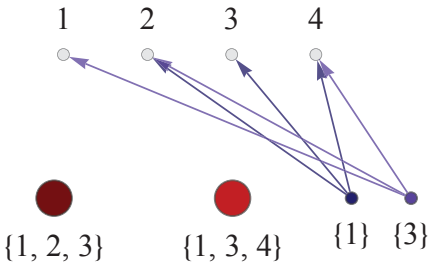

$\gamma \in \Gamma_G$	$\{2,1,3\}$	$\{4,1,3\}$	$\mathcal{K}_G$	$\{\{1\},\{3\}\}$			
v_{i_1}	2	4	$\xi \in \langle\mathcal{K}_G\rangle$	$\emptyset$	$\{1\}$	$\{3\}$	$\{1,3\}$
$\pi_G(\gamma)$	-1	-1	$\pi_G(\xi)$	1	1	1	-1
x_Γ	$\{2,4\}$		$i^{(c_\xi)}$	0	0111	1101	1010
$\lvert i^{(x_\Gamma)}\rangle$	$\lvert 0101\rangle$		$\lvert\psi_\emptyset(\xi)\rangle$	$\lvert 0101\rangle$	$\lvert 0010\rangle$	$\lvert 1000\rangle$	$-\lvert 1111\rangle$

(d)

FIG. 2: (Color online) Example for determination of X-chain states (see main text in section IV for details): (a) The graph state $|K_4^{-1}\rangle$. (b) The factorization diagram of $|K_4^{-1}\rangle$ (for an explanation, see Algorithm 14). (c),(d) The incidence structure of the X-chain generators and correlation group generators of $|K_4^{-1}\rangle$. The choices of these generators are not unique, and lead to different fundamental X-chain states $|i^{(x_\Gamma)}\rangle$. However, they arrive at the identical set of X-chain states $\{|\psi_\emptyset(\xi)\rangle, \xi \in \langle\mathcal{K}_G\rangle\}$.

Proof. According to property 1 in Corollary 12, one can infer that $|\psi_{\mathcal{K}_G}\rangle$ is stabilized by all graph state stabilizers $s_G^{(\xi)}$ with $\xi \in \langle\Gamma_G\rangle \times \langle\mathcal{K}_G\rangle$. As a result of Lemma 8, $|\psi_{\mathcal{K}_G}\rangle$ is stabilized by the whole graph state stabilizer group $\mathcal{S}_G$. According to the definition of graph states in the stabilizer formalism, one can infer that $|G\rangle = |\psi_{\mathcal{K}_G}\rangle$. The explicit form of $|\psi_{\mathcal{K}_G}\rangle$ in Eq. (33) is obtained by Proposition 11. □

Note that the graph state obtained by this theorem may differ from the real one by a global phase -1, i.e. $|G\rangle = -|\psi_{\mathcal{K}_G}\rangle$ [31]. We summarize the approach of X-chain factorization of a graph state representation in a so-called factorization diagram.

Algorithm 14 (Factorization diagram)**.**
The X-chain factorization of graph states can be described in the factorization diagram *shown in Fig. 3.*

1. *One decomposes the group $\mathcal{P}(V_G)$ into the direct product of the X-chain group $\langle\Gamma_G\rangle$ and the correlation group $\langle\mathcal{K}_G\rangle$ (Lemma 8).*

2. *From the X-chain group $\langle\Gamma_G\rangle$, one obtains the set*

of X-chain states $\Psi^{\emptyset}_{\mathcal{K}_G}$ (Proposition 10).

3. *From the correlation group $\langle \mathcal{K}_G \rangle$, one obtains graph states via the superposition of the X-chain states in $\Psi^{\emptyset}_{\mathcal{K}_G}$ (Theorem 13).*

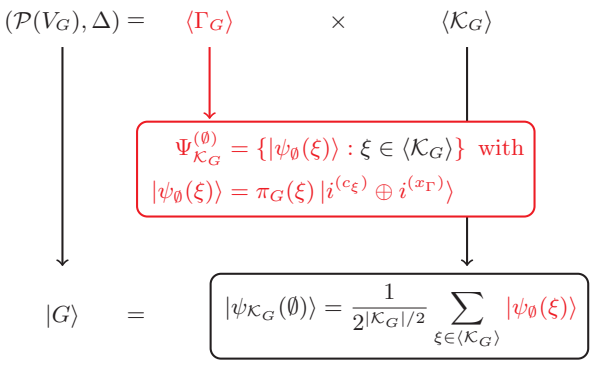

FIG. 3: (Color online) X-chain factorization diagram of graph states: A graphical summary of Proposition 10, 11 and Theorem 13. This diagram illustrates the algorithm for representing a graph state in the X-basis.

The arrows in the factorization diagram can be interpreted as a mapping from the sets of X-resources to their corresponding stabilized Hilbert subspaces. As we already discussed at the end of the section II, a graph state is mapped from the powerset of vertices by stabilizer induction, which is depicted in the left hand side of the equality in the diagram. The equation in the first row is the X-chain factorization of the group $(\mathcal{P}(V_G), \Delta)$ (Lemma 8). The arrow from the X-chain group Γ_G to the X-chain states $\Psi^{(\emptyset)}$ interprets the mapping from the X-chain group to the stabilized subspace spanned by $\Psi^{(\emptyset)}$ (Definition 9 and Proposition 10). The arrow from the correlation group $\langle \mathcal{K}_G \rangle$ through the X-chain states $\Psi^{(\emptyset)}$ to the $\mathcal{K}_G$-correlation state is a mapping from the subspace span$(\Psi^{(\emptyset)})$ to the $\mathcal{K}_G$-correlation state $|\psi_{\mathcal{K}_G}\rangle$, which is stabilized by the $\mathcal{K}_G$-stabilizers. This arrow-represented mapping is the summation (superposition) of the X-chain states over the correlation group $\langle \mathcal{K}_G \rangle$ (Proposition 11). Since the graph state $|G\rangle$ is the only stabilized state of the stabilizers induced by the group $\langle \Gamma_G \rangle \times \langle \mathcal{K}_G \rangle$, it is identical to the $\mathcal{K}_G$-correlation state $|\psi_{\mathcal{K}_G}\rangle$ (Theorem 13), which is represented by the equality of the last line in the factorization diagram. With the help of the factorization diagram in Fig. 2b, the graph state $|K_4^{\neg 1}\rangle$ is given by

$$|K_4^{\neg 1}\rangle = \frac{1}{2}\left(|1000\rangle + |0010\rangle + |0101\rangle - |1111\rangle\right). \quad (34)$$

Since the edge number $|E_{G[\xi]}|$ is identical to the product $\langle i_Z^{(\xi)}, i_Z^{(\xi)} \rangle_{A_G}$ in Eq. (10), according to the definition of the stabilizer-parity (Def. 4),

$$\pi_G(\xi) = (-1)^{\langle i_Z^{(\xi)}, i_Z^{(\xi)} \rangle_{A_G}}. \quad (35)$$

Hence the representation of graph states in the Z-basis in Eq. (10) can be reformulated as

$$|G\rangle = \frac{1}{2^{n/2}} \sum_{\xi \subseteq V_G} \pi_G(\xi)\, |i_Z^{(\xi)}\rangle. \quad (36)$$

Comparing this Z-representation with the representation of a graph state in the X-basis given in Eq. (33), the number of terms in the representation is reduced from $2^{|V_G|}$ to $2^{|\mathcal{K}_G|}$. The correlation group $\langle \mathcal{K}_G \rangle$ can be directly obtained if one knows the X-chain group. The X-chain group can be searched by a criterion that the cardinality of the intersection of the vertex neighborhood with the X-chain $|N_v \cap \xi|$ should be even for all $v \in V_G$ [8]. The search of the X-chains of a graph state $|G\rangle$ is equivalent to finding the 2-modulus-kernel of the adjacency matrix of the graph G. As this is efficient, the representation of graph states in the X-basis is feasible. The larger the X-chain group that a graph state possesses, the smaller is its correlation group and hence the more efficient is its X-chain factorization.

Note that not every graph state has non-trivial X-chains (non-trivial means not the empty set). For graph states without non-trivial X-chains, their X-chain factorization contains all X-basis states, and thus has the same difficulty as their Z-representation.

Besides, the X-chain factorization of graph states in Theorem 13 implies that the possible outcomes of X-measurements are only the X-chain states, $|\psi_\emptyset(\xi)\rangle$. Consequently two graph states with different X-chains can have different X-chain states, and hence are distinguishable via the X-measurement outcomes. In Table III, we list the X-chain generators and X-chain states of graph states with 3 vertices. Since the X-chain states of these graph states are different from each other, one can therefore distinguish these 8 graph states via local X-measurements with non-zero probability of success.

V. APPLICATION OF THE X-CHAIN FACTORIZATION

The representation of graph states in the X-chain factorization reveals certain substructures of graph states. In this section, we discuss its usefulness for the calculation of graph state overlaps, the Schmidt decomposition and unilateral projections in bipartite systems.

A. Graph state overlaps

In [17], the overlaps of graph states are the basis for genuine multipartite entanglement detection of randomized graph states with projector-based witnesses $W_G =$

$\|G\rangle$	Γ_G	$\Psi^{(\emptyset)}_{\mathcal{K}_G} = \{\|\psi_\emptyset(\xi)\rangle : \xi \in \langle \mathcal{K}_G \rangle\}$
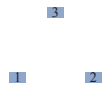	$\{\{1\},\{2\},\{3\}\}$	$\{\|000\rangle\}$
	$\{\{3\}\}$	$\{\|000\rangle, \|010\rangle, \|100\rangle, -\|110\rangle\}$
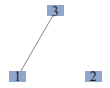	$\{\{2\}\}$	$\{\|000\rangle, \|001\rangle, \|100\rangle, -\|101\rangle\}$
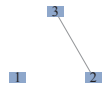	$\{\{1\}\}$	$\{\|000\rangle, \|001\rangle, \|010\rangle, -\|011\rangle\}$
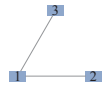	$\{\{2,3\}\}$	$\{\|000\rangle, \|100\rangle, \|011\rangle, -\|111\rangle\}$
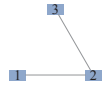	$\{\{1,3\}\}$	$\{\|000\rangle, \|100\rangle, \|101\rangle, -\|111\rangle\}$
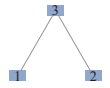	$\{\{1,2\}\}$	$\{\|000\rangle, \|001\rangle, \|110\rangle, -\|111\rangle\}$
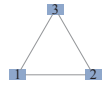	$\{\{1,2,3\}\}$	$\{\|100\rangle, \|010\rangle, \|001\rangle, -\|111\rangle\}$

TABLE III: X-chain states of 3-vertex graph states

$\mathbb{1}/2 - |G\rangle\langle G|$, see [18, 19], where G is a connected graph. An expectation value $\mathrm{tr}(|H\rangle\langle H|G\rangle\langle G|) > 1/2$ indicates the presence of genuine multipartite entanglement of the graph state $|H\rangle$.

In general, a graph state $|G\rangle = \prod_{e\in E_G} U_Z^{(e)}|0_X\rangle$ is created by control-Z operators $U_Z^{(e)}$, where

$$U_Z^{\{v_a,v_b\}} := |0\rangle\langle 0|^{(a)} \otimes \mathbb{1}^{(b)} + |1\rangle\langle 1|^{(a)} \otimes \sigma_Z^{(b)}. \quad (37)$$

Since the operators $U_Z^{(e)}$ commute for different edges e and are unitary, the overlap $\langle G|H\rangle$ is calculated by

$$\langle G|H\rangle = \langle 0_X^{\otimes n}| \prod_{e\in E_G \Delta E_H} U_Z^{(e)} |0_X^{\otimes n}\rangle = \langle 0_X^{\otimes n}|G\Delta H\rangle. \quad (38)$$

According to Eq. (10),

$$\langle G|H\rangle = \frac{1}{2^{n/2}} \sum_{i=0}^{2^n-1} (-1)^{\langle i_Z, i_Z\rangle_{A_{G\Delta H}}}, \quad (39)$$

where $G\Delta H$ is the symmetric difference of the graphs G and H. $G\Delta H$ is the graph $(V_{G\Delta H}, E_{G\Delta H})$, whose vertices and edges are $V_{G\Delta H} = V_G = V_H$ and $E_{G\Delta H} = E_G \cup E_H \setminus E_G \cap E_H$, respectively. However, the complexity of this calculation increases exponentially with the size of the system.

The quantity obtained from Eq. (10),

$$\langle 0_X^{\otimes n}|G\rangle = \frac{1}{2^{n/2}} \sum_{i=0}^{2^n-1} (-1)^{\langle i_Z, i_Z\rangle_A}, \quad (40)$$

corresponds to the difference of the positive and negative amplitudes of $|G\rangle$ in the Z-basis. We can define for each graph state $|G\rangle$ a Boolean function $f_G := \langle i_Z, i_Z\rangle_A \pmod 2$ with A being the adjacency matrix. The function f_G is balanced, if and only if $\langle 0_X^{\otimes n}|G\rangle = 0$, otherwise it is biased. We introduce the bias degree of a graph state and define its Z-balance as follows.

Definition 15 (Bias degree and Z-balanced graph states)**.**
The (Z-)bias degree β *of a graph state* $|G\rangle$ *with* n *vertices is defined as the overlap*

$$\beta(|G\rangle) := \langle 0_X^{\otimes n}|G\rangle, \quad (41)$$

where $|0_X\rangle = (|0_Z\rangle + |1_Z\rangle)/\sqrt{2}$*. A graph state with zero bias degree is called* Z-balanced*.*

The bias degree is related to the weight of a graph state, $\omega^-(G) := |\{i_Z : \langle i_Z|G\rangle / |\langle i_Z|G\rangle| = -1\}|$, which is equal to the number of minus amplitudes in $|G\rangle$ in the Z-basis [20]. The probability of finding a negative amplitude in the Z-basis is $1/2 - \beta(|G\rangle)/2$, which is equal to $\omega^-(G)/2^n$. Note that as a result of Eq. (36), the bias degree of a graph state is equal to the sum of its stabilizer parities.

$$\beta(|G\rangle) = \sum_{\xi\subseteq V_G} \pi_G(\xi). \quad (42)$$

As a result of Theorem 13, the bias degree $\langle 0_x \,|\, G\rangle$, depends only on the number of X-chain generators and the parity of their corresponding X-resources.

Corollary 16 (Graph state overlaps and bias degrees)**.** *The overlap of two graph states $|G\rangle$ and $|H\rangle$ is equal to the bias degree of the graph state $|G\Delta H\rangle$, i.e.*

$$\langle G|H\rangle = \beta(|G\Delta H\rangle). \tag{43}$$

The bias degree of a graph state $|G\rangle$ is equal to

$$|\beta(|G\rangle)| = \frac{1}{2^{(n-|\Gamma_G|)/2}} \prod_{\gamma\in\Gamma_G} \delta^1_{\pi_G(\gamma)}, \tag{44}$$

where Γ_G is the X-chain generating set of $|G\rangle$, δ is the Kronecker-delta and $\pi_G(\gamma)$ is the stabilizer-parity of X-chain generators γ.

Proof. First we prove that there does not exist ξ such that $c_\xi = x_\Gamma$. Assume $c_\xi = x_\Gamma$, then $|c_\xi \cap \gamma| \overset{\mathrm{mod}\,2}{=} |\xi \cap c_\gamma| = 0$. However, according to the definition of x_Γ (Def. 10), $|c_\xi \cap \gamma| = |x_\Gamma \cap \gamma| = 1$ which contradicts $|c_\xi \cap \gamma| = 0 \bmod 2$. Then the only possible zero X-chain state is $|i^{x_{(\Gamma)}}\rangle$. Therefore Theorem 13 leads to

$$|\beta(|G\rangle)| = \frac{1}{2^{(n-|\Gamma_G|)/2}} \langle 0_X|i^{(x_\Gamma)}\rangle. \tag{45}$$

According to the definition of the X-chain basis, $x_\Gamma = \emptyset$ if and only if $\pi_G(\gamma) = 1$ for all X-chain generators $\gamma \in \Gamma_G$, that means $\langle 0_X|i^{(x_\Gamma)}\rangle = \prod_{\gamma\in\Gamma_G} \delta^1_{\pi_G(\gamma)}$. □

In [20], the authors relate the weight $\omega^-(G)$ to the binary rank of the adjacency matrix of graphs. Our Corollary 16 is a similar result showing that the bias degree depends on the binary rank of the adjacency matrix, which is equal to $n - |\Gamma_G|$.

Here, we focus on the bias degree and Z-balance of graph states. Since the X-chain group of a graph state can be efficiently determined, instead of Eq. (39), Corollary 16 provides an efficient method to calculate the graph state overlap. As a result of Corollary 16, we arrive at the following corollary.

Corollary 17 (Z-balanced graph states)**.**
A graph state is Z-balanced, if and only if it has at least one X-chain generator γ^- with negative stabilizer-parity, i.e. $|E(G[\gamma^-])|$ is odd. Two graph states are orthogonal, if and only if $|G\Delta H\rangle$ is Z-balanced.

Knowing all the Z-balanced graph states with vertex number n allows to identify all pairs of orthogonal graph states with n vertices. Note that relabeling a graph state (graph isomorphism) does not change its bias degree, since the structure of the X-chain group does not change under graph isomorphism.

In Fig. 4, the Z-balanced graph states up to five vertices are listed. Every graph in the figure represents an isomorphic class. From these balanced graph states one can obtain orthogonal graph states via the graph symmetric difference. Examples of orthogonal graph states derived from the Z-balanced graph states $|C_3\rangle$ and $|C_5\rangle$ are shown in Fig. 5 and 6 , respectively, (C_3 and C_5 are the first and fifth graph in Fig. 4).

B. Schmidt decomposition

In this section, we discuss the Schmidt decomposition of graph states represented in the X-basis, which is derived via the X-chain factorization. The Schmidt decomposition of a graph state for an $A|B$-bipartition reads

$$|G\rangle = \frac{1}{2^{r_S/2}} \sum_{i=1}^{r_S} |\phi_i^{(A)}\rangle\, |\psi_i^{(B)}\rangle\,, \tag{46}$$

where $\langle\phi_i^{(A)}|\phi_j^{(A)}\rangle = \delta_{ij}$ and $\langle\psi_i^{(B)}|\psi_j^{(B)}\rangle = \delta_{ij}$. Here r_S is the Schmidt rank of the graph state $|G\rangle$ with respect to the partition A versus B. Its value

$$r_S = |S_A| := \left|\left\{ s_G^{(\xi)} \in S_G : \mathrm{supp}(s_G^{(\xi)}) \subseteq A \right\}\right| \tag{47}$$

is studied in the section III.B of [6] via the Schmidt decomposition of graph states in the Z-basis, where $\mathrm{supp}(s_G^{(\xi)})$ is the support of the stabilizer $s_G^{(\xi)}$. The $\mathrm{supp}(s_G^{(\xi)})$ is equal to the projection on the Hilbert space spanned by qubits corresponding to the vertices $\xi \cup c_\xi$, which is the set of vertices on which the stabilizer $s_G^{(\xi)}$ acts non-trivially (i.e. not equal to the identity).

We derive the Schmidt decomposition of graph states in the X-basis in the following steps. First, we generalize the X-chain factorization of graph states (Theorem 13) to the X-chain factorization of arbitrary correlation states (Theorem 18). Second, we introduce three correlation subgroups, whose correlation states are $A|B$-biseparable (Lemma 20). Third, we prove the orthonormality of these correlation states (Lemma 21). At the end, we arrive at the Schmidt decomposition in Theorem 22.

The X-chain factorization of graph states in Theorem 13 can be generalized to correlation states (introduced in Eq. (25) and (A15)) as follows.

Theorem 18 (X-chain factorization of $\mathcal{K}$-correlation states)**.**
Let $\langle\mathcal{K}_1\rangle, \langle\mathcal{K}_2\rangle \subseteq \langle\mathcal{K}_G\rangle$ be two disjoint correlation subgroups of a graph state $|G\rangle$, and $\mathcal{K} = \mathcal{K}_1 \cup \mathcal{K}_2$. Then the $\mathcal{K}$-correlation state is a superposition of $\mathcal{K}_1$-correlation states,

$$|\psi_{\mathcal{K}}(\xi)\rangle = \frac{1}{2^{|\mathcal{K}_2|/2}} \sum_{\xi'\in\langle\mathcal{K}_2\rangle} |\psi_{\mathcal{K}_1}(\xi\Delta\xi')\rangle \tag{48}$$

with $\xi \in \langle\mathcal{K}_G\rangle / \langle\mathcal{K}\rangle$ being an element in their quotient group. Theorem 13 is a special case of this theorem related by $\langle\mathcal{K}\rangle = \langle\mathcal{K}_1\rangle \times \langle\mathcal{K}_2\rangle = \emptyset \times \langle\mathcal{K}_G\rangle$.

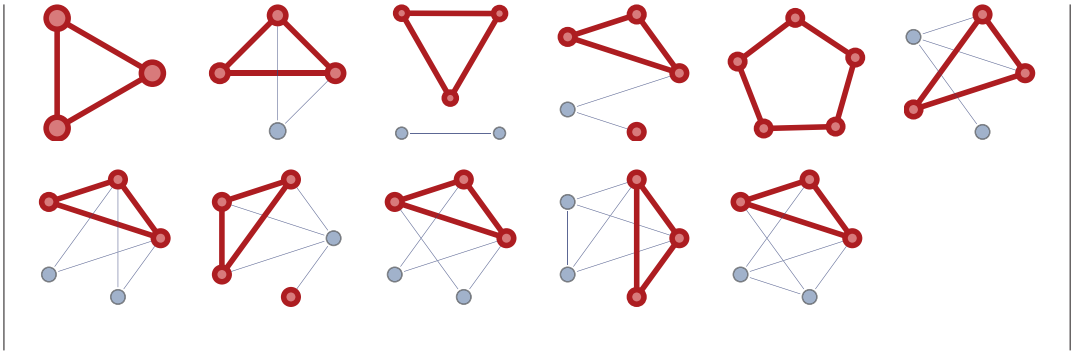

FIG. 4: (Color online) Z-balanced graph states (see Def. 15) up to 5 vertices: Each graph represents a graph isomorphic class. Each balanced graph state has at least one X-chain γ^- with negative parity. In each graph, the γ^--induced subgraph $G[\gamma^-]$ is highlighted in red with bold edges. Every highlighted γ^--induced subgraph has an odd edge number.

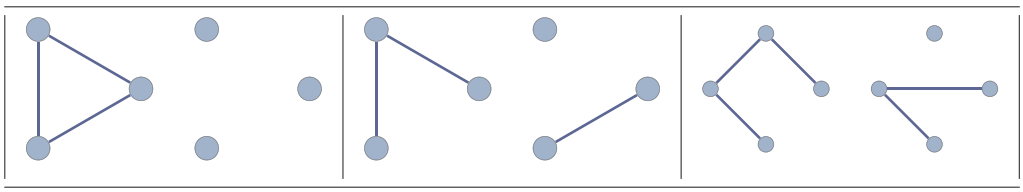

FIG. 5: Orthogonal graph states derived from the Z-balanced graph state $|C_3\rangle$: The graph states in each cell are orthogonal to each other. Their symmetric difference is identical to the cycle graph C_3, where C_3 is the first graph in Fig. 4.

Proof. According to the definition in Eq. (25) it holds

$$|\psi_{\mathcal{K}_1\cup\mathcal{K}_2}(\xi)\rangle = s_G^{(\xi)} \prod_{\kappa\in\mathcal{K}_2} \frac{1+s_G^{(\kappa)}}{\sqrt{2}} \prod_{\kappa\in\mathcal{K}_1} \frac{1+s_G^{(\kappa)}}{\sqrt{2}} \left|i^{(x_\Gamma)}\right\rangle. \tag{49}$$

Due to the commutativity of the graph state stabilizers it follows

$$|\psi_{\mathcal{K}}(\xi)\rangle = |\psi_{\mathcal{K}_1\cup\mathcal{K}_2}(\xi)\rangle = \prod_{\kappa\in\mathcal{K}_2} \frac{1+s_G^{(\kappa)}}{\sqrt{2}} |\psi_{\mathcal{K}_1}(\xi)\rangle. \tag{50}$$

According to Proposition 2, $s_G^{(\kappa_1\Delta\kappa_2)} = s_G^{(\kappa_1)} s_G^{(\kappa_2)}$, the product of $(1+s_G^{(\kappa)})$ with $\kappa\in\mathcal{K}_2$ becomes the sum of the stabilizers $s_G^{(\xi')}$ with $\xi'\in\langle\mathcal{K}_2\rangle$.

$$\begin{aligned} |\psi_{\mathcal{K}}(\xi)\rangle &= \frac{1}{2^{|\mathcal{K}_2|/2}} \sum_{\xi'\in\langle\mathcal{K}_2\rangle} s_G^{(\xi')} |\psi_{\mathcal{K}_1}(\xi)\rangle \\ &= \frac{1}{2^{|\mathcal{K}_2|/2}} \sum_{\xi'\in\langle\mathcal{K}_2\rangle} |\psi_{\mathcal{K}_1}(\xi\Delta\xi')\rangle, \end{aligned} \tag{51}$$

where the second equality is a result of property 2 in Corollary 12. □

Algorithm 19 (Factorization diagram of correlation states)**.**
Theorem 18 can be interpreted by the factorization diagram in Fig. 7.

1. *One decomposes the group $\mathcal{P}(V_G)$ into the direct product of the X-chain group $\langle\Gamma_G\rangle$ and the correlation group $\langle\mathcal{K}_G\rangle$.*
2. *From the X-chain group $\langle\Gamma_G\rangle$, one obtains the set of X-chain states $\Psi^{\emptyset}_{\mathcal{K}_G}$.*
3. *From the correlation group $\langle\mathcal{K}_1\rangle$, one obtains graph states via the superposition of the X-chain states in $\Psi^{\emptyset}_{\mathcal{K}_G}$ within $\langle\mathcal{K}_1\rangle$.*
4. *At the end the correlation state $|\psi_{\mathcal{K}_1\cup\mathcal{K}_2}(\xi)\rangle$ is the superposition of the $\mathcal{K}_1$-correlation states $|\psi_{\mathcal{K}_1}(\xi\Delta\xi')\rangle \in \Psi^{(\mathcal{K}_1)}_{\mathcal{K}_G}$ inside the correlation group $\xi'\in\langle\mathcal{K}_2\rangle$ (Theorem 18).*

The subspace of X-chain states $\mathrm{span}(\Psi^{(\emptyset)}_{\mathcal{K}_G})$ are projected via $\langle\mathcal{K}_1\rangle$-stabilizers to the space spanned by the $\mathcal{K}_1$-correlation states $|\psi_{\mathcal{K}_1}(\xi)\rangle$. Further, the subspace $\mathrm{span}(\Psi^{(\mathcal{K}_1)}_{\mathcal{K}_G})$ are then projected via $\langle\mathcal{K}_2\rangle$-stabilizers to the $\mathcal{K}_1\cup\mathcal{K}_2$-correlation states $|\psi_{\mathcal{K}_1\cup\mathcal{K}_2}(\xi)\rangle$. With this theorem, one can obtain the Schmidt decomposition of graph states, by appropriate selection of the correlation subgroup $\mathcal{K}_1$, such that its corresponding $\mathcal{K}_1$-correlation states are $A|B$-separable and mutually orthonormal.

Let $|G\rangle$ be a graph state with the correlation group

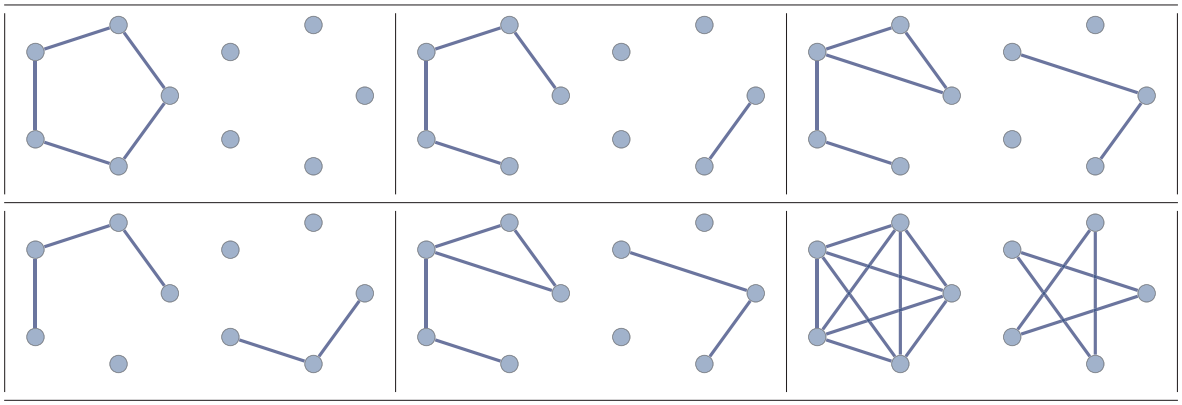

FIG. 6: Orthogonal graph states derived from the Z-balanced graph state $|C_5\rangle$: The graph states in each cell are orthogonal. Their symmetric difference is identical to the cycle graph C_5, where C_5 is the fifth graph in Fig. 4.

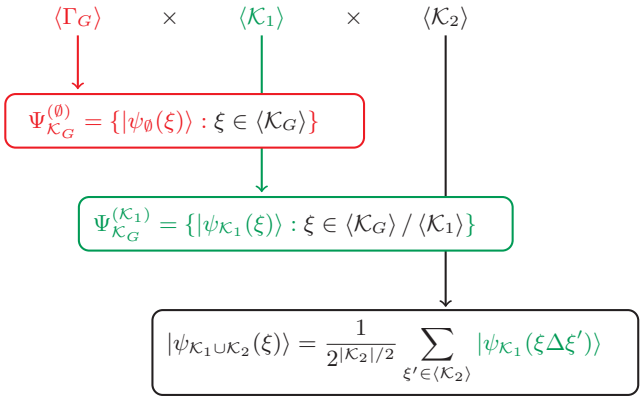

FIG. 7: (Color online) The X-chain factorization diagram of correlation states: A graphical summary of Theorem 18. The ξ in $|\psi_{\mathcal{K}_1\cup\mathcal{K}_2}(\xi)\rangle$ are elements in the quotient group, $\xi \in \langle\mathcal{K}_G\rangle / \langle\mathcal{K}_1 \cup \mathcal{K}_2\rangle$.

$\langle\mathcal{K}_G\rangle$ and $A|B$ be a bipartition of its vertices. In order to find the Schmidt decomposition, we select $\langle K_1\rangle$ as the disjoint union of three correlation subgroups specified as follows.

1. The correlation subgroup, whose elements possess a correlation index only in B:

$$\langle\mathcal{K}^{(B)}\rangle := \{\xi \in \langle\mathcal{K}_G\rangle : c_\xi \subseteq B\}\,. \tag{52}$$

2. The correlation subgroup, whose elements possess a correlation index only in A and only consists of vertices in A:

$$\langle\mathcal{K}^{(A)}_A\rangle := \{\xi \in \langle\mathcal{K}_G\rangle : c_\xi \subseteq A, \xi \subseteq A\}\,. \tag{53}$$

3. The correlation subgroup, whose elements possess a correlation index only in A, consists of vertices in B and has even number of edges between all $\beta \in \langle\mathcal{K}^{(B)}\rangle$:

$$\langle\mathcal{K}^{(A)}_{\sim B}\rangle := \{\xi \in \langle\mathcal{K}_G\rangle : c_\xi \subseteq A, \xi \not\subseteq A\} \cap \{\xi \in \langle\mathcal{K}_G\rangle : |E_G(\xi : \beta)| \overset{\mathrm{mod}\,2}{=} 0, \text{ for all } \beta \in \left\langle\mathcal{K}^{(B)}\right\rangle\}. \tag{54}$$

These three groups form a special group

$$\langle\mathcal{K}^{A\rfloor B}\rangle := \langle\mathcal{K}^{(A)}_A \cup \mathcal{K}^{(A)}_{\sim B}\rangle \times \langle\mathcal{K}^{(B)}\rangle \tag{55}$$

called *$A\rfloor B$-correlation group*. (The notation "$A\rfloor B$" is used, as the group is not symmetric with respect to exchanging A and B.) We will show in Lemma 20 that all $A\rfloor B$-correlation states $|\psi_{\mathcal{K}^{A\rfloor B}}(\xi)\rangle$ with $\xi \in \langle\mathcal{K}^{A\rightharpoonup B}\rangle$, shortly $|\psi_{A\rfloor B}(\xi)\rangle$, are $A|B$-separable. The corresponding quotient group is denoted as

$$\langle\mathcal{K}^{A\rightharpoonup B}\rangle := \langle\mathcal{K}_G\rangle / \langle\mathcal{K}^{A\rfloor B}\rangle \tag{56}$$

and called *$(A \rightharpoonup B)$-correlation group*. (The notation $A \rightharpoonup B$ is introduced, as there is again no symmetry under exchange of A and B, as the correlation index c_ξ of $\xi \in \langle\mathcal{K}^{A\rightharpoonup B}\rangle$ is always inside A.) We will show in Theorem 22 that the Schmidt rank of $|G\rangle$ is equal to the cardinality $|\langle\mathcal{K}^{A\rightharpoonup B}\rangle|$. That means that the correlation subgroup $\mathcal{K}^{A\rightharpoonup B}$ generates the $A|B$ correlation in the graph state $|G\rangle$. Note that we investigated many graphs and found their correlation subgroups $\langle\mathcal{K}^{(A)}_{\sim B}\rangle$ all to be empty. That means the group $\langle\mathcal{K}^{(A)}_{\sim B}\rangle$ may not exist for any graph state. However, this is still an open question.

In this $A\rfloor B$-factorization, the correlation group $\mathcal{K}_G$ is divided into four subgroups. Let us take the graph of "St. Nicholas's house" in Fig. 8a as an example. This "house" state $|G_{\text{House}}\rangle$ is divided into the bipartition $A = \{1, 2, 3\}$ versus $B = \{4, 5\}$. The correlation group factorization is shown in Fig. 8b. The X-chain group of $|G_{\text{House}}\rangle$ is $\{\{1, 2, 3\}\}$. The X-resources are factorized by the X-chain group, $\mathcal{P}(V_G) = \langle\Gamma_G\rangle \times \langle\mathcal{K}_G\rangle$,

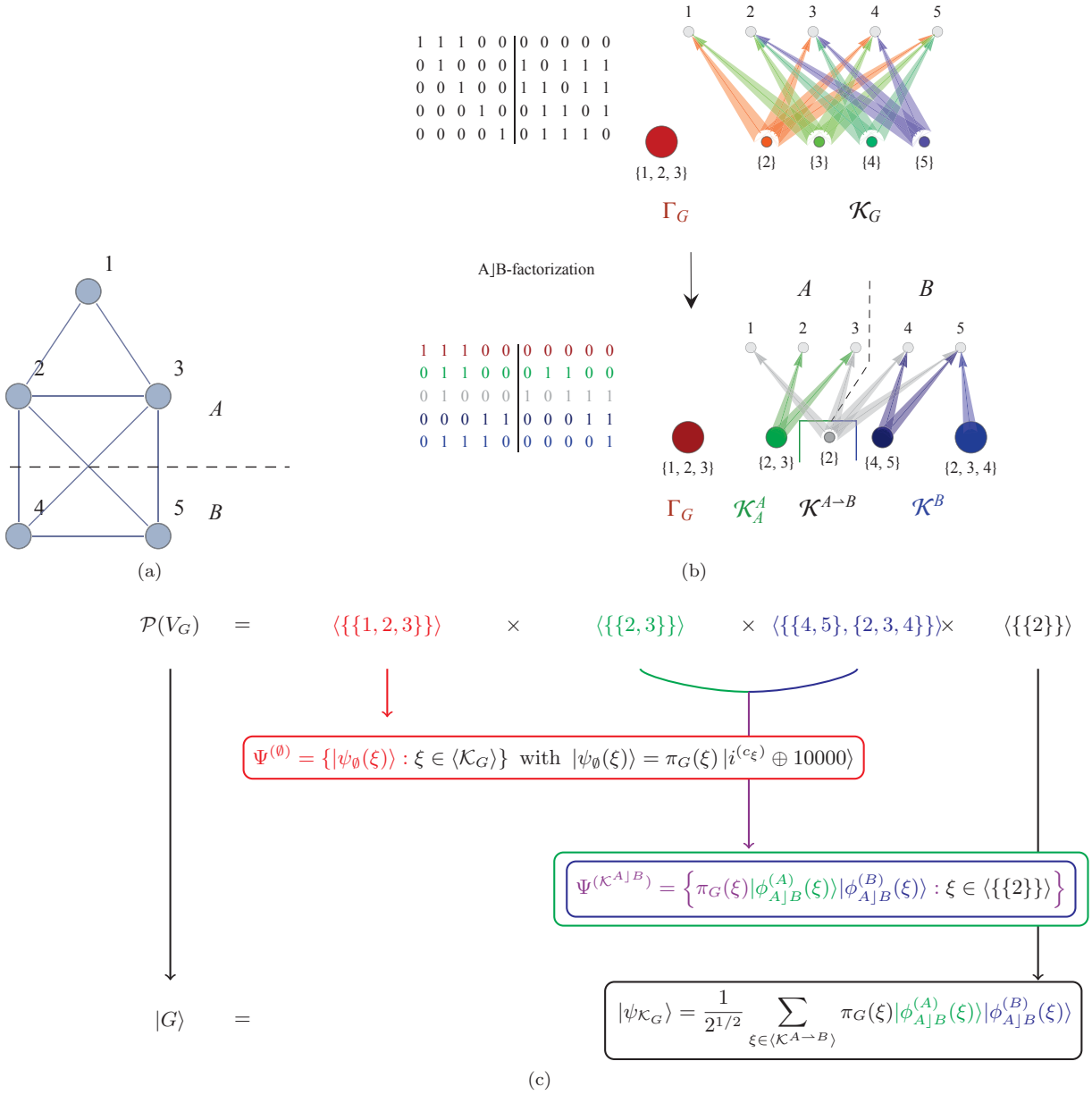

FIG. 8: (Color online) $A\rfloor B$-factorization of graph states: (a) The graph state $|G_{\text{House}}\rangle$ corresponding to a "St. Nicholas's house" is divided in two subsystems $A = \{1,2,3\}$ and $B = \{4,5\}$. (b) The binary representation of the X-chain factorization (the upper row) and $A\rfloor B$-factorization (the lower row). (c) The $A\rfloor B$-factorization diagram (see Algorithm 23) of the "St. Nicholas's house" graph state $|G_{\text{House}}\rangle$.

see the upper row in Fig. 8b. The array is the binary representation of the stabilizers induced by the X-chain generators $\Gamma = \{\{1,2,3\}\}$ and correlation group generators $\mathcal{K}_G = \{\{2\},\{3\},\{4\},\{5\}\}$, it corresponds to the incidence structure on its right hand side. In the second row of Fig. 8b, the X-resources, whose correlation indices lie in the system B, are first grouped together into $\langle\mathcal{K}^{(B)}\rangle = \langle\{\{4,5\},\{2,3,4\}\}\rangle$. Second, the X-resources ξ, whose correlation indices c_ξ and itself ξ are both contained by V_A, are grouped into $\langle\mathcal{K}^{(A)}_A\rangle = \langle\{\{2,3\}\}\rangle$. Third, the group $\mathcal{K}^{(A)}_{\sim B}$ is empty. At the end, the $(A \rightharpoonup B)$-correlation group is then $\langle\mathcal{K}^{A\rightharpoonup B}\rangle = \langle\{\{2\}\}\rangle$.

These three special correlation subgroups, $\langle\mathcal{K}^{(A)}_A\rangle$, $\langle\mathcal{K}^{(A)}_{\sim B}\rangle$ and $\langle\mathcal{K}^{(B)}\rangle$, project the space spanned by the X-chain states into a subspace spanned by their correlation states $|\psi_{A\rfloor B}(\xi)\rangle$. These states are $A|B$-separable states, which is stated in the following lemma.

Lemma 20 ($A|B$-Separability of $A\rfloor B$-correlation states)**.**
For $\xi \in \langle \mathcal{K}_G^{A\rightharpoonup B}\rangle$, the $(A \rightharpoonup B)$-correlation states

$$|\psi_{A\rfloor B}(\xi)\rangle = \pi_G(\xi)\,|\phi^{(A)}_{A\rfloor B}(\xi)\rangle|\phi^{(B)}_{A\rfloor B}(\xi)\rangle \tag{57}$$

are $A|B$-separable with $|\phi^{(A)}_{A\rfloor B}(\xi)\rangle := |\psi^{(A)}_{\mathcal{K}_A^{(A)}\cup\mathcal{K}_{\sim B}^{(A)}}(\xi)\rangle$ and $|\phi^{(A)}_{A\rfloor B}(\xi)\rangle := |\psi^{(B)}_{\mathcal{K}^{(B)}}(\xi)\rangle$ being the $(\mathcal{K}_A^{(A)} \cup \mathcal{K}_{\sim B}^{(A)})$- and $\mathcal{K}^{(B)}$-correlation states projected into the subspaces of A and B, respectively.

Proof. See Appendix A. □

Note that $|\psi_{A\rfloor B}(\xi)\rangle$ will be shown to be the Schmidt basis in Theorem 22. There, one will also see that the global phase $\pi_G(\xi)$ ensures positive Schmidt coefficients.

Let us continue to consider the "St. Nicholas's house" state as an example. According to Proposition 10, the fundamental X-chain state of $|G_{\text{House}}\rangle$ is $|i^{x_\Gamma}\rangle = |10000\rangle$. Then from the $\mathcal{K}_A^{(A)}$-correlation states,

$$|\psi_{\mathcal{K}_A^{(A)}}(\emptyset)\rangle = |\phi^{(A)}_{A\rfloor B}(\emptyset)\rangle \otimes |00\rangle \text{ and} \tag{58}$$

$$|\psi_{\mathcal{K}_A^{(A)}}(\{2\})\rangle = |\phi^{(A)}_{A\rfloor B}(\{2\})\rangle \otimes |00\rangle\,, \tag{59}$$

one can read off

$$|\phi^{(A)}_{A\rfloor B}(\emptyset)\rangle = \frac{|100\rangle - |111\rangle}{\sqrt{2}} \text{ and} \tag{60}$$

$$|\phi^{(A)}_{A\rfloor B}(\{2\})\rangle = \frac{|001\rangle + |010\rangle}{\sqrt{2}}. \tag{61}$$

From the $\mathcal{K}^{(B)}$-correlation states,

$$|\psi_{\mathcal{K}^{(B)}}(\emptyset)\rangle = |100\rangle \otimes |\phi^{(B)}_{A\rfloor B}(\emptyset)\rangle \text{ and} \tag{62}$$

$$|\psi_{\mathcal{K}^{(B)}}(\{2\})\rangle = |100\rangle \otimes |\phi^{(B)}_{A\rfloor B}(\{2\})\rangle, \tag{63}$$

one can read off

$$|\phi^{(B)}_{A\rfloor B}(\emptyset)\rangle = \frac{|00\rangle - |01\rangle - |10\rangle - |11\rangle}{2} \text{ and} \tag{64}$$

$$|\phi^{(B)}_{A\rfloor B}(\{2\})\rangle = \frac{-|00\rangle - |01\rangle - |10\rangle + |11\rangle}{2}. \tag{65}$$

According to Lemma 20, $A\rfloor B$-correlation states are

$$|\psi_{A\rfloor B}(\emptyset)\rangle = \left(\frac{|100\rangle - |111\rangle}{\sqrt{2}}\right)\left(\frac{|00\rangle - |01\rangle - |10\rangle - |11\rangle}{2}\right) \tag{66}$$

and since $\pi_G(\{2\}) = 1$

$$|\psi_{A\rfloor B}(\{2\})\rangle = \left(\frac{|001\rangle + |010\rangle}{\sqrt{2}}\right)\left(\frac{-|00\rangle - |01\rangle - |10\rangle + |11\rangle}{2}\right). \tag{67}$$

Orthonormality of the states within the subspaces still needs to be verified. This holds for the explicit example $|G_{\text{House}}\rangle$ in Eq. (66) and (67). In the general case, the orthonormality is shown in the following lemma.

Lemma 21 (Orthonormality of $(A \rightharpoonup B)$-correlation states)**.**
The components of $A\rfloor B$-correlation states on subspace A and B, $|\phi^{(A)}_{A\rfloor B}(\xi)\rangle$ and $|\phi^{(B)}_{A\rfloor B}(\xi)\rangle$, are orthonormal with respect to $\xi \in \langle \mathcal{K}^{A\leftarrow B}\rangle$ within the subspaces A and B, respectively, i.e.

$$\langle\phi^{(A)}_{A\rfloor B}(\xi_1)|\phi^{(A)}_{A\rfloor B}(\xi_2)\rangle = 0 \tag{68}$$

and

$$\langle\phi^{(B)}_{A\rfloor B}(\xi_1)|\phi^{(B)}_{A\rfloor B}(\xi_2)\rangle = 0$$

for all $\xi_1, \xi_2 \in \langle \mathcal{K}^{A\rightharpoonup B}\rangle$ and $\xi_1 \neq \xi_2$.

Proof. See Appendix A. □

We can now construct the Schmidt decomposition of graph states with $A\rfloor B$-correlation states as follows.

Theorem 22 (Schmidt decomposition in $A\rfloor B$-correlation states)**.**
The Schmidt decomposition of a graph state $|G\rangle$ is the superposition of its $A\rfloor B$-correlation states,

$$|G\rangle = \frac{1}{2^{|\mathcal{K}^{A\rightharpoonup B}|/2}} \sum_{\xi\in\langle\mathcal{K}^{A\rightharpoonup B}\rangle} \pi_G(\xi)\,|\phi^{(A)}_{A\rfloor B}(\xi)\rangle|\phi^{(B)}_{A\rfloor B}(\xi)\rangle. \tag{69}$$

The Schmidt rank r_S and geometric measure of the $A|B$-bipartite entanglement [21, 22] can be expressed by

$$\log_2(r_S) = \mathcal{E}_g^{A|B} = \left|\mathcal{K}^{A\rightharpoonup B}\right| \tag{70}$$

with $\mathcal{E}_g^{(A|B)}(|G\rangle) := -2\log_2\left(\min_\psi |\langle\psi_A\psi_B|G\rangle|\right)$.

Proof. Employing Theorem 13 and 18 together with Lemma 20 one can prove that the graph state $|G\rangle$ is equal to the superposition of all biseparable $A\rfloor B$-correlation states $|\psi_{A\rfloor B}(\xi)\rangle = \pi_G(\xi)|\phi^{(A)}_{A\rfloor B}(\xi)\rangle|\phi^{(B)}_{A\rfloor B}(\xi)\rangle$. As a result of the orthonormality of $|\phi^{(A)}_{A\rfloor B}(\xi)\rangle$ and $|\phi^{(B)}_{A\rfloor B}(\xi)\rangle$ (Lemma 21), Eq. (69) is a Schmidt decomposition. The bipartite geometric measure of entanglement is equal to the maximum singular value $s_{\max}$ of the matrix $M_{ij} := \{\langle i_A j_B|G\rangle\}_{i,j}$ with $i = 0, ..., 2^{|V_A|}-1$ and $i = 0, ..., 2^{|V_B|}-1$ [21]. For the bipartite case the singular value decomposition is equivalent to the Schmidt decomposition. Since the Schmidt coefficients are all $2^{-|\mathcal{K}^{A\rightharpoonup B}|/2}$, if follows that the geometric measure of bipartite entanglement of a

graph state, $\mathcal{E}_g^{A|B} := -2\log_2(s_{\max})$, is equal to log of the Schmidt rank, i.e. $\log_2(r_S) = \left|\mathcal{K}^{A\rightharpoonup B}\right|$. As a result, the $A\rfloor B$-correlation states $\pi_G(\xi)|\phi^{(A)}_{A\rfloor B}(\xi)\rangle|\phi^{(B)}_{A\rfloor B}(\xi)\rangle$ are the $A|B$-separable states, which are closest to $|G\rangle$. □

According to [7], the Schmidt rank is given by $\log_2|\{\sigma \in S_G : \mathrm{supp}(\sigma) \subseteq V_A\}|$ with $|V_A| \leq |V_B|$, which is $|V_A| - \left|\mathcal{K}^{(A)}_A\right| - |\Gamma_G \cap \mathcal{P}(V_A)|$ in the language of the X-chain factorization. The Schmidt rank is also equal to the cardinality of the matching [32] between A and B [23]. The matching is the set of edges between A and B, which do not mutually share any common vertex [11]. Hence the cardinality $\left|\mathcal{K}^{A\rightharpoonup B}\right|$ should be equal to the matching. However the proof of this equality is still an open question.

The result of this section can be summarized in an $A\rfloor B$-factorization diagram.

Algorithm 23 (Factorization diagram: Schmidt decomposition of graph states)**.**
The Schmidt decomposition of graph states in Theorem 22 can be summarized in the factorization diagram of Fig. 9.

1. *The group $\mathcal{P}(V_G)$ is decomposed into the direct product of $\langle\Gamma_G\rangle$, $\langle\mathcal{K}^{A\rfloor B}\rangle = \langle\mathcal{K}^{(A)}_A \cup \mathcal{K}^{(A)}_{\sim B}\rangle \times \langle\mathcal{K}^{(B)}\rangle$ and $\langle\mathcal{K}^{A\rightharpoonup B}\rangle$.*
2. *Via the X-chain group $\langle\Gamma_G\rangle$, one obtains the set of X-chain states $\Psi^{\emptyset}$.*
3. *The Schmidt basis states $|\phi^{(A)}_{A\rfloor B}(\xi\rangle)$ are constructed from the superposition of states in $\Psi^{\emptyset}$ inside the correlation group $\langle\mathcal{K}^{(A)}_A \cup \mathcal{K}^{(A)}_{\sim B}\rangle$ (Lemma 20).*
4. *Similar to the previous step, one obtains the states $|\phi^{(B)}_{A\rfloor B}(\xi)\rangle$ via the correlation group $\langle\mathcal{K}^{(B)}\rangle$ (Lemma 20).*
5. *Together with the stabilizer-parities $\pi_G(\xi)$, the set of $A\rfloor B$-correlation states $\Psi^{(A\rfloor B)}$ (Lemma 20) are constructed.*
6. *Via the $(A \rightharpoonup B)$-correlation group $\langle\mathcal{K}^{A\rightharpoonup B}\rangle$, one obtains the Schmidt decomposition from the superposition of states in* $\mathrm{span}(\Psi^{(A\rfloor B)})$ *(Lemma 21 and Theorem 22).*

The $A\rfloor B$-factorization diagram of $|G_{\mathrm{House}}\rangle$ is shown in Fig. 8c. As a result of this theorem, the Schmidt decomposition of this state is

$$|G_{\mathrm{House}}\rangle = \frac{1}{\sqrt{2}}\left(|\psi_{A\rfloor B}(\emptyset)\rangle + |\psi_{A\rfloor B}(\{2\})\rangle\right) \tag{71}$$

with $|\psi_{A\rfloor B}(\emptyset)\rangle$ and $|\psi_{A\rfloor B}(\{2\})\rangle$ being given in Eq. (66) and (67). The house state has Schmidt rank $r_S = 2$ and the geometric measure of bipartite entanglement $E_g^{(A|B)} = -2\log_2(\min_\psi|\langle\psi_A\psi_B|G_{\mathrm{House}}\rangle|) = 1$.

1. Entanglement localization of graph states protected against errors

In this section, we consider the localization of entanglement [10] on graph states shared between Alice and Bob ($A|B$-bipartition), see Fig. 10a. Alice measures the graph state with Pauli-measurements on her system, then tells Bob her measurement results via a classical channel. At the end, Bob should possess a bipartite maximally entangled state which he knows. A connected graph state is maximally "connected" with respect to entanglement localization, if every pair of vertices can be projected onto a Bell pair with local measurements [7]. The most simple approach to localize the entanglement of $|G\rangle$ in the subsystem $\{B_1, B_2\}$ is finding a path between B_1 and B_2, then removing vertices outside the path with Z-measurements and at the end measuring each vertex on the path between $\{B_1, B_2\}$ in the X-direction. However, the resulting state depends on the measurement outcomes. If errors occur in Alice's measurements, it will leads to a wrong state of Bob. Therefore error correction would be a nice feature in the entanglement localization of graph states.

Graph states are stabilizer states. These states can be exploited as quantum stabilizer codes [7, 14, 15, 24], which are linear codes and protect against errors. In the Schmidt decomposition, the measurement outcomes on the system A imply which states are projected in the system B. The existence of X-chains on Alice's side can provide simple repetition codes as the Schmidt basis in the Schmidt decomposition in X-basis. Therefore, instead of removing the vertices outside a selected path between B_1 and B_2, we will make X-measurements on them to take the benefit of X-chains for the error correction.

The graph state $|G\rangle$ in Fig. 10a is taken as an example. This state has the X-chain generating set $\Gamma_G = \{\{1,2\},\{1,3\},\{4,5\}\}$. The generating set of the three correlation groups (Eq. (52), (53) and (54)) for the Schmidt decomposition are $\mathcal{K}^{(A)}_A = \mathcal{K}^{(A)}_{\sim B} = \emptyset$ and $\mathcal{K}^{(B)} = \{\{1\}\}$, while the generating set of the $(A \rightharpoonup B)$-correlation group is $\mathcal{K}^{(A\rightharpoonup B)} = \{\{4\}\}$. According to Theorem 22 and with the help of Algorithm 23, one has

$$|\psi_{A\rfloor B}(\emptyset)\rangle = |000\rangle\,\frac{|00\rangle + |11\rangle}{\sqrt{2}} \tag{72}$$

and

$$|\psi_{A\rfloor B}(\{4\})\rangle = |111\rangle\,\frac{|00\rangle - |11\rangle}{\sqrt{2}}. \tag{73}$$

As a result, the Schmidt decomposition of the graph state is

$$|G\rangle = \frac{1}{\sqrt{2}}\left(|000\rangle\,\frac{|00\rangle + |11\rangle}{\sqrt{2}} + |111\rangle\,\frac{|00\rangle - |11\rangle}{\sqrt{2}}\right). \tag{74}$$

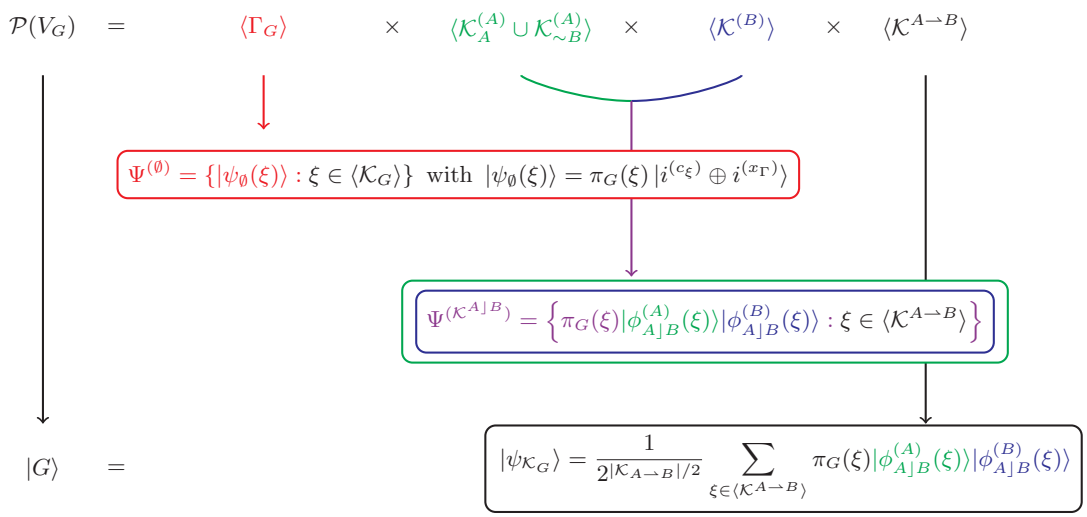

FIG. 9: (Color online) X-chain factorization diagram for the Schmidt decomposition of graph states in X-basis: A graphical summary of Lemma 20, 21 and Theorem 22.

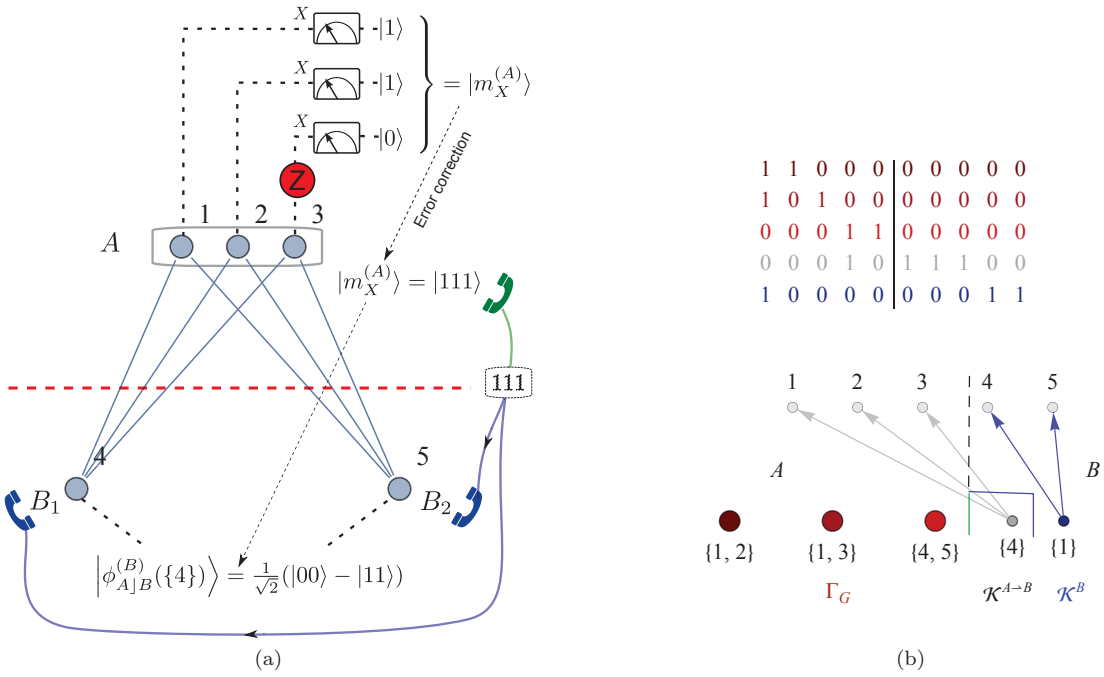

FIG. 10: (Color online) An example of entanglement localization of graph states protected against errors: a) Local X-measurements on subsystem A project the graph state $|G\rangle$ onto the maximally entangled state $|\phi^{(B)}_{A\rfloor B}(\xi)\rangle$ for subsystem B. Under the assumption of a single qubit error, the outcome $|m_X^{(A)}\rangle = |110\rangle$ indicates a Z-error on vertex 3. Alice sends Bod the corrected outcome (111), such that Bob knows from the Schmidt decomposition that he possesses the state $|\phi^{(B)}_{A\rfloor B}(\{4\})\rangle$. b) Binary representation and incidence structure after $A\rfloor B$-factorization.

In this example, one observes that there are 2 X-chain generators $\{1, 2\}$ and $\{1, 3\}$ on Alice's 3-qubit system. This encodes the following $[3, 1, 3]$ repetition code [14, 15, 24] in the Schmidt vectors on Alice's system:

$$|\phi^{(A)}_{A\rfloor B}(0)\rangle = |000\rangle \text{ and } |\phi^{(A)}_{A\rfloor B}(\{4\})\rangle = |111\rangle. \qquad (75)$$

These codes have the Hamming distance 3. Thus, a single Z-error can be corrected. After a measurement in the X-basis, Alice can therefore correct her result before sending it to Bob. In this approach, Bob will gain the correct acknowledgement of his maximally entangled state after Alice's measurement with confidence. Although the

repetition code cannot correct phase errors (the X-errors in X-measurements), it is already sufficient for our task, since a phase error on Alice's side does not change the measurement outcomes.

This application may be useful for quantum repeaters [25]. The parties B_1 and B_2 can be at a large distance, such that they are not able to create directly an entangled state between them. In this case, they need the help from Alice as a repeater station to project the entanglement onto B_1 and B_2.

VI. CONCLUSIONS

In this paper, we discussed properties of the representation of graph states in the computational X-basis. We introduced the framework of X-resources and correlation indices and linked them to the binary representation of graph states. A special type of X-resources was defined as X-chains: an X-chain is a subset of vertices for a given graph, such that the product of the stabilizer generators associated with these vertices contains only σ_X-Pauli operators. The set of X-chains of a graph state is a group, which can be calculated efficiently [8]. The X-chain groups revealed structures of graph states and showed how to distinguish them by local σ_X measurements. We introduced X-chain factorization (Lemma 8, 13) for deriving the representation of graph states in the X-basis, and it was shown that a graph state can be represented as superposition of all X-chain states (Theorem 13). This approach was illustrated in the so-called factorization diagram (Algorithm 14). The larger the X-chain group is, the fewer X-chain states are needed for representing the graph state.

We demonstrated various applications of the X-chain factorization. An important application is its usefulness for efficiently determining the overlap of two graph states (Corollary 16), for which no efficient algorithm was known before.

Further, we generalized the X-chain factorization approach such that it allows to find the Schmidt decomposition of graph states, which is the superposition of appropriately selected correlation states (Theorem 22, Algorithm 23 and Mathematica package in [9]).

Further benefits of the X-chain factorization are error correction procedures in entanglement localization of graph states in bipartite systems. This could be useful for quantum repeaters [25].

The results of this paper can be extended to general multipartite graph states, e.g. weighted graph states [26, 27] and hypergraph states [28–30]. Another possible extension of these results is to consider the representation of graph states in a hybrid basis, i.e. for a subset of the qubits one adopts the X-basis, while for the other parties one uses the Z-basis. The graph state in such a hybrid basis can even have a simpler representation (i.e. a smaller number of terms in the superposition) than the one obtained by X-chain factorization. Besides, in [6, 7, 20, 23], various multipartite entanglement measures for graph states were studied. We expect that the approach of X-chain factorization may also be useful in these cases.

Acknowledgments

This work was financially supported by the BMBF (Qcom-Q). We thank Michael Epping, Mio Murao and Yuki Mori for inspirations and useful discussions.

Appendix A: Proofs

Proposition 2 shows the isomorphism between the stabilizer group and power set of graph vertex set. It is proved as follows.

Proposition 2 (Isomorphism of vertex-induction operations)**.**
Let $(\mathcal{S}_G, \cdot)$ be the stabilizer group of a graph state $|G\rangle$, $\mathcal{P}(V_G)$ be the power set of the vertex set of G. The vertex-induction operation $s_G^{(\xi)}$ is a group isomorphism between $(\mathcal{P}(V_G), \Delta)$ and $(\mathcal{S}_G, \cdot)$, i.e.

$$(\mathcal{P}(V_G), \Delta) \overset{s_G^{(\xi)}}{\sim} (\mathcal{S}_G, \cdot), \tag{A1}$$

where Δ is the symmetric difference operation.

Proof of Proposition 2. Let $\xi_1, \xi_2 \subseteq V_G$ be two vertex subsets. Since the stabilizer group $\mathcal{S}_G$ is Abelian, one can resort the product as $s_G^{(\xi_1)} s_G^{(\xi_2)} = \prod_{i\in\xi_1\Delta\xi_2} g_i \prod_{i'\in\xi_1\cap\xi_2} (g_{i'})^2$. The property $(g_i)^2 = \mathbb{1}$ leads to $s_G^{(\xi_1)} s_G^{(\xi_2)} = s_G^{(\xi_1\Delta\xi_2)}$. Therefore $s_G^{(\xi)}$ is a group homomorphism $(\mathcal{P}(V_G), \Delta) \overset{s_G^{(\xi)}}{\to} (\mathcal{S}_{G_k}, \cdot)$. The kernel of $s_G^{(\xi)}$ is $\emptyset$, therefore $(\mathcal{P}(V_G), \Delta) \overset{s_G^{(\xi)}}{\sim} (\mathcal{S}_G, \cdot)$. □

Proposition 5 provides us a mathematical expression of J-induce graph state stabilizer. It is proven by counting of the exchanging times of Paul-X and Z operators.

Proposition 5 (Induced stabilizer)**.**
Let ξ be a vertex subset of a graph G. The ξ-induced stabilizer (see Def. 1) of a graph state $|G\rangle$ is given by

$$s_G^{(\xi)} = \pi_G(\xi)\, \sigma_X^{(\xi)} \sigma_Z^{(c_\xi)}, \tag{A2}$$

where c_ξ is the correlation index *of ξ and $\pi_G(\xi)$ is the stabilizer parity of ξ.*

Proof of Proposition 5. Let $\xi = \{j_1, ..., j_m\}$. Once we write down the ξ-induced stabilizers explicitly, we have

$$s_G^{(\xi)} = \sigma_x^{(j_1)} \sigma_z^{(N_{j_1})} \cdots \sigma_x^{(j_m)} \sigma_z^{(N_{j_m})} \tag{A3}$$

with N_j being the neighborhood of j. Now we shift σ_x operators to re-sort the expression such that all the σ_x are on the left side of σ_z. First, let us consider the last X-operator, $\sigma_x^{(j_m)}$. The number of $\sigma_z^{(j_m)}$ on the left hand side of $\sigma_x^{(j_m)}$ indicates how many times one needs to exchange $\sigma_x^{(j_m)}$ and $\sigma_z^{(j_m)}$. It is equal to the number of neighbors of j_m in the ξ-induced graph $G[\xi]$, namely $d_{j_m}(G[\xi])$. Due to the anti-commutativity of σ_x and σ_z, the shifting brings us a prefactor $(-1)^{d_{j_m}(G[\xi])}$. Recursively, shifting $\sigma_x^{(j_m-1)}$ to the left side of $\sigma_z^{(j_m-1)}$ brings us a prefactor $(-1)^{d_{j_{k-1}}(G[\xi]-j_m)}$ and so on. In total the times that one needs to exchange σ_x and σ_z is

$$d_{j_k}(G[\xi])+d_{j_{k-1}}(G[\xi]-j_m)+\cdots+d_2(G[\{j_1,j_2\}]), \quad \text{(A4)}$$

which is equal to the edge number $|E(G[\xi])|$. Hence, after the shifting, we obtain a product of re-sorted σ_x and σ_z operators with a prefactor $(-1)^{|E(G[\xi])|}$, i.e.

$$s_G^{(\xi)} = (-1)^{|E(G[\xi])|}\sigma_x^{(j)}\sigma_z^{(n_G(j_1))}\cdots\sigma_z^{(n_G(j_m))}, \quad \text{(A5)}$$

while $\sigma_z^{(N(j_1))}\cdots\sigma_z^{(N(j_m))} = \sigma_z^{c_G(\xi)}$. □

Lemma 8 regroups the power set of vertices with factorization regarding the X-chain group into the correlation group. Accordingly, one can regroup the graph state projector by stabilizers induced by the correlation group. It is a result of Proposition 2.

Lemma 8 (X-chain groups and correlation groups)**.** *Let $|G\rangle$ be a graph state. The set of X-chains together with the symmetric difference $(\mathcal{X}_G^{(\emptyset)},\Delta)$, is a normal subgroup of $(\mathcal{P}(V_G),\Delta)$. The quotient group $(\mathcal{P}(V_G)/\mathcal{X}_G^{(\emptyset)},\Delta)$ is identical to the set of all resource sets*

$$\mathcal{P}(V_G)/\mathcal{X}_G^{(\emptyset)} = \left\{\mathcal{X}_G^{(c)} : c\in\mathcal{C}_G\right\}, \quad \text{(A6)}$$

which we call call the correlation group *of $|G\rangle$. Let Γ_G and $\mathcal{K}_G$ denote the generating sets of $(\mathcal{X}_G^{(\emptyset)},\Delta)$ and $(\mathcal{P}(V_G)/\mathcal{X}_G^{(\emptyset)},\Delta)$, respectively. The stabilizer group $(\mathcal{S}_G,\cdot)$ is isomorphic to the direct product of the X-chain group and the correlation group,*

$$(\mathcal{S}_G,\cdot)\sim(\langle\Gamma_G\rangle,\Delta)\times(\langle\mathcal{K}_G\rangle,\Delta), \quad \text{(A7)}$$

As a result, the graph state $|G\rangle$ is the product of the X-chain group and correlation group inducing stabilizers, i.e.

$$|G\rangle\langle G| = \prod_{\kappa\in\mathcal{K}_G}\frac{1+s_G^{(\kappa)}}{2}\prod_{\gamma\in\Gamma_G}\frac{1+s_G^{(\gamma)}}{2}. \quad \text{(A8)}$$

Proof of Lemma 8. Let ξ_1 and ξ_2 be two elements of $\mathcal{X}_G^{(c)}$. The correlation index mapping, $c_G:(\mathcal{P}(V_G),\Delta)\to(\mathcal{C}_G,\Delta)$, is a group homomorphism, since $c_G(\xi_1\Delta\xi_2) = c_G(\xi_1)\Delta c_G(\xi_2)$. Due to the definition of X-chains that $c_G(\xi)=0$, $(\mathcal{X}_G^{(\emptyset)},\Delta)$ is the kernel of the mapping c_G. Since $(\mathcal{P}(V_G),\Delta)$ is Abelian, the kernel $(\mathcal{X}_G^{(\emptyset)},\Delta)$ and the correlation group $\mathcal{P}(V_G)/\mathcal{X}_G^{(\emptyset)}$ are both normal subgroups. The correlation group $\langle\mathcal{K}_G\rangle$ is obtained via

$$\begin{aligned}\langle\mathcal{K}_G\rangle &= \mathcal{P}(V_G)/\mathcal{X}_G^{(\emptyset)}\\ &= \left\{\xi\Delta\mathcal{X}_G^{(\emptyset)} : \xi\in\mathcal{P}(V_G)\right\}\\ &= \left\{\mathcal{X}_G^{(c)} : c\in\mathcal{C}_G\right\}. \end{aligned} \quad \text{(A9)}$$

As a result of group theory,

$$(\mathcal{P}(V_G),\Delta) = (\langle\Gamma_G\rangle,\Delta)\times(\langle\mathcal{K}_G\rangle,\Delta). \quad \text{(A10)}$$

According to Proposition 2, one obtains the isomorphism

$$(\mathcal{S}_{G_k},\cdot)\overset{s_{G_k}^{(\xi)}}{\sim}(\langle\Gamma_G\rangle,\Delta)\times(\langle\mathcal{K}_G\rangle,\Delta). \quad \text{(A11)}$$

The projector of graph state $|G\rangle\langle G|$ is the sum of all ξ-induced stabilizers, $s_G^{(\xi)}$, with $\xi\in\langle\Gamma_G\rangle\times\langle\mathcal{K}_G\rangle$. As a result,

$$\begin{aligned}|G\rangle\langle G| &= \sum_{\xi\in\mathcal{P}(V_G)} s_G^{(\xi)}\\ &= \prod_{\kappa\in\mathcal{K}_G}\frac{1+s_G^{(\kappa)}}{2}\prod_{\gamma\in-_G}\frac{1+s_G^{(\gamma)}}{2}. \end{aligned} \quad \text{(A12)}$$

□

Proposition 10 (X-chain states in X-basis)**.** *Let $|G\rangle$ be a graph state with the X-chain group $\langle\Gamma_G\rangle$ and the correlation group $\langle\mathcal{K}_G\rangle$. Let $\Gamma_G=\{\gamma_1,\gamma_2,...\}$, and $\gamma_i=\{v_{i_1},v_{i_2},\cdots\}$. The generating set Γ_G and $\mathcal{K}_G$ can be chosen as*

1. *$\Gamma_G=\{\gamma_1,...,\gamma_k\}$ such that $\gamma_i\not\subseteq\gamma_j$ for all $\gamma_i,\gamma_j\in\Gamma_G$,*
2. *$\mathcal{K}_G=\left\{\{v\}:v\in V_G\backslash\bigcup_{i=1}^k\{v_{i_1}\}\right\}$.*

Here, the first element of $\gamma_i=\{v_{i_1},v_{i_2},...\}$ is selected in the way such that $v_{i_1}\neq v_{j_1}$ for all $i\neq j$. Then the X-chain state $|\psi_\emptyset(\emptyset)\rangle$ of $|G\rangle$ is an X-basis state, $|i^{(x_\Gamma)}\rangle$, with

$$x_\Gamma = \{v_{i_1}:\pi_G(\gamma_i)=-1\}. \quad \text{(A13)}$$

Proof of Proposition 10. Let γ_i^- be an X-chain generator with negative parity $\pi_G(\gamma_i^-)=-1$, then $v_{i_1}\in x_\Gamma$. Since $v_{i_1}\in\gamma_i$ and $v_{i_1}\notin\gamma_j$ for all $j\neq i$, the intersection $\gamma_i^-\cap x_\Gamma=\{v_{i_1}\}$, hence $\pi_G(\gamma_i^-)\sigma_x^{(\gamma_i)}|i^{(x_\Gamma)}\rangle = |i^{(x_\Gamma)}\rangle$. For an X-chain generator γ_j^+ with positive parity $\pi_G(\gamma_i^+)=1$, the intersection $\gamma_i^+\cap x_\Gamma=\emptyset$, therefore

$\pi_G\left(\gamma_i^+\right)\sigma_x^{(\gamma_i)}|i^{(x_\Gamma)}\rangle = |i^{(x_\Gamma)}\rangle$. Hence the condition 1 in Definition 9 is fulfilled.

Let $\{v\} \in \mathcal{K}_G$ be a generator of correlation group, then $\sigma_x^{(\{v\})}|i^{(x_\Gamma)}\rangle = (-1)^{|x_\Gamma\cap\{v\}|}|i^{(x_\Gamma)}\rangle = |i^{(x_\Gamma)}\rangle$, since $|x_\Gamma \cap \{v\}| = 0$ according to the choice of $\mathcal{K}_G$. Hence, the condition 2 in Definition 9 is fulfilled. □

The Proposition 11 derives the correlation states as the summation of X-chain states. It follows directly from their definition.

Proposition 11 (X-chain states, $\mathcal{K}$-correlation states)**.** *Let $\xi \in \langle\mathcal{K}_G\rangle$ be an X-resource and $\langle\mathcal{K}\rangle \subseteq \langle\mathcal{K}_G\rangle$. An X-chain state is given as*

$$|\psi_\emptyset(\xi)\rangle = \pi_G(\xi)\left|i^{(x_\Gamma)} \oplus i^{(c_\xi)}\right\rangle, \tag{A14}$$

where $\pi_G(\xi)$ is the stabilizer parity of ξ (see Eq. (13)), and c_ξ is the correlation index of ξ.

A $\mathcal{K}$-correlation state is the superposition of X-chain states*,*

$$|\psi_\mathcal{K}(\xi)\rangle = \frac{1}{2^{|\mathcal{K}|/2}}\sum_{\xi'\in\langle\mathcal{K}\rangle}|\psi_\emptyset(\xi\Delta\xi')\rangle. \tag{A15}$$

Proof of Proposition 11. According to Proposition 2, $s_G^{(\xi)}\Delta s_G^{(\xi')} = s_G^{(\xi\Delta\xi')}$, the product of the operators in Eq. (25) can be reformulated to the sum of

$$|\psi_\mathcal{K}(\xi)\rangle = \frac{1}{2^{|\mathcal{K}|/2}}\sum_{\xi'\in\langle\mathcal{K}\rangle} s_G^{(\xi\Delta\xi')}\left|i^{(x_\Gamma)}\right\rangle. \tag{A16}$$

With the formulas in Proposition 5,

$$|\psi_\mathcal{K}(\xi)\rangle = \frac{1}{2^{|\mathcal{K}|/2}}\sum_{\xi'\in\langle\mathcal{K}\rangle}\pi_G(\xi\Delta\xi')\,\sigma_z^{(c_{\xi\Delta\xi'})}\sigma_x^{(\xi\Delta\xi')}\left|i^{(x_\Gamma)}\right\rangle. \tag{A17}$$

Since $\sigma_x^{(\kappa)}\left|i^{(x_\Gamma)}\right\rangle = \left|i^{(x_\Gamma)}\right\rangle$ for all $\kappa \in \langle\mathcal{K}\rangle$, one obtains

$$|\psi_\mathcal{K}(\xi)\rangle = \frac{1}{2^{|\mathcal{K}|/2}}\sum_{\xi'\in\langle\mathcal{K}\rangle}\pi_G(\xi\Delta\xi')\left|i^{(x_\Gamma)} \oplus i^{(c_{\xi\Delta\xi'})}\right\rangle. \tag{A18}$$

□

The following calculation is the proof of Corollary 12, which is employed in the proof of Theorem 13.

Proof of Corollary 12. The properties 2 and 3 are direct results of Proposition 11. The property 1 follows from the commutativity of graph state stabilizers. Let $\kappa = \gamma\Delta\kappa_0 \in \langle\Gamma_G\rangle \times \langle\mathcal{K}\rangle$ with $\gamma \in \langle\Gamma_G\rangle$ and $\kappa_0 \in \langle\mathcal{K}\rangle$, then

$$\begin{aligned} s_G^{(\kappa)}\phi_\mathcal{K}(\xi) &= s_G^{(\gamma)}s_G^{(\kappa_0)}s_G^{(\xi)}\prod_{\kappa'\in\mathcal{K}}\frac{1+s_G^{(\kappa')}}{\sqrt{2}}|x_\Gamma\rangle \\ &= s_G^{(\xi)}\frac{1}{2^{|\mathcal{K}|/2}}s_G^{(\kappa_0)}\sum_{\kappa'\in\langle\mathcal{K}\rangle}s_G^{(\kappa')}s_G^{(\gamma)}|x_\Gamma\rangle. \end{aligned}$$

Due to the definition of $|x_\Gamma\rangle$, it holds $s_G^{(\gamma)}|x_\Gamma\rangle = |x_\Gamma\rangle$. Since $\kappa_0 \in \langle\mathcal{K}\rangle$, the operator $s_G^{(\kappa_0)}\sum_{\kappa'\in\langle\mathcal{K}\rangle}s_G^{(\kappa')} = \sum_{\kappa'\in\langle\mathcal{K}\rangle}s_G^{(\kappa')}$ is not changed by $s_G^{(\kappa_0)}$, hence

$$s_G^{(\kappa)}\phi_\mathcal{K}(\xi) = s_G^{(\xi)}\frac{1}{2^{|\mathcal{K}|/2}}\sum_{\kappa'\in\langle\mathcal{K}\rangle}s_G^{(\kappa')}|x_\Gamma\rangle = \phi_\mathcal{K}(\xi). \tag{A19}$$

□

Lemma 20 shows us the $A|B$-separability of the correlation state $\left|(0,\mathcal{K}_A^{(A)}\uplus\mathcal{K}^{(B)})\right\rangle$. Its a result of the property of multiplication G-parities.

Lemma 24 (Multiplication of G-parity)**.**
Let G be a graph, then the multiplication of two the parities of two vertex subset $\pi_G(\xi_1)$ and $\pi_G(\xi_2)$ is equal to

$$\pi_G(\xi_1)\,\pi_G(\xi_2) = (-1)^{|E_G(\xi_1:\xi_2)|}\,\pi_G(\xi_1\Delta\xi_2). \tag{A20}$$

Proof. Since $(P(V),\Delta)$ is isomorphic to the stabilizer group $(S_G,\cdot)$, it holds then

$$s_G^{(\xi_1)}s_G^{(\xi_2)} = s_{G_k}^{(\xi_1\Delta\xi_2)}.$$

Reorder the σ_x and σ_z in both sides, such that σ_x are on the left side of σ_z, one obtains

$$\pi_G(\xi_1)\,\pi_G(\xi_2) = (-1)^{|E_G(\xi_1:\xi_2)|}\,\pi_G(\xi_1\Delta\xi_2). \tag{A21}$$

□

With this lemma one can prove Lemma 20 as follows.

Lemma 20 ($A|B$-Separability of $A\rfloor B$-correlation states)**.**
For $\xi \in \langle\mathcal{K}_G^{A\rightharpoonup B}\rangle$, the $(A\rightharpoonup B)$-correlation states

$$|\psi_{A\rfloor B}(\xi)\rangle = \pi_G(\xi)\,|\phi_{A\rfloor B}^{(A)}(\xi)\rangle|\phi_{A\rfloor B}^{(B)}(\xi)\rangle \tag{A22}$$

are $A|B$-separable with $|\phi_{A\rfloor B}^{(A)}(\xi)\rangle := |\psi^{(A)}_{\mathcal{K}_A^{(A)}\cup\mathcal{K}_{\sim B}^{(A)}}(\xi)\rangle$ and $|\phi_{A\rfloor B}^{(A)}(\xi)\rangle := |\psi^{(B)}_{\mathcal{K}^{(B)}}(\xi)\rangle$ being the $(\mathcal{K}_A^{(A)}\cup\mathcal{K}_{\sim B}^{(A)})$- and $\mathcal{K}^{(B)}$-correlation states projected into the subspaces of A and B, respectively.

Proof of Lemma 20. According to Proposition 11,

$$|\psi_{A\rfloor B}(\xi)\rangle = \sum_{\xi'\in\left\langle \mathcal{K}_A^{(A)}\cup\mathcal{K}_{\sim B}^{(A)}\cup\mathcal{K}^{(B)}\right\rangle} \pi_G\left(\xi'\Delta\xi\right)|x_\Gamma\oplus c_{\xi'}\oplus c_\xi\rangle. \tag{A23}$$

Each X-resource $\xi'\in\left\langle \mathcal{K}_A^{(A)}\cup\mathcal{K}_{\sim B}^{(A)}\cup\mathcal{K}^{(B)}\right\rangle$ can be decomposed as $\xi'=\alpha\Delta\beta=\alpha_A\Delta\alpha_B\Delta\beta$ with $\alpha_A\in\left\langle \mathcal{K}_A^{(A)}\right\rangle$ and $\alpha_B\in\left\langle \mathcal{K}_{\sim B}^{(A)}\right\rangle$ and $\beta\in\left\langle \mathcal{K}^{(B)}\right\rangle$. Due to Lemma 24

$$\pi_G\left(\xi'\Delta\xi\right)=(-1)^{|E_G(\xi:\alpha\Delta\beta)|}\pi_G\left(\alpha\Delta\beta\right)\pi_G\left(\xi\right) \text{ and } \pi_G\left(\alpha\Delta\beta\right)=(-1)^{|E_G(\alpha:\beta)|}\pi_G\left(\alpha\right)\pi_G\left(\beta\right) \tag{A24}$$

Since $\alpha_A\subseteq A$ and $c_\beta\subseteq B$, it holds $|E_G(\alpha_A:\beta)|\overset{\mathrm{mod}\,2}{=}|\alpha_A\cap c_\beta|\overset{\mathrm{mod}\,2}{=}0$, while $\alpha_B\in\left\langle \mathcal{K}_{\sim B}^{(A)}\right\rangle$ is defined by $|E_G(\alpha_B:\beta)|\overset{\mathrm{mod}\,2}{=}0$. Therefore the edge number is $|E_G(\alpha:\beta)|=|E_G(\alpha_A\Delta\alpha_B:\beta)|\overset{\mathrm{mod}\,2}{=}0$. Besides since $|E_G(\xi:\alpha\Delta\beta)|\overset{\mathrm{mod}\,2}{=}|E_G(\xi:\alpha)|+|E_G(\xi:\beta)|$, therefore

$$\pi_G\left(\xi'\Delta\xi\right)=(-1)^{|E_G(\xi:\alpha)|}(-1)^{|E_G(\xi:\beta)|}\pi_G\left(\alpha\right)\pi_G\left(\beta\right)\pi_G\left(\xi\right)$$

According to Eq. (13) in Proposition 5, the following equation holds

$$\pi_G\left(\xi\right)(-1)^{|E_G(\xi:\beta)|}\pi_G\left(\beta\right)=(-1)^{|E(G[\beta])|+|E_G(\xi:\beta)|+|E(G[\xi])|}=(-1)^{|E(G[\beta\Delta\xi])|}=\pi_G\left(\xi\Delta\beta\right). \tag{A25}$$

This equality also holds for α, therefore

$$\pi_G\left(\xi'\Delta\xi\right)=\pi_G\left(\alpha\Delta\xi\right)\pi_G\left(\beta\Delta\xi\right)\pi_G\left(\xi\right). \tag{A26}$$

Insert this equality into Eq. (33) one obtains

$$|\psi_{A\rfloor B}(\xi)\rangle=\pi_G\left(\xi\right)\sum_{\alpha\in\left\langle \mathcal{K}_A^{(A)}\right\rangle}\sum_{\beta\in\left\langle \mathcal{K}^{(B)}\right\rangle}\pi_G\left(\alpha\Delta\xi\right)\pi_G\left(\beta\Delta\xi\right)|i^{(x_\Gamma)}\oplus i^{(c_\alpha)}\oplus i^{(c_\beta)}\oplus i^{(c_\xi)}\rangle=\pi_G\left(\xi\right)|\phi_{A\rfloor B}^{(A)}(\xi)\rangle|\phi_{A\rfloor B}^{(B)}(\xi)\rangle \tag{A27}$$

with

$$|\phi_{A\rfloor B}^{(A)}(\xi)\rangle=|\psi_{\mathcal{K}_A^{(A)}\cup\mathcal{K}_{\sim B}^{(A)}}^{(A)}(\xi)\rangle=\sum_{\alpha\in\left\langle \mathcal{K}_A^{(A)}\cup\mathcal{K}_{\sim B}^{(A)}\right\rangle}\pi_G\left(\alpha\Delta\xi\right)|i^{(x_\Gamma^{(A)})}\oplus i^{(c_\alpha)}\oplus i^{(c_\xi^{(A)})}\rangle, \tag{A28}$$

and

$$|\phi_{A\rfloor B}^{(B)}(\xi)\rangle=|\psi_{\mathcal{K}^{(B)}}^{(B)}(\xi)\rangle=\sum_{\beta\in\left\langle \mathcal{K}^{(B)}\right\rangle}\pi_G\left(\beta\Delta\xi\right)|i^{(x_\Gamma^{(B)})}\oplus i^{(c_\beta)}\oplus i^{(c_\xi^{(B)})}\rangle. \tag{A29}$$

□

Lemma 21 is the key to derive Theorem 22. Its proof is as follows.

Lemma 21 (Orthonormality of $(A\rightharpoonup B)$-correlation states)**.**
The into A and B projected $A\rfloor B$-correlation states, $|\phi_{A\rfloor B}^{(A)}(\xi)\rangle$ and $|\phi_{A\rfloor B}^{(B)}(\xi)\rangle$, are orthonormal with respect to $\xi\in\langle\mathcal{K}^{A\rightharpoonup B}\rangle$ within the subspaces A and B, respectively, i.e.

$$\langle\phi_{A\rfloor B}^{(A)}(\xi_1)|\phi_{A\rfloor B}^{(A)}(\xi_2)\rangle=0 \tag{A30}$$

and

$$\langle\phi_{A\rfloor B}^{(B)}(\xi_1)|\phi_{A\rfloor B}^{(B)}(\xi_2)\rangle=0$$

for all $\xi_1,\xi_2\in\langle\mathcal{K}^{A\rightharpoonup B}\rangle$ and $\xi_1\neq\xi_2$.

Proof of Lemma 21. According to the definition of correlation states (Def. 9) and the unitarity of stabilizer $s_G^{(\xi_1)}$ and $s_G^{(\xi_2)}$, it holds

$$\langle\phi_{\mathcal{K}}(\xi_1)|\phi_{\mathcal{K}}(\xi_2)\rangle = \langle\phi_{\mathcal{K}}(0)|\phi_{\mathcal{K}}(\xi_1\Delta\xi_2)\rangle. \tag{A31}$$

One just needs to consider the overlap $\langle\phi^{(A)}_{A\rfloor B}(0)|\phi^{(A)}_{A\rfloor B}(\xi)\rangle$ and $\langle\phi^{(B)}_{A\rfloor B}(0)|\phi^{(B)}_{A\rfloor B}(\xi)\rangle$ with $\xi \in \langle\mathcal{K}_G^{A\rightharpoonup B}\rangle$. That means for all $\alpha \in \langle\mathcal{K}_A^{(A)} \cup \mathcal{K}_{\sim B}^{(A)}\rangle$ and $\beta \in \langle\mathcal{K}^{(B)}\rangle$, it holds

$$c_\alpha \oplus c_\beta \neq c_\xi. \tag{A32}$$

For $|\phi^{(A)}_{A\rfloor B}(\xi)\rangle$, due to the commutativity of graph state stabilizers, it holds

$$\langle\phi^{(A)}_{A\rfloor B}(0)|\phi^{(A)}_{A\rfloor B}(\xi)\rangle = \frac{1}{2^{\left|\mathcal{K}_A^{(A)}\cup\mathcal{K}_{\sim B}^{(A)}\right|}} \sum_{\alpha,\alpha'\in\left\langle\mathcal{K}_A^{(A)}\cup\mathcal{K}_{\sim B}^{(A)}\right\rangle} \pi_G(\alpha')\,\pi_G(\alpha\Delta\xi)\,\langle i(x_\Gamma^{(A)}) \oplus i(c_{\alpha'})|i(x_\Gamma^{(A)}) \oplus i(c_\alpha) \oplus i(c_\xi^{(A)})\rangle \tag{A33}$$

$$= \frac{1}{2^{\left|\mathcal{K}_A^{(A)}\cup\mathcal{K}_{\sim B}^{(A)}\right|}} \sum_{\alpha,\alpha'\in\left\langle\mathcal{K}_A^{(A)}\cup\mathcal{K}_{\sim B}^{(A)}\right\rangle : c_{\alpha\Delta\alpha'}=c_\xi^{(A)}} \pi_G(\alpha')\,\pi_G(\alpha\Delta\xi). \tag{A34}$$

If there exists $\lambda \in \left\langle\mathcal{K}_A^{(A)} \cup \mathcal{K}_{\sim B}^{(A)}\right\rangle$ such that $c_\lambda = c_\xi^{(A)}$, then $\xi\Delta\lambda \in \mathcal{K}^{(B)}$ (since $c_{\xi\Delta\lambda} \subseteq B$). This means $\xi \in \left\langle\mathcal{K}_A^{(A)} \cup \mathcal{K}_{\sim B}^{(A)}\right\rangle \times \left\langle\mathcal{K}^{(B)}\right\rangle$, which is in contradiction to the definition of $\xi \in \langle\mathcal{K}^{A\rightharpoonup B}\rangle$. Hence there are no pairs $\alpha, \alpha' \in \mathcal{K}_A^{(A)}$ such that $c_{\alpha\Delta\alpha'} = c_\xi^{(A)}$, therefore

$$\langle\phi^{(A)}_{A\rfloor B}(0)|\phi^{(A)}_{A\rfloor B}(\xi)\rangle = 0. \tag{A35}$$

Analogously for $|\phi^{(B)}_{A\rfloor B}(\xi)\rangle$, it holds

$$\langle\phi^{(B)}_{A\rfloor B}(0)|\phi^{(B)}_{A\rfloor B}(\xi)\rangle = \frac{1}{2^{\left|\mathcal{K}^{(B)}\right|}} \sum_{\beta,\beta'\in\left\langle\mathcal{K}^{(B)}\right\rangle : c_{\beta\Delta\beta'}=c_\xi^{(B)}} \pi_G(\beta')\,\pi_G(\beta\Delta\xi). \tag{A36}$$

If there exists no $\lambda \in \mathcal{K}^{(B)}$ such that $c_\lambda = c_\xi^{(B)}$, then $\langle\phi^{(B)}_{A\rfloor B}(0)|\phi^{(B)}_{A\rfloor B}(\xi)\rangle = 0$. If there exist such $\lambda \in \mathcal{K}^{(B)}$ then we substitute ξ by $\xi' := \xi\Delta\lambda$, then $\xi' \in \left\langle\mathcal{K}^{A\rightharpoonup B}\right\rangle$ still holds and $c_{\xi'}^{(B)} = 0$. Hence the overlap becomes

$$\begin{aligned}\langle\phi^{(B)}_{A\rfloor B}(0)|\phi^{(B)}_{A\rfloor B}(\xi)\rangle &= \frac{1}{2^{\left|\mathcal{K}^{(B)}\right|}} \sum_{\beta\in\left\langle\mathcal{K}^{(B)}\right\rangle} \pi_G(\beta)\,\pi_G(\beta\Delta\xi') = \frac{1}{2^{\left|\mathcal{K}^{(B)}\right|}} \sum_{\beta\in\left\langle\mathcal{K}^{(B)}\right\rangle} (-1)^{\left|E_G(\beta:\xi')\right|} \\ &= \frac{1}{2^{\left|\mathcal{K}^{(B)}\right|}} \prod_{\beta\in\mathcal{K}^{(B)}} \left(1 + (-1)^{\left|E_G(\beta:\xi')\right|}\right).\end{aligned} \tag{A37}$$

Since $\xi' \in \left\langle\mathcal{K}^{A\rightharpoonup B}\right\rangle$ and $\tilde{c}_{\xi'} \subseteq A$ implies that $\xi' \not\subseteq A$, under the assumption that $|E_G(\beta : \xi')| \overset{\mathrm{mod}\,2}{=} 0$ for all $\beta \in \mathcal{K}^{(B)}$, one can infer (according to the definition in Eq. (54)) that $\xi' \in \langle\mathcal{K}_{\sim B}^{(A)}\rangle$. This is in contradiction to the condition that $\xi' \in \left\langle\mathcal{K}^{A\rightharpoonup B}\right\rangle$. Therefore there must be at least one β_0, which has odd number of edges to ξ', i.e. $|E_G(\beta : \xi')| \overset{\mathrm{mod}\,2}{=} 1$. Hence

$$\langle\phi^{(B)}_{A\rfloor B}(0)|\phi^{(B)}_{A\rfloor B}(\xi)\rangle = 0. \tag{A38}$$

□

Appendix B: The list of notations

Here we present a list of symbols together with the page number where they occur for the first time.

A_G The adjacency matrix of the graph G. 3

$\beta(|G\rangle)$ The Z-bias degree of the graph state $|G\rangle$. 10

$\langle\mathcal{K}\rangle$ A general correlation subgroup of $\langle\mathcal{K}_G\rangle$. 5

$\langle\mathcal{K}^{A\rfloor B}\rangle$ The correlation subgroup, whose corresponding correlation state are the $A|B$-separable Schmidt basis. 13

$\langle\mathcal{K}^{A\leftarrow B}\rangle$ The correlation subgroup obtained by the quotient group $\mathcal{K}_G/\mathcal{K}^{A\rfloor B}$. 13

$\langle\mathcal{K}_A^{(A)}\rangle$ The correlation subgroup, whose elements and their corresponding correlation index are both in the subsystem A. 13

$\langle\mathcal{K}_G\rangle$ The correlation group of G generated by its generating set $\mathcal{K}_G$. 5

$\langle\mathcal{K}_{\sim B}^{(A)}\rangle$ A special correlation subgroup. 13

$\langle\mathcal{K}^{(B)}\rangle$ The correlation subgroup, whose elements possess correlation index only in the subsystem B. 13

c_ξ The correlation index of the vertex subset ξ. 3

$\mathcal{C}_G$ The set all correlation indices in G. 5

$|\psi_{\mathcal{K}}(\xi)\rangle$ A $\mathcal{K}$-correlation state. 6

$|\psi_{A\rfloor B}(\xi)\rangle$ A $\mathcal{K}^{(A\rfloor B)}$-correlation state. 13

$|\phi_{A\rfloor B}^{(A)}(\xi)\rangle$ The state projected from the $A\rfloor B$-correlation state $|\psi_{A\rfloor B}(\xi)\rangle$ onto the subsystem A. 15

$|\phi_{A\rfloor B}^{(B)}(\xi)\rangle$ The state projected from the $A\rfloor B$-correlation state $|\psi_{A\rfloor B}(\xi)\rangle$ onto the subsystem B. 15

$\Psi_{\mathcal{K}'}^{(\mathcal{K})}$ The set $\mathcal{K}$-correlation states $|\psi_{\mathcal{K}}(\xi)\rangle$ with $\xi \in \langle\mathcal{K}'\rangle / \langle\mathcal{K}\rangle$. 6

$\mathcal{E}_g^{A|B}$ $A|B$-bipartite geometric measure of entanglement. 15

G A graph. 1

g_i The graph state stabilizer generator associated to ith vertex. 2

$s_G^{(\xi)}$ The graph state stabilizer induced by the vertex subset ξ. 2

$\mathcal{S}_G$ The graph state stabilizer group of G. 2

E_G The edge set of G. 1

$G[\xi]$ The subgraph of G induced by vertices ξ. 1

N_v The neighborhood of v. 1

V_G The vertex set of G. 1

$|i_\alpha^{(\iota)}\rangle$ The α-basis state with binary number corresponding to the index set ι, $\alpha \in \{X, Y, Z\}$. 2

$\mathcal{P}(V_G)$ The power set of the vertex set V_G. 2

r_S The Schmidt rank. 11

$\pi_G(\xi)$ The stabilizer parity of ξ in G. 3

$\mathcal{X}_G^{(\emptyset)}$ The set of X-chains. 5

$\langle\Gamma_G\rangle$ The X-chain group generated by its generating set Γ_G. 5

$|i^{(x_\Gamma)}\rangle$ The basic X-chain state. 6

$|\psi_\emptyset(\xi)\rangle$ An X-chain state. 6

$\mathcal{X}_G^{(c)}$ The set of all X-resources of c-correlation. 5

[1] H. J. Briegel and R. Raussendorf. Persistent entanglement in arrays of interacting particles. *Phys. Rev. Lett.*, 86:910–913, 2001.

[2] R. Raussendorf and H. J. Briegel. A one-way quantum computer. *Phys. Rev. Lett.*, 86:5188–5191, 2001.

[3] R. Raussendorf and H. J. Briegel. Computational model underlying the one-way quantum computer. *Quant. Inf. Comp.*, 2:443, 2002.

[4] R. Raussendorf, D. E. Browne, and H. J. Briegel. Measurement-based quantum computation on cluster states. *Phys. Rev. A*, 68:022312, 2003.

[5] R. Raussendorf. *Measurement-based quantum computation with cluster states*. PhD thesis, LMU München, Germany, 2003.

[6] M. Hein, J. Eisert, and H. J. Briegel. Multiparty entanglement in graph states. *Phys. Rev. A*, 69:062311, 2004.

[7] M. Hein, W. Dür, J. Eisert, R. Raussendorf, M. V. den Nest, and H.-J. Briegel. Entanglement in graph states and its applications. *arXiv:quant-ph/0602096v1*, 2006.

[8] J.-Y. Wu, H. Kampermann, and D. Bruß. The search of X-chains of graph states. *In preparation*, 2015.

[9] J.-Y. Wu. The mathematica package of X-chain factorization: https://github.com/emmauelwjy/X-chain-Factorization.

[10] M. Popp, F. Verstraete, M. A. Martín-Delgado, and J. I. Cirac. Localizable entanglement. *Phys. Rev. A*, 71:042306, 2005.

[11] R. Diestel. *Graph theory*, volume 173 of *Graduate Texts in Mathematics*. Springer-Verlag, Heidelberg, 2005 edition, 2005.

[12] M. Van den Nest. *Local Equivalence of Stabilizer states and codes*. PhD thesis, Katholieke Universiteit Leuven, 2005.
[13] K. H. Rosen. *Handbook of discrete and combinatorial mathematics*. CRC press, 1999.
[14] D. Gottesman. *Stabilizer Codes and Quantum Error Correction*. PhD thesis, 1997.
[15] D. Gottesman. Class of quantum error-correcting codes saturating the quantum Hamming bound. *Phys. Rev. A*, 54:1862–1868, 1996.
[16] A. Calderbank, E. Rains, P. Shor, and N. Sloane. Quantum error correction and orthogonal geometry. *Phys. Rev. Lett.*, 78:405–408, 1997.
[17] J.-Y. Wu, M. Rossi, H. Kampermann, S. Severini, L. C. Kwek, C. Macchiavello, and D. Bruß. Randomized graph states and their entanglement properties. *Phys. Rev. A*, 89:052335, 2014.
[18] A. Acín, D. Bruß, M. Lewenstein, and A. Sanpera. Classification of mixed three-qubit states. *Phys. Rev. Lett.*, 87:040401, 2001.
[19] O. Gühne, P. Hyllus, D. Bruß, A. Ekert, M. Lewenstein, C. Macchiavello, and A. Sanpera. Detection of entanglement with few local measurements. *Phys. Rev. A*, 66:062305, 2002.
[20] A. Cosentino and S. Severini. Weight of quadratic forms and graph states. *Phys. Rev. A*, 80:052309, 2009.
[21] A. Shimony. Degree of entanglementa. *Annals of the New York Academy of Sciences*, 755(1):675–679, 1995.
[22] H. Barnum and N. Linden. Monotones and invariants for multi-particle quantum states. *Journal of Physics A: Mathematical and General*, 34(35):6787, 2001.
[23] M. Hajdušek and M. Murao. Direct evaluation of pure graph state entanglement. *New Journal of Physics*, 15(1):013039, 2013.
[24] M. A. Nielsen and I. L. Chuang. *Quantum Computation and Quantum Information (Cambridge Series on Information and the Natural Sciences)*. Cambridge University Press, 1 edition, 2004.
[25] H.-J. Briegel, W. Dür, J. I. Cirac, and P. Zoller. Quantum repeaters: The role of imperfect local operations in quantum communication. *Phys. Rev. Lett.*, 81:5932–5935, 1998.
[26] W. Dür, L. Hartmann, M. Hein, M. Lewenstein, and H.-J. Briegel. Entanglement in spin chains and lattices with long-range ising-type interactions. *Phys. Rev. Lett.*, 94:097203, 2005.
[27] L. Hartmann, J. Calsamiglia, W. Dür, and H. J. Briegel. Weighted graph states and applications to spin chains, lattices and gases. *Journal of Physics B: Atomic, Molecular and Optical Physics*, 40(9):S1, 2007.
[28] M. Rossi, M. Huber, D. Bruß, and C. Macchiavello. Quantum hypergraph states. *New Journal of Physics*, 15(11):113022, 2013.
[29] R. Qu, J. Wang, Z.-S. Li, and Y.-R. Bao. Encoding hypergraphs into quantum states. *Phys. Rev. A*, 87:022311, 2013.
[30] O. Gühne, M. Cuquet, F. E. S. Steinhoff, T. Moroder, M. Rossi, D. Bruß, B. Kraus, and C. Macchiavello. Entanglement and nonclassical properties of hypergraph states. *Journal of Physics A: Mathematical and Theoretical*, 47(33):335303, 2014.
[31] This global phase can be corrected by the sign of the sum of the parities of all X-resources in the correlation group $\langle \mathcal{K}_G \rangle$, $\alpha = Sign(\sum_{\xi \in \langle \mathcal{K}_G \rangle} (\pi_G(\xi)))$, i.e. $|G\rangle = \alpha \, |\psi_{\mathcal{K}_G}\rangle$.
[32] Note that the matching between two parties is not unique, but its cardinality is fix.

Acronyms

CC classical communication.
CP completely positive.
CPTP completely positive trace-preserving.
CZ control-Z.

Decomp decomposition.
DGO deterministic global operation.
DLO deterministic local operation.
DLOCC deterministic local operation and classical communication.

Ent entanglement.

Geo geometric, geometry.
GM genuinely multipartite.
GME genuine multipartite entanglement.
GO global operation.

LC local Clifford.
LHV local hidden variable.
LO local operation.
LOCC local operations and classical communication.

LU local unitary.

MBQC measurement based quantum computation.

NPT non-positive partital transpose.

PnCP positive and not completely positive.
POVM positive operator-valued measure.
PPT positive partial transpose.

RG randomized graph.
RUS repeat-until-success.

Schm Schmidt.
SGO stochastic global operation.
SLO stochastic local operation.
SLOCC stochastic local operation and classical communication.
SOP separable (Kraus) operator.

UPB unextendible product bases.

Notations

γ, Γ Bipartition, $\gamma|\bar{\gamma}$.

$\mathcal{E}_{\mathcal{I}}^{(A)}$ The I-concurrence regarding the bipartition $A|\bar{A}$.

$\mathcal{E}_{\mathrm{con}}^{(A)}$ The concurrence regarding the bipartition $A|\bar{A}$.

$\mathcal{E}_{F}^{(A)}$ The entanglement of formation regarding the bipartition $A|\bar{A}$.

$\mathcal{E}_{D}^{(A)}$ The distillable entanglement regarding the bipartition $A|\bar{A}$.

$\mathcal{E}_{T}^{P}$ Measure of P-partition entanglement of the type T.

S_T Entropy of the type T.

S_L Linear entropy.

S_V Von Neumann entropy.

$S_{ent}^{(A|B)}$ The entropy of entanglement with repect to the $A|B$ bipartition.

$\mathbb{F}_d^{\otimes n}$ Digit space with dimension d and length n.

$\langle \mathcal{K}_G^{A\rfloor B} \rangle$ The correlation subgroup, whose corresponding correlation states $|\psi_{\mathcal{K}_G^{A\rfloor B}}(\xi)\rangle$ are the $A|B$-separable Schmidt basis of $|G\rangle$.

$\Psi_{\mathcal{K}_G}^{\mathcal{K}}$ The set of $\mathcal{K}$-correlation states $|\psi_{\mathcal{K}}(\xi)\rangle$ with $\xi \in \langle \mathcal{K}_G \rangle \,/\, \langle \mathcal{K} \rangle$.

$\mathcal{K}_G$ The correlation group generators of the graph state $|G\rangle$.

Γ_G The X-chain generators of the graph state $|G\rangle$.

$G[\xi]$ The subgraph of G induced by vertices ξ.

$s_G^{(\xi)}$ The graph state stabilizer induced by the vertex subset ξ.

V_G The vertex set of the graph G.

d_v Vertex degree of v.

N_v The neighborhood of v.

S_n The star graph with n vertices.

$|G\rangle$ Graph states.

E_G The edges of a graph G.

$\beta(|G\rangle)$ The Z-bias degree of $|G\rangle$.

$|\psi_{\mathcal{K}}(\xi)\rangle$ The $\mathcal{K}$-correlation state of the graph state $|G\rangle$ with the argument ξ.

$|\psi_{\emptyset}(\xi)\rangle$ The X-chain state of the graph state $|G\rangle$ with the argument ξ.

ρ_G^p Randomized graph state ρ_G^p corresponding to the graph G with the randomness parameter p.

$\mathcal{S}_G$ The stabilizer group of the graph state $|G\rangle$.

$\mathbb{H}$ Hilbert space.

$\mathcal{B}$ The set of linear bounded operators on the Hilbert space $\mathbb{H}$: $\mathcal{B}(\mathbb{H})$.

$i_\gamma^{[j]}$ Permutation of i and j on the digits of the subsystem γ.

$|i_X^{(\iota)}\rangle$ The X-basis state with the binary number corresponding to the index set ι.

$\mathcal{M}$ Measurement.

$\mathcal{M}_\pi$ Projector-valued measure.

$\mathcal{M}_+$ Positive operator-valueed measure.

$\mathcal{M}_{\pi,\perp}$ von-Neumann measurement.

$\mathcal{N}^{(A)}$ The negativity regarding the bipartition $A|\bar{A}$.

$\mathcal{E}_{\mathcal{N}}^{(A)}$ The logarithmic negativity regarding the bipartition $A|\bar{A}$.

$\mathcal{Q}$ A quantum observable.

$\mathcal{P}(A)$ The power set of A.

p Probability.

$\mathfrak{O}$ Quantum operation.

R_p Randomization operator $R_p(|G\rangle) = \rho_G^p$.

$\mathrm{rank}(\rho)$ The rank of ρ.

$\rho^{(\gamma)}$ The reduced state of ρ on the subsystem γ after tracing out the compliment subsystem $\bar{\gamma}$.

ρ Mixed states.

$|\psi\rangle, |\phi\rangle$ Pure states.

$\mathrm{tr}(\rho)$ The trace of ρ.

ξ A vertex subset of a graph $\xi \subseteq V_G$..

γ, Γ X-chain generator γ, X-chain group Γ.

Index

Bibliography

[1] A. Einstein, B. Podolsky, and N. Rosen. Can quantum-mechanical description of physical reality be considered complete? *Phys. Rev.*, 47:777–780, 1935.

[2] C. A. Kocher and E. D. Commins. Polarization correlation of photons emitted in an atomic cascade. *Phys. Rev. Lett.*, 18:575–577, 1967.

[3] S. J. Freedman and J. F. Clauser. Experimental test of local hidden-variable theories. *Phys. Rev. Lett.*, 28:938–941, 1972.

[4] A. Aspect, P. Grangier, and G. Roger. Experimental tests of realistic local theories via bell's theorem. *Phys. Rev. Lett.*, 47:460–463, 1981.

[5] A. Aspect, J. Dalibard, and G. Roger. Experimental test of bell's inequalities using time-varying analyzers. *Phys. Rev. Lett.*, 49:1804–1807, 1982.

[6] G. Weihs, T. Jennewein, C. Simon, H. Weinfurter, and A. Zeilinger. Violation of bell's inequality under strict einstein locality conditions. *Phys. Rev. Lett.*, 81:5039–5043, 1998.

[7] M. A. Rowe, D. Kielpinski, V. Meyer, C. A. Sackett, W. M. Itano, C. Monroe, and D. J. Wineland. Experimental violation of a bell's inequality with efficient detection. *Nature*, 409(6822):791–794, 2001.

[8] M. Ansmann, H. Wang, R. C. Bialczak, M. Hofheinz, E. Lucero, M. Neeley, A. D. O'Connell, D. Sank, M. Weides, J. Wenner, A. N. Cleland, and J. M. Martinis. Violation of bell's inequality in josephson phase qubits. *Nature*, 461(7263):504–506, 2009.

[9] M. Giustina, A. Mech, S. Ramelow, B. Wittmann, J. Kofler, J. Beyer, A. Lita, B. Calkins, T. Gerrits, S. W. Nam, R. Ursin, and A. Zeilinger. Bell violation using entangled photons without the fair-sampling assumption. *Nature*, 497(7448):227–230, 2013.

[10] J. S. Bell. On the Einstein-Podolsky-Rosen paradox, "physics 1, 195 (1964)". *Physics Rev. Mod. Phys*, 38(3):447, 1966.

[11] J. F. Clauser, M. A. Horne, A. Shimony, and R. A. Holt. Proposed experiment to test local hidden-variable theories. *Phys. Rev. Lett.*, 23:880–884, 1969.

[12] J. F. Clauser and M. A. Horne. Experimental consequences of objective local theories. *Phys. Rev. D*, 10:526–535, 1974.

[13] Schrödinger. Die gegenwärtige situation in der quantenmechanik. *Naturwissenschaften*, 23:823–844, 1935.

[14] R. F. Werner. Quantum states with Einstein-Podolsky-Rosen correlations admitting a hidden-variable model. *Phys. Rev. A*, 40:4277–4281, 1989.

[15] A. Peres. Separability criterion for density matrices. *Phys. Rev. Lett.*, 77:1413–1415, 1996.

[16] M. Horodecki, P. Horodecki, and R. Horodecki. Separability of mixed states: necessary and sufficient conditions. *Physics Letters A*, 223(1C2):1 – 8, 1996.

[17] P. Horodecki. Separability criterion and inseparable mixed states with positive partial transposition. *Physics Letters A*, 232(5):333 – 339, 1997.

[18] C. H. Bennett, D. P. DiVincenzo, T. Mor, P. W. Shor, J. A. Smolin, and B. M. Terhal. Unextendible product bases and bound entanglement. *Phys. Rev. Lett.*, 82:5385–5388, 1999.

[19] N. J. Cerf, C. Adami, and R. M. Gingrich. Reduction criterion for separability. *Phys. Rev. A*, 60:898–909, 1999.

[20] D. P. DiVincenzo, T. Mor, P. W. Shor, J. A. Smolin, and B. M. Terhal. Unextendible product bases, uncompletable product bases and bound entanglement. *Communications in Mathematical Physics*, 238(3):379–410, 2003.

[21] B. M. Terhal. Bell inequalities and the separability criterion. *Physics Letters A*, 271(5-6):319 – 326, 2000.

[22] M. Lewenstein, B. Kraus, J. I. Cirac, and P. Horodecki. Optimization of entanglement witnesses. *Phys. Rev. A*, 62:052310, 2000.

[23] M. Lewenstein, B. Kraus, P. Horodecki, and J. I. Cirac. Characterization of separable states and entanglement witnesses. *Phys. Rev. A*, 63:044304, 2001.

[24] D. Bruß, J. I. Cirac, P. Horodecki, F. Hulpke, B. Kraus, M. Lewenstein, and A. Sanpera. Reflections upon separability and distillability. *Journal of Modern Optics*, 49(8):1399–1418, 2002.

[25] O. Gühne, P. Hyllus, D. Bruss, A. Ekert, M. Lewenstein, C. Macchiavello, and A. Sanpera. Experimental detection of entanglement via witness operators and local measurements. *Journal of Modern Optics*, 50(6-7):1079–1102, 2003.

[26] A. K. Ekert. Quantum cryptography based on bell's theorem. *Phys. Rev. Lett.*, 67:661–663, 1991.

[27] C. H. Bennett, G. Brassard, C. Crépeau, R. Jozsa, A. Peres, and W. K. Wootters. Teleporting an unknown quantum state via dual classical and einstein-podolsky-rosen channels. *Phys. Rev. Lett.*, 70:1895–1899, 1993.

[28] C. H. Bennett and S. J. Wiesner. Communication via one- and two-particle operators on einstein-podolsky-rosen states. *Phys. Rev. Lett.*, 69:2881–2884, 1992.

[29] D. Deutsch and R. Jozsa. Rapid solution of problems by quantum computation. *Proceedings of the Royal Society of London. Series A: Mathematical and Physical Sciences*, 439(1907):553–558, 1992.

[30] L. K. Grover. A fast quantum mechanical algorithm for database search. *Proceedings, 28th Annual ACM Symposium on the Theory of Computing (STOC)*, pages 212–219, 1996.

[31] P. W. Shor. Polynomial-time algorithms for prime factorization and discrete logarithms on a quantum computer. *SIAM Review*, 41(2):303–332, 1999.

[32] R. P. Feynman. Simulating physics with computers. *Int. J. Theor. Phys.*, 21:467C488, 1982.

[33] D. Deutsch. Quantum theory, the church-turing principle and the universal quantum computer. *Proceedings of the Royal Society of London. A. Mathematical and Physical Sciences*, 400(1818):97–117, 1985.

[34] P. W. Shor. Scheme for reducing decoherence in quantum computer memory. *Phys. Rev. A*, 52:R2493–R2496, 1995.

[35] A. M. Steane. Error correcting codes in quantum theory. *Phys. Rev. Lett.*, 77:793–797, 1996.

[36] C. H. Bennett, D. P. DiVincenzo, J. A. Smolin, and W. K. Wootters. Mixed-state entanglement and quantum error correction. *Phys. Rev. A*, 54:3824–3851, 1996.

[37] V. Vedral, M. B. Plenio, M. A. Rippin, and P. L. Knight. Quantifying entanglement. *Phys. Rev. Lett.*, 78:2275–2279, 1997.

[38] V. Vedral and M. B. Plenio. Entanglement measures and purification procedures. *Phys. Rev. A*, 57:1619–1633, 1998.

[39] G. Vidal. Entanglement monotones. *Journal of Modern Optics*, 47(2-3):355–376, 2000.

[40] D. Bruß and C. Macchiavello. Multipartite entanglement in quantum algorithms. *Phys. Rev. A*, 83:052313, 2011.

[41] D. M. Greenberger, M. A. Horne, and A. Zeilinger. Going beyond bells theorem. In *Bells theorem, quantum theory and conceptions of the universe*, pages 69–72. Springer, 1989.

[42] M. Hillery, V. Bužek, and A. Berthiaume. Quantum secret sharing. *Phys. Rev. A*, 59:1829–1834, 1999.

[43] W. Dür, G. Vidal, and J. I. Cirac. Three qubits can be entangled in two inequivalent ways. *Phys. Rev. A*, 62:062314, 2000.

[44] M. Fleischhauer and M. D. Lukin. Quantum memory for photons: Dark-state polaritons. *Phys. Rev. A*, 65:022314, 2002.

[45] H. J. Briegel and R. Raussendorf. Persistent entanglement in arrays of interacting particles. *Phys. Rev. Lett.*, 86:910–913, 2001.

[46] R. Raussendorf and H. J. Briegel. A one-way quantum computer. *Phys. Rev. Lett.*, 86:5188–5191, 2001.

[47] A. Acín, D. Bruß, M. Lewenstein, and A. Sanpera. Classification of mixed three-qubit states. *Phys. Rev. Lett.*, 87:040401, 2001.

[48] M. Bourennane, M. Eibl, C. Kurtsiefer, S. Gaertner, H. Weinfurter, O. Gühne, P. Hyllus, D. Bruß, M. Lewenstein, and A. Sanpera. Experimental detection of multipartite entanglement using witness operators. *Phys. Rev. Lett.*, 92:087902, 2004.

[49] B. Jungnitsch, T. Moroder, and O. Gühne. Taming multiparticle entanglement. *Phys. Rev. Lett.*, 106:190502, 2011.

[50] J.-Y. Wu, H. Kampermann, D. Bruß, C. Klöckl, and M. Huber. Determining lower bounds on a measure of multipartite entanglement from few local observables. *Phys. Rev. A*, 86:022319, 2012.

[51] M. Hein, W. Dr, J. Eisert, R. Raussendorf, M. V. den Nest, and H.-J. Briegel. Entanglement in graph states and its applications. *arXiv:quant-ph/0602096v1*, 2006.

[52] R. Diestel. *Graph theory*, volume 173 of *Graduate Texts in Mathematics*. Springer-Verlag, Heidelberg, 2005 edition, 2005.

[53] A. Cabello, L. E. Danielsen, A. J. López-Tarrida, and J. R. Portillo. Optimal preparation of graph states. *Phys. Rev. A*, 83:042314, 2011.

[54] J.-Y. Wu, M. Rossi, H. Kampermann, S. Severini, L. C. Kwek, C. Macchiavello, and D. Bruß. Randomized graph states and their entanglement properties. *Phys. Rev. A*, 89:052335, 2014.

[55] Y. L. Lim, A. Beige, and L. C. Kwek. Repeat-until-success linear optics distributed quantum computing. *Phys. Rev. Lett.*, 95:030505, 2005.

[56] Y. L. Lim, S. D. Barrett, A. Beige, P. Kok, and L. C. Kwek. Repeat-until-success quantum computing using stationary and flying qubits. *Phys. Rev. A*, 73:012304, 2006.

[57] A. Beige, Y. Lim, and L. Kwek. A repeat-until-success quantum computing scheme. *New Journal of Physics*, 9(6):197, 2007.

[58] G. Tóth and O. Gühne. Detecting genuine multipartite entanglement with two local measurements. *Phys. Rev. Lett.*, 94:060501, 2005.

[59] G. Tóth and O. Gühne. Entanglement detection in the stabilizer formalism. *Phys. Rev. A*, 72:022340, 2005.

[60] J.-Y. Wu, H. Kampermann, and D. Bruß. X-chains reveal substructures of graph states. *e-print: arXiv:1504.03302*, 2015.

[61] M. Popp, F. Verstraete, M. A. Martín-Delgado, and J. I. Cirac. Localizable entanglement. *Phys. Rev. A*, 71:042306, 2005.

[62] H.-J. Briegel, W. Dür, J. I. Cirac, and P. Zoller. Quantum repeaters: The role of imperfect local operations in quantum communication. *Phys. Rev. Lett.*, 81:5932–5935, 1998.

[63] M.-D. Choi. Completely positive linear maps on complex matrices. *Quantum Computation and Quantum Information Theory: Reprint Volume with Introductory Notes for ISI TMR Network School, 12-23 July 1999, Villa Gualino, Torino, Italy*, 10:174, 2000.

[64] K.-E. Hellwig and K. Kraus. Pure operations and measurements. *Communications in Mathematical Physics*, 11(3):214–220, 1969.

[65] K.-E. Hellwig and K. Kraus. Operations and measurements ii. *Communications in mathematical physics*, 16(2):142–147, 1970.

[66] K. Kraus, A. Böhm, J. Dollard, and W. Wootters, editors. *States, Effects, and Operations: Fundamental Notions of Quantum Theory*. Lecture Notes in Physics. Springer Berlin Heidelberg, 1983.

[67] W. F. Stinespring. Positive functions on $c*$-algebras. *Proc. Amer. Math. Soc.*, 6:211, 1955.

[68] B. Cirel'son. Quantum generalizations of bell's inequality. *Letters in Mathematical Physics*, 4(2):93–100, 1980.

[69] N. Gisin. Bell's inequality holds for all non-product states. *Physics Letters A*, 154(5):201 – 202, 1991.

[70] N. Gisin and A. Peres. Maximal violation of bell's inequality for arbitrarily large spin. *Physics Letters A*, 162(1):15 – 17, 1992.

[71] R. F. Werner and M. M. Wolf. Bell inequalities and entanglement. *arXiv*, quant-ph/0107093v2, 2001.

[72] S. Popescu and D. Rohrlich. Generic quantum nonlocality. *Physics Letters A*, 166(5):293 – 297, 1992.

[73] H.-T. Lim, Y.-S. Kim, Y.-S. Ra, J. Bae, and Y.-H. Kim. Experimental realization of an approximate partial transpose for photonic two-qubit systems. *Phys. Rev. Lett.*, 107:160401, 2011.

[74] H.-P. Breuer. Optimal entanglement criterion for mixed quantum states. *Phys. Rev. Lett.*, 97:080501, 2006.

[75] H.-P. Breuer. Separability criteria and bounds for entanglement measures. *Journal of Physics A: Mathematical and General*, 39(38):11847, 2006.

[76] O. Gühne and N. Lütkenhaus. Nonlinear entanglement witnesses. *Phys. Rev. Lett.*, 96:170502, 2006.

[77] E. Størmer. Positive linear maps of operator algebras. *Acta math*, 110(3-4):233–278, 1963.

[78] K.-C. Ha and S.-H. Kye. Entanglement witnesses arising from exposed positive linear maps. *Open Systems & Information Dynamics*, 18(04):323–337, 2011.

[79] S. L. Woronowicz. Positive maps of low dimensional matrix algebras. Technical report, Centre National de la Recherche Scientifique, 13-Marseille (France). Centre de Physique Theorique, 1975.

[80] M. Horodecki, P. Horodecki, and R. Horodecki. Mixed-state entanglement and distillation: Is there a "bound" entanglement in nature? *Phys. Rev. Lett.*, 80:5239–5242, 1998.

[81] M. A. Nielsen and I. L. Chuang. *Quantum Computation and Quantum Information (Cambridge Series on Information and the Natural Sciences)*. Cambridge University Press, 1 edition, 2004.

[82] J. E. de Pillis. Linear transformations which preserve hermitian and positive semidefinite operators. *Pacific Journal of Mathematics*, 23(1), 1967.

[83] A. Jamiołkowski. Linear transformations which preserve trace and positive semidefiniteness of operators. *Reports on Mathematical Physics*, 3(4):275 – 278, 1972.

[84] N. Gisin. Hidden quantum nonlocality revealed by local filters. *Physics Letters A*, 210(3):151 – 156, 1996.

[85] C. H. Bennett, H. J. Bernstein, S. Popescu, and B. Schumacher. Concentrating partial entanglement by local operations. *Phys. Rev. A*, 53:2046–2052, 1996.

[86] C. H. Bennett, D. P. DiVincenzo, C. A. Fuchs, T. Mor, E. Rains, P. W. Shor, J. A. Smolin, and W. K. Wootters. Quantum nonlocality without entanglement. *Phys. Rev. A*, 59:1070–1091, 1999.

[87] E. M. Rains. Rigorous treatment of distillable entanglement. *Phys. Rev. A*, 60:173–178, 1999.

[88] E. Chitambar and R. Duan. Nonlocal entanglement transformations achievable by separable operations. *Phys. Rev. Lett.*, 103:110502, 2009.

[89] R. Horodecki, P. Horodecki, M. Horodecki, and K. Horodecki. Quantum entanglement. *Rev. Mod. Phys.*, 81:865–942, 2009.

[90] C. H. Bennett, G. Brassard, S. Popescu, B. Schumacher, J. A. Smolin, and W. K. Wootters. Purification of noisy entanglement and faithful teleportation via noisy channels. *Phys. Rev. Lett.*, 76:722–725, 1996.

[91] M. B. Plenio and S. Virmani. An introduction to entanglement measures. *Quant.Inf.Comput.7:1-51*, 2006.

[92] S. Hill and W. K. Wootters. Entanglement of a pair of quantum bits. *Phys. Rev. Lett.*, 78:5022–5025, 1997.

[93] W. K. Wootters. Entanglement of formation of an arbitrary state of two qubits. *Phys. Rev. Lett.*, 80:2245–2248, 1998.

[94] W. K. Wootters. Entanglement of formation and concurrence. *Quantum Info. Comput.*, 1(1):27–44, 2001.

[95] A. Uhlmann. Fidelity and concurrence of conjugated states. *Phys. Rev. A*, 62:032307, 2000.

[96] P. Rungta, V. Bužek, C. M. Caves, M. Hillery, and G. J. Milburn. Universal state inversion and concurrence in arbitrary dimensions. *Phys. Rev. A*, 64:042315, 2001.

[97] G. Vidal and R. F. Werner. Computable measure of entanglement. *Phys. Rev. A*, 65:032314, 2002.

[98] F. G. S. L. Brandão. Quantifying entanglement with witness operators. *Phys. Rev. A*, 72:022310, 2005.

[99] F. G. S. L. Brandão and R. O. Vianna. Witnessed entanglement. *International Journal of Quantum Information*, 04(02):331–340, 2006.

[100] P. W. Shor, J. A. Smolin, and B. M. Terhal. Nonadditivity of bipartite distillable entanglement follows from a conjecture on bound entangled werner states. *Phys. Rev. Lett.*, 86:2681–2684, 2001.

[101] D. M. Greenberger, M. A. Horne, A. Shimony, and A. Zeilinger. Bells theorem without inequalities. *Am. J. Phys*, 58(12):1131–1143, 1990.

[102] R. Qu, J. Wang, Z.-S. Li, and Y.-R. Bao. Encoding hypergraphs into quantum states. *Phys. Rev. A*, 87:022311, 2013.

[103] M. Rossi, M. Huber, D. Bruß, and C. Macchiavello. Quantum hypergraph states. *New Journal of Physics*, 15(11):113022, 2013.

[104] O. Gühne, G. Tóth, and H. J. Briegel. Multipartite entanglement in spin chains. *New Journal of Physics*, 7(1):229, 2005.

[105] Z.-H. Ma, Z.-H. Chen, J.-L. Chen, C. Spengler, A. Gabriel, and M. Huber. Measure of genuine multipartite entanglement with computable lower bounds. *Phys. Rev. A*, 83:062325, 2011.

[106] A. Sanpera, D. Bruß, and M. Lewenstein. Schmidt-number witnesses and bound entanglement. *Phys. Rev. A*, 63:050301, 2001.

[107] M. Hein, J. Eisert, and H. J. Briegel. Multiparty entanglement in graph states. *Phys. Rev. A*, 69:062311, 2004.

[108] B. Jungnitsch, T. Moroder, and O. Gühne. Entanglement witnesses for graph states: General theory and examples. *Phys. Rev. A*, 84:032310, 2011. Introduction of Graph-diagonal state Multipartite Entanglement Witness for, Graph-diagonal State.

[109] P. Erdős and A. Rényi. On random graphs. *Publ. Math. Debrecen*, 6:290–297, 1959.

[110] M. Van den Nest. *Local Equivalence of Stabilizer states and codes*. PhD thesis, Katholieke Universiteit Leuven, 2005.

[111] J.-Y. Wu, H. Kampermann, and D. Bruß. The search of X-chains in graph states. *In preparation*, 2015.

[112] J.-Y. Wu. The mathematica package of X-chain factorization: https://github.com/emmauelwjy/X-chain-Factorization.

[113] W. Dür, L. Hartmann, M. Hein, M. Lewenstein, and H.-J. Briegel. Entanglement in spin chains and lattices with long-range ising-type interactions. *Phys. Rev. Lett.*, 94:097203, 2005.

[114] L. Hartmann, J. Calsamiglia, W. Dür, and H. J. Briegel. Weighted graph states and applications to spin chains, lattices and gases. *Journal of Physics B: Atomic, Molecular and Optical Physics*, 40(9):S1, 2007.

[115] O. Gühne, M. Cuquet, F. E. S. Steinhoff, T. Moroder, M. Rossi, D. Bruß, B. Kraus, and C. Macchiavello. Entanglement and nonclassical properties of hypergraph states. *Journal of Physics A: Mathematical and Theoretical*, 47(33):335303, 2014.

[116] A. Cosentino and S. Severini. Weight of quadratic forms and graph states. *Phys. Rev. A*, 80:052309, 2009.

[117] M. Hajdušek and M. Murao. Direct evaluation of pure graph state entanglement. *New Journal of Physics*, 15(1):013039, 2013.

Ich versichere an Eides statt, dass die Dissertation von mir selbständig und ohne unzulässige fremde Hilfe unter Beachtung der "Grundsätze zur Sicherung guter wissenschaftlicher Praxis an der Heinrich-Heine-Universitt Düsseldorf" erstellt worden ist.

Dsseldorf, den 22. April 2015

(Junyi Wu)

Hiermit erkläre ich, dass ich die Dissertation keiner anderen Fakultät bereits vorgelegt habe und keinerlei vorherige erfolglose Promotionsversuche vorliegen.

Düsseldorf, den 22. April 2015

(Junyi Wu)